

ASSESSMENT OF CATHETER-MANOMETER SYSTEMS USED

FOR INVASIVE BLOOD PRESSURE MEASUREMENT

P.A. HEIMANN

Submitted to the University of Cape Town
in partial fulfillment of the requirements for the degree of
Master of Science in Medicine in the field of
Biomedical Engineering

March 1989

The University of Cape Town has been given
the right to reproduce this thesis in whole
or in part. Copyright is held by the author.

The copyright of this thesis vests in the author. No quotation from it or information derived from it is to be published without full acknowledgement of the source. The thesis is to be used for private study or non-commercial research purposes only.

Published by the University of Cape Town (UCT) in terms of the non-exclusive license granted to UCT by the author.

ABSTRACT

Direct measurement of blood pressure using a fluid-filled catheter and an electromechanical transducer is widely accepted in clinical practice. However, errors associated with the measurement are often not appreciated and these catheter-manometer systems are frequently unable to accurately reproduce applied pressures.

To assess the accuracy of catheter-manometer systems used for invasive arterial blood pressure measurements, *in vitro* and *in vivo* evaluations were performed.

The frequency response (described in terms of damped natural frequency and damping factor) for a variety of cannulae, pressure tubing and stopcocks (and combinations thereof) and their dependence on various parameters (catheter length, lumen diameter, fluid temperature and catheter material) were measured using an hydraulic pressure generator. The design and construction details of the pressure generator are presented.

It was found that the damped natural frequency of the catheter-manometer system is directly proportional to lumen diameter of the pressure tubing/catheter. Furthermore, damping factor is inversely related to the damped natural frequency and stiffer catheter material (for identical radius ratios) results in higher damped natural frequency. Catheter length is inversely related to damped natural frequency and the resonant frequency decreases for an increase in fluid operating temperature.

It was established that all catheter-manometer systems tested

were under-damped ($0.15 < \beta < 0.37$) and that the damped natural frequency ranged from 10.5 Hz for 1500 mm to 27.0 Hz for pressure tubing of 300 mm in length. Furthermore, catheter-manometer systems which had pressure tubing in excess of 300 mm in length did not comply with the bandwidth requirements for accurate dynamic blood pressure measurement.

For the in vivo assessment of the catheter-manometer system, the blood pressure waveform was analysed in the time and frequency domains. It was established that in 60 percent of the cases, the systolic pressure peak was higher when measured by a narrow bandwidth catheter-manometer system compared to that measured by a wide bandwidth system. Furthermore, values of dp/dt maximum were lower for wide bandwidth catheter-manometer systems than those measured by narrow bandwidth systems for heart rates above 90 beats per minute.

In the frequency domain analysis, artifact was sometimes found to occur at frequencies higher than the bandwidth of the catheter-manometer system. This high frequency artifact was found to distort the blood pressure waveform and resulted in false high dp/dt and peak systolic pressures.

ACKNOWLEDGMENTS

I would like to express special thanks to my supervisors Professor WB Murray (University of Natal), Dr. DA Boonzaier (Biomedical Engineering, UCT), Dr. PW le Roux Murray (South African Medical Research Council) and Mladen Poluta (Biomedical Engineering, UCT) for their guidance and enthusiasm throughout the project.

I am also grateful to:

Professor AR Coetzee for his support in allowing me to use the facilities of the F1 cardiac theatre at the Tygerberg Hospital.

Dr. Peter Hatting and Dr. C van der Merwe from the Department of Anaesthesiology, Tygerberg Hospital. Special thanks are due to the clinical technology staff at Tygerberg Hospital for their support, especially Mr Greg Hutchinson and Mr Johan van Rensburg.

All the staff of the Biomedical Engineering Department (UCT) for their assistance, and especially to Mr M Price for the construction of the catheter-manometer testing equipment.

Mr Paul Selby, Mr MM Blanckenberg, Miss Janet Butler and Miss Margie Walter for their special assistance.

My family and friends for their support and encouragement throughout, and the South African Medical Research Council for funding the research.

CONTENTS

Abstract	i1
Acknowledgments	i3
Contents	i4
List of Abbreviations	i11
List of Symbols	i12
List of Figures	i13
List of Tables	i18
Glossary	i21
1. INTRODUCTION	1
1.1 Incentive leading to the study	1
1.2 Aims of the thesis	4
1.3 Thesis contents	4
2. LITERATURE REVIEW	6
2.1 Introduction	7
2.2 Catheter-manometer modelling	11
2.2.1 Distributed parameter models	11
2.2.2 Lumped parameter models	18
2.3 Catheter-manometer system characterisation	23
2.3.1 Transient method of catheter-manometer characterisation	24
2.3.2 Steady state method of catheter-manometer characterisation	26
2.4 Frequency response evaluation	29
2.4.1 Catheter-manometer system evaluation	29
2.4.2 Swan Ganz catheter response evaluation	32
2.4.3 Compensation techniques	35

3.	BASIS FOR PROPOSED INVESTIGATION	37
3.1	Introduction	38
3.2	Limitations of catheter-manometer models	39
3.2.1	General limitations	39
	(i) Catheter compliance and fluid temperature	39
	(ii) Pressure chamber compliance	41
3.2.2	Limitations of the distributed parameter model	43
	(i) Multiple sites of reflections	43
	(ii) Unequal transmission times of frequency components	44
	(iii) Frequency dependence of fluid resistance and inertance	44
3.2.3	Limitations of the lumped parameter model	46
	(i) Reflections in the catheter-manometer	46
	(ii) Unequal attenuation of wave transmission	46
3.2.4	Summary	46
3.3	Catheter-manometer characterisation techniques	47
3.3.1	The transient method	47
3.3.2	The steady state method	50
3.3.3	Summary	51
3.4	Catheter-manometer system evaluation/assessment	52
3.4.1	Summary	53
3.5	Details of proposed investigation	54
3.5.1	Modelling	54
3.5.2	Characterisation technique	55
3.5.3	Evaluation	55
4.	EQUIPMENT AND PROCEDURES FOR DYNAMIC CATHETER-MANOMETER SYSTEM TESTING	57
4.1	Introduction	58
4.2	Catheter-manometer testing equipment	59
4.2.1	Ideal catheter-manometer test equipment requirements	59
4.2.2	Review of test system requirements	61

4.3	Pressure chamber design	62
4.3.1	General design	62
4.3.2	Mathematical and hydraulic analysis of the pressure chamber	63
4.3.3	Pressure generator construction	68
4.3.3.1	Introduction	68
4.3.3.2	Construction of the pressure chamber	69
4.4	In vitro catheter-manometer evaluation	75
4.4.1	The test system	75
4.4.2	Test equipment configuration	77
4.4.3	Test procedure	78
4.5	In vivo catheter-manometer evaluation	80
4.5.1	Introduction	80
4.5.2	In vivo testing configuration	81
4.5.3	Recording procedure	82
4.5.4	Signal analysis	83
4.5.4.1	Time domain analysis	83
4.5.4.2	Frequency domain analysis	83
4.6	Software development	84
4.6.1	Introduction	84
4.6.2	Computer hardware requirements	85
4.6.3	Micro-computer system used for the research	86
4.6.4	Brief program description	87
4.6.4.1	MEAS.THE	87
4.6.4.2	ANAL.THE	89
5.	RESULTS	91
5.1	Introduction	92
5.2	In vitro result	93
5.2.1	Pressure tubing	93
5.2.1.1	Physical properties of pressure lines	93
5.2.1.2	Effect of lumen diameter on damped natural frequency.	94
5.2.1.3	Effect of pressure tubing length on damped natural frequency	96
5.2.1.4	Relationship of the damping factor and damped natural frequency.	97
5.2.1.5	Effect of pressure tubing radius ratio on the damped natural frequency and damping factor.	99
5.2.1.6	Effect of boiled and non-boiled saline on the damped natural frequency.	101
5.2.1.7	Effect of twisting and coiling of pressure tubing on the damped natural frequency.	103

5.2.2	Catheters	106
5.2.2.1	Effect of stopcocks and flush devices on damped natural frequency	106
5.2.3	Cannulae	108
5.2.3.1	Effects of cannula lumen diameter on the damped natural frequency.	108
5.2.3.2	Effect of cannula lumen diameter on the damping factor.	110
5.2.4	Catheter-manometer systems	111
5.2.4.1	Effect of the damped natural frequency and damping factor in catheter-manometer systems with different pressure tubing length.	111
5.2.4.2	The effect of cannulae gauge and pressure tubing length on the damped natural frequency of catheter-manometer systems.	114
5.2.4.3	Effect of saline temperature on the frequency response parameters of catheter-manometer systems.	115
5.2.4.4	Effect of boiled vs. non-boiled saline on the frequency response parameters of catheter-manometer systems.	118
5.2.5	Effect of different transducer and transducer domes on the frequency response of catheter-manometer systems.	119
5.3	In vivo results	120
5.3.1	Introduction	120
5.3.2	The frequency content of the recorded blood pressure waveforms	122
5.3.3	Effect of low-pass filtering on the higher frequency components of the blood pressure pulse.	124
5.3.4	Effect of wide and narrow bandwidth catheter-manometer systems on blood pressure pulse.	127
5.3.5	Effect of fast heart rate on the pulse spectral characteristics for wide and narrow bandwidth catheter-manometer systems	128
5.3.6	Effect of wide and narrow bandwidth catheter-manometer systems on peak systolic and end diastolic blood pressures.	130
5.3.7	Effect of wide and narrow bandwidth systems on dp/dt maximum.	131
5.3.8	Effect of wide and narrow bandwidth systems on the Power Density Spectra of the blood pressure pulse.	132
5.4	Relationship between model derived frequency response parameters and measured frequency response.	132

6	DISCUSSION	134
6.1	In vitro results	135
6.1.1	Measurement technique	135
6.1.2	Discussion and interpretation of results	135
6.1.2.1	Pressure tubing	135
6.1.2.2	Stopcocks and flush devices	137
6.1.2.3	Cannulae	138
6.1.2.4	Catheter-manometer systems	138
6.1.2.5	Gardner representation of frequency response parameters	139
6.2	In vivo results	144
6.2.1	General statement on the recorded signals	144
6.2.2	High frequency artifact addition for narrow catheter-manometer systems.	144
6.2.3	Heart rate and its effect on signal fidelity.	146
6.2.4	Peak systolic and end diastolic blood pressure values	146
6.2.5	Fourier transforms	147
6.3	Catheter-manometer system models	147
7	CONCLUSIONS AND RECOMMENDATIONS	148
7.1	Conclusion	149
7.2	Recommendations	151
7.2.1	General recommendations	151
7.2.2	Catheter-manometer system	152
7.2.2.1	Pressure tubing dimensions	152
7.2.2.2	Catheters	152
7.2.2.3	Cannulae	152
7.3	Future work	153
	REFERENCES	154

APPENDICES

A	Blood pressure measurement	A1
A1	Clinical aspects of blood pressure	A2
A2	Invasive blood pressure measurement technique	A12
A3	Advantages and risks of invasive blood pressure measurement	A18
A4	System requirements for invasive blood pressure measurement	A20
B	Modelling and characterisation of the catheter-manometer system	B1
B1	Modelling and characterisation of catheter-manometer systems	B2
B1.1	The distributed parameter model	B2
B1.2	The lumped parameter model	B17
B2	Fundamentals of second order systems	B23
C	Pressure generator and compensation network design and construction	C1
C1	Pressure generator construction and evaluation	C2
C2	Electronic compensation network for pressure generator	C9
C3	Equipment set up for in vitro testing	C26
D	Construction plan for test equipment	D1
E	Software operation	E1
E1	Guidelines on the operation of MEAS.THE	E2
E2	Guidelines on the operation of ANAL.THE	E26
E3	Examples of hardcopy presentation	E52
F	Software listing	F1
F1.1	MEAS.THE	F2
F1.2	ANAL.THE	F24

G	Results listing	G1
	G2 In vitro results	G2
	G3 In vivo results	G14
	G4 Calculated frequency responses for catheter- manometer systems	G19
H	Equipment specification	H1
	H1 Racal store 7DS tape recorder	H2
	H2 Bio-tek blood pressure system analyser	H6
	H3 Blood pressure amplifier BAP 001	H7
	H4 HP Vectra	H8
	H5 Microlink	H9
I	Data constants	I1
	I1 Data table on polymers	I2

LIST OF ABBREVIATIONS

A	-	ampere
AC	-	alternating current
A/D	-	analogue to digital
AP	-	arterial pressure
atm	-	atmosphere
AV	-	arterio-venous (shunt)
bpm	-	beats per minute
BW	-	bandwidth
cc	-	cubic centimetre
CGA	-	Color Graphics Adapter
cm	-	centimetre
CO	-	cardiac output
CPB	-	cardiopulmonary bypass
CVP	-	central venous pressure
dB	-	decibel
DC	-	direct current
Del	-	delete
Dn	-	down
ECG	-	Electrocardiogram
EGA	-	Enhanced Graphic Adapter
FFT	-	Fast Fourier Transform
FM	-	frequency modulation
GPiB	-	General Purpose Interface Bus
HP	-	Hewlett-Packard
HP-IB	-	Hewlett-Packard Interface Bus
hr	-	hour
Hz	-	hertz
IEEE	-	Institute for Electrical and Electronic Engineers
Ins	-	insert
IV	-	intra-venous
k	-	kilo
kB	-	kilo byte
kg	-	kilo gram
M	-	mega
MAP	-	mean arterial pressure
max	-	maximum
min	-	minimum
ml	-	millilitre
mmHg	-	millimetres of mercury
n	-	nano
N	-	Newton
Pa	-	Pascal
PDS	-	Power Density Spectra
PE	-	polyethylene
Pg	-	page
PP	-	polypropylene
PVC	-	polyvinyl-chloride
sec	-	second
SI	-	System Internationale
SV	-	stroke volume
T	-	Teflon
V	-	volt
vs.	-	versus

LIST OF SYMBOLS

B	-	reflection coefficient
c_o	-	frictional coefficient (fluid)
c_T	-	frictional coefficient (pressure chamber)
C	-	capacitance
CO_2	-	carbon dioxide
E	-	Young's modulus
f_n	-	undamped natural frequency (Hz)
f_p	-	resonant frequency (Hz)
F	-	force
h	-	thickness of membrane
K	-	spring constant
k_o	-	distributed coefficient of elastance
k_T	-	pressure-mass coefficient
k_v	-	pressure-volume coefficient
k_w	-	compressibility of water
l	-	length
L	-	inductance
m_o	-	mass-flow inertance
m_T	-	coefficient of inertia
M	-	mass
M_p	-	resonant peak
O_2	-	oxygen
ρ	-	fluid density
r	-	radius
R	-	resistance
t_w	-	catheter wall thickness
v	-	volume
ν	-	fluid viscosity
ω	-	angular frequency (rad/sec)
ω_n	-	undamped natural frequency (rad/sec)
ω_p	-	resonant frequency (rad/sec)
Z_o	-	characteristic fluid impedance
Z_T	-	terminal mechanical impedance
$^{\circ}C$	-	degrees Celsius
Ω	-	ohm
\propto	-	proportional
Ω	-	frequency ratio
β	-	damping factor
π	-	pi
σ	-	variance
θ	-	angle
δ	-	damping
α	-	pole/zero ratio
μ	-	micro
Φ	-	propagation constant

LIST OF FIGURES

Chapter 1

- Figure 1.1 Reversal of the usual relationship between aortic and radial pulse pressure after CPB 2

Chapter 2

- Figure 2.1 Diagram of a catheter-manometer system 10
Figure 2.2 Fluid analogue model of a catheter-manometer model by Fry (1960) 12
Figure 2.3a Electrical analogue model by Andersen and Bergsten (1982) 13
Figure 2.3b Electrical analogue model by Andersen and Bergsten (1982) 14
Figure 2.3c Electrical analogue model by Andersen and Bergsten (1982) 14
Figure 2.4 Electrical analogue model by Yeomanson and Evans (1983) 16
Figure 2.5 Mechanical analogue model 18
Figure 2.6a Analogous circuit for catheter-manometer system by Taylor et al (1986) 21
Figure 2.6b Simplified circuit for figure 2.6a 22
Figure 2.7 Typical system used for the transient method of frequency response testing 25
Figure 2.8 Transient response display 26
Figure 2.9 Typical system used for the steady state method of frequency response testing 27
Figure 2.10 Amplitude response obtained by the steady state method 28

Chapter 3

- Figure 3.1a Photograph showing the non-uniform radius of a pressure lumen 40
Figure 3.1b Photograph showing a non-concentric lumen of a cannula 41
Figure 3.2a Second order catheter-manometer system and the equivalent electrical model 48
Figure 3.2b Second order catheter-manometer system and the equivalent electrical model 49

Chapter 4

Figure 4.1	Schematic diagram of the dynamic of the catheter-manometer testing system	59
Figure 4.2	Amplitude response requirements of the pressure generator	61
Figure 4.3	Diagram of forces acting on pressure generator chamber	63
Figure 4.4	Approximate model for the pressure generator connected to a catheter-manometer system	65
Figure 4.5	Amplitude and phase response of the pressure generator	71
Figure 4.6	Amplitude and phase response using the phase-lag compensator	72
Figure 4.7	Improved amplitude and phase response of the pressure generator and pole-zero compensator	73
Figure 4.8	The pressure chamber	74
Figure 4.9	The catheter-manometer test equipment	74
Figure 4.10	Diagram of the test system	76
Figure 4.11	Reference and output transducer signals for test system	78
Figure 4.12	In vivo test system configuration	81
Figure 4.13	Function key flowchart of MEAS.THE	87
Figure 4.14	Function key flowchart of ANAL.THE	89

Chapter 5

Figure 5.1	f_d vs. lumen diameter for pressure tubing	94
Figure 5.2	f_d vs. pressure tubing length	96
Figure 5.3	f_d vs. the inverse of pressure tubing length	97
Figure 5.4	Relationship of f_d and β for pressure tubing (300 mm)	98
Figure 5.5	Inverse of β and f_d for pressure tubing	99
Figure 5.6	f_d vs. radius ratio for pressure tubing	100
Figure 5.7	f_d vs. pressure tubing length for boiled and non-boiled saline	102
Figure 5.8	β vs. f_d for different lengths of pressure tubing. Boiled and non-boiled saline	103
Figure 5.9	Frequency response of twisted, coiled and straight pressure tubing	105
Figure 5.10	f_d and β for pressure tubing compared to catheters	107
Figure 5.11	f_d vs. cannula gauge	108
Figure 5.12	f_d vs. lumen diameter for cannulae	109
Figure 5.13	f_d vs. β for different cannula gauges	110
Figure 5.14	Frequency response of catheter-manometer system - 20 gauge cannula	111
Figure 5.15	Frequency response of catheter-manometer system - 22 gauge cannula	112

Figure 5.16	Frequency response of catheter-manometer system - 24 gauge cannula	113
Figure 5.17	f_d vs. β for catheter-manometer systems with different cannula gauges and pressure tubing length	114
Figure 5.18	f_d of catheter-manometer systems at 25°C and 37 °C (20 gauge cannula)	115
Figure 5.19	f_d of catheter-manometer systems at 25°C and 37 °C (22 gauge cannula)	116
Figure 5.20	f_d of catheter-manometer systems at 25°C and 37 °C (24 gauge cannula)	117
Figure 5.21	f_d vs. β for catheter-manometer systems (20 gauge cannula) for boiled and non-boiled saline	118
Figure 5.22	Pulse alternans	121
Figure 5.23	Atrial fibrillation	121
Figure 5.24	FFT and blood pressure waveform measured by a wide bandwidth catheter-manometer system	122
Figure 5.25	FFT and blood pressure waveform measured by a narrow bandwidth catheter-manometer system	123
Figure 5.26	Filtered (33 and 25 Hz) blood pressure waveform	124
Figure 5.27	FFT of filtered (33 and 25 Hz) blood pressure waveform	125
Figure 5.28	Filtered (17 and 25 Hz) blood pressure waveform	126
Figure 5.29	FFT of filtered (33 and 25 Hz) blood pressure waveform	126
Figure 5.30	Double peak recorded by narrow bandwidth catheter-manometer system	127
Figure 5.31	FFT of blood pressure pulse at 76 bpm	128
Figure 5.32	FFT of blood pressure pulse at 113 bpm	129
Figure 5.33	Peak systolic blood pressure recorded by a wide and narrow bandwidth catheter-manometer system	130
Figure 5.34	Comparison of measured and calculated frequency response parameters	132
Figure 5.35	Comparison of measured and calculated (lumped and distributed) frequency response parameters	133
 Chapter 6		
Figure 6.1	Gardners representation chart	140
Figure 6.2	Gardners representation of catheters	141
Figure 6.3	Gardners representation of catheter-manometer systems	142
Figure 6.4	Gardners representation of Swan Ganz catheters	143

Appendix A

Figure A1.1	Blood pressure pulse and the corresponding blood flow	A3
Figure A1.2	The phases of the pressure pulse	A4
Figure A1.3	Differences in pulse pressure at several sites in the arterial system	A11
Figure A2.1	Recommended system for long-duration intravascular monitoring	A13
Figure A4.1	Ideal amplitude and phase response for blood pressure measurement systems	A21

Appendix B

Figure B1.1	Vector diagram of forces of a second order system	B3
Figure B1.2	Vector diagram representing pressures in a second order system	B7
Figure B1.3	Electrical analogue model described by Andersen and Bergsten (1982)	B9
Figure B1.4	Electrical analogue model described by Yeomanson and Evans (1983)	B12
Figure B1.5	Mechanical analogue model of a second order system	B17
Figure B1.6	Amplitude ratio of a second order system	B20
Figure B1.7	Phase response of a second order system	B22
Figure B2.1	Force-mass-friction system	B23
Figure B2.2	Peak resonance, resonant frequency and bandwidth for a second order system	B26

Appendix C

Figure C1.1	Pressure generator (model A)	C2
Figure C1.2	Pressure generator (model B)	C7
Figure C1.3	Frequency response of catheter-manometer test equipment	C8
Figure C2.1	Block diagram of a simple linear system	C9
Figure C2.2	Block diagram of a single-loop feedback system	C10
Figure C2.3	Characteristic roots of pressure generator	C12
Figure C2.4	Nichols chart	C13
Figure C2.5	Frequency response of pressure generator and phase-lag compensator	C14
Figure C2.6	Characteristic roots of the pressure generator and pole-zero compensator	C16
Figure C2.7	Block diagram of pole-zero compensator	C17
Figure C2.8	Block diagram of variable pole-zero compensator	C18
Figure C2.9	Electronic circuit of compensator	C19

Figure C2.10	Summation circuit	C20
Figure C2.11	Non-inverting amplifier circuit	C22
Figure C2.12	Integrator circuit	C23
Figure C2.13	Printed circuit board outlay	C25
Figure C3.1	Pressure generator system	C26
Figure C3.2	Cannula sliding device	C28

Appendix D

Drawing D1	Pressure generator (model A)	D2
Drawing D2	Pressure generator (model B)	D3
Drawing D3	Assembled pressure chamber	D4
Drawing D4	Stand	D5
Drawing D5	Pressure chamber	D6
Drawing D6	Base	D7
Drawing D7a	Cannula sliding device (side view)	D8
Drawing D7b	Cannula sliding device (front view)	D8

Appendix E

Figure E1.1	Opening menu of MEAS.THE	E2
Figure E1.2	Key to box diagrams used in flowcharts	E4
Figure E1.3	Flow diagram of main subroutine of MEAS.THE	E5
Figure E1.4	Flowchart of data entry routines	E8
Figure E1.5	The array editor	E11
Figure E1.6	Read data menu of MEAS.THE	E13
Figure E1.7	Flowchart for data read and data analysis routines	E16
Figure E1.8	Printer and plotter menu	E18
Figure E1.9	Amplitude response display	E19
Figure E1.10	Flowchart for printing routines	E20
Figure E2.1	Opening menu of ANAL.THE	E27
Figure E2.2	Flowchart for main routine for ANAL.THE	E34
Figure E2.3	Flowchart of the view menu	E36
Figure E2.4	Scroll window	E37
Figure E2.5	Flowchart for the analysis menu	E40
Figure E2.6	Screen display for time menu	E42
Figure E2.7	Flowchart for the time analysis routine	E43
Figure E2.8	Time analysis information window	E45
Figure E2.9	Screen display of the time analysis results	E46
Figure E2.10	Frequency analysis menu and a PDS display	E47
Figure E2.11	Screen display for frequency domains results	E48
Figure E2.12	Flowchart of the frequency domain subroutines	E49
Figure E2.13	Flowchart of the printer routine	E50
Figure E2.14	Example of time analysis report	E51

LIST OF TABLES

Chapter 2

Table 2.1	System requirements for accurate blood pressure measurement	8
Table 2.2	Resonant frequency for catheter-manometer system	31
Table 2.3	Resonant frequency for pressure tubing	32
Table 2.4	Frequency response of cardiac catheters	33
Table 2.5	Frequency response of cardiac catheters	34

Chapter 5

Table 5.1	Characteristics of pressure tubing	93
Table 5.2a	f_d and β for pressure tubing (300 mm and 1200 mm)	104
Table 5.2b	Change in f_d and β for coiled, twisted and straight pressure tubing	104
Table 5.3	Change in frequency response for catheters and pressure tubing	106

Appendix A

Table A2.1	Conversion table for pressure units	A17
Table A4.1	Transducer requirements for accurate blood pressure measurement	A27
Table A4.2	Ancillary blood pressure system requirements	A31

Appendix B

Table B1.1	Compliance values of catheters and transducers	B11
Table B1.2	Bessel functions	B16

Appendix C

Table C1.1	Resonant frequency of pressure generator (model A)	C4
Table C1.2	Improved frequency response of pressure generator (model A)	C5
Table C1.3	Improved frequency response of pressure generator (model B)	C6
Table C2.1	Component list	C24

Appendix E

Table E1.1	Active function keys for main menu, MEAS.THE	E3
Table E1.2	Active function keys for the data entry menu	E6
Table E1.3	Control keys of the array editor	E12
Table E1.4	Active function keys for the data read menu	E14
Table E1.5	Active function keys for the printer menu	E17
Table E1.6	Scroll control keys	E24
Table E1.7	Marker bar control keys	E25
Table E2.1	Active function keys for the data read menu, ANAL.THE	E28
Table E2.2	Clock rates	E29
Table E2.3	Scroll control keys	E35
Table E2.4	Marker bar control keys	E38
Table E2.5	Active function keys for data analysis menu	E39
Table E2.6	Active function keys for the time analysis	E41
Table E2.7	Editor-marker control keys	E44
Table E2.8	Active function keys for the frequency domain analysis	E46
Table E2.9	Active function keys for the printer routines	E48

Appendix G

Table G2.1	Index of pressure tubing	G3
Table G2.2	f_d and β for pressure tubing	G4
Table G2.3	f_d and β for pressure tubing coiled around an 8 cm diameter cylinder	G4
Table G2.4	f_d and β for pressure tubing coiled around an 15 cm diameter cylinder	G5
Table G2.5	f_d and β for pressure tubing twisted through 720° around its longitudinal axis	G5
Table G2.6	f_d and β for polyethylene pressure tubing (ID = E). Boiled saline	G6

Table G2.7	f_d and β for polyethylene pressure tubing (ID = E). Non-boiled saline	G6
Table G2.8	f_d and β for catheter system	G7
Table G2.9	Cannulae characteristics	G8
Table G2.10	f_d and β for cannulae not pressurized externally	G9
Table G2.11	f_d and β for cannulae pressurized by 100 mmHg externally	G9
Table G2.12a	f_d for catheter-manometer systems. Boiled saline at 25 °C	G10
Table G2.12b	β for catheter-manometer systems. Boiled saline at 25 °C	G10
Table G2.13a	f_d for catheter-manometer systems. Non-boiled saline at 25 °C	G11
Table G2.13b	β for catheter-manometer systems. Non-boiled saline at 25 °C	G11
Table G2.14a	f_d for catheter-manometer systems. Boiled saline at 37 °C	G12
Table G2.14b	β for catheter-manometer systems. Boiled saline at 37 °C	G12
Table G2.15	f_d and β for Swan Ganz catheters (7F)	G13
Table G2.16	f_d and β for Swan Ganz catheters (5F)	G13
Table G3.1	Patient index	G14
Table G3.2	Heart rate, dp/dt max and mean blood pressure	G15
Table G3.3	Peak systolic, end diastolic and time delays of blood pressure waveforms	G16
Table G3.4	Relative amplitude of harmonics (first four)	G17
Table G3.5	Relative amplitude of harmonics (five to eight)	G18
Table G3.6	Calculated frequency response using the Bruner model	G19
Table G3.7	Calculated frequency response using Yeomanson and Evans model	G20

Appendix I

Table I1.1	Data constants
------------	----------------

GLOSSARY

Allen test

Test for adequacy of blood circulation in the hand (see Appendix A2.1).

Amplitude response

Amplitude response is defined as the ratio of the output of a system with respect to the input (i.e. the gain) as a function of frequency of an applied sinusoidal signal.

Artifacts

Erroneous or false components present in the output signal. Artifacts in monitoring systems are due to a variety of causes: the most common artifacts are caused by inadequate dynamic response, movements of pressure tubing, and improper calibration of the measurement system.

Balancing

Zeroing of the output from the catheter-manometer system by opening the transducer diaphragm to atmospheric pressure and adjusting the monitor readout to zero (see Appendix A2.2).

Bandwidth

The bandwidth, BW, of a catheter-manometer system is defined as the frequency at which the magnitude of the amplitude response drops to 70.7 percent of its zero-frequency value, or 3 dB down from its zero-frequency gain.

Cardiac output (CO)

The volume of blood pumped by the heart in one minute (measured in liters per minute). Normal value for an average resting adult male is approximately 5 liters per minute.

CO = stroke volume x heart rate.

Catheter-tip transducer

A miniature pressure transducer on the distal end of a catheter intended for direct intravascular measurements, i.e. with no hydraulic coupling.

Compliance

Expresses the stiffness of a catheter-manometer system: The greater the stiffness, the lower the compliance. Expressed in traditional units of $\text{mm}^3/100 \text{ mmHg}$ or SI-units m^5N^{-1} . (Also called volume displacement and is defined as dv/dp)

Damping factor

A numerical quantity describing the decay of oscillations in a resonant system. Values between 0 and 1 describe an underdamped system, values greater than 1 describe an overdamped system; 0.2 being a typical value in a fluid-filled catheter-manometer system.

Dicrotism

The quality of having two sphygmographic waves or elevations to one beat of the pulse.

dp/dt

Rate of change in pressure per unit time, normally measured in units of mmHg/s. Important indicator of cardiac contractility.

Disposable dome

A plastic chamber which isolates the sterile fluid connection to the patient from the non-sterile transducer.

Distortion

The artifactual response of a measuring system due to insufficient bandwidth (low resonant frequency), non-linear phase response, and/or static errors.

Dynamic response

See frequency response.

Fidelity

An indication of the quality of dynamic response. High fidelity, as in sound reproduction systems, refers to a system which faithfully reproduces the input signal.

Continuous infusion device

A device that flushes the catheter by slow infusion of heparinized saline (usually 3 ml/h). The flush device isolates the infusion system from the pressure transducer and prevents the catheter being blocked.

Frequency response

The amplitude and phase responses, as a function of frequency, of a system (DiStefano, 1967). Amplitude and phase responses fully describe the characteristics of any system.

Gain

The magnitude of the amplitude response of a system. The gain is a function of frequency.

The gain of transducers is measured in:

$$\mu\text{V (output) / V (excitation) / mmHg (pressure applied)}$$

Harmonic

A harmonic is one of the component frequencies of a complex waveform and is an integral multiple of the fundamental frequency. Any waveform can be broken down into its harmonics by Fourier transformation.

Measurement error

Inaccuracy caused by incorrect system calibration, application or reading of measuring apparatus and by artifactual distortions in the measuring device itself. The errors are classified as static or dynamic. Static errors apply in most measurement situations and dynamic errors arise only when the input (e.g. pressure) changes rapidly.

Damped natural frequency

The resonant frequency at which an underdamped measuring system oscillates when subjected to a step input.

Overshoot (second-order system)

The difference between the maximum amplitude attained by the output and the steady-state value in response to a unit step input.

In an underdamped blood pressure measurement system the pressure pulse waveform may exhibit itself as an overshoot of the systolic portion of the waveform followed by ringing.

Phase response

Phase response is defined as the phase of the output of a system with respect to the input, as a function of the frequency of an applied sinusoidal signal.

Resonance

Amplification of oscillations that occurs when the frequency of an applied signal equals the natural frequency of the measuring system.

Ringing

The result of an underdamped catheter-transducer system. Best characterized by small oscillations seen on the pressure waveform after peak systole.

Peak systolic and end diastolic pressure

The maximum pressure during systole and the minimum pressure during diastole, respectively.

Pressure Transducer

An electromechanical device that transforms hydraulic pressure into an electrical signal.

CHAPTER ONE

INTRODUCTION

1.1 Incentive leading to the study

It was first mentioned in a publication in 1939 (Hamilton and Dow) that peak systolic arterial pressure increases by up to 40 mmHg relative to central aortic systolic pressure as the site of measurement is moved distally in the large arteries, while the mean pressure usually decreases by less than 8 mmHg.

This normal increase in peripheral systolic pressure does not always occur. Stern et al (1985) found that in almost 70 percent of the patients that were studied in their classic work, radial artery peak systolic pressure was lower than central systolic pressure during the immediate cardiopulmonary post-bypass (CPB) period (figure 1.1). The decrease was large enough to be of clinical concern (12-32 mmHg). For all the patients, the difference between aortic and radial mean blood pressure measured prior to CPB was in the range of 0 to 8 mmHg (mean = 3 mmHg, median = 2.5 mmHg), while in the post-bypass period this range increased from 1 to 22 mmHg (mean = 9 mmHg, median = 8 mmHg).

Stern concluded that the radial artery systolic pressure often did not accurately reflect central aortic pressure in the immediate cardiopulmonary post-bypass period.

Stern associated the change with the warming of blood at the end of cardiopulmonary bypass and suggested a lower vascular resistance in the forearm as a possible explanation for the apparent reversal. Pauca and Meredith (1987) discovered that the reversal also caused clinically significant errors in patients with AV fistulae and thus confirmed Stern's perception that a lowered forearm resistance was indeed the reason for the reversal.

This reversal has more recently been found to occur during CPB performed at the Tygerberg Hospital, and typically lasts between 10 and 60 minutes, post-bypass, gradually reverting to normal.

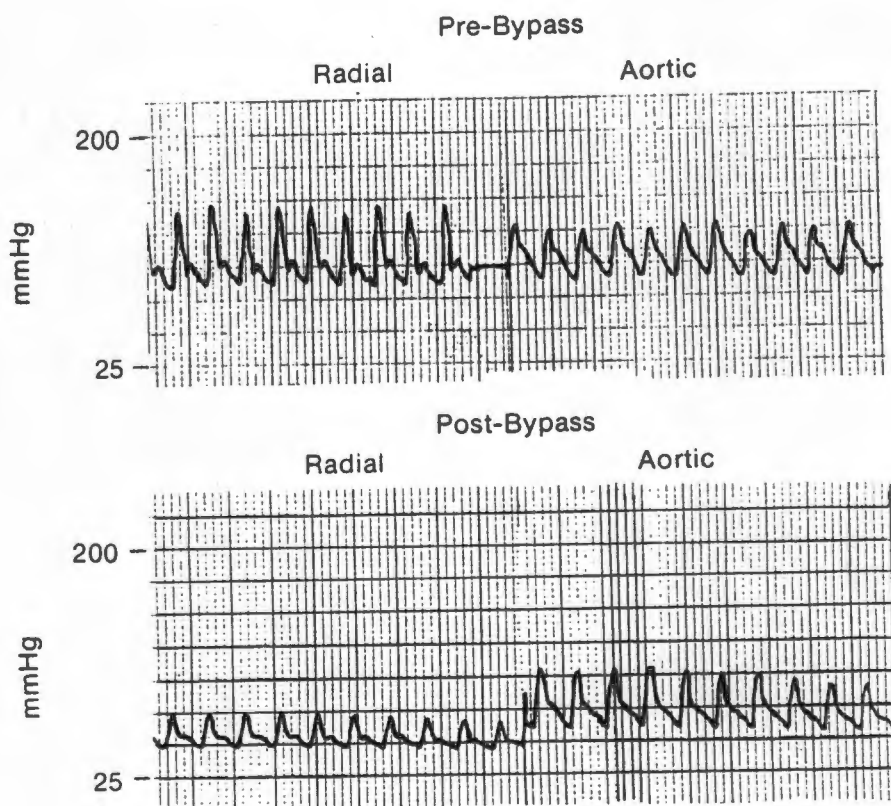


Figure 1.1

Reversal of the usual relationship between the aortic and the radial artery pulse pressure after CPB (Stern et al, 1985).

In order to investigate possible explanations for the above-mentioned reversal, many relevant factors and parameters need to be considered. Some of these are: cardiac output, arterial blood flow, arterial pressure, venous pressure, peripheral vascular resistance, p_{O_2} (partial pressure of oxygen in ml/l), p_{CO_2} (partial pressure of carbon dioxide in ml/l), venous return, heart rate, ECG waveforms and core temperature. Nevertheless, blood pressure, blood flow and peripheral resistance have been identified by McDonald (1974), Stern et al (1985) and Pauca and Meredith (1987) as the key parameters for the explanation of the above mentioned reversal in arterial blood pressure.

It was initially hoped to investigate all three of these parameters (blood pressure, blood flow and peripheral vascular resistance) in close detail. A model for the arterial tree of the forearm and hand would be formulated on the basis of pressure measurements taken while withdrawing a Miller catheter from a central site distally to the point of insertion near the wrist. Ethical considerations prevented the use of a catheter-tip manometer inserted via the radial artery and it was decided that a model based solely on the two pressure measurement points readily available (central and radial) would not be of sufficient accuracy or benefit.

It was also felt that to properly examine the above-mentioned problem, measurements of pressure and flow would have to be accurate, reliable and reproducible. Stern et al (1985) and others had raised the issue of possible measurement system artifact and inaccuracies in quantifying these parameters. On closer investigation, it was realised that both pressure and flow

measurement are complex and often oversimplified procedures. Detailed analysis of pressure and flow waveforms requires complete understanding of the methods and equipment used and calibration of the measurement system. To restrict the scope of this work, it was decided to concentrate on invasive blood pressure measurement. As most invasive measurements are performed using catheter-manometer systems, the thesis focuses on catheter-manometer systems used in clinical practice.

1.2 Aims of the thesis

- to present a critique on two of the modelling methods used in the analysis of the catheter-manometer system.
- in vitro testing of catheter-manometer system dynamic response.
- in vivo assessment of the relative fidelity of blood pressure measurements using different catheter-manometer systems.

1.3 Thesis contents

Chapter 2 presents a literature review on catheter-manometer models and techniques for the assessment of catheter-manometer systems. Chapter 3 deals with the evaluation of these catheter-manometer models and the methodology of in vitro and in vivo assessment of catheter-manometer systems. In chapter 4, the hardware, software and procedures for the dynamic testing of the catheter-manometer system are presented.

The results are presented in chapter 5. The discussion follows in chapter 6 while the conclusion and recommendations is given are chapter 7.

The appendices contain the body of results and detailed discussions of relevant issues that are briefly mentioned in the text.

CHAPTER TWO

LITERATURE REVIEW

2.1 Introduction

Assessment of invasive blood pressure measurement systems requires an understanding of blood pressure fundamentals, viz. generation, transmission and attenuation of the pressure pulse (the reader is referred to Appendix A, section 1 for a presentation of these aspects). It is imperative to understand the physiology of blood pressure dynamics before objectively assessing the performance of blood pressure measurement systems, as the dynamics have a direct bearing on the requirements of these systems (Bruner et al, 1981a). In particular, the frequency response of the system should be sufficient to ensure distortionless processing of the signal, whose frequency content (dealt with in appendix A, section 4.2) is a function of measurement site (including distance from heart), anatomical features of the site such as vessel diameter and wall elasticity, and peripheral resistance (Bruner, 1978; Bruner et al, 1981a; Caro et al, 1978; Hasegawa and Rodbard, 1979; O'Rourke, 1968 and Smith, 1978).

System requirements for accurate invasive blood pressure measurements have been established (Appendix A4.4, A4.5 and A4.6) and are summarised in table 2.1.

■ Linearity	:	± 2% error for pressure range of - 20 to 250 mmHg.
■ Hysteresis	:	± 2% error for pressure range of - 20 to 250 mmHg
■ Temperature coefficient of sensitivity	:	± 0.05 mV/cmHg/°C for temp. range of 15 to 40 °C
■ Temperature coefficient at zero pressure	:	± 0.3 mmHg/°C for temp. range of 15 to 40 °C
■ Sensitivity drift	:	1 mmHg / 8 hours
■ Pressure measurement range	:	-20 to 400 mmHg

Table 2.1

System requirements for accurate blood pressure measurement (AAMI, 1984).

An invasive blood pressure measurement system typically comprises the following stages:

- signal pickup (catheter-tip transducer or transducer coupled via fluid-filled catheter)
- amplifier
- recorder/monitor

Although the catheter-tip transducer is currently the most accurate invasive measuring device, for reasons of optimal frequency response, cost considerations prevent its widespread use.

While each of the blood pressure measurement stages has an effect on the overall performance/response of the measurement system, it has been found that the catheter-manometer stage is the limiting factor in dynamic performance of the system (Bruner, 1978).

In order to determine and comprehend which parameters of the catheter-manometer system affect and limit the dynamic response, the catheter-manometer system must be modelled and analysed in terms of these parameters.

For the purpose of this thesis, the catheter-manometer is defined to comprise the following (figure 2.1):

- cannula
- pressure tubing
- stopcock(s)
- flush device
- pressure chamber (including the membranes of the pressure dome and transducer)

Although the transducer is not defined as a part of the catheter-manometer system, the characteristics of the pressure chamber are determined by both the transducer diaphragm and the membrane of the pressure dome. The influence of the pressure dome membrane, however, which isolates the patient from the transducer, is insignificant compared to that of the transducer diaphragm, as the latter has a lower compliance (Yeomanson and Evans, 1983).

Furthermore, the combination of cannula and pressure tubing will be referred to as "the catheter". An exception to the above is

the so-called Swan Ganz catheter, used to measure blood pressure and cardiac output, by means of the thermo-dilution technique. Although Swan Ganz catheters will be considered in subsequent sections, no references alluding to modelling of Swan Ganz catheters were found.

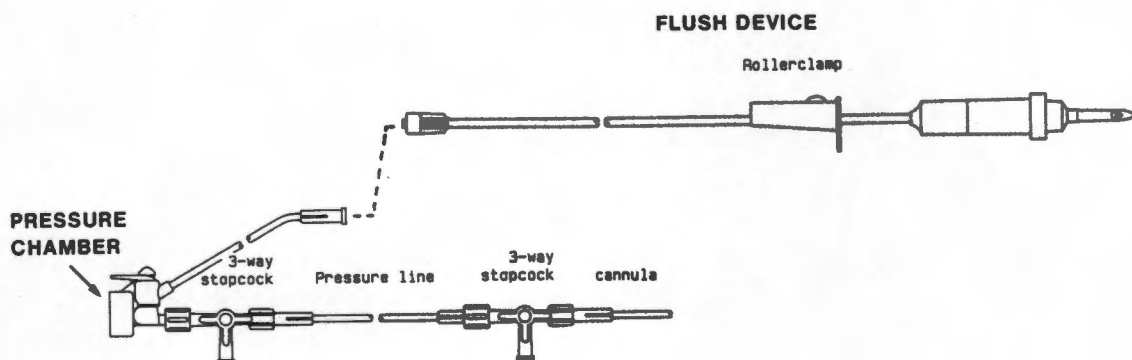


Figure 2.1

Diagram of a catheter-manometer system.

This Chapter will review:

1. Existing catheter-manometer models (distributed and lumped models) in terms of the system parameters.
2. The in vitro characterisation techniques.
3. The in vitro characterisation of the catheter-manometer system parameters, and those of Swan Ganz catheters.

2.2 Catheter-manometer modelling

The following sections will briefly review these different catheter-manometer models. Models requiring further explanations are discussed in Appendix B.

2.2.1 Distributed parameter models

The schematic representation of a fluid analogue model (Fry, 1960) of a catheter-manometer system is given in figure 2.2. The model consists of a catheter M (cannula and pressure tubing), attached to a pressure chamber (dome), M_{dome} . The pressure dome has an elastic diaphragm K, the characteristics of which are determined by the elastance of the pressure chamber membrane and the diaphragm of the transducer.

In this model, Fry described the physical characteristic of the catheter and the pressure dome in terms of impedances. The impedance of the catheter was called the characteristic (fluid) impedance Z_0 , which is determined by the distributed fluid inertance or mass flow m_0 , the distributed fluid friction c_0 and the distributed fluid elastance k_0 of the catheter. The impedance of the pressure chamber was called the terminal mechanical impedance Z_T , which is determined by the coefficient of inertia m_T , the coefficient of friction c_T and the coefficient of elastance or pressure-mass coefficient k_T of the pressure chamber.

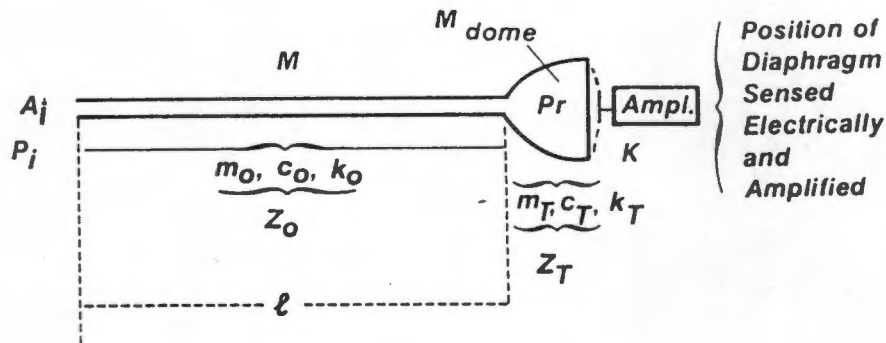


Figure 2.2

The fluid analogue model of a catheter-manometer system (Fry, 1960). For a pressure increase (relative to the pressure P_r in the pressure dome) of P_i , at the opening A_i , a movement of incompressible fluid would occur into the pressure chamber M_{dome} , consequently increasing the fluid mass contained in the pressure chamber. This increase of fluid mass in the pressure chamber displaces the membrane of the pressure dome and subsequently the diaphragm of the transducer (this is indicated by the dotted line). The position of the diaphragm is sensed and converted to an electrical signal which is then amplified by some appropriate scheme to display the value of applied pressure, assuming proper calibration of the system.

Formulating the amplitude and phase response of the catheter-manometer model, the relationship between pressure within the pressure dome P_r , and that at the opening of the catheter P_i , is given by (Fry, 1960);

$$\frac{P_r}{P_i} = \frac{k_T}{j\omega(Z_T \cosh \Phi l + Z_o \sinh \Phi l)} \quad (2.1)$$

In equation 2.1, Φ is the propagation constant of the catheter, l is the length of the catheter and the amplitude and phase responses are given by the amplitude and phase plots of P_r/P_i respectively.

In Appendix B, section 1.1.1 the relationship between the fluid dynamic parameters and the system response is discussed.

Andersen and Bergsten (1982) also devised a distributed model which is shown in figure 2.3(a). The model is represented by the electrical analogue given in terms of fluid-dynamic parameters. A simplified model is given in figure 2.3(b), where the capacitance representing catheter and fluid compliance has been combined.

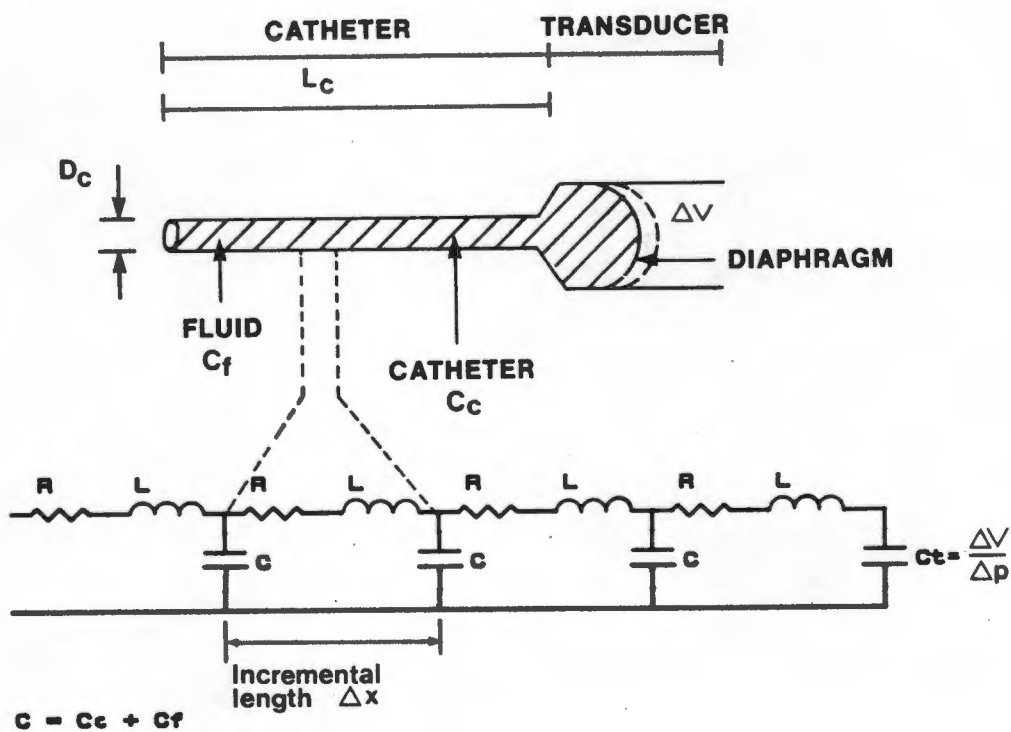
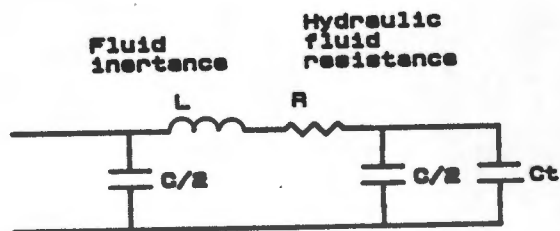


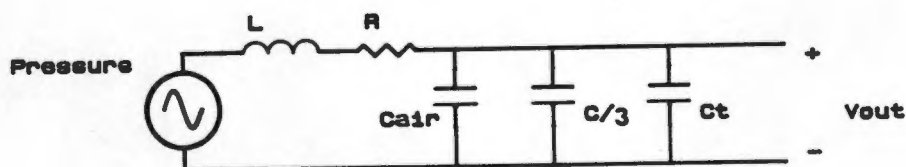
Figure 2.3(a)

The electrical analogue model described by Andersen and Bergsten (1982). The pressure chamber has a compliance C_t . The compliance of the catheter is C_c and that of the fluid is given by C_f . The lumen diameter of the catheter is given by D_c and its length by L_c . R is the resistance per unit length related to the viscosity of the fluid and L is the inductance per unit length representing the radial inertia of the fluid.

In the simplified circuit, the capacitor on the left in figure 2.3(b) shunts the circuit's input voltage without any influence on the input voltage (pressure). Furthermore, the distribution of compliances within the catheter resulted in the compliance of the pressure chamber being reduced from $C/2$ to $C/3$ (figure 2.3c).



b)



c)

Figure 2.3(b and c)

C is the combined catheter and fluid compliance. The fluid inertia is represented by L and the flow resistance due to viscosity is represented by R . C_t is the compliance of the pressure chamber.

Andersen and Bergsten stated that this model was a simple second-order system with one degree of freedom and found the resonant frequency to be given by:

$$f_p = \frac{1}{2 \cdot L \cdot (C_t + C/3)^{\frac{1}{2}}} \quad (2.2)$$

and the damping factor by,

$$\beta = \frac{(C_t + CR/3)}{(2 \cdot (L \cdot (C_t + C/3))^{1/2})^{1/2}} \quad (2.3)$$

A further improvement of the model was to include the compliance of air bubbles trapped in the system. This is shown by the capacitor (C_{air}) in figure 2.3(c).

The above equations are given in terms of fluid-analogue parameters in Appendix B1.1.2.

Another distributed model of the catheter-manometer is shown in figure 2.4. This circuit was first described by Hansen and Wardburg in 1950 and improved by Yeomanson and Evans (1983). In this model the catheter forms part of the coupling between the pressure chamber, impedance Z_t , and the vascular system (or any other pressure source of relatively large compliance) that is modelled as a zero impedance voltage source, V_s . At both ends of the pressure tubing are Luer fittings of small impedances Z_{fs} and Z_{ft} , one of which is usually connected to a cannula, impedance Z_n .

The pressure recorded by the transducer is represented in the electrical analogue by the voltage (V_{tc}) across the transducer impedance (due to compliance) Z_{tc} , which is given by the simple potential division of V_r (the potential across the transducer and the Luer fitting):

$$V_{tc} = \frac{V_s'}{\cosh \Phi l + (Z_o/Z_r) \sinh \Phi l} \cdot \frac{Z_{tc}}{Z_{tc} + Z_{td} + Z_{ft}} \quad (2.4)$$

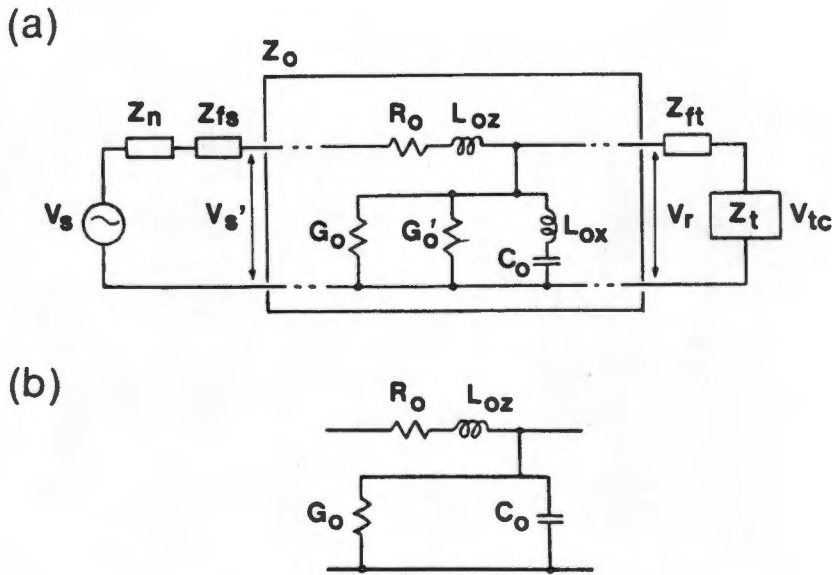


Figure 2.4

Electrical analogue of the catheter-manometer system, R_0 is the resistance per unit length due to the fluid viscosity, L_{0z} is the inductance per unit length corresponding to the axial inertia of the mass of the liquid, C_0 the capacitance per unit length representing the compliance of the catheter walls, G_0 is the conductance per unit length to account for the hysteresis losses in the catheter wall and G_0' is the conductance per unit length due to the inelastic behaviour of the fluid. L_{0x} represents the inductance per unit length representing the radial inertia of the fluid and the catheter wall. Z_0 in (a) may be approximated by the circuit shown in (b) (Yeomanson and Evans, 1983).

where Z_0 is the characteristic impedance of the catheter, Z_r is the sum of the impedances of the transducer and that of the catheter Luer fittings, l the length of the catheter and Φ is the propagation constant of the catheter (The formulae are derived in in Appendix B1.1.3).

Furthermore, the impedance of the transducer is written as

$$Z_t = Z_{tc} + Z_{td} \quad (2.5)$$

where Z_{tc} is the compliant impedance of the transducer diaphragm and Z_{td} is that of the membrane of the pressure dome.

The frequency response is given by the magnitude and phase plots of $V_{tc}/V_{s'}$:

$$\frac{V_{tc}}{V_{s'}} = \frac{1}{\cosh \Phi l + (Z_o/Z_r)\sinh \Phi l} \cdot \frac{Z_{tc}}{Z_{tc} + Z_{td} + Z_{ft}} \quad (2.6)$$

2.2.2 Lumped parameter models

In the mechanical analogue model of the catheter-manometer, the system is regarded as analogous to a simple second-order system (Fry, 1960; McDonald, 1974; Bruner, 1978; Bergel, 1972) consisting of a mass (the effective mass of the fluid in the catheter) suspended from a spring (the pressure chamber) which is viscously damped by a dash pot (the viscous resistance of the fluid in the catheter lumen) as shown in figure 2.5.

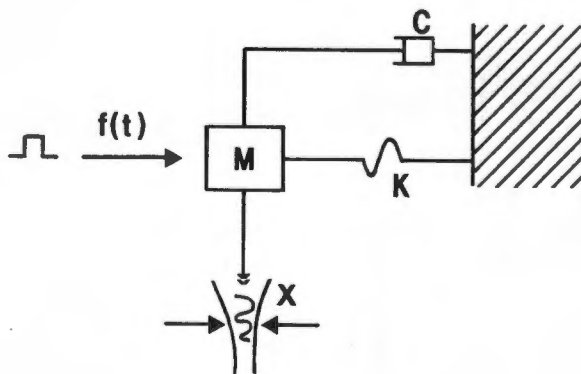


Figure 2.5

The mechanical analogue model where the mass M , is restrained by a spring K and a viscous dashpot, C . x is the distance for which the mass is displaced when a force $f(t)$ is applied.

The behaviour of this system may be predicted by studying the forces acting on the fluid mass in figure 2.5. For this system the sum of the forces acting at any point in the system must be zero which implies that the applied force will be opposed by a force that has three components, one related to acceleration, one to friction (velocity) and one to the spring (displacement).

Therefore:

$$\text{External force} = \text{Acceleration force} + \text{Friction force} + \text{Spring force}$$

or

$$f(t) = M \frac{d^2x}{dt^2} + C \frac{dx}{dt} + kx \quad (2.7)$$

where M is the mass of the system, C the friction coefficient and K is the spring constant.

The pressure that would be recorded at the pressure chamber is proportional to x. In evaluating catheter-manometer systems it is important to establish how the variation of x with time follows the variation of the external force f(t) with time. Taking equation 2.7 and setting f(t) = A cos wt where A is the amplitude of the pressure and w is the angular frequency in radians/second, x can be solved for and is given in equation 2.8 (Fry, 1960).

F and ϕ represent arbitrary constants determined from the initial conditions of the catheter-manometer model and the applied driving forces.

$$x = \left[F e^{-Ct/2M} \cos \left[\left[\frac{K}{M} - \frac{C^2}{4M^2} \right]^{\frac{1}{2}} t - \phi \right] \right] + \left[\frac{A \cos (wt - \phi)}{(K - Mw^2)^2 + (wC)^2} \right]$$

transient
response

steady state
response

(2.8)

The two major bracketed terms represent the transient response and the steady state response, respectively. The transient response is the response of the system to a change in the steady

state conditions, such as a sudden increase in pressure, amplitude or frequency of the driving force. The steady state represents the response of the system when the driving force remains unchanged.

In Appendix B1.2 this system is dealt with in detail.

Bruner (1978) also described a lumped parameter model for the catheter-manometer system and identified resonant frequency and the damping factor as the parameters that characterised the frequency response. The damping factor β was given as:

$$\beta = \frac{4v}{r^3} \cdot (1/\pi E)^{\frac{1}{2}} \quad (2.9)$$

while the resonant frequency was

$$f_p = \frac{1}{2 \cdot \pi} \cdot \left[\frac{\pi \cdot r^2 \cdot E}{p \cdot l} \right]^{\frac{1}{2}} \quad (2.10)$$

where

- v = fluid viscosity
- r = radius of catheter
- E = stiffness of the catheter
- p = fluid density
- l = length of catheter

McDonald (1974) described a mechanical analogue model similar to that of Fry (1960). Other researchers (Krovetz et al, 1974 and Gardner, 1981) only referred to this catheter-manometer model.

Taylor et al (1986) developed a method by which they measured electrical analogue values for fluid resistance (resistance), inertance (inductance) and compliance (capacitance). These electrical values were used to formulate a lumped parameter model of the catheter-manometer system which is shown in figure 2.6(a).

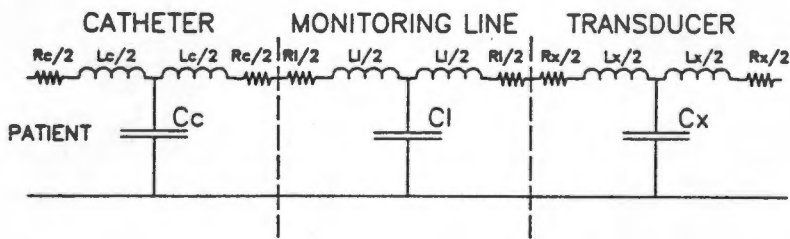


Figure 2.6(a)

Analogous circuit for a catheter-manometer system (Taylor, 1986). Subscript c refers to the catheter, l to the pressure tubing and x to the transducer (Taylor et al, 1986).

In order to appropriately designate the resistive and inductive terms, the derived values were evenly distributed on both sides of the lumped capacitance for each section (cannula, pressure tubing, and transducer) of the model. The circuit was simplified through the combination of series elements and is given in figure 2.6(b).

In this model the damped natural frequency (f_n) and the damping factor (β) are represented in terms of the inductance and capacitance. The damped natural frequency is given by

$$f_n = 1/(2\pi\sqrt{LC}) \quad (2.11)$$

while the damping factor is given by

$$\beta^2 = (1 - (1 - (1/M_p)^2)^{1/2})/2 \quad (2.12)$$

where M_p is the gain at resonance (Equation 2.12 is derived in Appendix B, section 2.1).

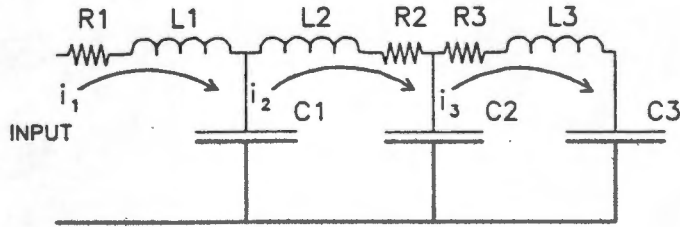


Figure 2.6(b)

Simplified circuit of that shown in figure 2.6(a). The electrical current in the circuit is represented by i .

2.3 Catheter-manometer system characterisation

The previous section presented models that have attempted to characterise catheter-manometer systems in terms of various parameters. Not all of these parameters, and in particular those related to fluid analogue models, are easily measured in practice. Latimer and Latimer (1969) devised a method for measurement of the mechanical hysteresis loss of plastic materials using derived parameters and were able to calculate the characteristic impedance of catheters and transducers and thus their frequency response. The reader is referred to the article of Latimer and Latimer (1969) for a detailed discussion as both their model and the measurement technique is beyond the scope of this thesis. The damping factor and the amplitude response of a system however, can be measured with ease using the appropriate technique and the assumption that the catheter-manometer is a second-order system.

In the following section a brief description and review of catheter-manometer characterisation techniques will be given.

Two methods of catheter-manometer system evaluation have been identified: (1) the transient method and (2) the steady state method.

2.3.1 Transient method of catheter-manometer characterisation

Fry (1960), Crul (1965), McDonald (1974), Krovetz et al (1974), Hök (1976), Boonzaier (1978) and Fourie et al (1987) have described the transient method of catheter-manometer characterisation in detail. In this method, the parameters required to describe the frequency response of the catheter-manometer system are: the damping factor β and the undamped natural frequency, w_n . These parameters are calculated from the system response to a stepwise change (as shown in figure 2.8) at the input of the catheter-manometer system.

The apparatus used was described by the above mentioned researchers. A typical system used is shown in figure 2.7. A latex rubber membrane is attached with a rubber O-ring seal to a pressure chamber which is half-filled with debubbled saline. The chamber is then pressurised by inflating the chamber using a sphygmomanometer. The membrane is then ruptured and this results in a sharp step change in pressure at the input to the catheter under test. The response of the catheter under test is recorded and is shown in figure 2.8.

The damping factor β is then calculated using (Fry , 1960):

$$\beta = \left[\frac{(\ln x_2/x_1)^2}{\pi^2 + (\ln x_2/x_1)^2} \right]^{\frac{1}{2}} \quad (2.13)$$

where $(\ln x_2/x_1)$ is the natural logarithm of the ratio of two successive excursions in the transient response as shown in figure 2.8.

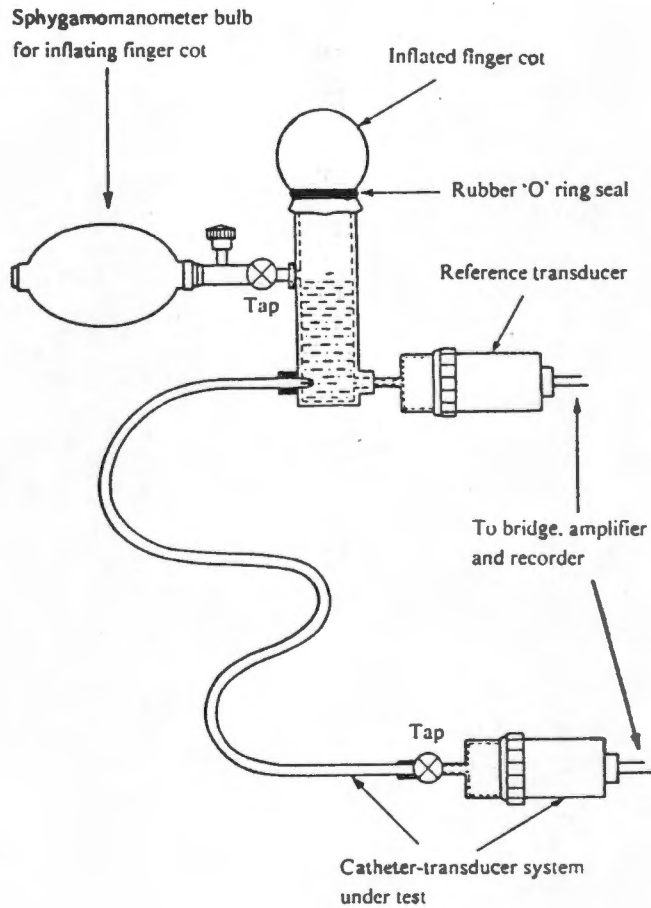


Figure 2.7

The balloon-popping chamber used to produce step changes in pressure. The balloon is burst by a flame or hot wire (Boonzaier, 1978).

Knowing β , the undamped natural frequency w_n may be derived from:

$$w_n = w_d / (1 - \beta^2)^{1/2} \quad (2.14)$$

where w_d is the damped natural frequency and represents the frequency of the oscillations of the overshoot (which is derived from the wavelength of the oscillation). This parameter is measured in radians per second and thus w_n will have the same units.

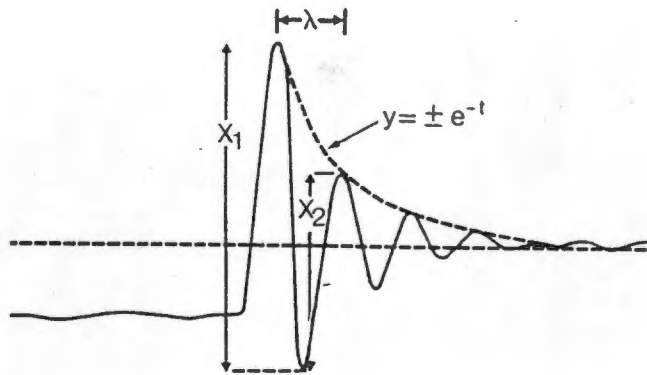


Figure 2.8

The transient response of a catheter-manometer system to a step change in pressure. X_1 and X_2 is are the amplitudes of any two successive excursions (Fourie et al, 1987).

2.3.2 Steady state method of catheter-manometer characterisation

A typical system used for this steady state method of testing is shown in figure 2.9.

The steady state method consists of measuring the response of the catheter-manometer system or of individual components of the system (cannula, pressure tubing, and combinations thereof) to an applied sinusoidal pressure signal at frequencies extending from zero to a frequency at which the catheter-manometer response has decreased to an arbitrary value. This directly represents the amplitude response of the system, as shown in figure 2.10.

The damping ratio may be obtained using the following formula (Fry 1960):

$$\beta = ((1 - w_p^2 / w_n^2) / 2)^{1/2} \quad (2.15)$$

As before, β is the damping ratio, w_p is the resonant frequency measured from the amplitude response curve, and w_n is the undamped natural frequency.

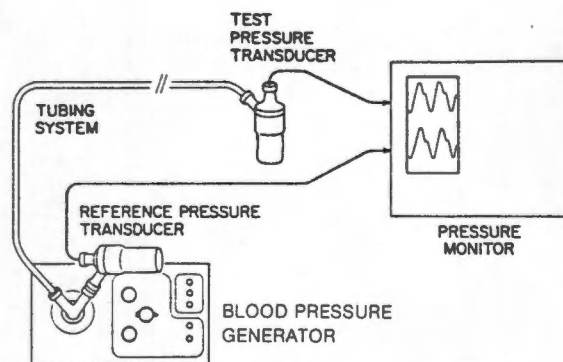


Figure 2.9

A typical system used for the steady state method of catheter-manometer frequency response testing (Shinozaki et al, 1980).

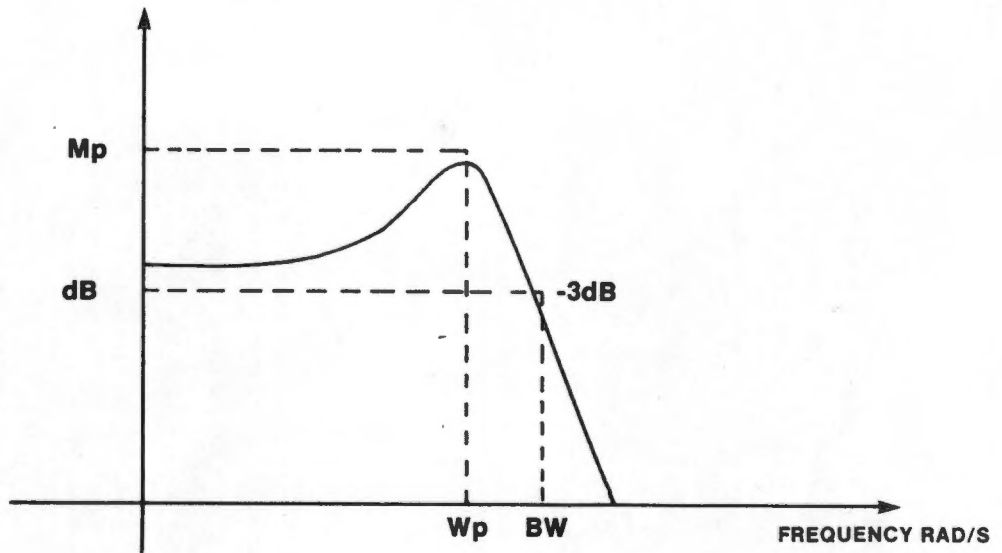


Figure 2.10

Amplitude response obtained by the steady state method. M_p represents the gain at resonance ω_p and the bandwidth is shown by BW .

2.4 Frequency response evaluation

2.4.1 Catheter-manometer system evaluation

Evaluations of catheter-manometer systems have been described by a number of researchers:

Fourie et al (1987) used the transient method to determine the frequency response of 50 cm long pressure tubing (lumen diameter 1.5 mm). The undamped natural frequency for the pressure tubing connected to a Statham (P23AA) transducer was found to be 23.0 Hz ($\beta = 0.16$). Furthermore, the addition of 0.05 ml air into the catheter-manometer system resulted in a decrease of the undamped natural frequency to a value of 5.1 Hz ($\beta = 0.20$). McDonald (1974) and Falsetti et al (1974) have also shown that the damped natural frequency of a catheter-manometer decreases if air is trapped within the system.

Shinozaki et al (1980) also evaluated the frequency response of various combinations of pressure tubing, cannula and pressure domes/transducers using the steady state method. The range of the resonant frequencies measured for 90 cm long pressure tubing of different makes was from 39 to 54 Hz while the resonant frequency for cannulae ranged between 81 Hz and 265 Hz. Furthermore, peak systolic and end diastolic pressure values measured were found to be very similar (the weighted sum of percentage difference was less than 10) to the applied pressure values. This observation was in conflict with that of Miller and Zbilut (1983), who established that measured pressures (with the applied pressure waveform unchanged) differed for various lengths and makes of pressure tubing. In particular, they found that recorded peak systolic pressure was higher for all tubing tested

(by up to 48 mmHg, mean = 15.9 mmHg) when compared to the applied peak systolic pressure of 150 mmHg.

In another study, Shapiro and Krovetz (1970) evaluated catheter-manometer systems by the direct method. They found that tubing length was inversely related to the undamped natural frequency. This ranged from 65.3 Hz for pressure tubing of 10 cm in length to 18.1 Hz for tubing of 100 cm in length (lumen diameter 0.76 mm). This concurred with the study of Shinozaki et al (1980). Furthermore, it was found that the frequency response was directly related to tubing lumen diameter and that tubing of similar dimensions (length - 10 cm and lumen diameter - 1.02 mm) constructed from stiff material had a higher damped natural frequency ($w_d = 80$ Hz) than that constructed from more compliant material ($w_d = 22$ Hz). Angle attachments and the effect of coiled tubing was investigated and appeared to decrease the frequency response of the catheter-manometer systems.

Yeomanson and Evans (1983) however, found that twisting the pressure tubing (Portex 200/495 - 150 cm) by an application of a torsional force two or three times around the central axis increased the resonant frequency response from 45 Hz to 49 Hz. This was attributed to a decrease in the compliance of the tube.. In this study, the resonant frequencies for catheter-manometer systems (combinations of 16 to 25 gauge cannulae connected to 150 cm pressure tubing) ranged from 25 Hz to 45 Hz. The direct method of catheter-manometer evaluation was also used in the classic study by Gardner (1981). Resonant frequency ranged from 15 Hz ($\beta = 0.72$) for an 18 gauge cannula (CAP Sorenson) connected to a 75 cm pressure tube to 48 Hz ($\beta = 0.14$) for a Vinca 18 gauge cannula connected to 75 cm of pressure tubing.

In a study by Ladin et al (1983), the frequency response was measured for a catheter-manometer system (4 feet of pressure tubing) by the transient method described by Gardner. The resonant frequency of the catheter-manometer systems was in the range of 14-18 Hz and the damped natural frequency was in the range of 15-19 Hz. The damping coefficients were in the range of 0.15-0.3. Furthermore, frequency domain analysis of blood pressure signals recorded from the catheter-manometer system evaluated by Ladin et al (1983) revealed that systolic spikes did not originate in the pressure tubing or in the amplifier system.

In summary, the results are listed in tables 2.2 and 2.3.

Cannula	Pressure tubing	Yeomanson	Gardner
CAP 18 G	+ (600)	-	15* (0.72)
Vinca 18 G	PE (600)	-	48* (0.14)
Vinca 18 G	PVC (600)	-	38* (0.10)
Medicut 16 G	Portex (1500)	42	-
Medicut 18 G	Portex (1500)	40	-
Gillette 19G	Portex (1500)	35	-
Gillette 21G	Portex (1500)	30	-
Gillette 23G	Portex (1500)	25	-
Gillette 25G	Portex (1500)	22	-
Vinca 18 G	+ (2000)	-	16* (0.20)
Vinca 18 G	PVC (2000)	-	45* (0.13)

Table 2.2

Resonant frequency (Hz) for catheter-manometer systems. The length of the pressure tubing is given in mm (in brackets). Other values listed in brackets are the damping coefficients. (refers to damped natural frequency, + information not supplied).*

Type (length)	Yeomanson	Fourie	Gardner	Shinozaki
Vygon (500)	-	23* (0.16)	-	-
Cobe (750)	-	-	-	46
Vygon (750)	77	-	-	-
Vygon (1000)	58	-	-	-
Vygon (1500)	42	-	-	-
Cobe (1500)	-	-	-	32
Portex (1500)	45	-	-	-
- (1500)	-	-	24* (0.28)	-
Norton (1800)	25	-	-	-
Cobe (2000)	-	-	-	23
Vygon (2000)	32	-	-	-

Table 2.3

Resonant frequency (Hz) for pressure tubing. The length is given in mm. Other values listed in brackets are the damping coefficients. (refers to damped natural frequency).*

2.4.2 Swan Ganz catheter response evaluation

Only a few researchers and product suppliers have investigated the frequency response characteristics of the cardiac catheter.

One of these, Fourie et al (1987), found that the undamped natural frequency of the 7F Swan Ganz catheter was 5.7 Hz ($\beta = 0.36$) and that of the 5F Swan Ganz catheter was only 3.9 Hz ($\beta = 0.5$) and suggested that the 5F Swan Ganz catheter was not suited for clinical or laboratory use because of its low undamped natural frequency.

Shinozaki et al (1980) however, found that the resonant frequency of 7F Swan Ganz catheters was in the range of 12 Hz to 25 Hz. In this study no reference was made to the damping factor.

In the study of Gardner (1981) the resonant frequencies ranged from 9.5 Hz ($\beta = 0.32$) for a 5F Swan Ganz catheter to 15.5 Hz ($\beta = 0.20$) for a 7F Swan Ganz catheter.

Falsetti et al (1974) measured the frequency response of four catheters used to measure left ventricular pressures. The steady state method of evaluation was used and the pressure chamber had a constant amplitude response for a bandwidth of 125 Hz. The damped natural frequencies and damping ratios measured are given in table 2.4. Furthermore, Falsetti et al (1974) stated that an increase in temperature did not significantly change the frequency response of the catheters; however, the effect of the transmural pressures (mean external pressures applied to the catheter) of 150 mmHg decreased the damping ratio. No apparent relationship between damped natural frequency and damping ratio was found. Inadequate damped natural frequency caused an error (4 to 30 percent, no mean value given) in the measured value of end diastolic pressure while the percentage error in peak dp/dt caused by inadequate bandwidth ($f_n = 10$ Hz, $\beta = 0.1$) was 30 percent.

Catheter (size)	f_d (Hz)		β	
	mean	SD	mean	SD
Gensini (7F)	59.8	13.3	0.109	0.03
Transeptal (8.4F)	66.7	7.5	0.158	0.03
Pigtail (8.4F)	50.8	8.7	0.137	0.03
Femoral (8F)	45.1	11.0	0.216	0.15

Table 2.4

Catheters and frequency characteristics - damped natural frequency and damping factor (Falsetti et al, 1974).

Damenstein et al (1976), used a pressure generator based on a modified version of Stegall's (1967) design. In vitro catheter evaluations consisted of establishing the damping factor and damped natural frequency of 0.8 m long Lehman and Pediatric NIH cardiac catheters (4F, 5F, 6F and 7F). The mean pressure was varied between 20 mmHg and 120 mmHg (in steps of 20 mmHg), while the sinusoidal pressure variation was 16 mmHg peak-to-peak. Results indicated that the mean static pressure did not influence the frequency response of the catheters. Damped natural frequency, damping factor and the frequency ranges for which the amplitude response was constant are presented in table 2.5.

Catheter type	f_d (Hz)	β	Useful frequency range (Hz)
4F	14	0.25	d.c. - 5
4F	24	0.23	d.c. - 8
5F	13	0.22	d.c. - 4
5F	16	0.20	d.c. - 5
6F	40	0.15	d.c. - 15
6F	36	0.13	d.c. - 15
7F	54	<0.10	d.c. - 35
7F	44	<0.10	d.c. - 20

Table 2.5

Damped natural frequency, damping factor and useful frequency range of cardiac catheters measured by Damenstein et al (1976).

2.4.3 Compensation techniques

From the foregoing discussion it is apparent that insufficient bandwidth (low undamped natural frequency) and excessively damped or under-damped catheter-manometer systems negatively affect the blood pressure signal fidelity. Although it is not the aim of this thesis to discuss the compensation techniques used in alleviating this problem, a few compensation techniques will be described below:

Boonzaier (1978) used a digital filtering technique for a real-time correction of resonance artifact in catheter systems. He established that derived dynamic parameters, e.g. dp/dt could thus be obtained from the original systems which would not have been possible without the filtering technique.

Similarly, Damenstein et al (1976) designed and implemented an electronic compensator so that the bandwidth and damping factors of cardiac catheters were increased. A feature of this equipment was that it could be tuned to individual catheters whereas the filtering technique of Boonzaier (1978) was fixed for a certain make and tuning required a reference intravascular signal.

Krovetz et al (1974) and Patel et al (1965) found that correcting frequency dependent phase and amplitude distortions in blood pressure signals by using harmonic analysis was not successful and that overcorrection occurred for frequencies higher than resonance. A further problem in harmonic analysis/compensation was that the correction formula used in vivo was established in vitro and the probable discrepancy between the actual in vivo response and in vitro response limited the effectiveness of this method.

Bernouw et al (1983) designed a compensation network that continuously optimised the dynamic response of catheter-manometer systems, in situ. This was achieved by determining the resonant frequency of the catheter-manometer system in situ and then compensating accordingly. The advantage of this system was that it compensated the blood pressure signal automatically irrespective of system parameters; however, it must be assumed for this system that the resonant frequency of the catheter-manometer system did not change when connected to the patient.

Summary

In many of the articles reviewed, little mention is made of the number and reproducibility of the measurements and hence of the accuracy of the findings. In particular, there are large deviations in the values of the system parameters given.

Only a few researchers have specified the importance of both resonant frequency and damping factor in the evaluation of second order catheter-manometer systems. These factors have resulted in an uncertainty on the part of the users of catheter-manometer systems, when using published material as a guide.

In the next chapters the importance and method of accurate frequency response evaluation of catheter-manometer systems will be investigated and discussed, firstly in terms of possible measurement errors in the assessment technique and secondly, in the application of test results.

CHAPTER THREE

BASIS FOR PROPOSED INVESTIGATION

3.1 Introduction

In the previous chapter a review of catheter-manometer system modelling and the characterisation and measurement techniques of system parameters was presented. The models have largely been of a mathematical nature (Fry, 1960; McDonald, 1974). The few quantitative studies of system parameters (Taylor et al, 1986); Latimer and Latimer 1969 and Andersen and Bergsten, 1982) have not validated the theoretical models, which have certain limitations (discussed in section 3.2). The model of Yeomanson and Evans (1983) was the exception as they showed that their model agreed with the frequency response measurements obtained. Furthermore, evaluation techniques currently used have certain limitations as the method of measuring the frequency response directly affects the catheter-manometer system parameters and therefore its response. Examining the literature review (section 2.2) and the requirements of catheter-manometer systems for accurate blood pressure measurement (Appendix A4), it becomes evident that the response requirements for accurate pressure measurement are not met by all the catheter-manometer systems discussed in the literature review. In section 3.4 a critique will be presented on the above.

3.2 Limitations of catheter-manometer models

In the catheter-manometer models described in chapter 2 various factors and parameters that influence the frequency response of the catheter-manometer systems have either not been investigated and/or not been included in the models. Some of these factors influence all models (discussed in section 3.2.1) while other factors relate specifically to either the distributed model (section 3.2.2) or the lumped parameter model (section 3.2.3).

3.2.1 General limitations

(i) Catheter compliance and fluid temperature

One limitation of both lumped and distributed parameter models presented was that none attempted to quantify the influence of either catheter or fluid temperature. Although, Yeomanson and Evans (1983); Andersen and Bergsten (1982) and Hansen and Wardburg (1950) found that catheters became more compliant with higher temperatures which negatively influenced the frequency response, they did not include this aspect in their models. The change in frequency response is explained by the fact that higher compliance increased the damping factor which resulted in a lower resonant frequency and thus a lower bandwidth. With the rise in temperature it was also found that air bubbles diffused out of the fluid and caused a sharp increase in compliance: however, no values are given as to which extent temperature influences the frequency response. Falsetti et al (1974) did not encounter this phenomenon in his research.

Another restriction of the model was that the lumen of catheters/cannulae was assumed to be symmetrical. It was however found in this thesis that most pressure tubing and cannulae tested had a lumen that was non-concentric. This is shown in figure 3.1(a) and 3.1(b). It is expected that the non-symmetrical lumen will effect the accuracy of the mass flow inertance and distributed coefficients (as they are determined by the lumen radius) of the models.

Measurement equipment used for the detection and measurement of such changes in lumen diameter, without the destruction of the catheter-manometer, was not available and thus tests to determine the effect of non-symmetrical/symmetrical lumen on the frequency response could not be performed. However it should be noted that the wall thickness of pressure tubing with non-concentric lumen is not constant and that the compliance thus varies non-linearly with catheter length and frequency.

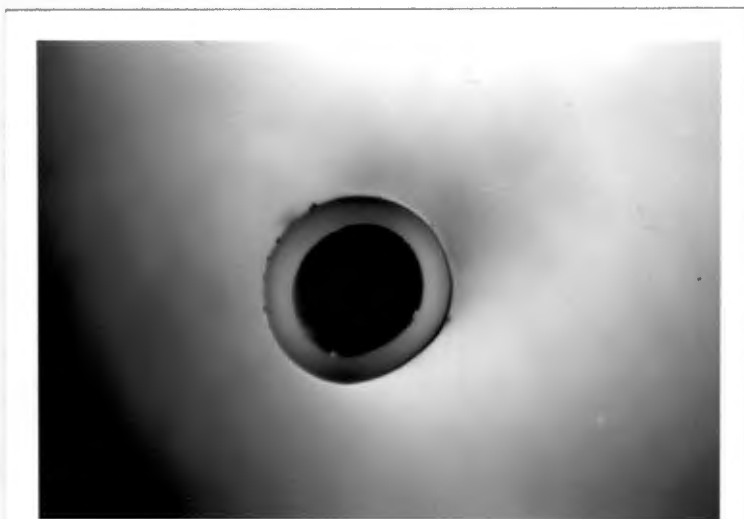


Figure 3.1(a)

Photograph showing the non-uniform radius of a pressure tube lumen.

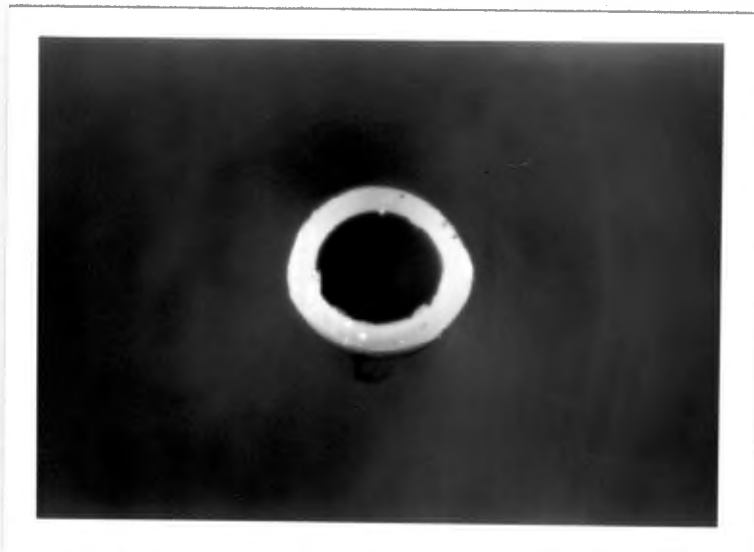


Figure 3.1(b)

Photograph showing a non-concentric lumen of a cannula.

(ii) Pressure chamber compliance

In the distributed catheter-manometer models of Fry (1960); Yeomanson and Evans (1983) and Andersen and Bergsten (1982) the pressure chamber compliance was assumed to be lumped and thus the pressure chamber compliance could be approximated by the compliance of the transducer diaphragm (calculated by the elastic modulus and the physical dimensions of the transducer diaphragm). However, Fox et al (1978) found that the frequency response of numerous pressure chambers differed when measured with similar transducers, indicating that the pressure chamber compliance was not only determined by the compliance of the transducer diaphragm.

The assumptions mentioned above may thus be inadequate as the transducer diaphragm compliance does not include the compliance of the transducer dome and the Luer-fitting taps. Furthermore, it is assumed that the diaphragm of the transducer is optimally clamped to the membrane of the pressure dome which in practice is very difficult to achieve.

The above mentioned factors will influence the total compliance of the pressure chamber and indeed Yeomanson and Evans (1983) and Latimer and Latimer (1969) found that the total compliance of the pressure chamber was 2 to 3 times higher than the compliance calculated by using the compliance of the transducer diaphragm alone. As the total compliance of the catheter-manometer system (the sum of pressure chamber and catheter compliance) is a limiting factor on overall frequency response of the catheter-manometer system, the accuracy of the model is limited by using transducer diaphragm compliance only.

It is however important to note that the calculation of the individual compliances of the transducer membrane, Luer fittings, pressure dome and fluid compliance are too complex and thus total pressure chamber compliance must thus be measured. This measurement is difficult and only Latimer and Latimer (1969) and Yeomanson and Evans (1983) have devised methods by which the compliance of their pressure chambers was measured directly. The compliance values supplied by manufacturers for pressure chambers have been questioned by Yeomanson and Evans (1983) and thus models using manufacturers' values for compliances may be incorrect.

3.2.2 Limitations of the distributed parameter model

In the distributed model, transmission line errors can arise both from the intrinsic transmission properties of the system which are determined by the parameters Z_0 and Z_T (section 2.2.1), as well as from the noise which is related to extrinsic motions imposed on the catheter-manometer system and is indirectly related to the above mentioned parameters. These extrinsic and intrinsic pressure recording errors, which have not been included in the distributed parameter model are discussed below;

(i) Multiple sites of reflections

The amplitude and the phase of the reflection that will occur in the distributed parameter model are given by the reflection coefficient, B , defined as:

$$B = \frac{Z_T - Z_0}{Z_T + Z_0} \quad (3.1)$$

where Z_0 (characteristic impedance of the catheter) and Z_T (terminal impedance of the pressure chamber) are complex numbers. If the terminal impedance is equal to the characteristic impedance, $B = 0$ and no reflections would occur. This is the ideal situation for an accurate pressure transmitting system; however, it is clear that Z_0 and Z_T are frequency dependent and thus it is impossible in practice to match the impedances of the pressure chamber and that of the pressure dome for all frequencies.

Although reflections have been included in the distributed model, multiple wave reflections from points of transition where the impedance of the catheter-manometer system changes (for example at stopcocks) have not been included. Therefore, in a distributed parameter model, reflections will only occur at the catheter tip and the entrance to the pressure chamber.

(ii) Unequal transmission times of frequency components

Phase shift of the various frequency components during the transmission down the catheter-manometer line is a further source of wave distortion. For accurate wave transmission it is necessary that each frequency component of the transmitted wave travels at the same velocity. If, however, one frequency component travels faster than the other, the shape of the waveform will progressively be distorted.

For the distributed parameter models the assumption is made that all frequency components travel at the same velocity.

(iii) Frequency dependence of fluid resistance and inertance

The electrical analogue model described by Yeomanson and Evans (1983) was a distributed parameter model. This model has a number of shortcomings that influence the accuracy of the model.

The impedance of a fluid filled tube as described by equation B1.24 is analogous to electrical impedance which has a real and an imaginary component: $Z = R + j\omega L$, where R is the fluid resistance and L the inductance or the reactance of the fluid. As the angular frequency ω tends to zero the resistive term reduces

to the Poiseuille fluid resistance and the inductance becomes simply the mass of fluid per unit area. Yeomanson and Evans (1983) however showed that both the resistance and inertance of a fluid were frequency dependent and could thus not be approximated by a real and imaginary component.

Further it was stated that fluid viscosity and, to a lesser extent, fluid density are temperature and frequency dependent.

A further limitation of the model of Yeomanson and Evans (1983) was that compliance values were determined with zero mean pressure in the catheter and pressure chamber and thus were higher by 2 percent than those determined at a mean pressure of 100 mmHg. This observation was explained by the fact that compliance of the catheter-manometer system decreased when the fluid pressure in the catheter-manometer system was increased. These factors were not included in the model.

3.2.3 Limitations of the lumped parameter model

(i) Reflections in the catheter-manometer

Similar to the distributed parameter model, multiple wave reflections have not been included in the lumped parameter model. Furthermore, the resonant frequency is determined entirely by fluid and catheter-manometer system parameters (seen in equation 2.10) and not by the interaction of standing waves and frequency dependent catheter-manometer system parameters.

(ii) Unequal attenuation of wave transmission.

The transmitted wave in the catheter-manometer system is attenuated exponentially with the distance travelled. The rate of this exponential attenuation is determined by equation B2.2 (Fry, 1960). Referring again to the real part of equation B2.2 it can be seen that the attenuation is a function of the physical characteristics of the catheter, the contained fluid and the frequency. This relationship between the physical characteristics of the catheter and those of the fluid are not accounted for in the lumped parameter model.

3.2.4 Summary

From the discussion of the modelling techniques of catheter-manometer system it is apparent that certain assumptions (such as lumped parameters, fixed catheter compliance and frequency independence) limit the accuracy of models.

Taylor et al (1986) indicated, that the lumped parameter model used to describe the mechanical analogue was not accurate in assessing the effect of catheter properties (materials and dimensions) on its frequency response.

3.3 Catheter-manometer characterisation techniques

Two characterisation techniques of catheter-manometer systems were described in section 2.3.

3.3.1 The transient method

The transient method was used by a number of workers and is well defined (section 2.3.1); however, the accuracy of this method depends not only on the measurement itself but also on the frequency response of the paper recorder which displays the oscillatory response of a system to a step input. In chapter 4 the test system requirements are given and thus it can be seen that the paper recorder should ideally have a bandwidth greater than 200 Hz. Although none of the researchers using the transient method have indicated the response of their equipment, it was established (by applying a step response to the input of the recorder and measuring the output response) that the bandwidth of some strip chart recorders were lower than 30 Hz. Gardner (1981) stated that the transient method was superior to the steady state method as it can be used to test the entire catheter-manometer system in the clinical setting while connected to the patient. The reproducibility of results was limited and Gardner suggested that the test should be repeated several times to improve accuracy of the measurement.

A limitation of the transient method used by Gardner was that the damping factor and damped natural frequency obtained, possibly were not that of the catheter-manometer system alone, but of the combination of catheter-manometer system and patient. No

indication was given whether the catheter-manometer system was isolated (disconnected by closing a stopcock) from the patient which would imply that the frequency response obtained for the catheter-manometer system would exclude that of the cannula and thus be higher.

A further limitation of this transient method is that the position of the flush device (and thus the source for the step input) within the catheter-manometer system will influence the frequency response measurement as shown in figure 3.2(a) and

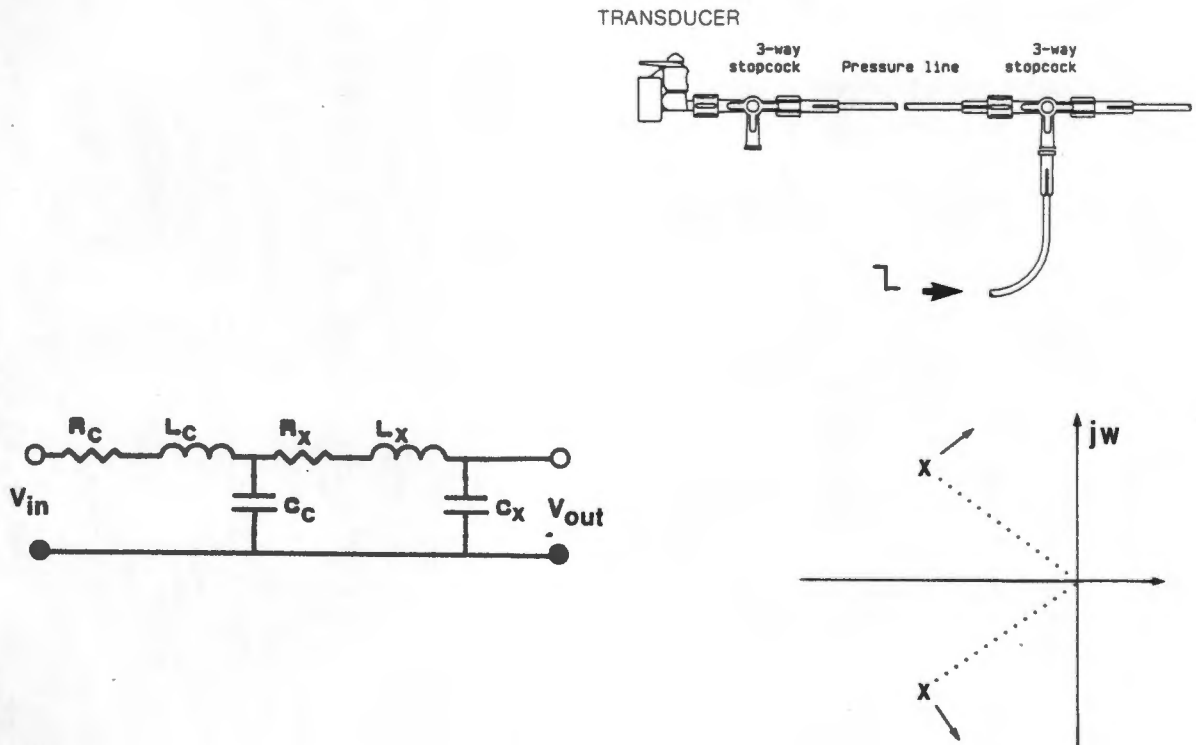


Figure 3.2(a)

Second-order catheter-manometer system and the equivalent electrical model. Subscript x represents the transducer and c the catheter. The poles (X) and zeros (O) are displayed in the s-plane. The arrows indicate the general direction the poles will move for $w > 0$.

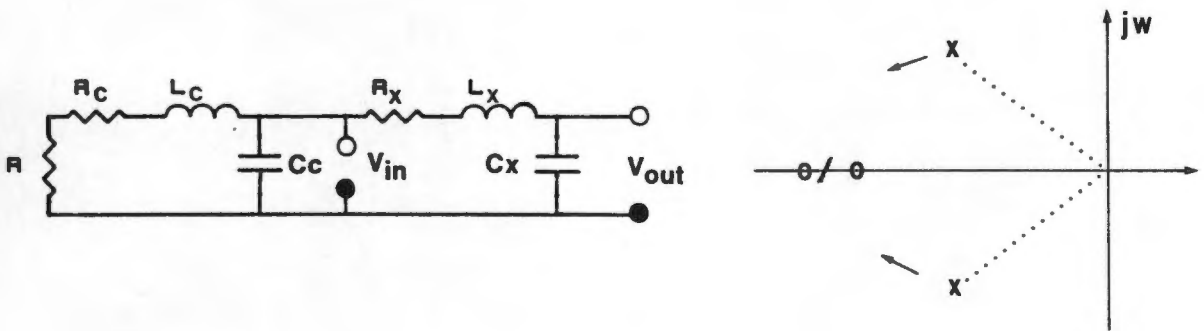
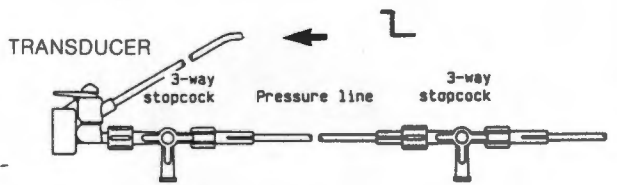


Figure 3.2(b)

Second-order catheter-manometer system and the equivalent electrical model. Subscript x represents the transducer and c the catheter. The poles (X) and zeros (O) are displayed in the s -plane. The arrows indicate the general direction the poles will move for $w > 0$.

3.2(b). In both cases, the actual damped natural frequency and the damping factor of the catheter-manometer system are the same since the catheter-manometer system was not changed (the poles of both systems are the same); however, in figure 3.2(a) the positions of the zeroes are different from those in figure 3.2(b) as they are determined by the relationship of the input signal site to output signal site. The difference in the positions of

the zeroes have the result that the measured damping factor and damped natural frequency are unlike. Fourie et al (1987); Ladin et al (1983) and Gardner (1981) have not mentioned or investigated this aspect.

Shapiro and Krovetz (1970) concluded that the transient method was not accurate enough to detect small changes in the damped natural frequency. They suggested the steady state method.

3.3.2 The steady state method

The major limitation of the steady state method is that the frequency response tests cannot be performed in situ and thus are limited to the in vitro situation.

As described in section 2.4 many researchers have used the steady state method; however, certain important parameters that affect the overall accuracy of the tests were not investigated and/or mentioned.

Miller and Zbilut (1983), Gardner (1981) and Shinozaki et al (1980) used the BIO-TEK (Model 601, Bio-Tek Instruments, Burlington, Vermont, USA) blood pressure system analyser as the pressure source. None of the above researchers measured and/or stated the bandwidth of this analyser; however, in this thesis (see Appendix H2), the BIO-TEK equipment was tested and it was found that the amplitude response of this system was flat to 68 Hz and the bandwidth (80 Hz) was too low for accurate measurement of catheter-manometer frequency response (the ideal requirements for accurate frequency response testing are presented in chapter

4, section 2.1). The compliance of the pressure generating source of the BIO-TEK equipment (an important parameter discussed in section 4.3.2) was not given and thus the measurement technique may be inaccurate.

Furthermore, no indication is given at what temperature the frequency response tests were performed.

3.3.3 Summary

Two methods (steady state and the transient method) have been employed to evaluate the frequency response of catheter-manometer systems.

The apparatus and evaluation procedure/techniques used by a number of researchers to perform the evaluations suggested that inaccuracies may have influenced their results. In chapter 4 the evaluation procedure will be discussed in detail.

3.4 Catheter-manometer system evaluation/assessment

Previous workers have measured catheter-manometer responses that are sufficient to comply with the minimum bandwidth requirements of 25 Hz (see appendix A4). However, the measured responses differ considerably (chapter 2, table 2.1 and table 2.2).

Shapiro and Krovetz (1970) stated that the damped natural frequency of pressure tubing was inversely related to length which would imply that a 500 mm length of pressure tubing should have a significantly higher damped natural frequency than pressure tubing of 1500 mm (for similar lumen diameter and material). This is not apparent if the results listed in table 2.2 in chapter 2 are compared. A possible explanation for the difference in damped natural frequency may be that the transient method was used by Fourie et al (1987) and the steady state method by Gardner (1981), Yeomanson and Evans (1983) and Shinozaki et al (1981).

It is also interesting to note that Gardner and Fourie et al listed the damping coefficients for their catheter-manometer/pressure tubing tests while Yeomanson and Evans (1983) only presented the amplitude response plots for the systems that were evaluated. This implies that only Gardner and Fourie et al (of the researchers mentioned) have formulated their results in terms of system parameters that fully describe the response of a second-order catheter-manometer system (Lam, 1979). Although Gardner found that air bubbles decreased the frequency response of the catheter-manometer system, he did not mention any attempt to de-bubble the saline by boiling the fluid. Furthermore only the highest damped natural frequency is reported and no indication of the range of frequency response values is given.

Some of the catheter-manometer systems listed in table 2.1 are not locally available. Those which are available have not been evaluated or characterised in terms of system parameters that describe their frequency response. It is thus important and imperative that: (1) locally available (in South Africa) catheter-manometer systems are evaluated in terms of the system parameters describing the frequency response and (2) to establish both in vitro and in vivo situations that the minimum bandwidth requirements are achieved and also what the effect is, if the bandwidth requirements are not met.

3.4.1 Summary

Frequency response results can be categorised into two fields: those obtained by the steady state method of evaluation and those by the transient method. The literature review suggests that there is no link between the results of the two methods.

The methodology of frequency response presentation suggests a major limitation as most of the results are presented without any statistical indication of their validity.

3.5 Details of proposed investigation

3.5.1 Modelling

The catheter-manometer system may be analysed as a second order system. This assumption is backed by many researchers (Fry, 1960; McDonald, 1974; Bruner, 1978 and Gardner, 1981). Analysis of these models indicate that the catheter-manometer system can be simplified and that the frequency response may be characterised by the damping factor and resonant frequency.

In the proposed investigation the above mentioned assumption will be tested by using the in vivo frequency response results of catheter-manometer systems and comparing these to the calculated values using the model of Yeomanson and Evans (1983) and Bruner (1978). It was decided to use the models of the above mentioned researchers, since the parameters required for calculating the frequency response of catheters are listed in the literature (and thus available to the clinical technologist) and no complex measurements for fluid and catheter compliance, impedance and inductance have to be performed.

Furthermore, it was necessary to establish which of the two modelling approaches (distributed or lumped parameter) described the in vivo catheter-manometer system frequency response more accurately.

3.5.2 Characterisation technique

The steady state method will be used to establish the parameters mentioned in section 2.3.2 as the transient method is not considered optimal for proper characterisation of the system. The frequency response testing equipment available for this steady state method of testing was evaluated and it was found that the bandwidth of the BIO-TEK equipment was not wide enough. Furthermore, the amplitude response was not constant over its bandwidth and therefore a system which complied to the requirements for accurate in vivo testing had to be designed and constructed (design, construction and software development will be discussed in detail in chapter 4).

Software had to be developed for the acquisition, manipulation and evaluation of in vitro response data of catheter-manometer systems.

3.5.3 Evaluation

In the analysis of the in vitro results, damping factor and resonant frequency will be used to establish the frequency response of pressure tubing, cannulae, catheters and catheter-manometer systems.

The effects on the damped natural frequency and damping factor of the following will be investigated:

- pressure tubing length
- lumen diameter
- compliance

- radius ratio
- coiling and twisting pressure tubing
- cannula lumen diameter
- cannula compliance
- stopcocks and flush devices
- fluid temperature

Various combinations of cannulae and catheters will be evaluated to establish the best possible frequency response for a locally available catheter-manometer system.

These results will then be used to compare blood pressure measurements obtained by wide and narrow bandwidth systems. The comparison of results will be performed in both the time and frequency domains (described in chapter 4, section 6) to establish what effect that catheter-manometer system has on absolute pressure values and the waveform of the blood pressure signal.

Software will be developed for the analysis and relative comparison of the blood pressure waveform, recorded by a wide and a narrow bandwidth catheter-manometer system.

CHAPTER FOUR

EQUIPMENT AND PROCEDURES FOR DYNAMIC CATHETER-MANOMETER

SYSTEM TESTING

4.1 Introduction

In the previous chapter, the transient and steady state methods of frequency response testing were described. The aim of both tests is to determine the damped natural frequency and the damping factor of the catheter-manometer system. It is however important to note that the transient frequency response measurement technique has various disadvantages regarding accuracy and sensitivity. Shapiro and Krovetz (1970) stated that changes in damped natural frequency due to the effect of stopcocks and coiling in the pressure line was greater than 3 Hz and this change was significant in narrow bandwidth catheter-manometer systems: however, these changes in damped natural frequency were not detected by the transient method.

This practically excludes the transient method for extensive catheter-manometer analysis. The steady state method was therefore used and a schematic block diagram representing the system is shown in figure 4.1.

This chapter will deal with the requirements, design and construction of the test equipment essential for in vitro frequency response testing, the in vivo evaluation procedures and software development.

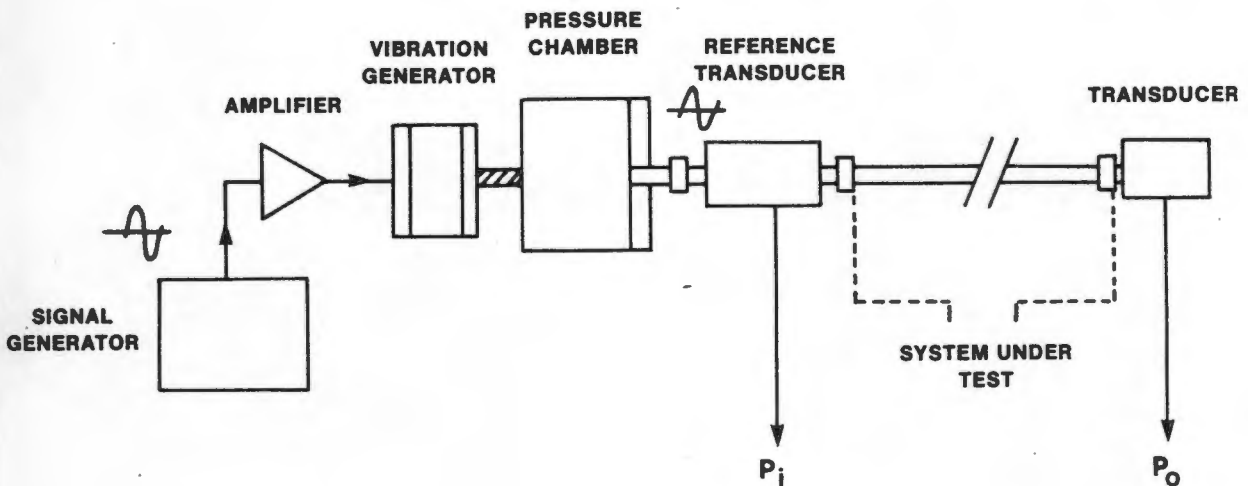


Figure 4.1.

Schematic diagram of the dynamic catheter-manometer testing system. The signal generator provides a sinusoidal voltage, which is amplified, to a vibration generator which in turn produces a mechanical, sinusoidal movement of the membrane. The fluid in the pressure chamber is regarded as incompressible and thus a sinusoidal hydraulic pressure is generated in the pressure chamber and also in the system under test. The changing hydraulic pressure is measured at both ends of the catheter-manometer system (system under test) and these two pressure signals (P_i and P_o) are used to derive catheter-manometer system response.

4.2 Catheter-manometer testing equipment

4.2.1 Ideal test equipment requirements

An ideal pressure generator (vibration generator and pressure chamber) should generate a hydraulic sinusoidal pressure with an amplitude independent of frequency over the frequency range of interest and of the hydraulic impedance of the load connected to the pressure generator.

For the above to be true, the hydraulic impedance of the pressure generator, determined by the inertia of the fluid, the stiffness of the membrane and by the friction within the pressure generator should be small compared to that of the catheter-manometer system (Vierhout and Vendrik, 1961).

Vierhout and Vendrik (1964) established that if the hydraulic impedance of the pressure chamber is less than one percent of the hydraulic impedance of the catheter-manometer system under test, the amplitude of the pressure wave generated in the pressure chamber is constant (within one percent) over the entire bandwidth of the test system. This requirement is important since the amplitude response of the pressure generator must not affect the amplitude response of the system under test.

Furthermore, the bandwidth of the pressure generator needs to be at least five times greater (Vierhout and Vendrik, 1964) than the bandwidth of any catheter-manometer system to be tested to ensure that the frequency response of the pressure generator does not affect the accuracy of the results. Figure 4.2 displays the ideal amplitude and bandwidth requirements for the pressure generator.

Another requirement is that the linearity must be maintained for a large volume displacement of the membrane of the pressure chamber, because the test must be performed for a large range of mean pressures and the pulse amplitude of the pressure generator must be independent of this mean pressure.

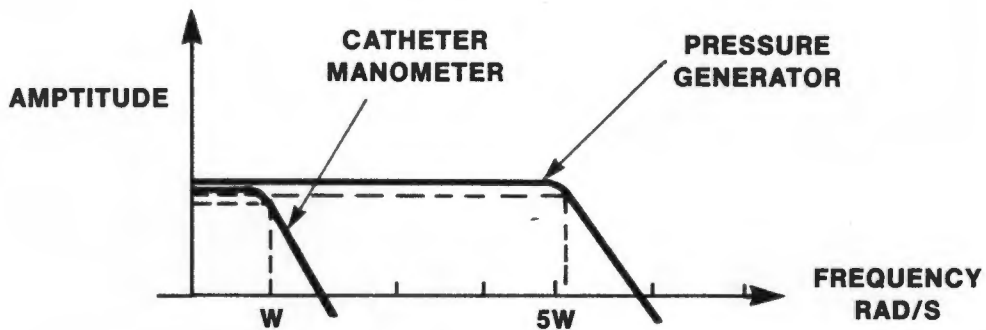


Figure 4.2

Amplitude response requirements of the pressure generator. The corner frequency (and thus the bandwidth) of the pressure generator should be 5 times higher than the bandwidth of the catheter-manometer system.

4.2.2 Review of test system requirements

From the discussion of the bandwidth requirements of catheter-manometer systems in chapter 2 and the optimal test system requirements stated in section 4.2.1, the bandwidth of the pressure generator should be greater than 100 Hz.

Nobel (1959), Stegall (1967), Ardill et al (1967) and Shelton and Watson (1968) claimed that their pressure generator designs indeed exceeded the bandwidth of 100 Hz; however, none of the above researchers have considered hydraulic impedance as a factor in their pressure generator designs. It is thus questionable if the amplitude responses were constant over the frequency range indicated. Vierhout and Vendrik (1964) included the hydraulic impedance requirement into their design but their pressure generator had a bandwidth of only 50 Hz.

4.3 Pressure chamber design

4.3.1 General design

In the section 4.2.1 it was mentioned that the hydraulic impedance of the chamber should not be greater than one percent of that of the system under test (Vierhout and Vendrik, 1964).

$$z_{\text{chamber}} < 1/100 (z_{\text{catheter-manometer}}) \quad (4.1)$$

Equation 4.1 is the fundamental requirement for the pressure generator and ensures that the sinusoidal pressure applied at the input to the catheter-manometer system under test has an amplitude which is independent of frequency and of the properties of the catheter-manometer system.

The hydrodynamic impedance of the pressure chamber is a function of fluid inertia, fluid friction and membrane stiffness. The relationship between these variables and that of hydrodynamic impedance may be best described in the following way: the sum of the inertial force of the moving fluid in the pressure chamber (F_f), the restoring forces of the membrane (F_M) and the force caused by the viscous resistance of the generator (F_{GF}) must be small in comparison with the force exerted by the vibration generator F_G (Vierhout and Vendrik, 1964). This ensures that the fluid pressure in the catheter or the system under test (P_i) is practically equal to the fluid pressure in the pressure chamber of the pressure generator P_G (figure 4.3). Further the friction forces of the pressure generator must be very small so that the above mentioned relationship between the variables that determine the hydrodynamic impedance is not affected.

Figure 4.3 illustrates the relationship of the forces in the pressure generator and the vibration generator.

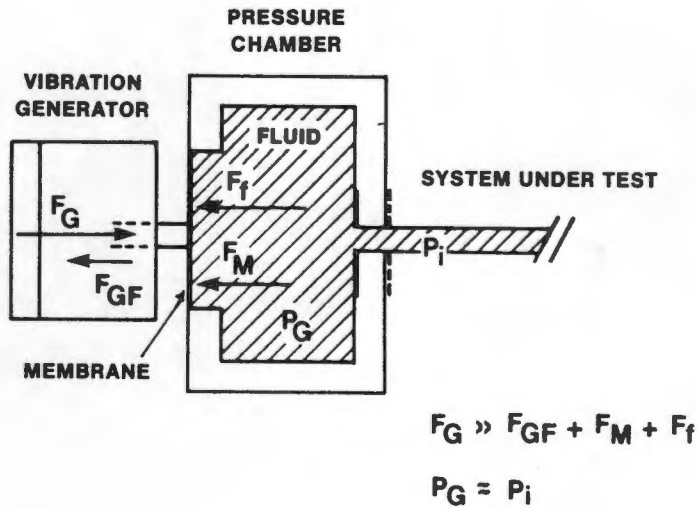


Figure 4.3

The pressure generator and the relationship of the different forces acting on the chamber. F_G is the force exerted by the vibration generator and F_f is the inertial force of the fluid. F_M and F_{GF} is the restoring force of the membrane and the friction force of the vibration generator respectively.

4.3.2 Mathematical and hydraulic analysis of the pressure chamber

The test system is closed; thus there are no external forces acting on the system and the only movement permitted is that of the membrane. Under these conditions the pressure developed in the chamber is proportional to the power supplied to the vibration generator - the pressure then equals the solenoid force (the force produced by the vibration generator) per unit area of the membrane (Vierhout and Vendrik, 1964; Ardill et al, 1967).

In figure 4.3, the solenoid force of the vibration generator F_G acts on the membrane. If the chamber is a closed system, the fluid acts on the membrane with an opposing pressure F_f ;

$$F_f \propto \frac{F_G}{\pi r^2} \quad (4.2)$$

where r is the radius of the membrane.

If a catheter-manometer system is then connected to the chamber and a displacement of the membrane occurs, the restoring forces determine the hydraulic impedance of the generator. The smaller these forces are the smaller the impedance (Vierhout and Vendrik, 1964). This impedance is non-resistive since the reaction forces are proportional to the displacement. The compliance (C_g) of the membrane itself, being the ratio between the volume displacement and the pressure difference which causes this displacement, is given in equation 4.3 (Vierhout and Vendrik, 1964; McDonald, 1974).

$$C_g = \frac{\pi r^6}{16Eh^3} \quad (4.3)$$

E is the Young's modulus of the membrane material, r and h the radius and the thickness of the membrane respectively. Applying this formula, the calculated compliance of the membrane and therefore of the pressure generator shown schematically in figure 4.3 and described in detail in Appendix D is $48 \text{ mm}^3/100\text{mmHg}$.

Figure 4.4 shows the electrical model of a pressure generator of internal hydraulic compliance C_g , connected via a catheter with hydraulic resistance R , self inductance L and compliance C , to a manometer with hydraulic compliance C_m .

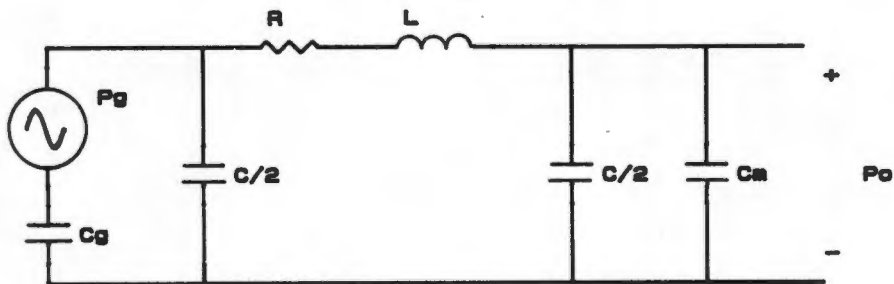


Figure 4.4

An approximate model for the pressure generator connected to a catheter-manometer system (Vierhout and Vendrik, 1964).

The reaction forces of the vibrating generator are negligible in comparison with force F_G (the reaction forces are designed to be small in the vibrating generator). Hence the internal hydraulic impedance of the generator is almost entirely determined by C_g . If the restoring force is not negligible, a capacitance would be in series with C_g , making the resulting hydraulic capacity or compliance smaller and thus the hydraulic impedance larger. This would be unfavourable.

It has been shown theoretically and experimentally that commercially available catheters can be approximated by the circuit in figure 4.4 (Vierhout and Vendrik, 1964).

Furthermore, the output pressure P_o of the generator is

$$P_o = P_g \cdot \frac{C_g}{C_g + C_m + C} \cdot \frac{\frac{1}{j\omega(C_m + C/2)} + \frac{1}{j\omega(C_g + C/2)}}{\frac{1}{j\omega(C_m + C/2)} + \frac{1}{j\omega(C_g + C/2)} + R + j\omega L} \quad (4.4)$$

where P_g is the pressure generated by the pressure chamber (Vierhout and Vendrik, 1964).

The undamped natural frequency f_n is

$$f_n = \frac{1}{2\pi} \left[\frac{1}{L} \left(\frac{1}{C_m + C/2} + \frac{1}{C_g + C/2} \right) \right]^{\frac{1}{2}} \quad (4.5)$$

and the damping factor β is

$$\beta = \frac{1}{2} \cdot R \cdot \left[\frac{(C_m + C/2)(C_g + C/2)}{C_m + C_g + C} \cdot \frac{1}{L} \right]^{\frac{1}{2}} \quad (4.6)$$

From equations 4.5 and 4.6 (Vierhout and Vendrik, 1964) it can be seen that with decreasing values of C_g , f_n increases and β decreases. The undamped natural frequency of a pressure generator equals the f_n of an ideal generator (for $C_g = \infty$) multiplied by the factor,

$$1 + \left[\frac{C_m + C/2}{C_g + C/2} \right]^{\frac{1}{2}}$$

while the damping factor equals the damping factor of an ideal generator divided by the same factor. For low values of β the undamped natural frequency f_n is almost equal to the damped natural frequency f_d .

For the measurement error to be smaller than one percent,

$$C_g + \frac{C}{2} \geq 50 \left[C_m + \frac{C}{2} \right] \quad (4.7)$$

From equation 4.7, the maximum and minimum values for C_g , the compliance of the pressure generator, can be calculated. For larger inner diameter catheters and cannulae, C is in the order of $0.2 \text{ mm}^3/100\text{mmHg}$. Hence for manometers with $C_m = 0.1 \text{ mm}^3/100\text{mmHg}$, C_g must be greater than $10 \text{ mm}^3/100\text{mmHg}$. For polyethylene pressure tubes, C_g must be greater than $25 \text{ mm}^3/100\text{mmHg}$ (Vierhout and Vendrik, 1964).

McDonald (1974) established that a catheter-manometer system has at most a compliance of $2 \text{ mm}^3/100\text{mmHg}$. The pressure generator however has a compliance which is 24 times higher, thus the

restoring force of the membrane may be neglected. The reason for this is that the volume displaced in the pressure chamber is very small. The displacement depends on the compliance of the tested device, thus the compliance of the tested device is smaller in comparison to that of the pressure generator.

From the above mentioned discussion it is clear that the pressure generator requirements were met.

4.3.3 Pressure generator construction

4.3.3.1 Introduction

Various design and construction methods have been suggested for sinusoid-producing pressure generators. Many of these designs have distinct disadvantages and in particular those which depend on cyclical compression of an elastic medium such as air (Ardill et al, 1967). Amplitude deviation at low frequencies is common for compressions that are neither strictly isothermal nor adiabatic. It is also difficult to achieve symmetrical waves from a non adiabatic system, at frequencies higher than 100 hertz.

Using water or saline as the compression medium the above mentioned disadvantages are minimized. Nobel (1959), Linden (1959) and Vierhout and Vendrik (1961) used fluid filled chambers with a membrane fixed to the one end of the chamber. The force was exerted on the membrane by means of a crystal, a loudspeaker and the moving coil of a telephone system respectively.

The designs of Nobel (1959) and Linden (1959) were questioned by Vierhout and Vendrik regarding the high internal impedance of the pressure chamber. They suggested a low pressure chamber impedance design with a crystal and loud speaker as the driving force.

It was found in this thesis (Appendix C1) that the system used by Vierhout and Vendrik depended on the frequency characteristics of the speaker. At low frequencies (1-6 Hz) the speaker response was attenuated and this influenced the entire frequency response of the test system. Furthermore, the frequency range for which the catheter-manometer systems were tested was within the audio range of sound and subsequently the sound emitted by the speaker, inconvenienced the person performing the testing procedure.

Ardill et al (1967) and Shapiro and Krovetz (1970) used moving coil vibrators for their mechanical generating force and claimed that the frequency response of the test equipment exceeded 180 Hz; however, they either failed to examine or mention the importance of the internal impedance of the pressure chamber.

The considerable differences in the driving systems and the compliance of the pressure chambers led to contradictory results. It was decided to construct a simple, inexpensive, sinusoidal pressure generator that meets the requirements discussed in section 4.2.

4.3.3.2 Construction of the pressure chamber

For optimal frequency bandwidth of the test equipment, the fluid filled pressure chamber design was used. The fluid used in the chamber was physiological saline, as this was the actual fluid used in the clinical environment (for catheter-manometer systems).

The initial pressure chamber design was based on the designs of Vierhout and Vendrik (1961) and Krovetz and Goldbloom (1974). In this design, a loud speaker was used to oscillate a mylar diaphragm of 0.38 mm thickness. The chamber was constructed (refer to Appendix C1) from perspex and was fitted to a baseplate as shown in drawing 1 in appendix D. The total deflection of this mylar diaphragm did not exceed 1.5 mm which resulted in a maximum mean pressure of 60 mmHg being generated within the pressure chamber. An oscillation of ± 20 mmHg around this mean was only achieved. This unfavourable result was attributed to the stiffness of the membrane; however, decreasing the thickness of the membrane resulted in limited improvement. Furthermore the vibrations created by the audio range of the loud speaker distorted the shape of the generated pulse in the pressure chamber. An improved design was considered by using a vibrating generator (Griffin XEH-600-L) and a redesigned base-plate and pressure chamber. The designs of the individual parts of the test equipment are given in Appendix D in drawings D3 to D6.

A polyvinyl chloride (PVC) membrane of 0.35 mm thickness was made by the Department of Polymer Science at the University of Stellenbosch. The shape of the membrane reduced the magnitude of the deflection forces of the vibration generator and allowed for a positive mean pressure in the pressure chamber of up to 150 mmHg.

The frequency response of the pressure generator was however not suited for catheter-manometer testing as the frequency bandwidth was low (Appendix C1 lists the response values) and the damping factor was low (high resonant peak at resonance). The amplitude and phase response of the system is shown in figure 4.5.

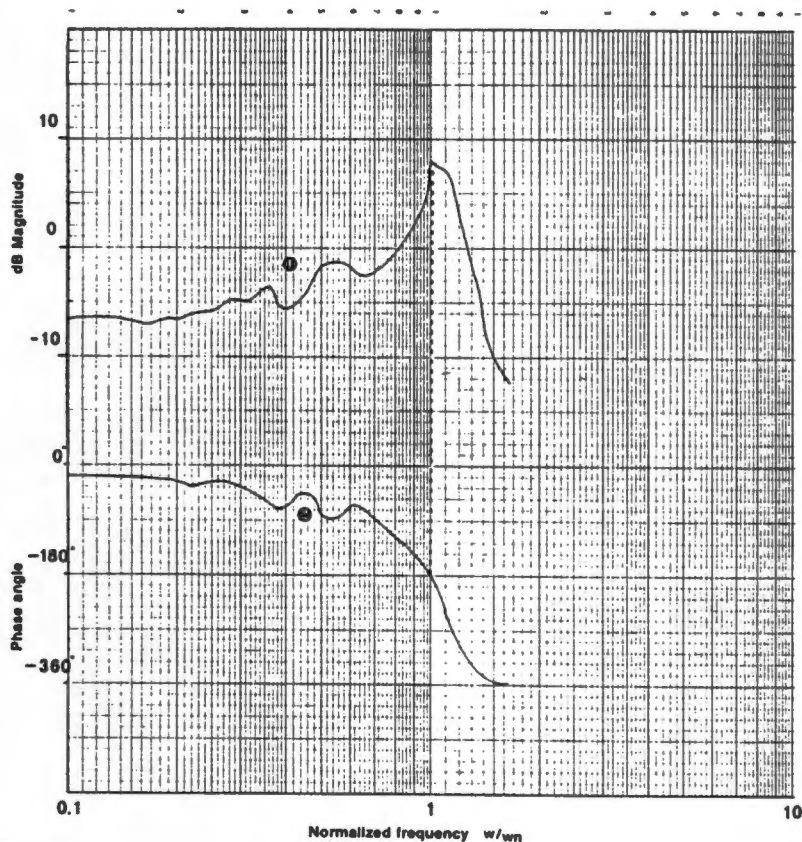


Figure 4.5

The amplitude and phase response of the pressure generator.

For the design described above the bandwidth was less than $w/w_n = 0.35$ (48 Hz) and thus a compensation network was required.

It was established that the system was of a third or fourth order since the phase shifted through 360° but it was assumed that the system could be approximated by a second order system because of its response, closely matching that normally attributed to a second order system.

A phase lag control circuit was designed (Appendix C2.2) and tested. The compensated amplitude and phase response is shown in figure 4.6.

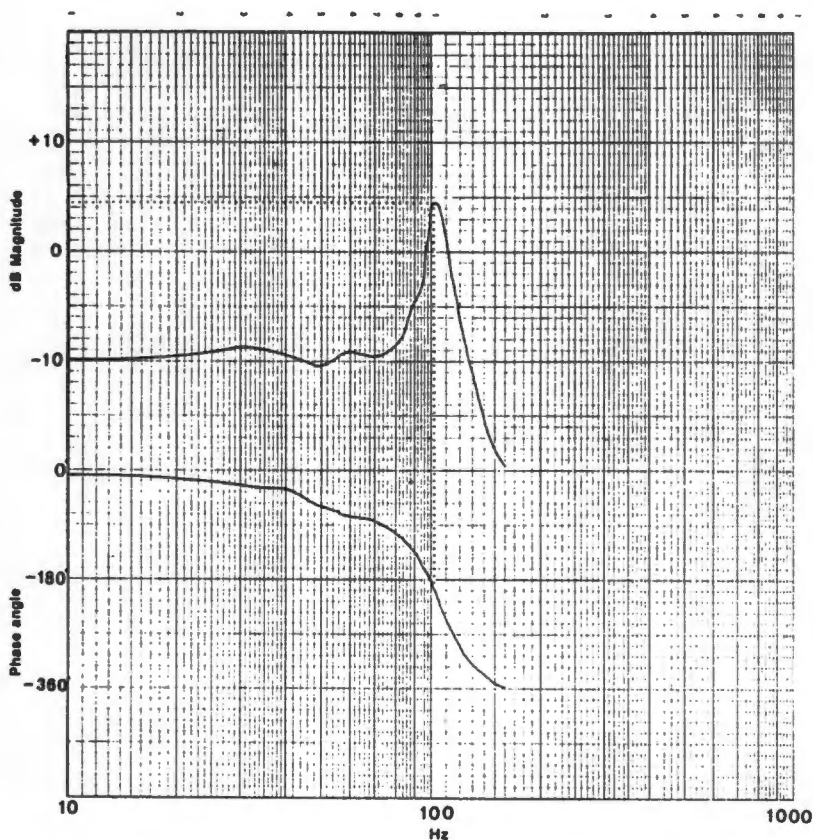


Figure 4.6

The amplitude and phase response using the phase-lag compensation circuit.

There was a marked improvement in bandwidth; however the gain at resonance was too large. It was then decided to use the pole-zero cancellation technique to optimise the response of the pressure generator. This method is described in detail in Appendix C2.3. The subsequent response is indicated in figure 4.7.

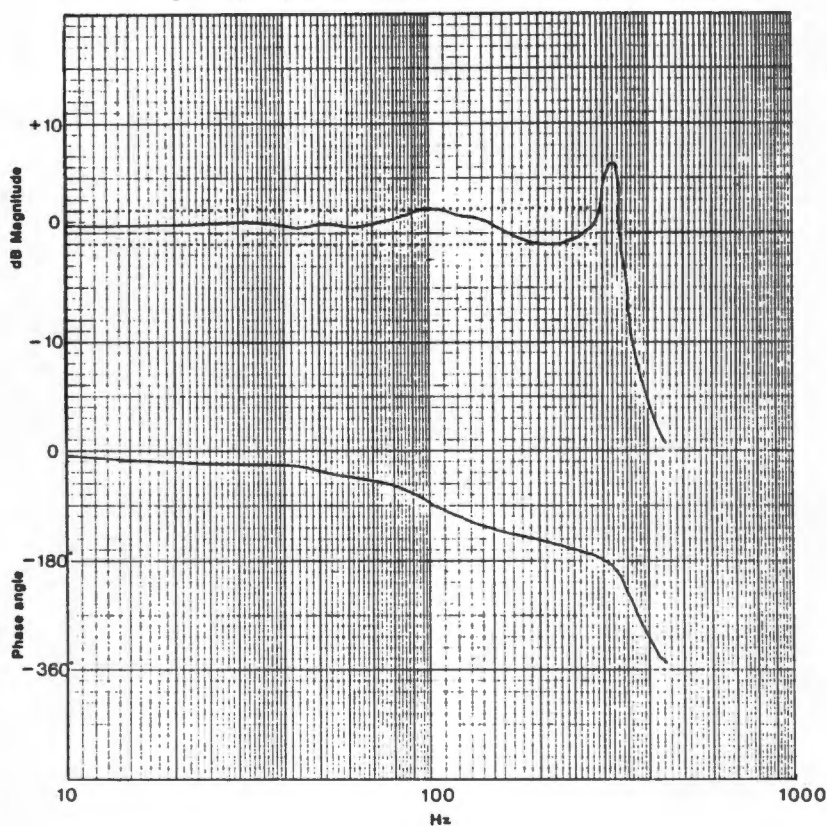


Figure 4.7

Improved amplitude and phase response of the pressure generator and pole-zero compensator.

The pressure chamber and test equipment is shown in figure 4.8 and 4.9 respectively and a detailed discussion of the construction procedure, for both the mechanical components and electronic compensation network, is given in Appendix C2.4 and Appendix D respectively.

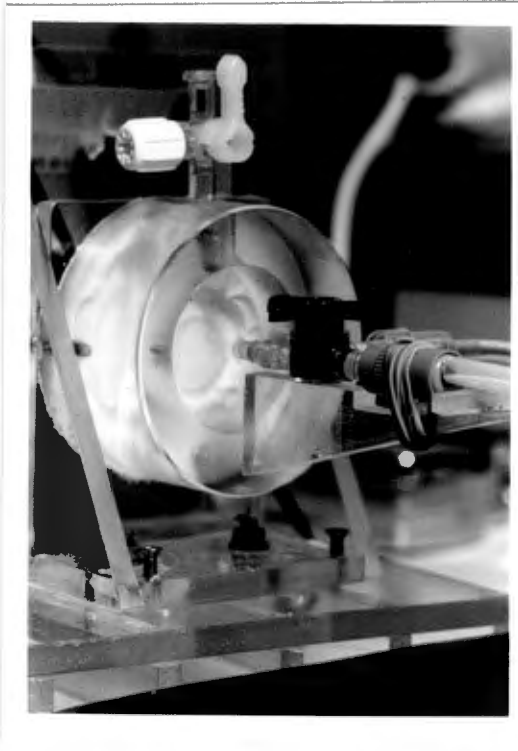


Figure 4.8

The pressure chamber.



Figure 4.9

The catheter-manometer test equipment.

4.4 In vitro catheter-manometer evaluation

In chapter 2 the importance of determining the damping factor and resonant frequency of catheter-manometer systems was mentioned, as this allowed the representation of the catheter-manometer system as a second order system. This made it possible to easily and reliably predict dynamic response and hence fidelity of a dynamic pressure measurement system.

In this section the method of in vitro testing of catheter-manometer systems is described in detail.

4.4.1 The test system

Figure 4.10 is a schematic representation of the testing equipment.

The AC voltage source is a Function Generator (HP 3314A) coupled via a compensator to an frequency amplifier (designed and constructed by the Department of Physics, UCT) has a bandwidth of 5 kHz.

The purpose of the amplifier is to provide the power levels needed by the vibrating generator for proper operation. As indicated in the diagram, a reference transducer (AME 840) at the output of the pressure chamber, was connected to the electronic compensator system to ensure that the output amplitude was constant with frequency to at least 100 Hz.

Distal to the reference pressure transducer, a three way stopcock was connected with a side arm leading to a flush system. This system was used to infuse previously boiled saline into either

the pressure chamber or the catheter-manometer system under test, connected distally to the stopcock. The system under test consisted of cannulae and/or pressure tubing followed by a transducer and stopcock. This second transducer was connected to a transducer amplifier module (Simonsen and Weel, BAP 001), from which a signal was tapped off directly after the pre-amplification stage (bandwidth of this stage > 500 Hz). The purpose was to eliminate the effects of filtering in the module. This signal was connected to a gain/phase meter (HP 3050) and oscilloscope (Kikusui COM 7101A).

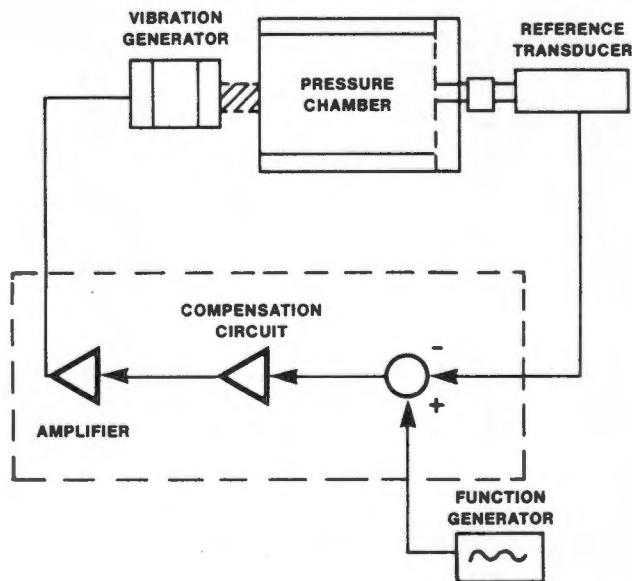


Figure 4.10

Diagram of the test system.

4.4.2 Test equipment configuration

To prevent air bubbles from being trapped in the pressure chamber and system under test, these are flushed with 90 percent alcohol before each test to remove any fatty substances. Furthermore, the formation of air bubbles in the catheter-manometer system is prevented by flushing the catheter-manometer with CO₂ and by pre-boiling the saline which is then cooled to 25 °C. The saline reservoir is a glass bottle as to prevent air diffusing through the container, as would be the case with the plastic container it is supplied in.

The procedure of filling the pressure chamber and the system under test with saline is described in Appendix C3.

The fluid pressure within the pressure chamber and the system under test is increased to at least 100 mmHg so as to simulate mean central arterial blood pressure (the blood pressure monitor has been calibrated using a sphygmomanometer) while the peak pressure is adjusted to 120 mmHg by the volume control of the signal amplifier. The pressure generator thus produces a sinusoidal pressure wave (120/80 mmHg) at the input of the system under test which is displayed by the pressure monitor and the oscilloscope. Furthermore, the output pressure of the system under test is also displayed on the oscilloscope (the reader is referred to figure 4.11).

4.4.3 Test procedure

The test procedure for cannulae and/or pressure tubing was as follows:

- The function generator (figure 4.10) is set to 1 Hz.
- The gain reading is normalized (the signal from transducer T_2 is normalised to that from the reference transducer T_1 , to give a reading of 0 dB).
- The frequency is then increased in steps of 2 Hz and the readings of the gain/phase meter are recorded.

Figure 4.11 shows typical signal traces for the reference and output transducers.

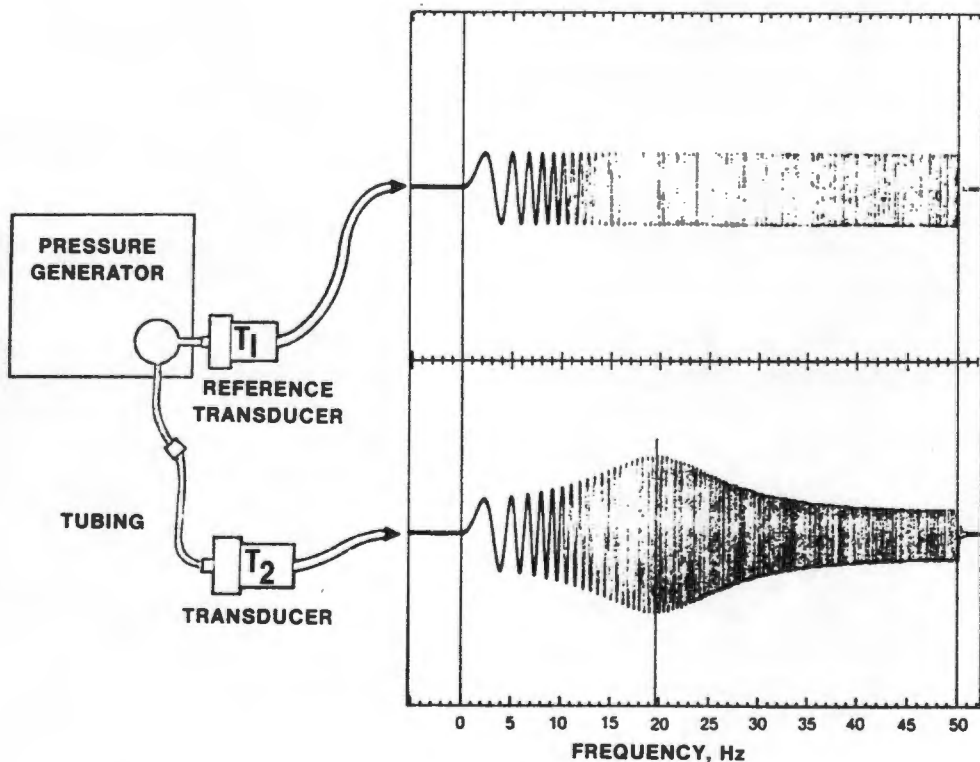


Figure 4.11

Reference and output transducer signals for increasing frequency (Gardner, 1981).

After each test the system was flushed as described in points 5 to 8 in Appendix C3 and the test procedure listed above was repeated. The tests were repeated at least five times or until the spread of the maximum gain value for each test was at a minimum. This was achieved by calculating the standard deviation of the gain values.

For the first 38 systems tested (refer to section 4.6.4.1), the test procedure and the recording of results were performed manually. The frequency and corresponding gain values (in decibels) were then entered into a computer by using software (MEAS.THE) discussed in section 4.6.4.1.

For the remaining 32 tests, the signal generator was set to automatically sweep a frequency range of 1 to 100 Hz in 4 seconds. It was established when using sweep times of 4, 8, 12 and 16 seconds, that no significant change in frequency response resulted. A sweep time of 4 seconds was therefore used in order to reduce each test period.

The responses were recorded on to magnetic tape (RACAL 7DS, FM recorder - specifications given Appendix H1) and subsequently analysed by the program MEAS.THE to obtain the resonant frequency and damping ratio for each system tested.

4.5 In vivo catheter-manometer evaluation.

4.5.1 Introduction

The effect of the bandwidth of catheter-manometer systems on the blood pressure signal transmission is demonstrated by in vivo testing. In these tests, it was hoped to compare blood pressure recorded by a conventional catheter-manometer system to that recorded by a wide bandwidth system, such as a catheter-tip transducer system. However, ethical consideration prevented the insertion of the catheter-tip transducer into the radial artery. In vivo testing was thus limited to the comparison of wide and narrow bandwidth conventional catheter-manometer systems.

Blood pressure waveforms from patients undergoing cardiac surgery at Tygerberg Hospital were recorded by using catheter-manometer systems for which the highest damped natural frequencies of 12.4 Hz (for 300 mm pressure tubing) and 24.9 Hz (for 1500 mm pressure tubing) were established from in vitro tests, respectively. The site of blood pressure measurement was the radial artery for all patients evaluated, because of good collateral circulation of blood in the hand and easy access to the artery. The arm was extended horizontally at right angles to the body and was supported by an arm rest. A catheter-manometer system, described in the next section, was connected to the patient according to the procedure described in Appendix A2.1.

4.5.2 In vivo testing configuration

The catheter-manometer configuration is shown in figure 4.12.

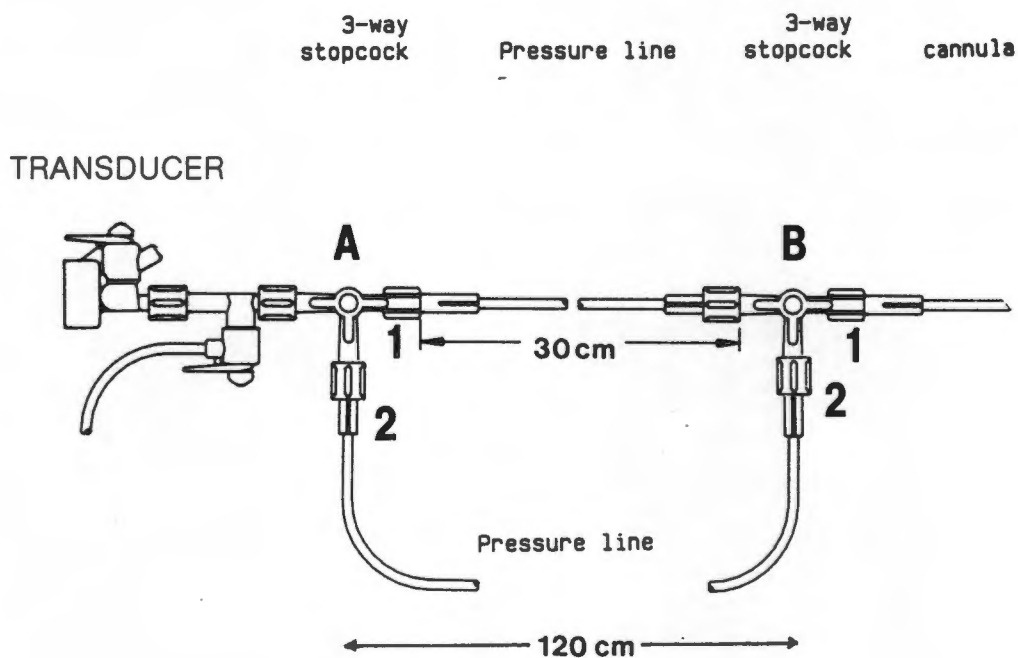


Figure 4.12

The cannula is inserted into the radial artery and is connected to a stopcock. Two pressure lines are fixed to the stopcocks (A and B), allowing alternate blood pressure measurements.

The configuration of the catheter-manometer system allows alternate blood pressure measurements, by selecting the appropriate stopcock port, through long and short pressure lines. Furthermore, the pressure transducer is identical for both measurements and thus reduces possible error.

The blood pressure signal is amplified by a Simonsen and Weel blood pressure monitor system (BAP 001 module) and the tapped off signal (obtained after the pre-amplification stage of the module) is recorded by an FM tape recorder (RACAL 7DS) for subsequent storage and analysis.

4.5.3 Recording procedure

Recording of blood pressure was performed prior to the CPB period. During the recording period the ventilator was switched off to prevent the influence of respiratory pressure changes (Valsalva manoeuvre).

The recording procedure was as follows:

- Stopcock A and B in position 1
- Ventilator switched off.
- Ten seconds of blood pressure recording by the narrow bandwidth catheter-manometer system.
- Stopcock A and B switched to position 2
- Ten seconds of blood pressure recording by the wide bandwidth catheter-manometer system.
- Ventilator switched on.

The recording procedure was repeated five times with a ten minute interval between each test.

The recorded signal was digitized (by an A/D converter described in section 4.6.3) and analysed by a micro-computer and appropriate software described in section 4.6 and listed in Appendix F.

4.5.4 Signal analysis

The recorded signal was analysed in the time and frequency domains to establish the effect that high and low resonant frequency catheter-manometer systems have on the frequency content and pulse shape of the blood pressure waveforms.

The points listed below were considered important in establishing and demonstrating this effect:

4.5.4.1 Time domain analysis

- Amplitude of peak systole, end diastole and of the dicrotic notch.
- Mean pressure value
- Maximum dp/dt value
- Time length of the anacrotic, predicrotic and the dicrotic waves of the blood pressure signal.
- Heart rate

4.5.4.2 Frequency domain analysis

- The Fast Fourier Transform of the blood pressure signal
- The power density spectrum of the signal

4.6 Software development

4.6.1 Introduction

The considerable volume of data recorded in testing the frequency response of catheter-manometer systems and in the analysis of blood pressure waveforms in both the time and frequency domains, necessitated the use of a computer. It was decided to use a personal computer.

Commercially available software, e.g. ASYSTANT (Macmillan Software Company) was not used, due to the high cost of such software and more importantly, the inflexibility of existing software when specific functions are desired.

Two software application programs were developed. The first (MEAS.THE) was used for data acquisition and in calculating the resonant frequency and the damping factors of catheter-manometer systems. The second (ANAL.THE) was used for the input of clinical waveforms (recorded on magnetic tape during cardiac bypass operations) and the subsequent analysis and representation of the results.

This section elaborates on the computer system requirements and briefly reviews the purpose of each program. A detailed program description including flow charts and function key summaries is presented in Appendix E. The program listings are given in Appendix F.

4.6.2 Computer hardware requirements.

The software was developed to operate on any IBM compatible micro-computer. Memory requirements are 640 kB (RAM), and for the signal analysis program, a clock speed of 8 MHz or higher is recommended due to the large number of mathematical calculations for the Fourier transformation. A mathematics co-processor is required to run both MEAS.THE and ANAL.THE (both programs use 80287/8087 - co-processor commands). Furthermore this addition will enhance the speed performance of the system.

Disk drive requirements are either two diskette drives (360 kbytes) or one diskette and one hard drive (10 Mbyte).

FORTH was used as the programming language and a support package, ASYST (A Scientific System - version 1.25), developed by Macmillan Software Company, was used to complement and enhance the analysis capabilities of the fourth generation software language. Excellent presentation is achieved if an HP74 series plotter and an EPSON compatible printer are linked to the micro-computer via the parallel interface port.

In addition to the hardware requirements mentioned above an analogue-to-digital converter (A/D card) is needed to digitise the data.

The software is developed to control either an RS232 port or an Hewlett-Packard Interface Bus (HP-IB)/IEEE-488 bus (the IEEE-488 is an adaptation of the HP-IB and a version of this bus is called the General Purpose Interface Bus, GPIB). This option thus allows the processor to control most of the commercially available A/D cards and HP-IB/IEEE-488 systems.

The software is written for the EGA colour card (option of the HP Vectra); however the Hercules monochrome card can likewise be used. The resolution of the monitor for the colour display was 600 x 350 pixels.

4.6.3 Micro-computer system used for the research

The Hewlett Packard Vectra (12 MHz clock and 80287 co-processor) system which was supplied by the South African Medical Research Council was used. The GPIB is a standard feature with this system and thus data acquisition is controlled effectively with the support software package, ASYST.

The system has one hard drive (30 Mb) and a 360 kbyte, 5½ inch diskette drive. The system board supports both ROM/EPROM (Read Only Memory/Erasable Programmable Read Only Memory) and R/W (Read/Write) memory. The system board also has 640 kbyte memory size (RAM).

The input/output (I/O) bus is an extension of the microprocessor address and data bus, the IEEE-488 bus, and this was linked to the MICROLINK system (Biodata). The MICROLINK device is an interface designed to allow flexible interchange of data between external instruments, such as laboratory equipment and magnetic tape recorders, and micro-computers that have the ability to act as controllers of the IEEE-488 bus.

The MICROLINK used in this research work was a modular system which had a 16 channel (8 bit) A/D converter module (01/AN16/32), a high speed clock module (00/HSC) and a 2 channel 8 bit D/A converter module (02/ANIDS).

In Appendix H4 and H5, brief technical descriptions of the HP Vectra and the MICROLINK system are respectively given.

4.6.4 Brief program description

4.6.4.1 MEAS.THE

The first 38 catheter-manometer frequency response measurements were not directly digitised, as the measuring instruments (the gain/phase meter, the oscilloscope and blood pressure monitor) did not have a bus compatible with the IEEE-488 bus used by the HP Vectra micro-computer. Furthermore, the FM tape recorder (RACAL 7DS) was only acquired at a later stage. Thus the initial results were recorded manually; however, once the recorder and the multi-channel A/D converter were obtained, the derivation of in vitro catheter-manometer frequency response parameters was automated. Two program versions were thus developed: one (version 1.00) for the analysis of manually acquired data and the other (version 1.25) for automated data acquisition.

In figure 4.13 the function key flowchart of MEAS.THE is given. The flowcharts for version 1.00 and version 1.25 are identical.

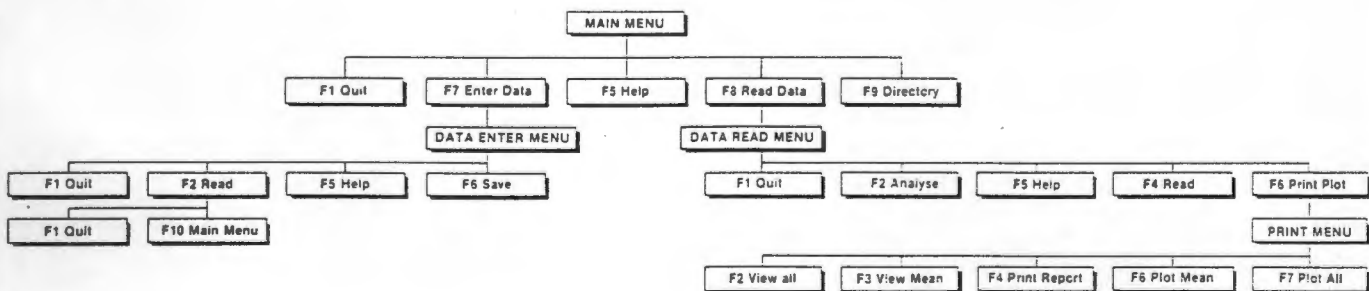


Figure 4.13

The function key flowchart of MEAS.THE. The menu levels are schematically represented.

From the function key flowchart of MEAS.THE it is seen that three sub-menus can be called:

(i) Data enter menu

This menu activates the subroutines for the manual data entry procedures (version 1.00) of the software. This section was developed to be user friendly and to provide the user with a time efficient method of entering data into the micro-computer. The automated version (1.25) of the program controls the digitizing process of the frequency response measurement and creates data files compatible to the manual data entry procedure.

Both program versions allow extensive data manipulation within the data files. This includes data correction, alternative indexing and data sorting. These data manipulations are discussed in detail in Appendix E. Furthermore, the program has the option of saving the data and/or reading the data from disk.

(ii) Data read menu

This menu activates the subroutines that control the access of stored data and the analysis thereof. Data analysis includes the calculation of damping factor and the resonant frequency. Furthermore, the program gives an indication of variance of the obtained results. This function was included in the program so as to give the user an indication of the repeatability of the results.

(iii) Print menu

The print menu gives the user the option to view the results on the screen and print and/or plot the results.

4.6.4.2 ANAL.THE

This program was developed to digitise and analyse the data (blood pressure waveforms) that was recorded on magnetic tape.

Figure 4.14 presents the function key flowchart of ANAL.THE.

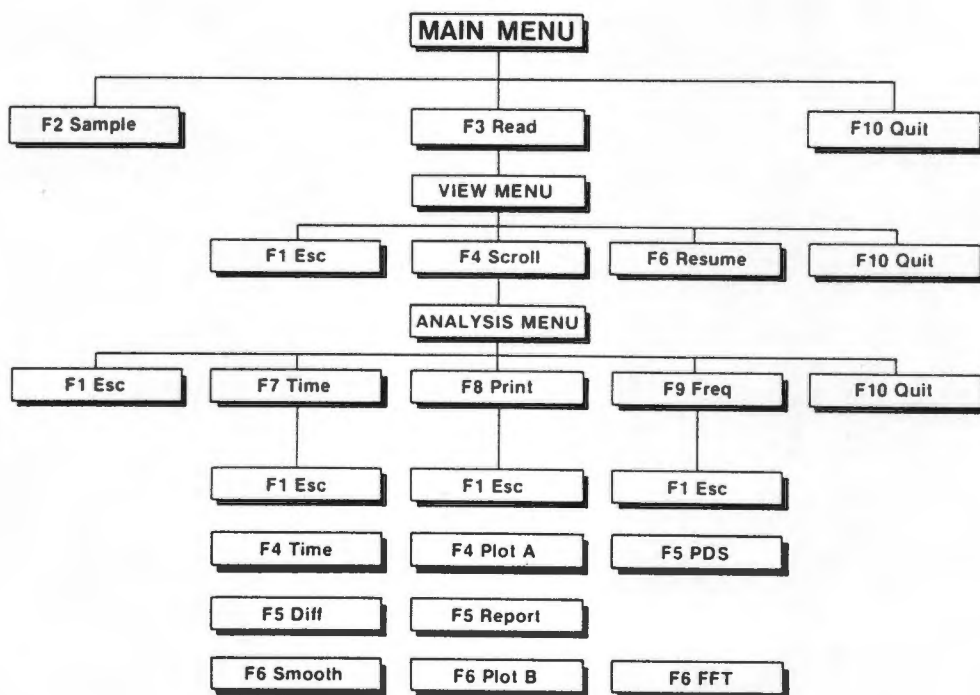


Figure 4.14

The function key flowchart of ANAL.THE. The menu levels are schematically represented.

The program is divided into three sub-menus. The first is the main menu, the second is the view menu and the third is the analysis menu.

(i) Main menu

The first section of the program controls the input/output (I/O) routines of the data acquisition phase of the program, data storage and the reading of stored data from diskette.

(ii) View menu

The second section of the program consists of data control and data manipulation. The data control enables the user to view the data and mark individual pulses of the stored data.

(iii) Analysis menu

The last section relates to the data analysis in the time and frequency domains and the hardcopy presentation of results. Hard copy presentation includes both plotting and printing of results.

CHAPTER FIVE

RESULTS

5.1 Introduction

The presentation of results is given in two sections. The first section lists the in vitro frequency response results. These results are used in the second section to investigate the effect of different catheter-manometer system bandwidths on the the clinical recorded blood pressure waveforms.

The data points on the accompanying graphs represent an average of five trials for which each test was performed.

Saline was pre-boiled and debubbled as described and was used at 25 °C if not indicated otherwise.

The complete listing of the in vitro data is given in Appendix G2 while in vivo data is given in appendix G3.

For the frequency response parameters of pressure tubing (section 5.2.1), catheters (section 5.2.2), cannulae (section 5.2.3) and catheter-manometer systems (section 5.2.4) it must be observed that the damped natural frequencies and damping factors listed are the response of both the system under test and that of the transducer.

5.2 IN VITRO RESULTS

5.2.1 Pressure tubing

5.2.1.1 Physical properties of pressure lines

Table 5.1 lists the characteristics (material, internal diameter and wall thickness) of the different pressure tubing used. The parameters were measured using a measuring microscope (MITUTOYO-AY5) and they are the average value of three measurement trials.

Pressure tubing (ID = E) was cut to the length as indicated by the '*' in the ID (identification) column.

ID	Length	Type	Internal diameter	Wall thickness
A	300	PE	1.49	0.87
B	300	PE	1.41	0.78
H	300	PE	1.53	0.90
I	300	PE	1.53	0.60
J	300	PE	1.44	0.82
C	300	T	1.47	0.53
G	300	T	1.39	0.44
E*	400	PE	1.66	0.82
E*	600	PE	1.66	0.82
E*	900	PE	1.66	0.82
E*	1000	PE	1.66	0.82
D	1200	PE	1.56	0.82
E	1200	PP	1.66	0.82
K	1200	PP	1.68	0.75
L	1200	PP	1.44	0.56
F	1500	PP	1.53	0.47

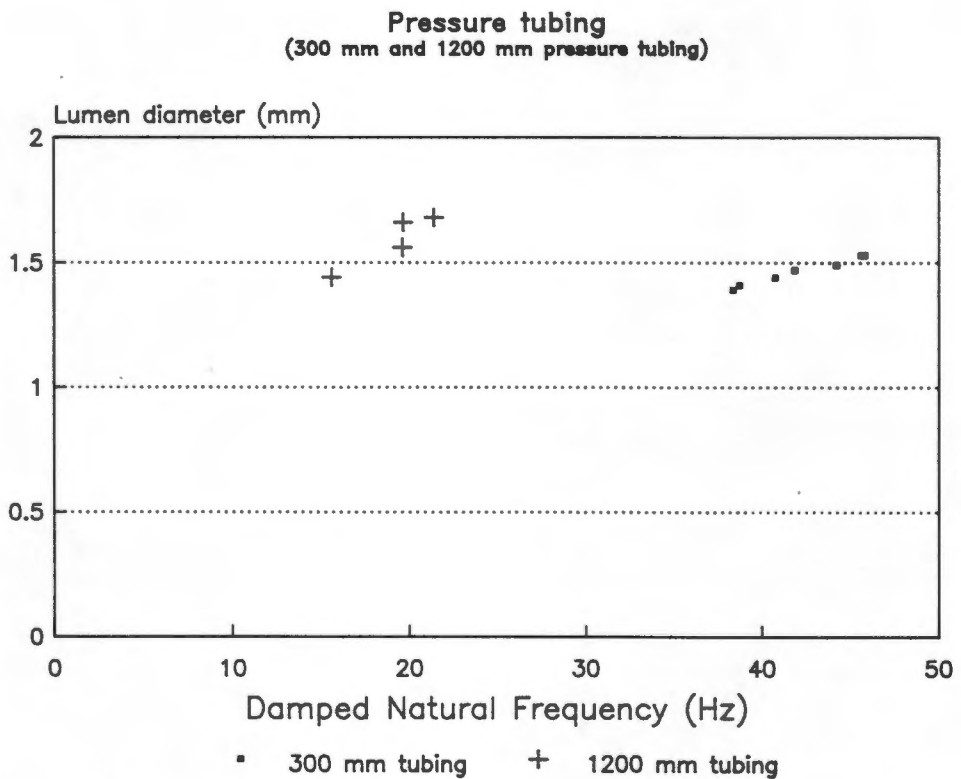
Table 5.1

Characteristics of pressure tubing tested (in millimetres). The materials are listed under the column heading "Type".
PE = Polyethylene, PP = Polypropylene, T = Teflon

Table 5.1 indicates that lumen diameter and the wall thickness of the pressure lines are unrelated to length and material.

5.2.1.2 Effect of lumen diameter on damped natural frequency

In figure 5.1, the relationship of lumen diameter and damped natural frequency is shown. The pressure lines of 300 mm are made from polyethylene, if not stated otherwise, and those of 1200 mm from polypropylene.



boiled saline, 25 degrees C

Figure 5.1

Damped natural frequency vs. lumen diameter for pressure tubing of 300 mm and 1200 mm lengths.

There is an indication that for both polyethylene and polypropylene pressure lines, the damped natural frequency is directly proportional to the lumen diameter. The rate of increase of the damped natural frequency for larger lumen diameter pressure lines is higher for 300 mm tubing than for tubing of 1200 mm in length. The results indicate that pressure tubing of 300 mm has a damped natural frequency (f_d range = 38.4 Hz to 45.8 Hz) while pressure tubing of 1200 mm has a damped natural frequency range of 15.6 Hz to 21.4 Hz for lumen diameter tested.

5.2.1.3 Effect of pressure tubing length on damped natural frequency

Table G2.6 lists the range of damped natural frequency for different pressure tubing length.

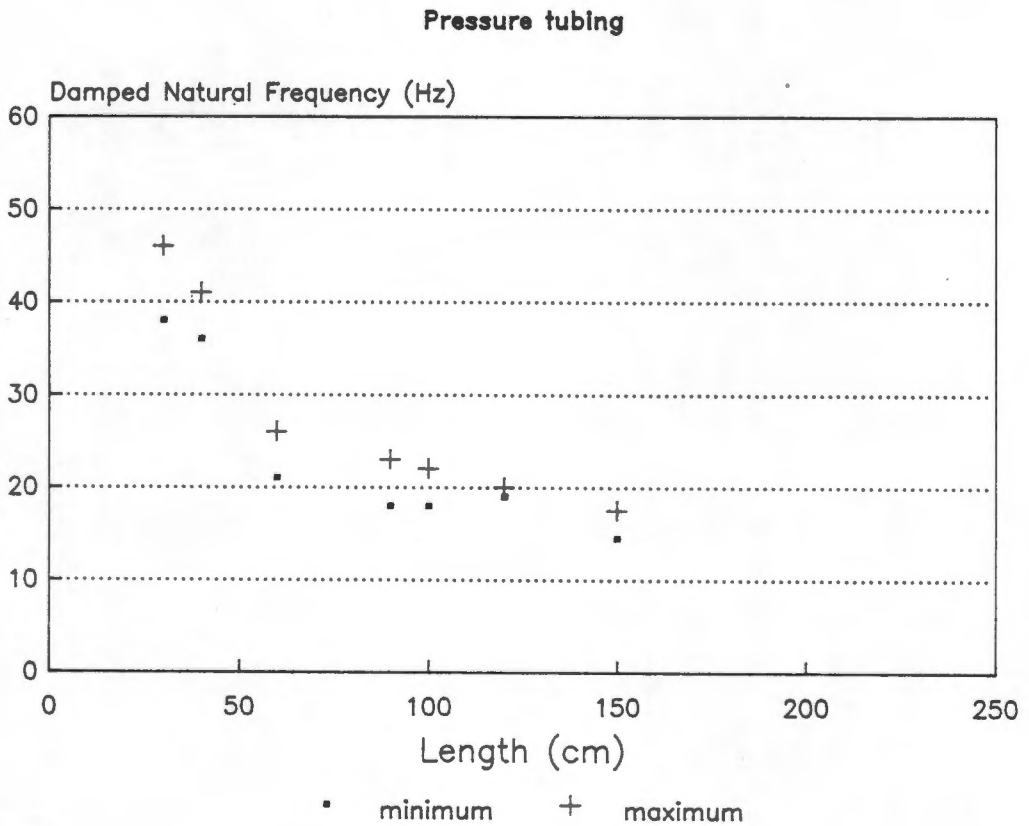
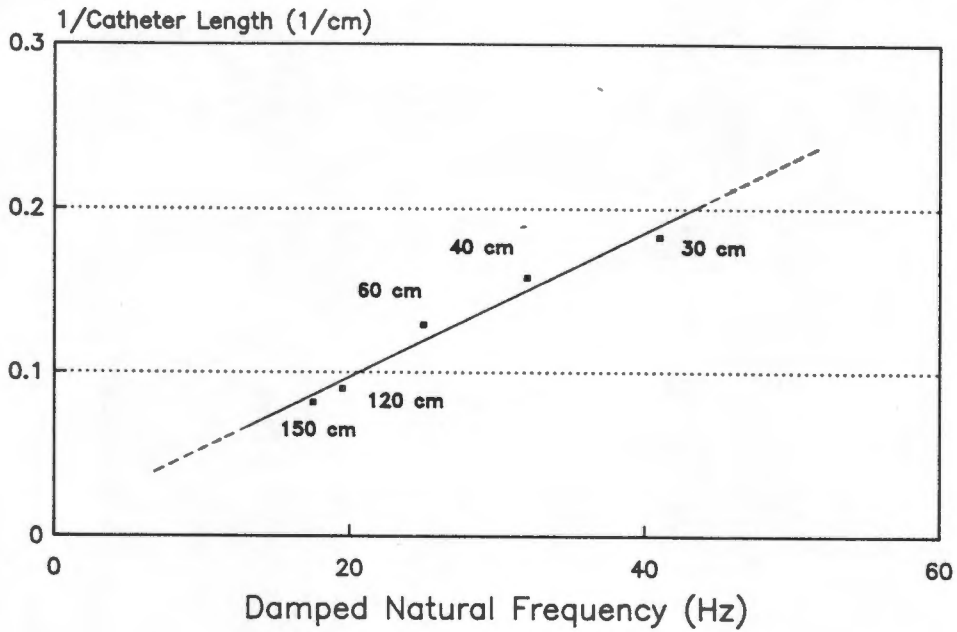


Figure 5.2

The relationship of pressure tube length and damped natural frequency. Minimum and maximum values indicate the range of f_d ($ID = E$).

Pressure tube length was inversely related to damped natural frequency for all pressure lines tested as shown in figure 5.3.

**Pressure Tubing
DNF vs. Catheter Length**



boiled saline, 25 C

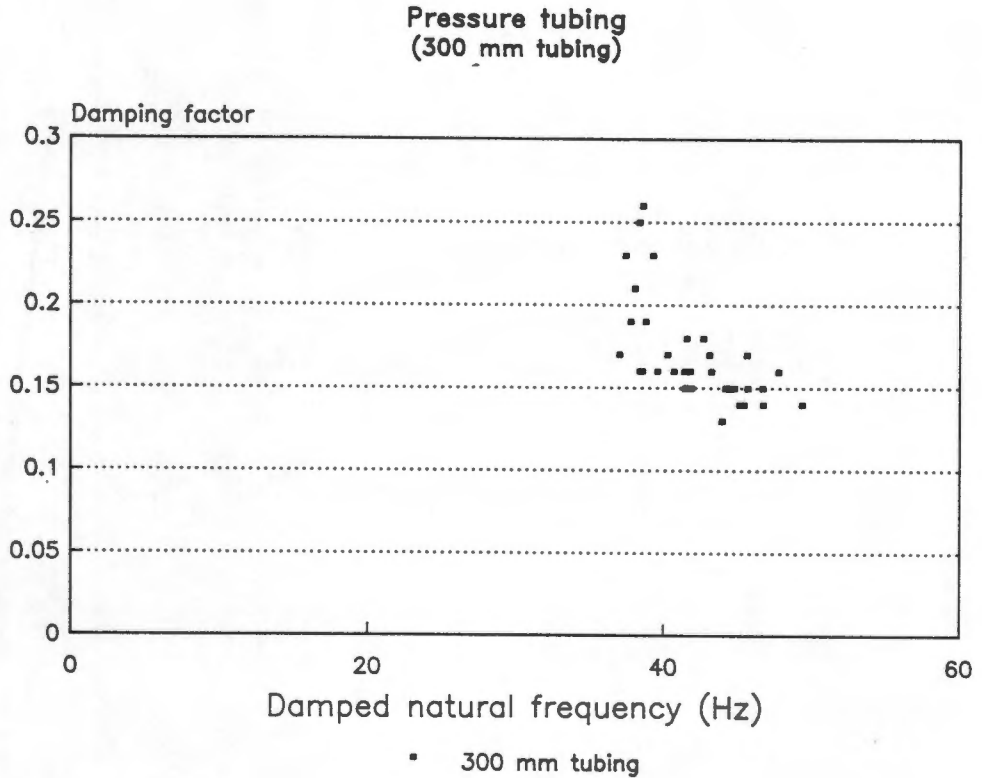
Figure 5.3

A plot of damped natural frequency vs. the inverse of tube length.

5.2.1.4 Relationship of the damping factor and damped natural frequency.

Figure 5.4 shows damping factor versus the damped natural frequency for different pressure tubing (ID's: A,B,H,I,J,C and G) of 300 mm length. All data points are represented in this figure to indicate the spread of results. Figure 5.5 shows the inverse relationship of damping factor vs. damped natural frequency for 300 mm and 1200 mm pressure tubing.

Table G2.2 lists the ranges and standard deviations of damped natural frequency and damping factors represented in the figures 5.4 and 5.5.

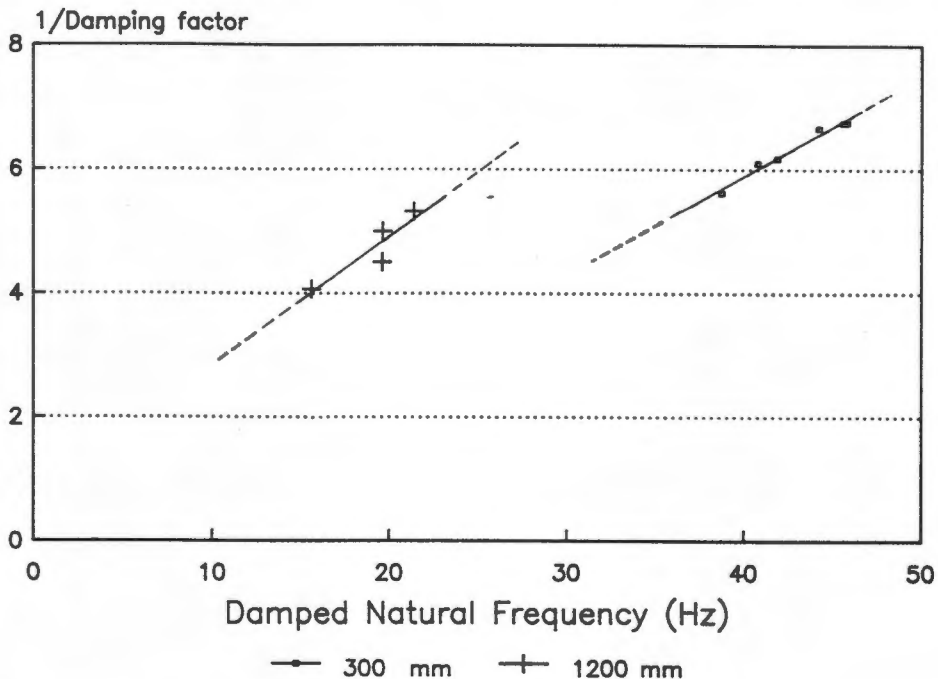


boiled saline, 25 degrees C

Figure 5.4

Relationship between the damping factor and the damped natural frequency for pressure tubing of 300 mm length (ID = E).

Pressure tubing
(300 mm and 1200 mm pressure tubing)



boiled saline, 25 degrees C

Figure 5.5

Inverse of damping factor vs. damped natural frequency. Data points represent the mean values for the different pressure tubing tested.

5.2.1.5 Effect of pressure tubing radius ratio on the damped natural frequency and damping factor

Pressure lines made of different materials but with similar lumen diameters were not available and thus the relationship between damped natural frequency and material could not be established exactly. It was however possible to predict that stiffer materials than polyethylene and polypropylene, such as Teflon and Teflon FEP, had higher damped natural frequencies by calculating

the radius ratio. This radius ratio (the ratio of the lumen radius to that of the outer radius) was then plotted against the damped natural frequency (figure 5.6) for pressure lines of different materials. Table G1.1, in appendix G, lists the radius ratio for different lengths of pressure tubing.

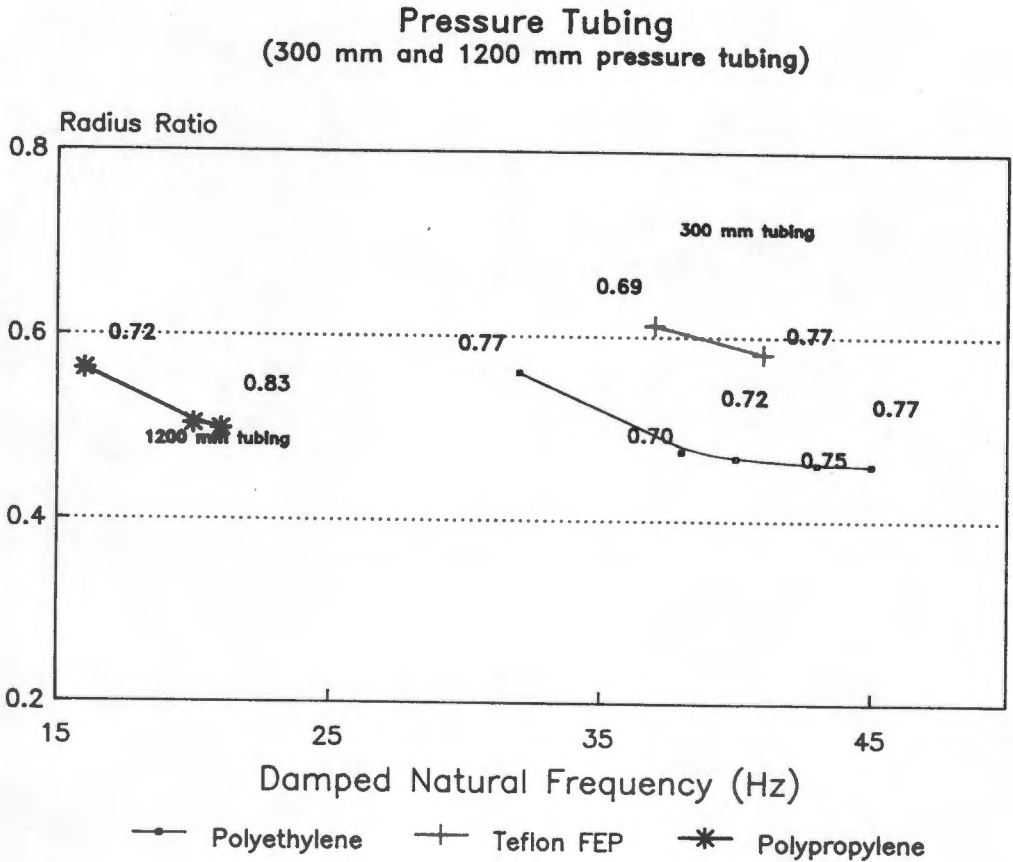


Figure 5.6

Damped natural frequency vs. radius ratio (for different materials). Values in the graph represent the lumen radius of the pressure lines.

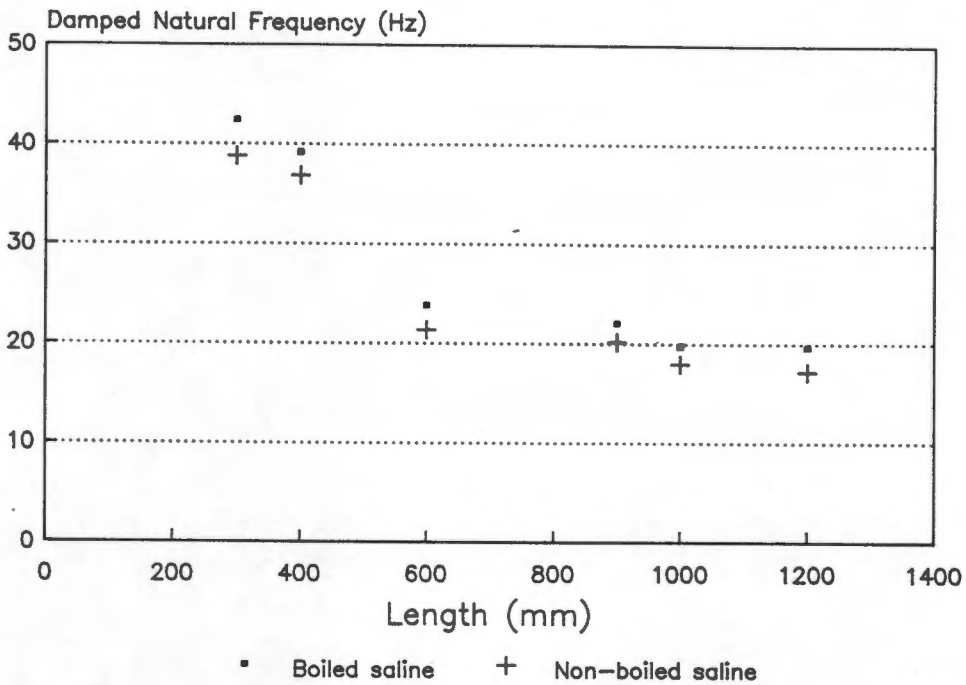
It is apparent from the graph that for any series the damped natural frequency is raised if the radius ratio is decreased, provided the internal diameter of the pressure tube is enlarged

simultaneously. The reason for this behaviour is that for a decrease of radius ratio (the wall thickness is increased) the compliance of the tube is lowered. This decrease in compliance of the tube has a higher damped natural frequency as a result (Shapiro and Krovetz, 1970). The simultaneous increase of the internal diameter furthermore guarantees a better frequency response, as stated in section 5.2.2 and seen from figure 5.6. As an example, a polyethylene pressure tube (ID = I) with a radius ratio of 0.582 and a damped natural frequency of 32 Hz was compared to a Teflon pressure line (ID = C) with a radius ratio of 0.565. The difference in radius ratio was less than 3 percent and was ignored. Both tubes had an internal radius of 0.77 mm and it was measured that the Teflon pressure tube had a damped natural frequency of 40.8 Hz. This indicates that the damped natural frequency is higher for stiffer material for the same radius ratio and internal diameter.

5.2.1.6 Effect of boiled and non-boiled saline on the damped natural frequency.

Figure 5.7 shows that the damped natural frequency is higher (mean = 2.4 Hz, SD = \pm 0.64, range = 1.8-4.0 Hz) for pressure tubing tested (ID = E) with boiled saline than that using non-boiled saline. The results are listed in table G2.6 for boiled saline and in table G2.7 for non-boiled saline.

**Pressure tubing
boiled vs non-boiled saline**



25 degrees C

Figure 5.7

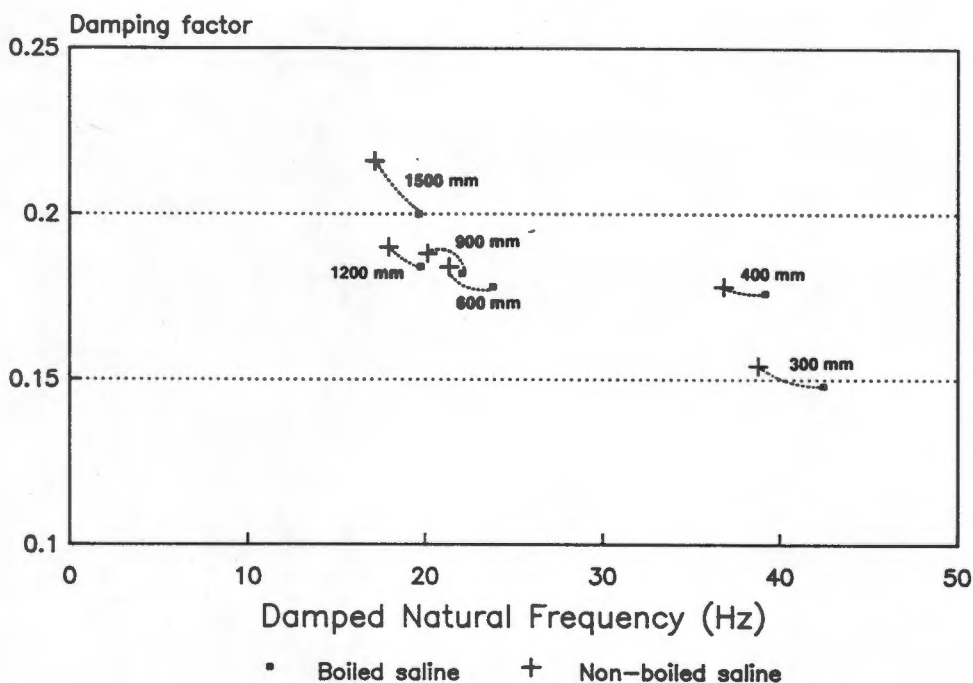
Damped natural frequency vs. pressure tubing length for boiled and non-boiled saline.

Figure 5.8 shows the damped natural frequency vs. the damping factor for pressure tubing of different lengths (for non-saline and boiled saline).

This decrease in damped natural frequency is in the range of 5 to 10 percent while the increase in damping factor is in the range of 2.0 to 2.7 percent.

In figure 5.8 the dotted line connects the average data values for pressure tubing of the same length. The data points are obtained from tables G2.6 and G2.7.

**Pressure tubing
(boiled / non-boiled saline)**



25 degrees C

Figure 5.8

Damping factor vs. damped natural frequency for different lengths of pressure tubing. Boiled and non-boiled saline.

5.2.1.7 Effect of twisting and coiling of pressure tubing on the damped natural frequency.

Table 5.2(a) lists the average values for damped natural frequencies and damping factors for all 300 mm and 1200 mm pressure tubing tested. The complete listing of f_d and β for the individual pressure tubes is given in table G2.2. Values in table 5.2(a) are used to calculate the changes in damped natural frequency and damping factor in table 5.2(b).

l (mm)	Damped natural frequency			Damping factor		
	range	SD	mean	range	SD	mean
Pressure tubing straight						
300	38.4-45.8	± 3.09	42.2	0.15-0.25	± 0.033	0.17
1200	15.6-21.4	± 2.46	19.1	0.19-0.25	± 0.026	0.22

Table 5.2(a)

Damped natural frequencies (Hz) and damping factors for 300 mm and 1200 mm pressure tubing.

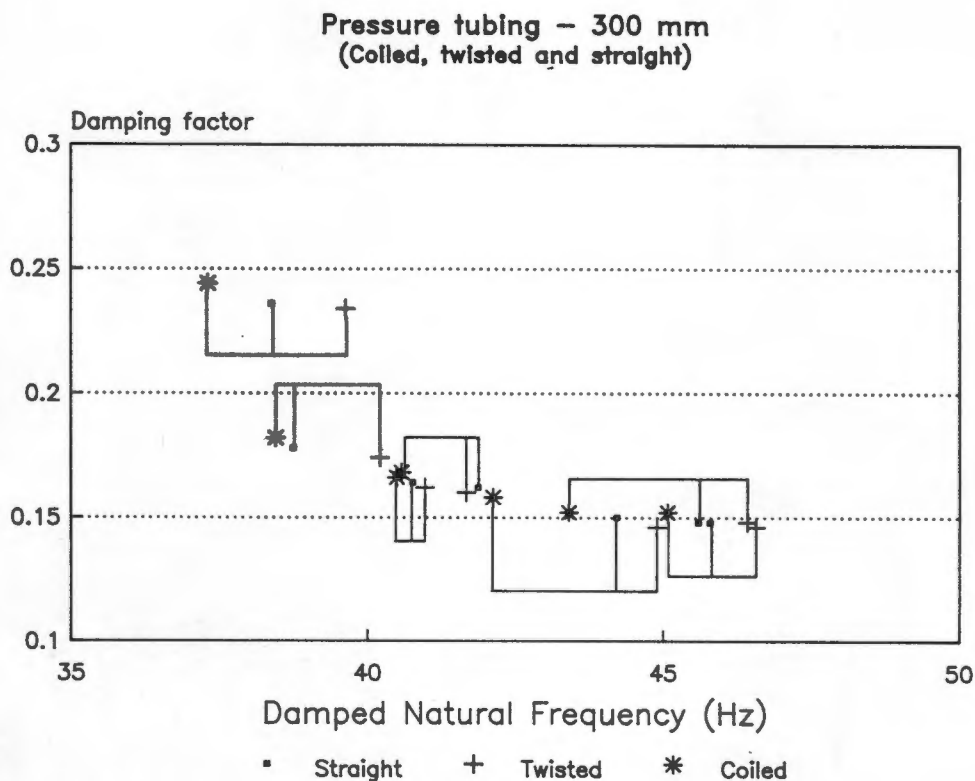
l (mm)	Change in f_d			Change in β		
	range	SD	mean	range	SD	mean
Pressure tubing coiled around a 8 cm diameter cylinder						
300	-0.2 < -2.2	±0.806	- 1.10	0.002 >0.012	±0.003	+0.003
1200	-0.6 < -1.6	±0.440	- 1.10	0.004 >0.009	±0.002	+0.003
Pressure tubing coiled around a 15 cm diameter cylinder						
300	-0.2 < -1.9	±0.492	-0.82	0.002 >0.004	±0.002	+0.002
1200	-0.3 < -1.3	±0.427	-0.76	0.001 >0.007	±0.004	+0.003
Pressure tubing twisted through 720 °						
300	+1.3 > +3.3	±0.833	+2.00	-0.004 <-0.011	±0.006	-0.006
1200	+1.0 > +2.6	±0.700	+1.75	-0.002 <-0.010	±0.005	-0.005

Table 5.2(b)

Decrease (-)/increase(+) in damped natural frequency and damping factor for tests indicated.

Coiling of 300 mm pressure tubing around an 8 cm diameter cylinder decreased the damped natural frequency by average of 2.6 percent while the damping factor increased by 1.8 percent. After coiling a 300 mm pressure tube around a 15 cm diameter cylinder, f_d only decreased by and average of 1.9 percent and β increased by 1.6 percent. Twisting the pressure tube through 720 ° around

its longitudinal axis increased f_d by 10.5 percent and β decreased by 3.5 percent. Similar results were found for pressure tubing of 1500 mm length.



boiled saline, 25 degrees C

Figure 5.9

Frequency response of twisted, coiled and straight pressure tubing. Identical systems are joined by solid lines.

Figure 5.9 represents the effect of twisted, coiled and straight pressure tubing (300 mm) on the damping factor and damped natural frequency. Connecting lines indicate which data points on the graph represent the same tubing.

5.2.2 Catheters

5.2.2.1 Effect of stopcocks and flush devices on the damped natural frequency

The effect that the addition of stopcocks and flush devices have on the damped natural frequency and damping factor is indicated in table 5.3 and G2.8.

ID	f_{d1} (Hz)	β_1 ($\times 10^{-2}$)	f_{d2} (Hz)	β_2 ($\times 10^{-2}$)
A	44.2 (± 2.28)	0.15 (± 0.60)	29.8 (± 0.22)	0.23 (± 0.68)
C	49.1 (± 1.33)	0.16 (± 0.40)	27.5 (± 0.50)	0.29 (± 0.55)
I	45.8 (± 1.06)	0.15 (± 0.74)	27.1 (± 0.24)	0.29 (± 0.79)
G	40.8 (± 1.36)	0.16 (± 1.04)	30.9 (± 0.26)	0.25 (± 1.04)
E	19.7 (± 0.38)	0.20 (± 1.02)	16.6 (± 0.34)	0.19 (± 0.38)
K	21.4 (± 1.26)	0.19 (± 0.45)	15.9 (± 0.53)	0.19 (± 0.34)
L	15.6 (± 0.93)	0.25 (± 0.44)	15.3 (± 0.40)	0.29 (± 0.61)
F	12.9 (± 1.52)	0.21 (± 0.74)	12.3 (± 0.48)	0.32 (± 1.37)

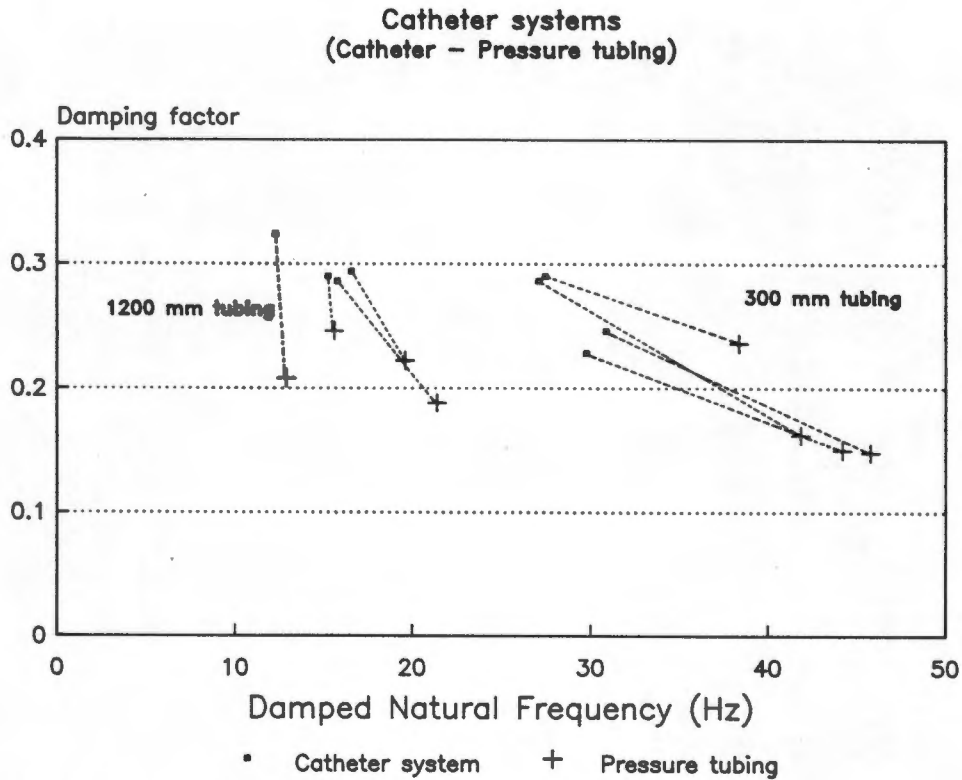
Table 5.3

The change in frequency response, for systems connected to stopcocks, flushing devices and intraflows. Subscript 1 denotes frequency response for pressure lines only and subscript 2, for pressure tubing connected to a stopcock which is connected to a flush device. The values in brackets represent the standard deviation.

Damped natural frequency decreased significantly with the addition of the above mentioned devices. The average decrease in damped natural frequency for catheters (pressure tubing = 300 mm) was 36 percent (mean = 16.15 Hz, SD = ± 5.11). The damping factor increased by 71 percent (mean = 0.11, SD = $\pm 2.91 \times 10^{-2}$). For catheters with 1200 mm pressure tubing the damped natural

frequency decreased by an average of 13.7 percent (mean = 2.38 Hz, SD = ± 2.43) and the damping factor increased by 13.6 percent (mean = 0.041 Hz, SD = $\pm 4.90 \times 10^{-2}$).

These results are graphically presented in figure 5.10.



Boiled saline, 25 degrees C

Figure 5.10

Graph indicating the decrease in damped natural frequency and the increase in damping factor for pressure tubing compared to pressure tubing with additions.

5.2.3 Cannulae

5.2.3.1 Effects of cannula lumen diameter on the damped natural frequency.

Table G2.9 in appendix G lists the dimensions of cannulae tested, whereas table G2.10 lists the frequency response parameters of the cannulae. The frequency response parameters of cannulae exerted to 100 mmHg external pressure is listed in table G2.11. This was achieved by inserting a cannula in a tube and pressurising the saline between tube and cannula to 100 mmHg.

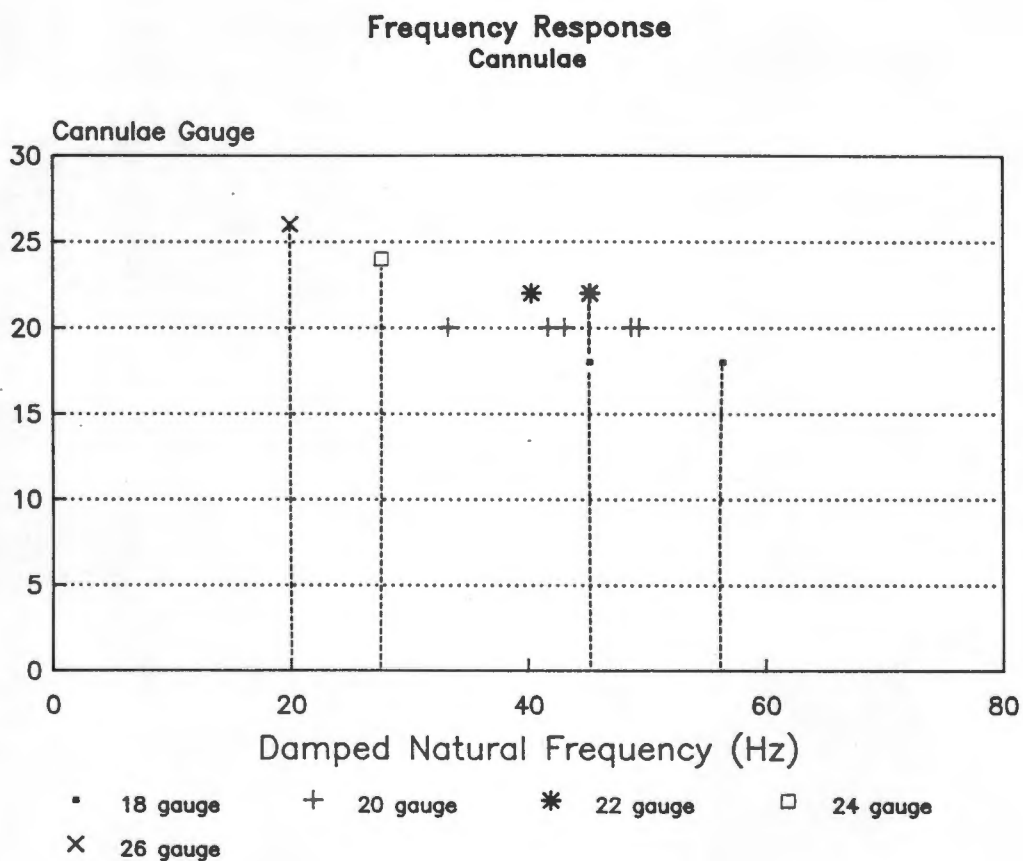


Figure 5.11

Relationship between damped natural frequency and cannulae gauge. Vertical lines represent the maximum damped natural frequency for the individual cannulae gauge.

Figure 5.11 shows that with an increase of cannula lumen radius or a decrease in cannula gauge, the damped natural frequency increased. The dotted lines represent the maximum damped natural frequency obtained by the individual cannulae.

The relationship of internal diameter and damped natural frequency is linear and is shown in figure 5.12.

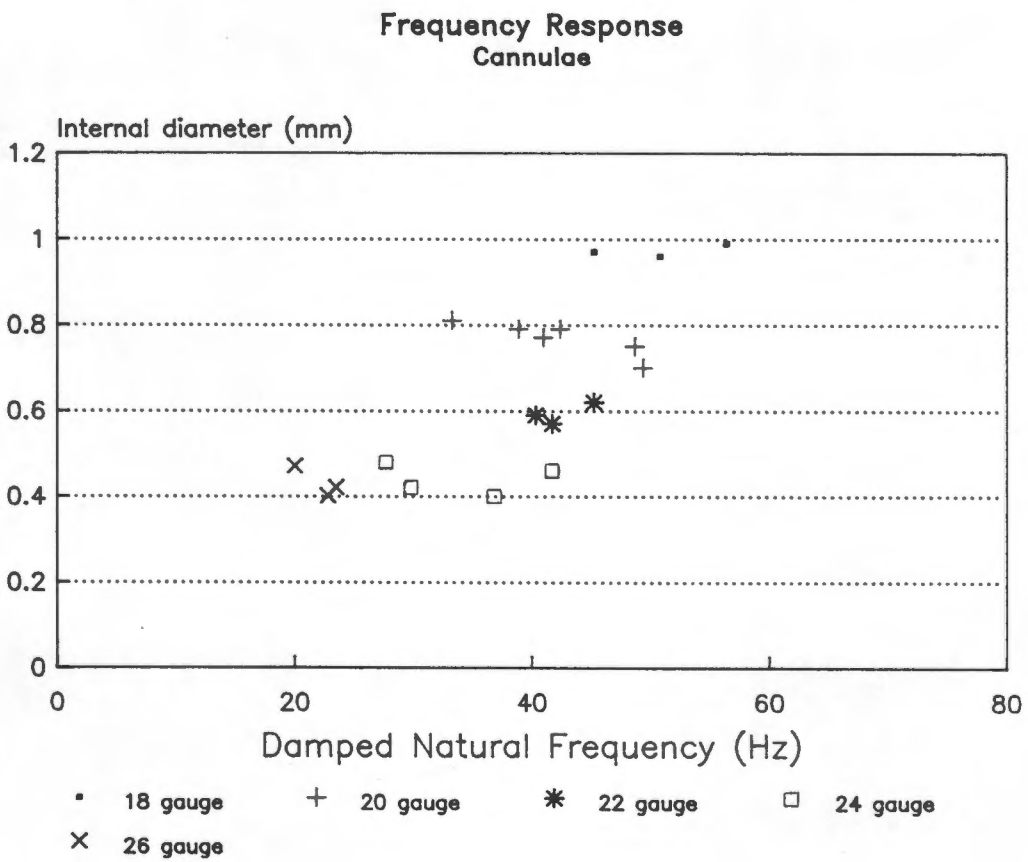


Figure 5.12

The relationship between the internal diameter and the damped natural frequency of cannulae.

5.2.3.2 Effect of cannula lumen diameter on the damping factor.

The damping factor increased and the damped natural frequency decreased for cannulae with reduced lumen diameter. This is shown in figure 5.13.

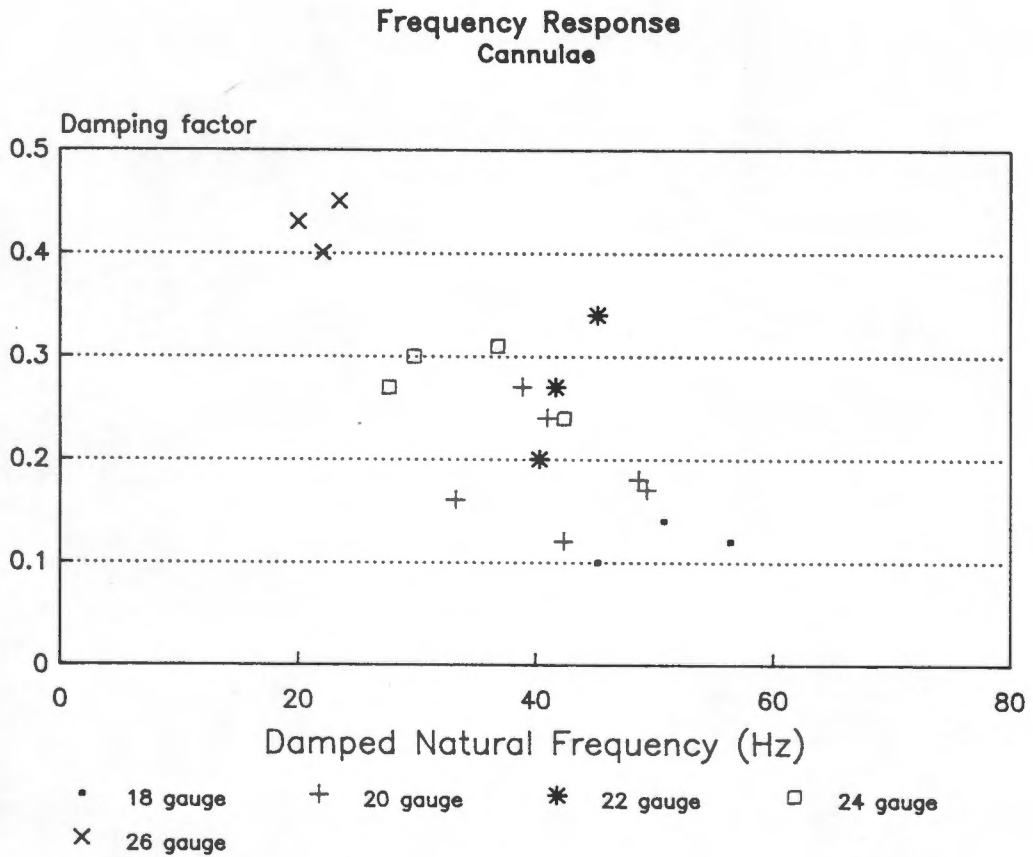


Figure 5.13

Damped natural frequency versus damping factor for different cannula gauges.

5.2.4 Catheter-manometer systems

5.2.4.1 Damped natural frequency and damping factor in catheter-manometer systems with different pressure tubing length.

After connecting a cannula to the system described in section 5.2.2, the damped natural frequency decreased even further. In tables G2.12(a) and G2.12(b) the results for various combinations of cannulae and pressure tubing systems (pressure tubing, stopcocks and flushing device) are given.

Catheter-manometer systems 20 gauge cannulae - boiled saline

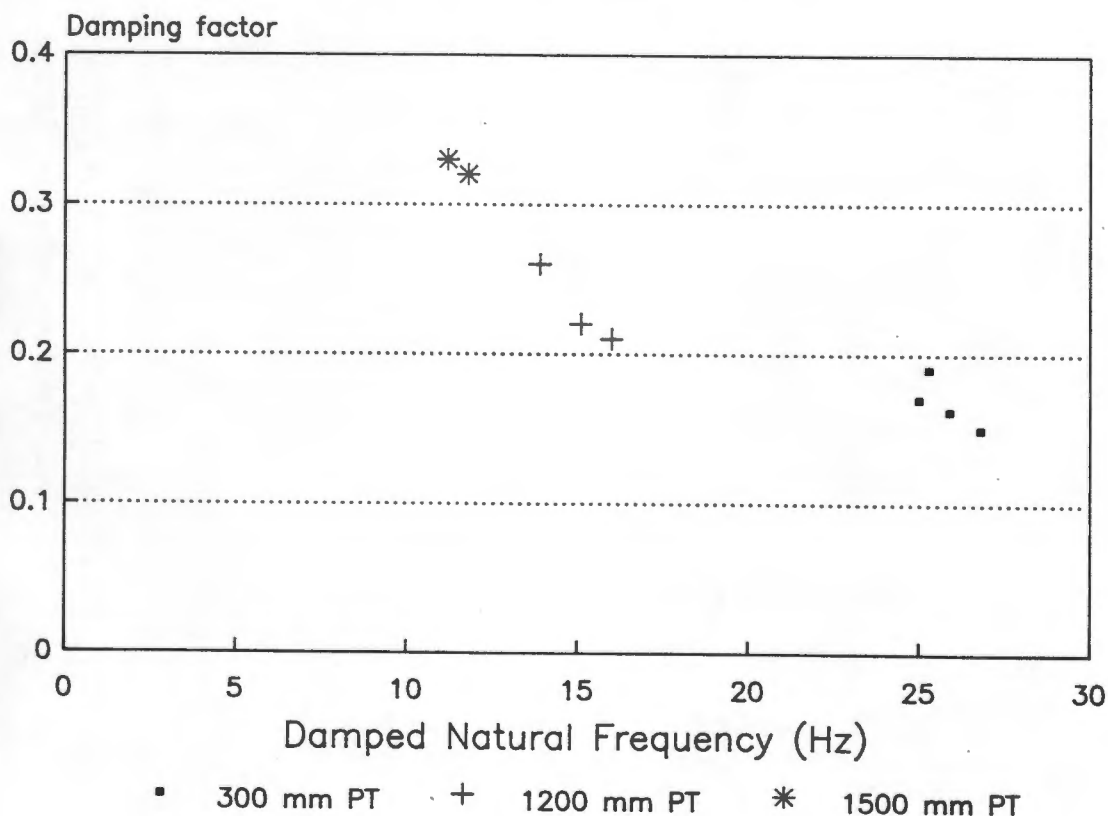


Figure 5.14

Frequency response parameters for catheter-manometer systems with pressure tubing of increasing length. A 20 gauge cannula is used.

Figures 5.14, 5.15 and 5.16 present the damped natural frequency versus the damping factor of catheter-manometer systems for 20 gauge, 22 gauge and 24 gauge cannulae respectively.

**Catheter-manometer systems
22 gauge cannulae - boiled saline**

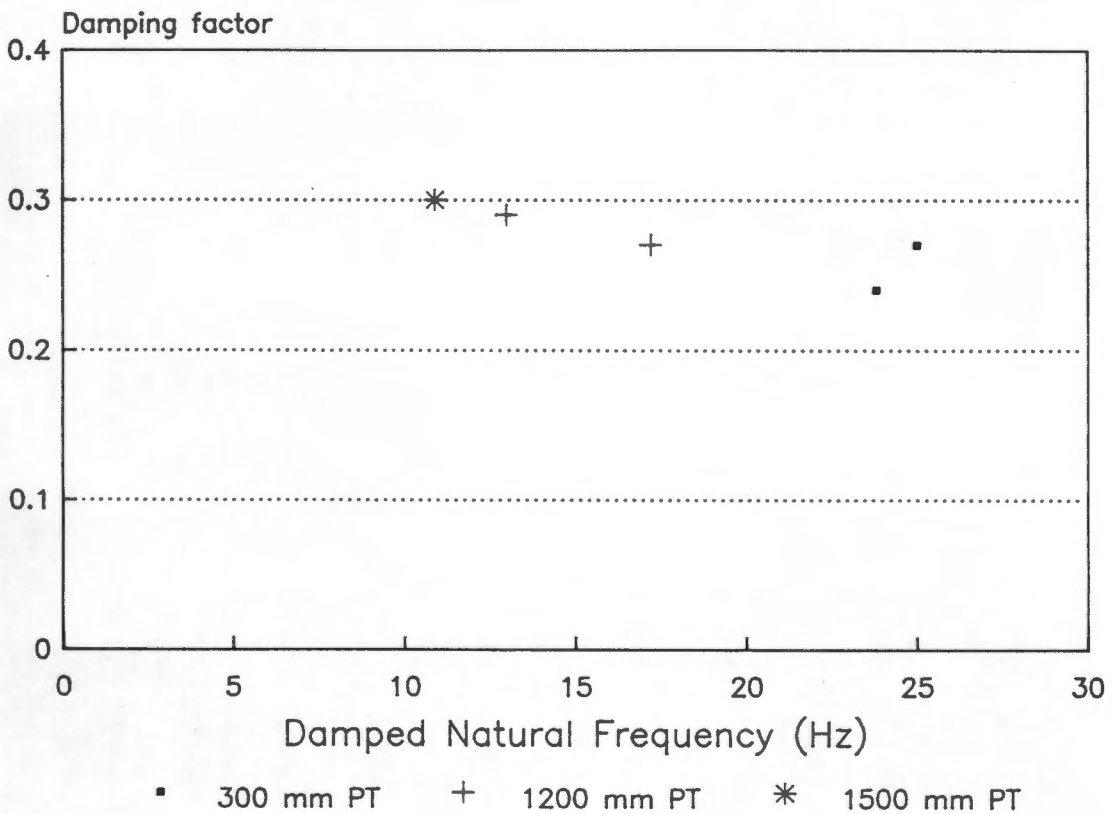


Figure 5.15

Frequency responses for catheter-manometer systems for pressure tubing of increased length. A 22 gauge cannula is used.

Catheter-manometer systems
24 gauge cannulae - boiled saline

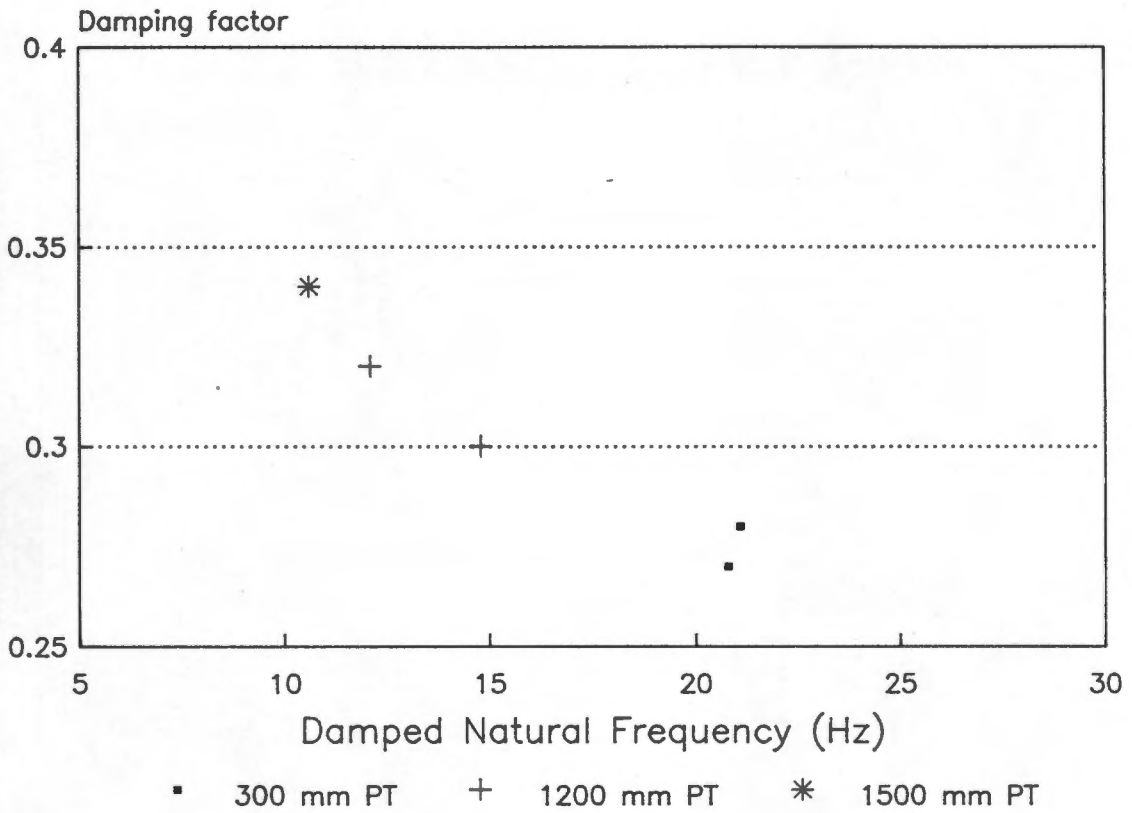


Figure 5.16

Frequency responses for catheter-manometer systems for pressure tubing of increased length. A 24 gauge cannula is used.

5.2.4.2 The effect of cannulae gauge and pressure tubing length on the damped natural frequency of catheter-manometer systems.

In figure 5.17, frequency response parameters of catheter-manometer systems for increased pressure tubing length and cannulae gauge are shown.

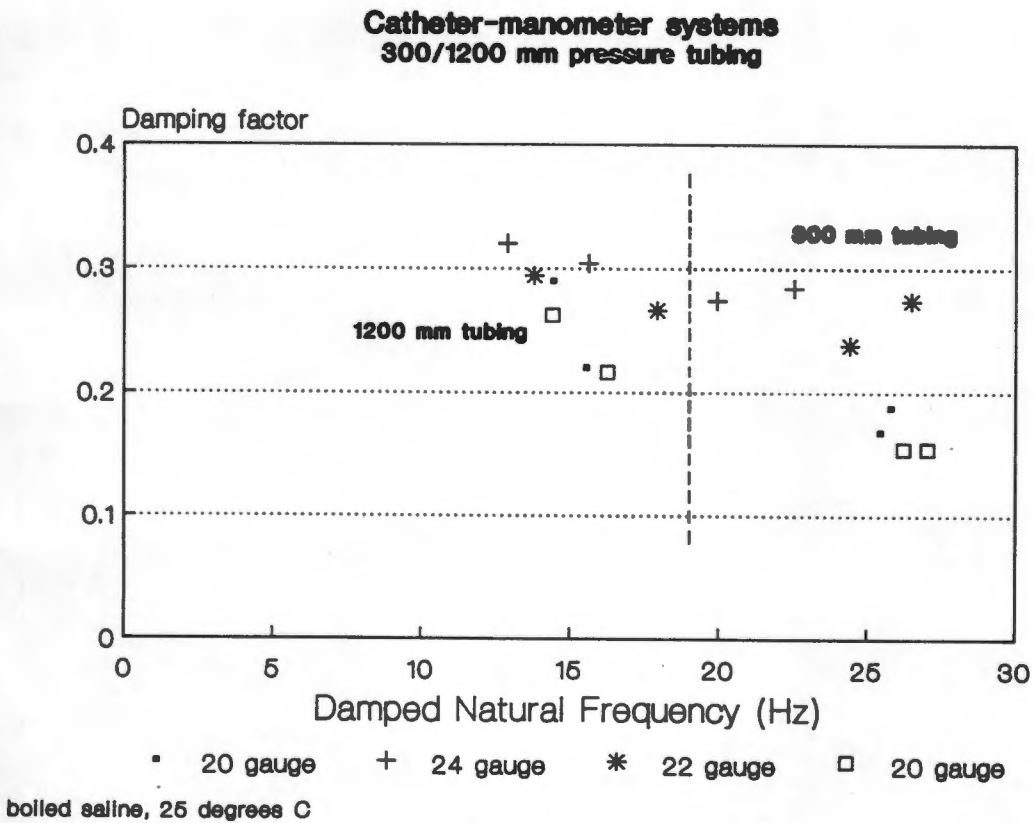


Figure 5.17

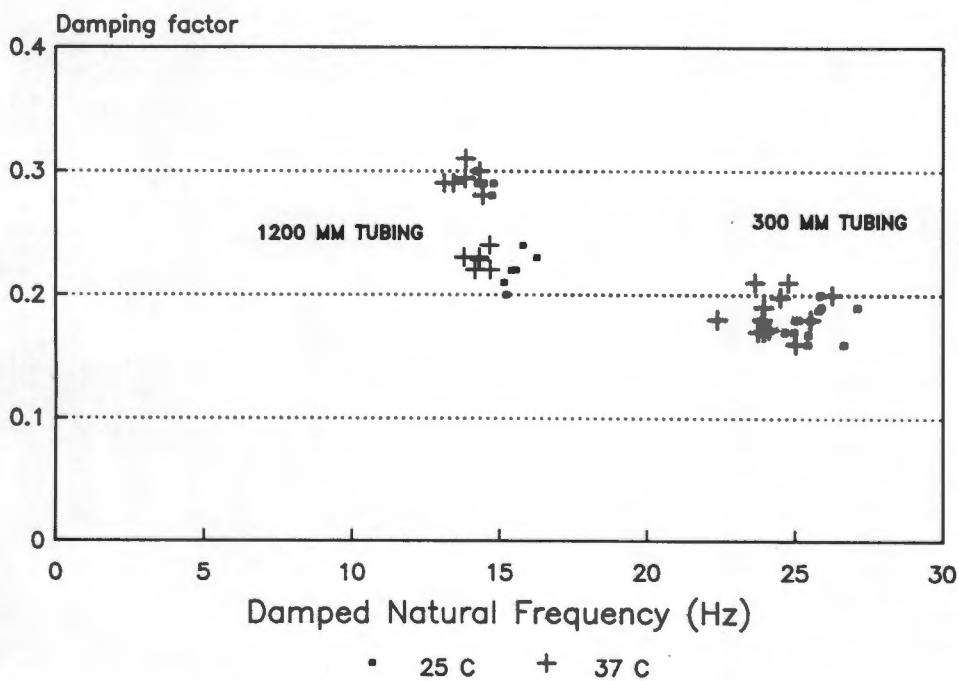
Damped natural frequency versus damping factor for catheter-manometer systems with different cannulae gauges and pressure tubing length.

5.2.4.3 Effect of saline temperature on the frequency response parameters of catheter-manometer systems.

Table G2.14(a) and G2.14(b) lists the frequency response parameters obtained by testing the effect of saline temperature (boiled and debubbled and used at 37 °C and 25 °C) within the catheter-manometer system.

The saline container, pressure tubing, stopcocks and flush device were placed in a flask which was filled with saline at the required temperature, twenty minutes before testing. This ensured

**Catheter-manometer systems
(boiled saline at 25 C and 37 C)**



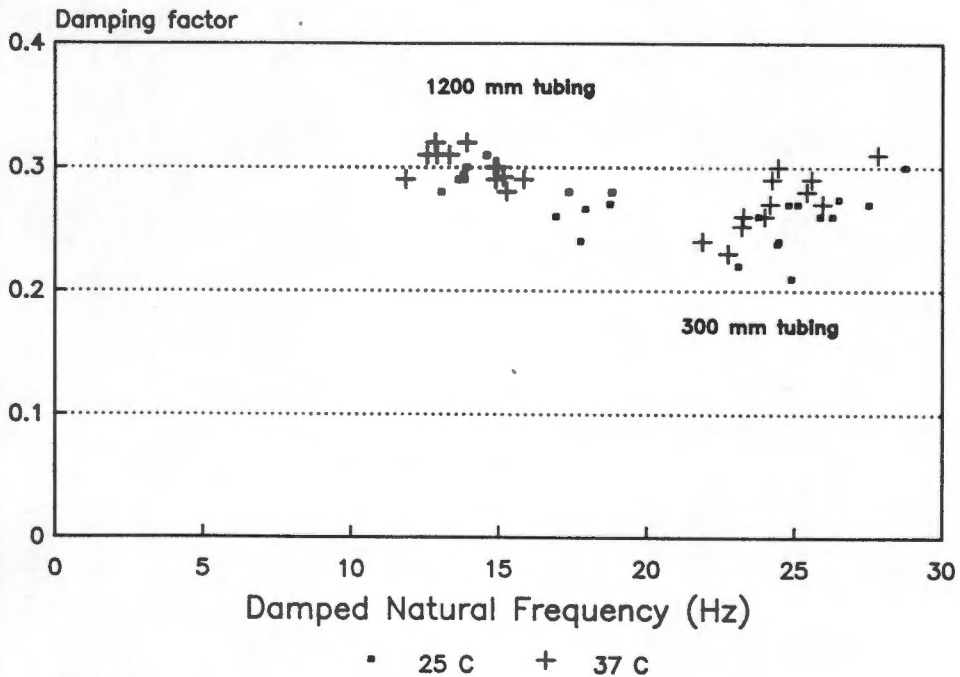
20 gauge cannula - 300/1200 mm tubing

Figure 5.18

Damped natural frequency for catheter-manometer systems (20 gauge cannula) at a temperature of 25 °C and 37 °C. All data points are displayed.

that the test system was at the same temperature as the saline. The temperature in this flask was then continuously measured and maintained (by a laboratory heater) during the testing procedure. Figure 5.18, 5.19 and 5.20 show that the damped natural frequency decreases if the saline temperature is increased from 25 °C to 37 °C.

**Catheter-manometer systems
(bolloed saline at 25 C and 37 C)**

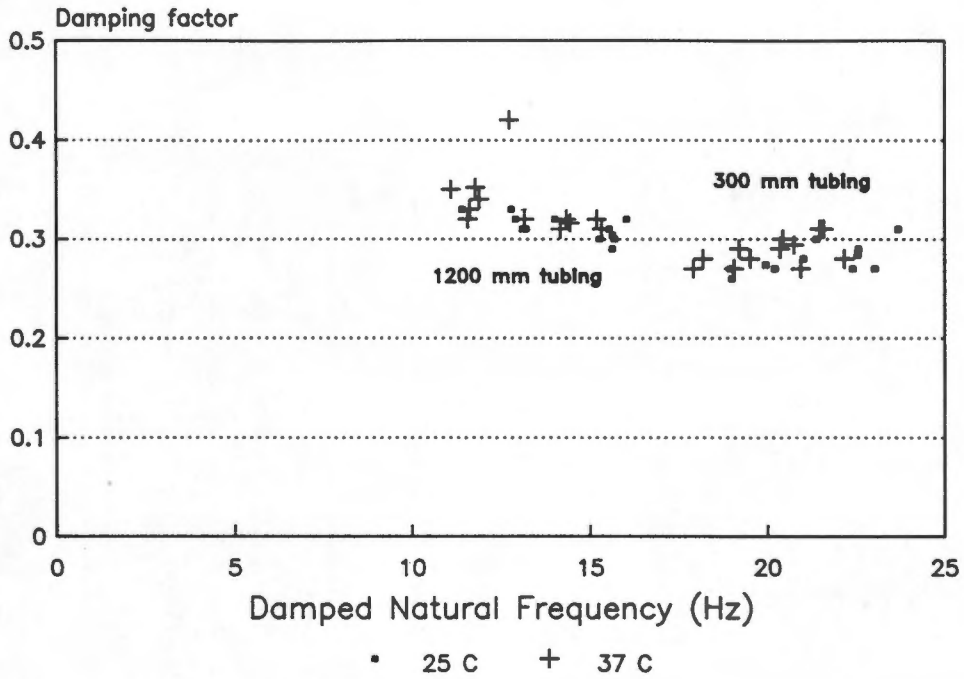


22 gauge cannula - 300/1200 mm tubing

Figure 5.19

Damped natural frequency for catheter-manometer systems (22 gauge cannula) at a temperature of 25 °C and 37 °C. All data points are displayed.

Catheter-manometer systems
(bolloed saline at 25 C and 37 C)



24 gauge cannula - 300/1200 mm tubing

Figure 5.20

Damped natural frequency for catheter-manometer systems (24 gauge cannula) at a temperature of 25 °C and 37 °C. All data points are displayed.

5.2.4.4 Effect of boiled vs. non-boiled saline on the
frequency response parameters of catheter-manometer
systems.

Tables G2.13(a) and G2.13(b) list the damped natural frequency and damping factor for catheter-manometer systems obtained by using non-boiled saline. The damped natural frequency decreased as shown in figure 5.21.

Catheter-manometer systems
20 g cannulae - boiled/non-boiled saline
300 mm and 1200 mm tubing

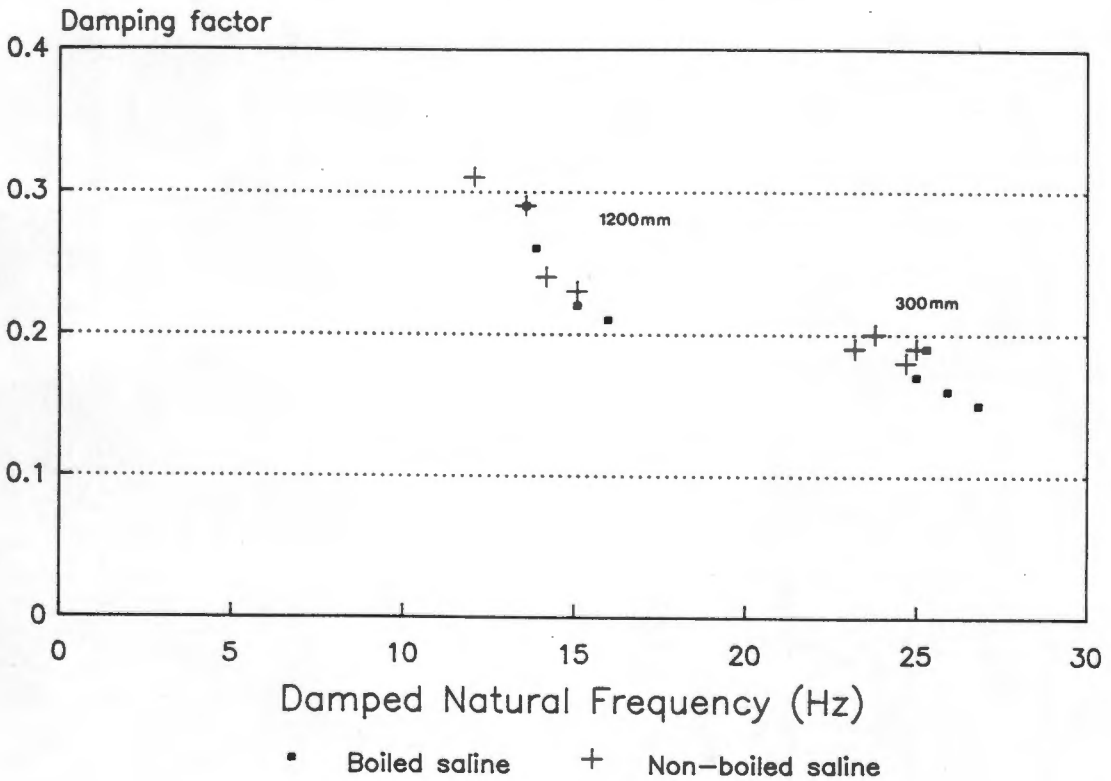


Figure 5.21

Damped natural frequency vs. damping factor for catheter-manometer systems (20 gauge cannula) for boiled and non-boiled saline.

5.2.5 Effect of different transducer and transducer domes on the frequency response of catheter-manometer systems.

Fox et al (1978) used the steady state method to establish the frequency response of transducers. They found that the bandwidth of transducers and pressure chambers tested ranged from 70 to 105 Hz. Fox et al, found that the bandwidth of the AME 840 transducer and pressure chamber was 71 Hz.

No attempt was made in this thesis to investigate and measure the effect of different transducer domes, membranes and transducers on the frequency response of catheter-manometer systems as this was beyond the scope of this thesis however: it was established that the bandwidth of both the transducer and pressure generator used for the in vitro tests was higher than 110 Hz.

5.3 IN VIVO RESULTS

5.3.1 Introduction

The recording system used for the blood pressure data acquisition was described in chapter 4. The blood pressure signals of eight patients were recorded on magnetic tape and subsequently digitised on the computer system.

The recording for each patient was done before the bypass period and consisted of five measurements trials for both a wide (1500mm pressure line) and narrow (300mm pressure line) bandwidth system. Each measurement consisted of two ten second recordings using the wide and narrow bandwidth systems, one directly following the other. During each measurement, the ventilator was disconnected from the patient to eliminate the influence of Valsalva. Furthermore, the patient was not touched during the recording period to prevent any artifact being recorded. The period between each measurement was about five minutes, this period depending on the operation and the anaesthesiologist's approval.

On displaying the recorded signal on the computer, for six patients, pulse alternans (figure 5.22) and atrial fibrillation (figure 5.23 - diagnosed with a reference to an ECG trace) were spotted. These variations in pulse waveform were not clearly visible on the display of the blood pressure monitoring system used in theatre and were thus unfortunately recorded. Calculation of the average waveform or pulse shape for the analysis process thus became extremely difficult and the procedure had to be repeated many times to obtain consistent values.

Appendix G3.1 lists the index and results of the in vivo tests.

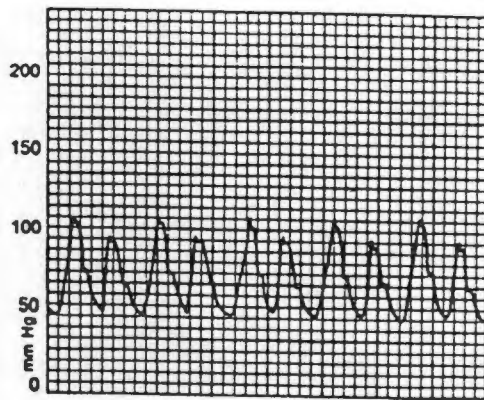


Figure 5.22

Pulse alternans

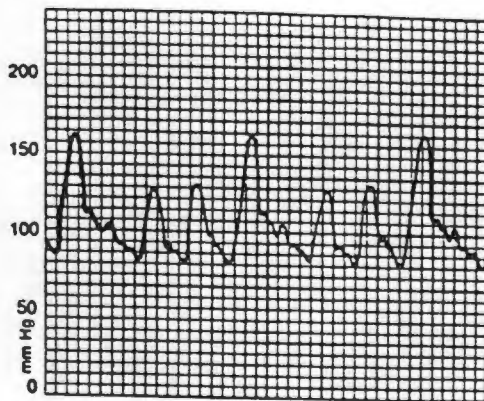


Figure 5.23

Atrial fibrillation

5.3.2 The frequency content of the recorded blood pressure waveforms.

The recorded blood pressure waveforms, revealed high frequency components irrespective of whether a wide or narrow bandwidth catheter-manometer system was used. The signal components in the frequency domain are obtained by the Fourier transform of the time domain signal and typical examples are given in figure 5.24 and Figure 5.25, respectively.

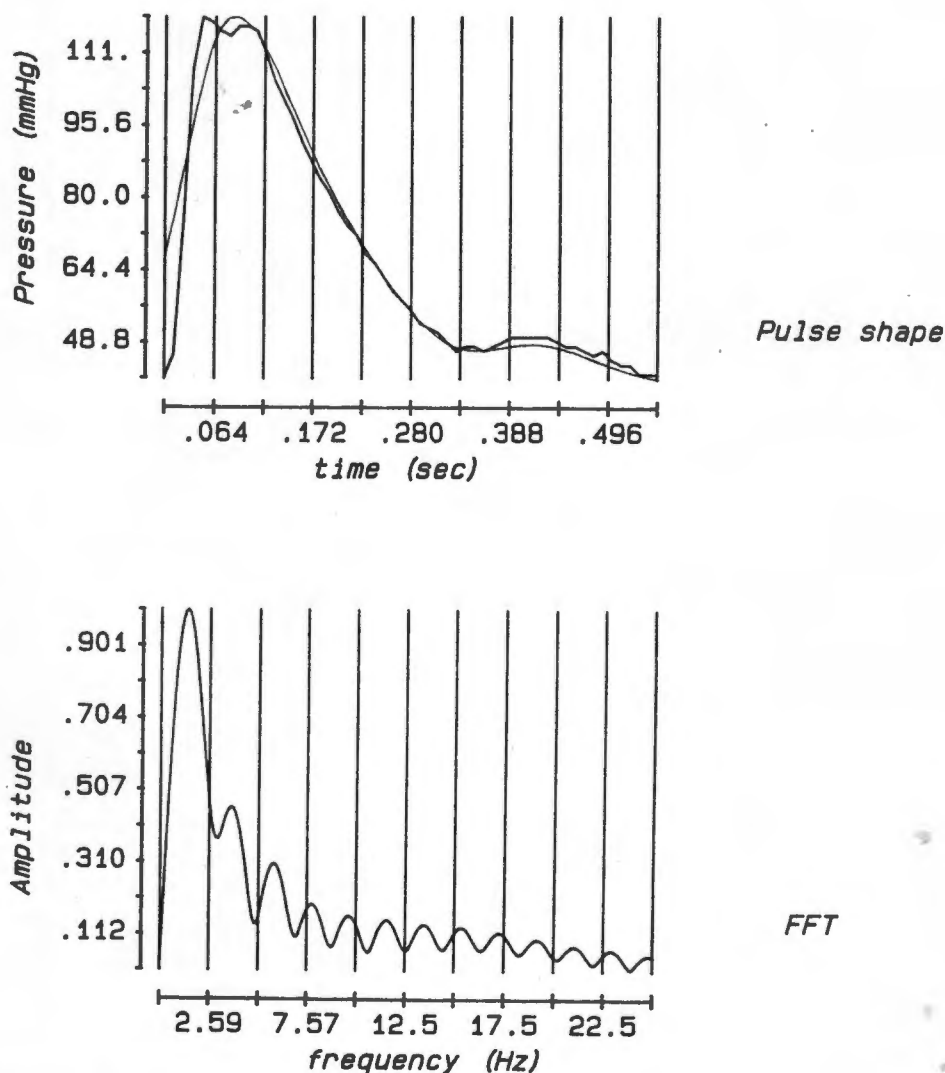
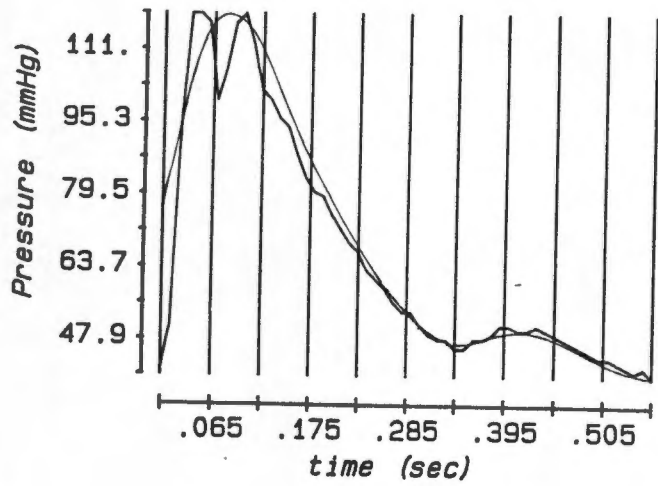
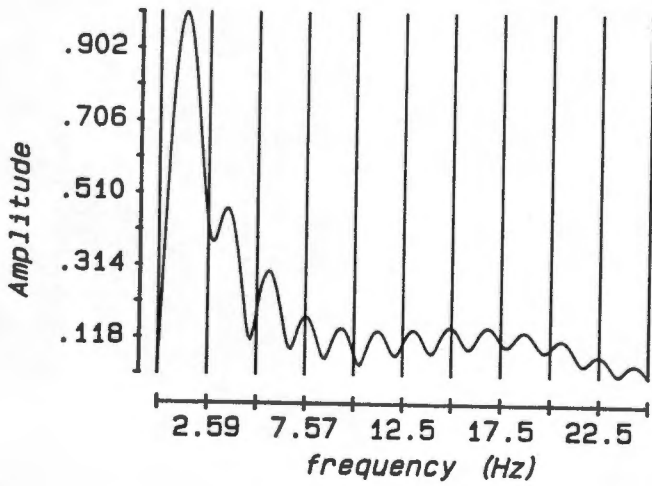


Figure 5.24

Fast Fourier transform (lower display) of a blood pressure pulse (upper display) measured by a catheter-manometer system with a damped natural frequency 24.9 Hz. Trace 2 in the upper display represents the low-pass (-3 dB = 33 Hz) filtered blood pressure waveform.



Pulse shape



FFT

Figure 5.25

Fast Fourier transform (lower display) of a blood pressure pulse (upper display) measured by a catheter-manometer system with a damped natural frequency 12.4 Hz. Trace 2 in the upper display represents the low-pass (-3 dB = 33 Hz) filtered blood pressure waveform.

5.3.3 Effect of low-pass filtering on the higher frequency components of the blood pressure pulse.

Filtering the blood pressure waveforms represented in figure 5.24 and figure 5.25, using a digital lowpass filter, for decreasing cutoff frequencies, it is possible to establish the effect of the higher frequency components mentioned above.

For the wide bandwidth catheter-manometer system (damped natural frequency of 24.9 Hz) the recorded pulse is filtered at 25 and 33 Hz. The resultant signal and corresponding Fast Fourier transform changed insignificantly from the unfiltered signal. Figure 5.26 represent the original and the filtered (cutoff frequencies set for 25 Hz and 33 Hz) blood pressure waveforms of figure 5.24. The FFT's of the waveforms in figure 5.26 are shown in figure 5.27.

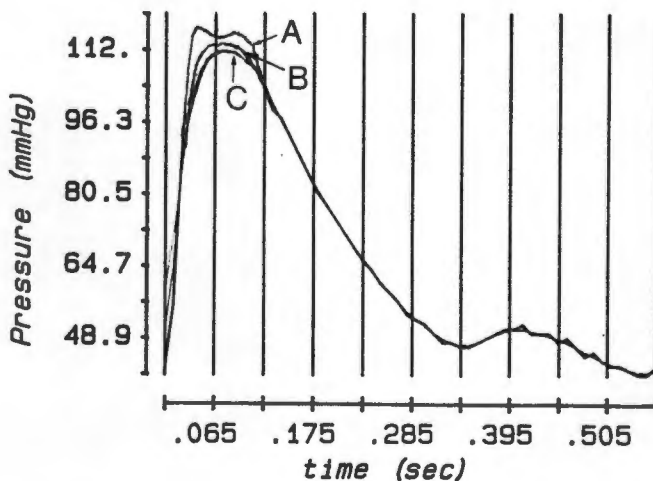


Figure 5.26

Unfiltered (A) and digital low pass filtered (cutoff frequency at 33 Hz (B) and 25 Hz (C)) blood pressure waveform.

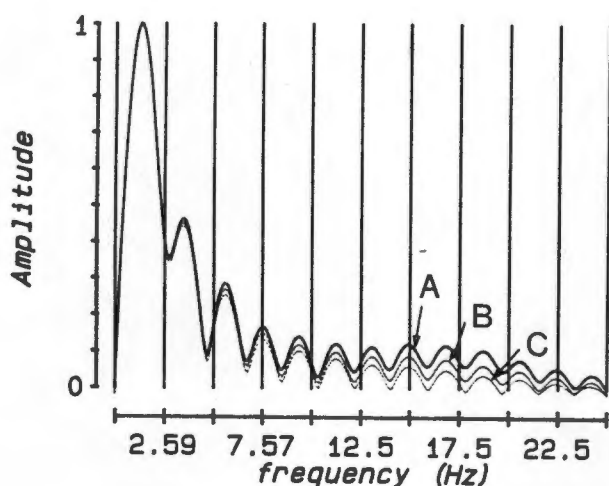


Figure 5.27

Fast Fourier transformation of the unfiltered (A) and digital low pass filtered (cutoff frequency at 33 Hz (B) and 25 Hz (C)) blood pressure waveform.

The narrow bandwidth catheter-manometer system (damped natural frequency of 12.4 Hz) waveforms are filtered by digital filters at cutoff frequencies of 17 and 25 Hz. The low cutoff frequency of 17 Hz (of the digital filter) represents the frequency at which more than 70 percent attenuation would occur for frequencies higher than 17 Hz being transmitted through the catheter-manometer system.

It is evident from the figures below that frequency components higher than 17 Hz are present in the blood pressure signals measured by narrow bandwidth catheter-manometer systems.

Figure 5.28 represents the filtered and unfiltered blood pressure signal of figure 5.25. The FFT of the blood pressure waveform shown in figure 5.28 is given in figure 5.29.

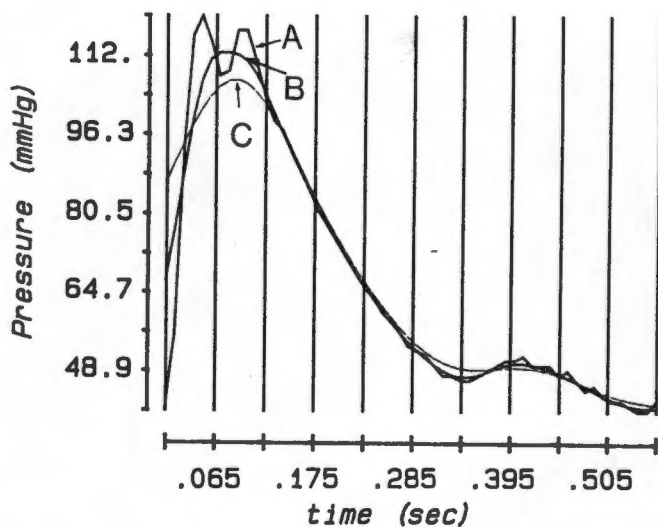


Figure 5.28

Low pass filtering at 17 Hz (B) and 25 Hz (C) for the blood pressure signal shown in figure 5.25.

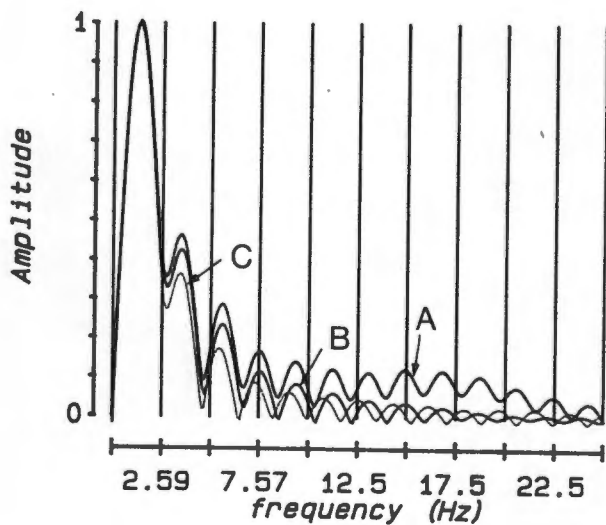


Figure 5.29

FFT of the blood pressure signals shown in figure 5.28.

5.3.4 Effect of wide and narrow bandwidth catheter-manometer systems on the blood pressure pulse.

Although the blood pressure waveform differed in all patients, there is an indication that there is a difference in pulse shape for systems of high and low resonant frequency. This change however, was dependent on the initial pulse shape and the heart rate, and varied notably from pulse to pulse and patient to patient. It was thus not possible to determine a specific relationship between catheter-manometer bandwidths and waveform contours.

In figure 5.30, a blood pressure pulse with a double peak recorded with a narrow bandwidth catheter-manometer system is shown. This double peak is clearly reduced for the wide bandwidth system.

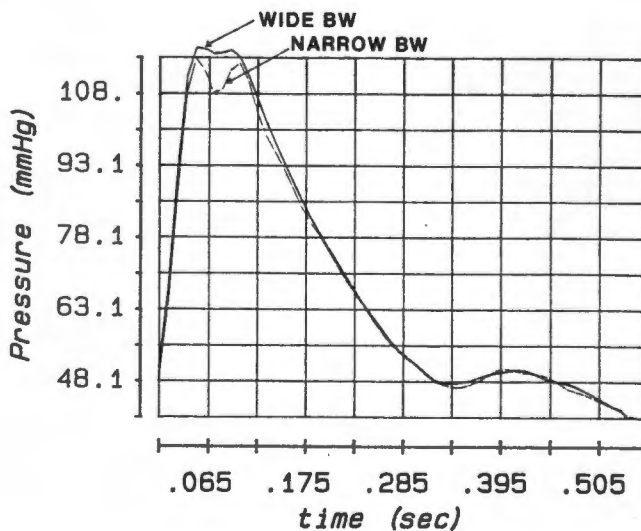


Figure 5.30

Double peak recorded with a narrow bandwidth catheter-manometer system.

5.3.5 Effect of fast heart rate on the pulse spectral characteristics for wide and narrow bandwidth catheter-manometer systems.

The effect of increased heart rate in the frequency domain results in the fundamental harmonic of the blood pressure signal being shifted to higher frequencies. The successive harmonics are shifted likewise and thus the bandwidth of the blood pressure signal for the same number of harmonics is increased.

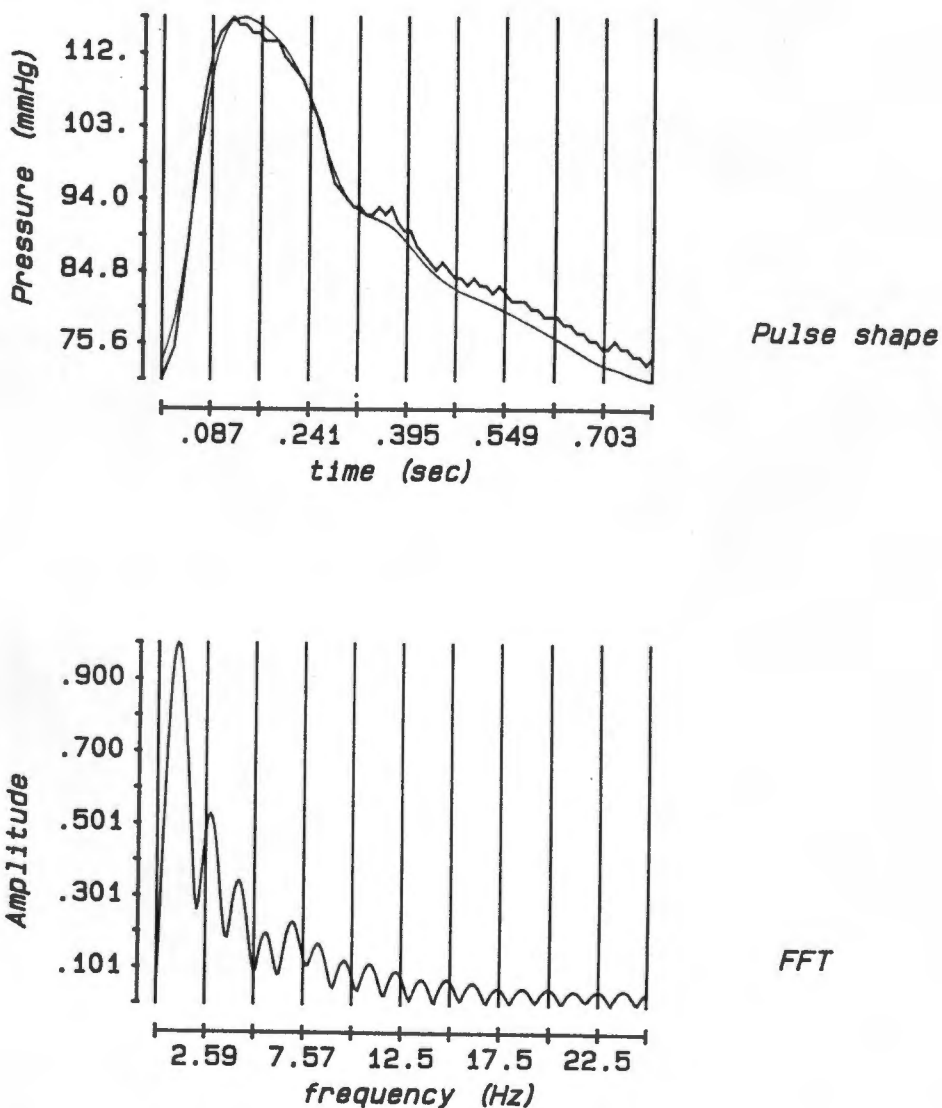


Figure 5.31

Frequency domain representation for a blood pressure pulse at 76 beats per minute.

Figures 5.31 and 5.32 show the waveform and Fourier transforms of a blood pressure pulse (from the same patient) for two different heart rates.

Appendix G3.2.2 lists the relative amplitudes of the frequency domain.

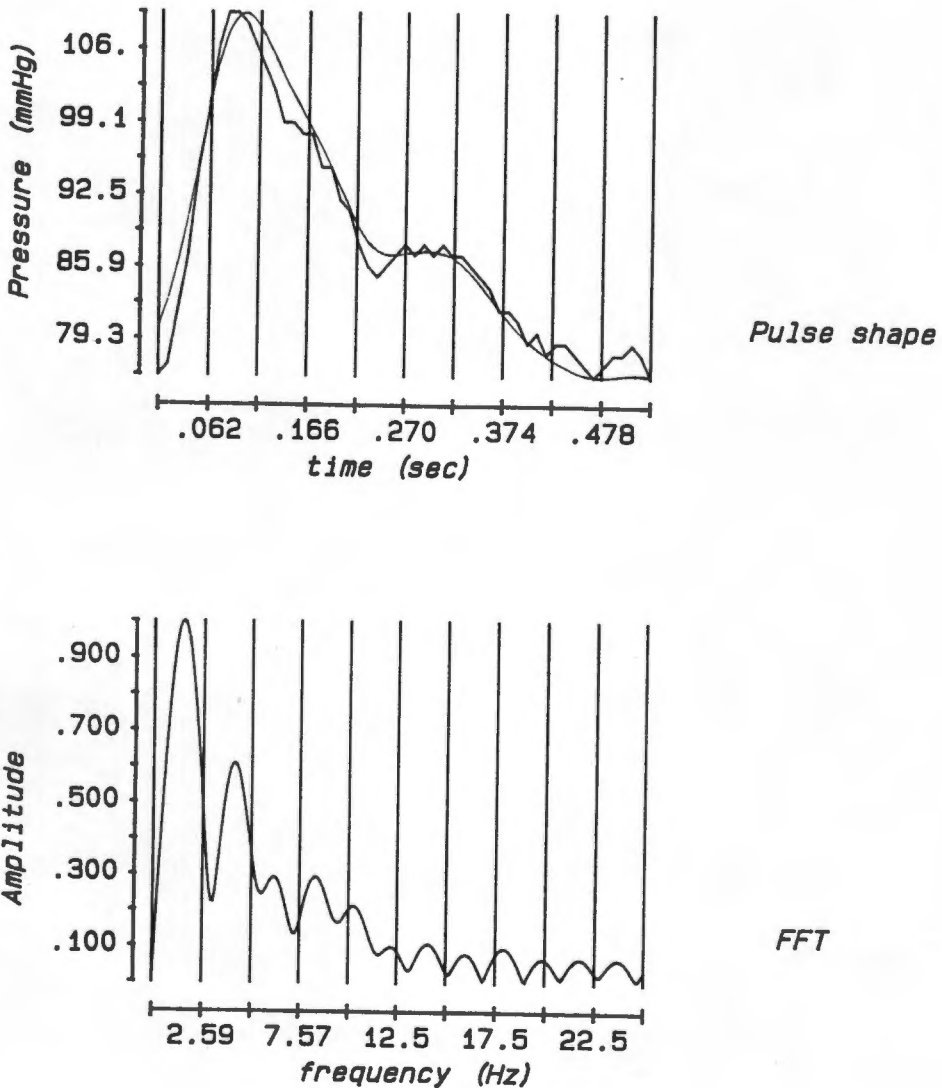


Figure 5.32

Frequency domain representation of a blood pressure pulse at 113 beats per minute.

5.3.6 Effect of wide and narrow bandwidth catheter-manometer systems on peak systolic and end diastolic blood pressures.

In 60 percent of the signals recorded (by a narrow bandwidth catheter-manometer system) the systolic peak pressure was higher than that recorded by a wide bandwidth catheter-manometer system.

Peak systolic blood pressures recorded by the narrow bandwidth catheter-manometer and that recorded by a wide bandwidth system is shown in figure 5.33.

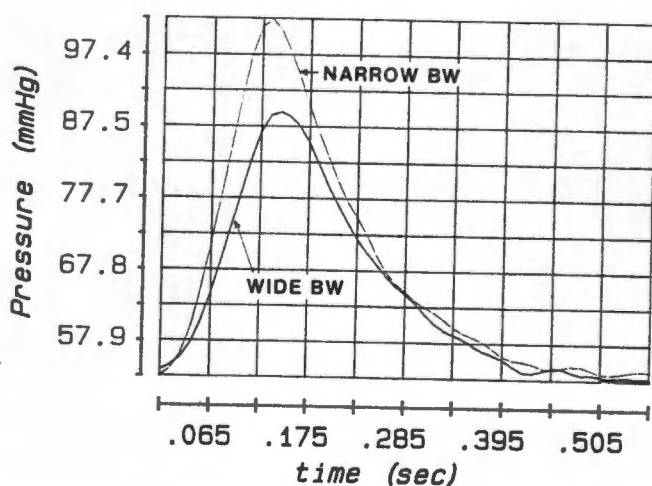


Figure 5.33

Peak systolic blood pressure for a narrow and wide bandwidth catheter-manometer system.

5.3.7 Effect of wide and narrow bandwidth catheter-manometer systems on maximum dp/dt

For blood pressure signals with a heart rate lower than 90 beats per minute, maximum dp/dt of the anacrotic wave was higher for blood pressure signals measured by a high wide bandwidth catheter-manometer system than for those measured by a narrow bandwidth system.

This trend is reversed for heart rates above 90 beats per minute.

5.3.8 Effect of wide and narrow bandwidth catheter-manometer systems on the Power Density Spectra of the blood pressure pulse.

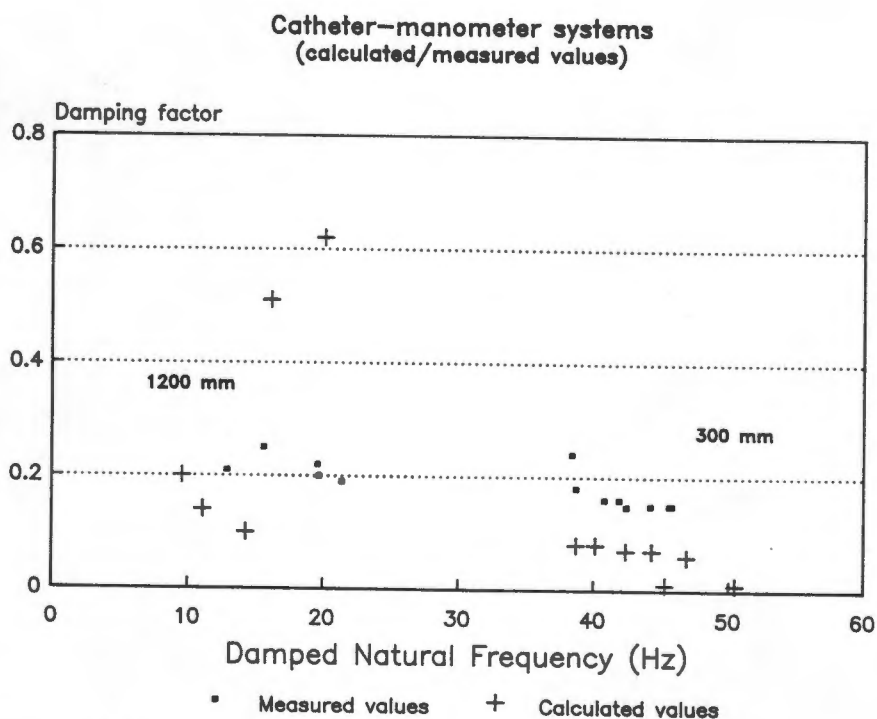
The power density spectrum of the blood pressure signal revealed that the maximum signal power was distributed within 5 Hz of the fundamental frequency.

Using either the wide bandwidth or narrow bandwidth catheter-manometer system resulted in insignificant changes in the Power Density Spectra of the blood pressure pulse.

5.4 Relationship between model derived frequency response parameters and measured frequency response.

In figure 5.34 the calculated damped natural frequency and damping factor for the catheter-manometer model by Bruner (1978) are compared to the in vitro measured parameters. Figure 5.35 compares the calculated parameters for the models of Bruner and Yeomanson and Evans (1983).

Appendix G3.3 lists the calculated values and parameters used in calculating the frequency response parameters.



25 degrees boiled saline

Figure 5.34

Comparison between the measured frequency response parameters and the calculated parameters using the model by Bruner (1978).

Catheter-manometer systems
(distributed/lumped parameter model)

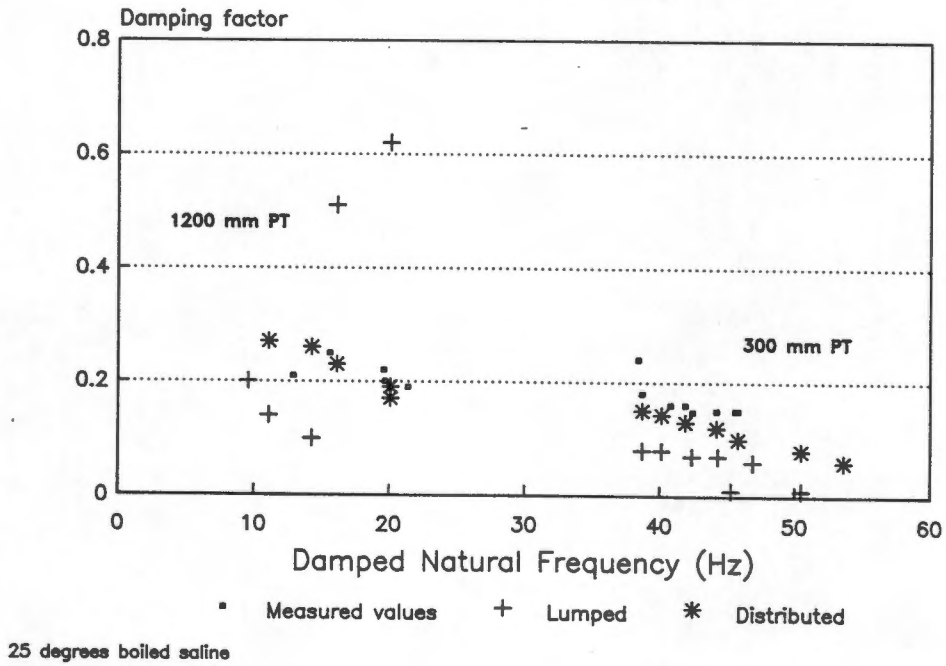


Figure 5.35

Comparison between the calculated frequency response parameters using the models by Bruner (1978) and Yeomanson and Evans (1983).

CHAPTER SIX

DISCUSSION

6.1 In vitro results

6.1.1 Measurement technique

The accuracy of results for the in vitro assessment of catheter-manometer systems depended on the ability of the researcher to identify and establish experimental conditions for which repeatable results were obtainable. These conditions were only achieved for systems which were correctly set up, flushed and debubbled. Air bubbles, even if small in size, ($< 1 \text{ mm}^3$) were found to increase the system compliance and resulted in an erroneous measurement. The measurement technique was thus an important factor in the overall fidelity of results.

Although the measurements for each test showed some variance, mean values with acceptable deviations were obtained and thus comparison and assessment of catheter-manometer systems and/or parts thereof was possible.

6.1.2 Discussion and interpretation of results

6.1.2.1 Pressure tubing

Examining the effects of the physical properties (lumen diameter, length, material and radius ratio) of pressure tubing on the frequency response parameters, it was found that damped natural frequency:

- 1) is directly proportional to lumen diameter (within experimental error) for all lengths of pressure tubing;
- 2) is inversely related to pressure tubing length;
- 3) is inversely related to the damping factor;

- 4) is higher for stiffer materials (e.g. Teflon) than for materials such as polyethylene and polypropylene for the same pressure tubing dimensions;
- 5) is higher for pressure tubing filled with boiled and debubbled saline (at 25 °C) than for un-boiled saline (also at 25 °C);
- 6) decreases for an increased saline temperature;
- 7) is decreased if pressure tubing is coiled;
- 8) is increased if pressure tubing is twisted around its longitudinal axis.

Further to point (1) above, it was established that an increased lumen diameter did not necessarily result in a proportional increase in damped natural frequency since the radius ratio did not remain constant for the pressure tubing tested (the wall thickness was found to decrease with increasing lumen diameter). This resulted in a higher compliance of the tube and thus a lower damped natural frequency.

The decrease in damped natural frequency for increased pressure tubing length (point 2) is caused by a higher pressure tubing compliance (equation B1.12) and increased fluid resistance and inertance (equations B1.10 and B1.11 respectively).

The above mentioned parameters also determine the damping factor given in equation B1.14. The inverse relationship (point 3) is apparent from equation B2.12.

Point 4 is explained by the higher Young's modulus of Teflon (Appendix I) compared to that of polypropylene. An increase in Young's modulus decreases the compliance of pressure tubing (equation B1.12).

The damped natural frequency decreased if the coupling fluid was un-boiled and/or at a higher (37 °C) temperature when compared to the fluid at 25 °C (points 5 and 6). This relationship is explained by the fact that more air bubbles are present in the un-boiled fluid and the fluid compliance is thus increased whereas higher fluid temperatures promote the formation of air bubbles in the fluid.

The resistance and inertia of fluid in pressure tubing increase for smaller and non-symmetrical lumen diameters (Caro et al, 1978). This is the apparent reason for the decrease of damped natural frequency for coiled pressure tubing. Twisting the pressure tubing on the other hand will tension the tubing material which will then have a lower compliance.

From the above discussion it can be inferred that the compliance of the pressure tube and/or the fluid is a major influence on the frequency response of the system.

6.1.2.2 Stopcocks and flush devices.

It was shown in section 5.2.2 that the addition of stopcocks and flush devices decreased f_d significantly (mean change = 36 percent). The main reason for this decrease was that the lumen diameter of a stopcock differs from that of the pressure tubing, resulting in an impedance mismatch between pressure tube and stopcock (Fry, 1960). This junction between the stopcock and the pressure tubing also becomes a source for wave reflection which influences the fidelity of the transmitted waveform. Furthermore, fluid inertance and resistance (equation B1.11 and

B1.10) increase for smaller lumen diameter and thus the stopcock acts as a hydraulic damper.

Similarly, the branching of the pressure tube to the flush device and the flush valve (figure 2.1) itself increases the catheter compliance since there is an effective increase in pressure tubing length. Hydraulic damping also occurs with the decrease of pressure tube lumen diameter due to the rollerclamp of the flush device.

6.1.2.3 Cannulae

The frequency response of cannulae tested was sufficient for optimal signal transmission; however, cannulae fitted with valves (to prevent bleed back during cannulation) had a higher compliance which again decreased f_d and increased β . It must also be noted that the damped natural frequency was higher (mean = 1.4 Hz, range = 0.0 - 2.3 Hz) when an external pressure of 100 mmHg was applied to the cannula: the compliance of the cannula is decreased since the lumen diameter of the cannula is decreased by the applied external pressure. This more closely simulates the in-vivo measurement situation when the cannula is inserted into an artery.

6.1.2.4 Catheter-manometer systems

The damped natural frequency of catheters decreased when cannulae were connected. This decrease is again attributed to the impedance mismatch between the cannula and the catheter.

Short catheters (300 mm pressure tubing) when connected to 20 and

22 gauge cannulae had a damped natural frequency greater than 25 Hz. Bruner (1978) suggested this as the minimum requirement for accurate blood pressure measurement. However, catheters with pressure tubing exceeding 300 mm with 24 gauge cannulae and pressure tubing exceeding 400 mm with 20 and 22 gauge cannula were found to not comply with this requirement.

It must be noted that the in vitro results obtained reflect the frequency response for catheter-manometer systems in controlled situations (preboiled saline used at 25 °C) whereas saline used in a typical theatre situation is seldom boiled and debubbled and thus the damped natural frequency for the same combinations of cannulae and catheters would be even lower than the measured values.

6.1.2.5 Gardner representation of frequency response parameters

The relationships between damped natural frequency, lumen diameter, damping factor and compliance have been described in the previous sections. It is apparent that these relationships are all inter-linked; however, the representation of all associations in one graph is formidable.

Gardner (1981) presented a method by which the frequency response of catheter-manometer system is described in terms of damping and damped natural frequency (note: damping = damping factor / critical damping). This method allows a visual inspection as to whether the catheter-manometer system is underdamped, optimally damped or over-damped, for a given damped natural frequency.

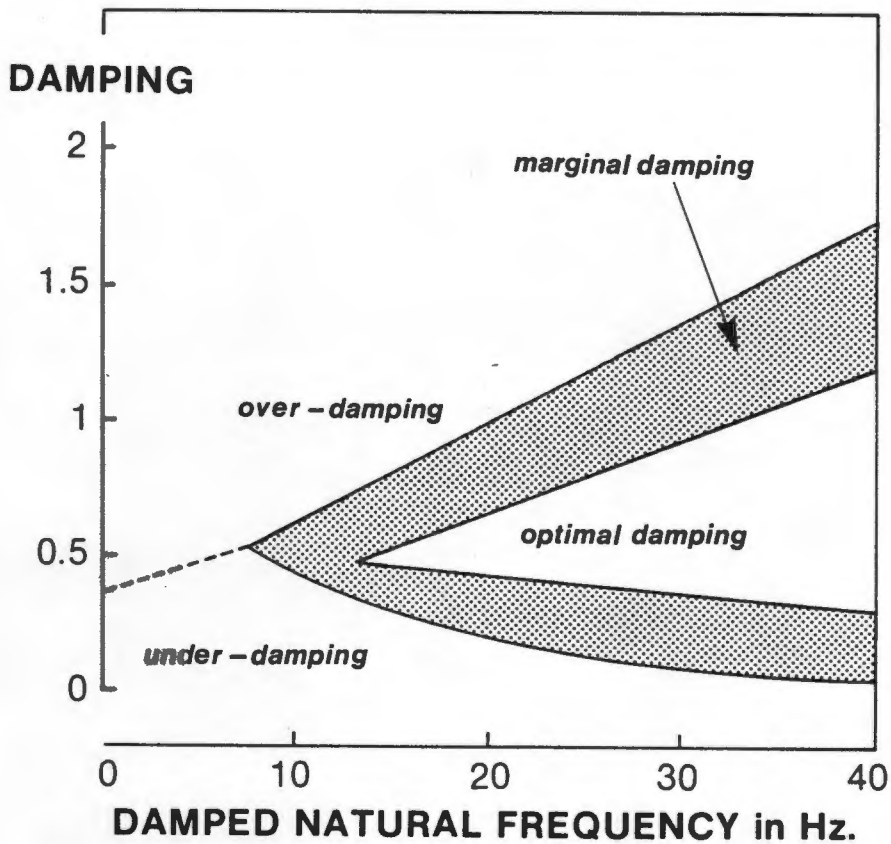


Figure 6.1

Chart to illustrate the areas of under-damping, over-damping, marginal damping and optimal damping (Gardner, 1981).

The chart described by Gardner is given in figure 6.1. Optimal system response is obtained if the catheter-manometer system has a damped natural frequency and damping within the region indicated. Marginal system response is obtained if damping and damped natural frequency lie within the gray area of figure 6.1. Areas of under-damping and over-damping are also indicated.

Frequency response parameters for catheters described in section 5.2.2 are shown in figure 6.2. Catheters with pressure lines of a length of 300 mm are marginally damped, whereas longer lines are under-damped.

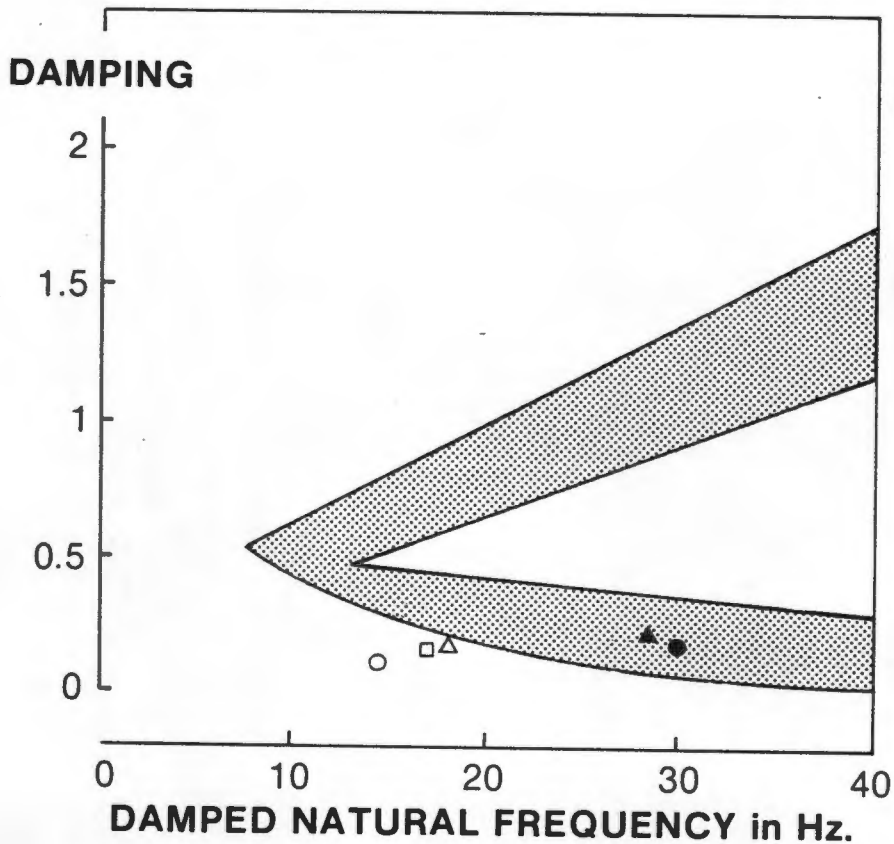


Figure 6.2

Damped natural frequency versus damping for catheters. Solid points represent 300 mm pressure tubing whereas the other points represent 1200 mm pressure tubing.

Catheter-manometer systems listed in tables G2.12(a) and G2.12(b) are represented in figure 6.3. Once again, only the systems with pressure tubing of 300 mm are marginally damped. This confirms that catheter-manometer systems with pressure lines exceeding 300 mm in length are insufficiently damped (Gardner representation) and thus contribute to a lower fidelity of the transmission system.

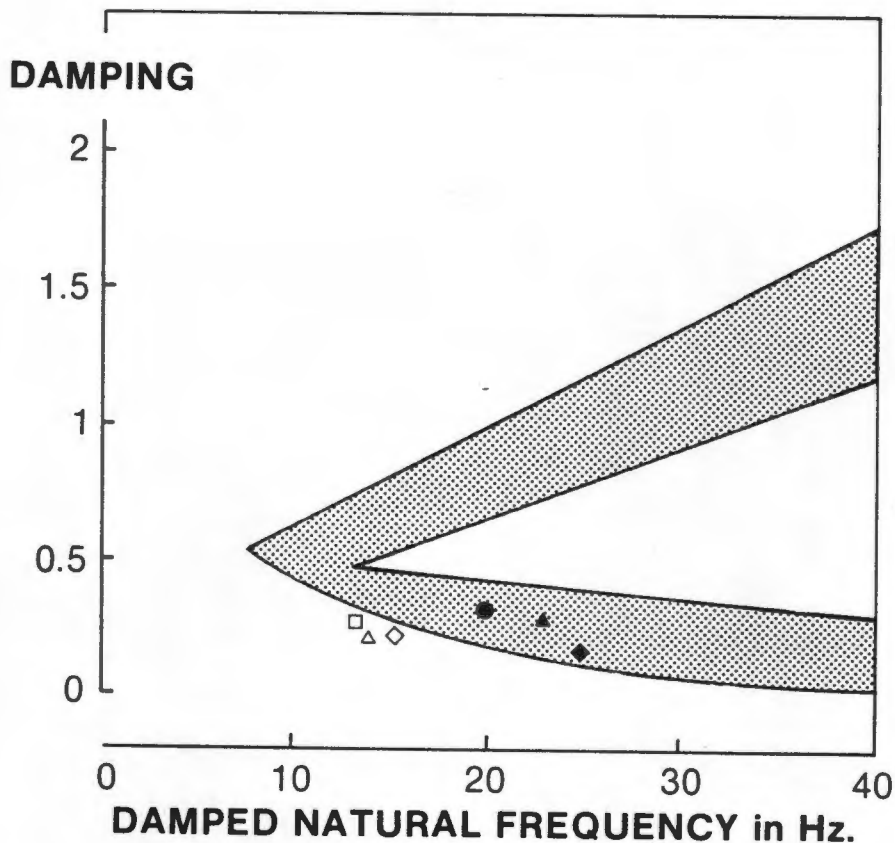


Figure 6.3

Damped natural frequency versus damping for selected catheter-manometer systems. Solid markers represent systems with pressure tubing of 300 mm in length and the open markers represent systems of 1200 mm pressure tubing.

In figure 6.4 the damped natural frequency and damping of the proximal and distal orifices of a 7F Swan Ganz catheter are shown. This system is also insufficiently damped.

Although the pulse amplitude of the blood pressure typically recorded by the Swan Ganz catheter is lower (pulmonary circulation) than that of the conventional catheter-manometer system (systemic circulation), the bandwidths of the Swan Ganz catheters tested are also lower and thus the possibility of waveform distortion remains.

Tables G2.15 and G2.16 in section G2.5.1 list the damped natural frequency and damping factors for these catheters.

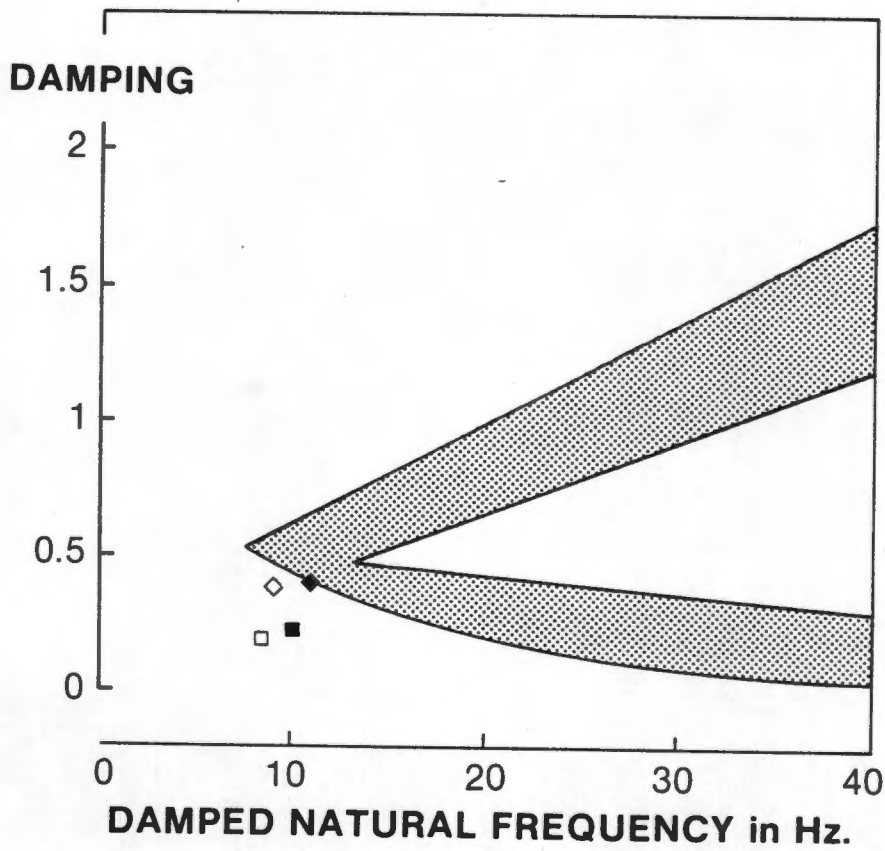


Figure 6.4

Damped natural frequency versus damping for 5F (■) and 7F (◆) Swan Ganz catheters.

6.2 In vivo results

6.2.1 General statement on the recorded signals

As mentioned previously the ventilator was disconnected during the recording period. The aim was to limit the effect of the Valsalva manoeuvre; however, as a result the heart rate changed (increased). Consequently, time and/or frequency related parameters such as the Fourier transforms and dp/dt values of blood pressure signals (from the same patient) measured by wide and narrow bandwidth catheter-manometer systems could not be meaningfully compared, since these parameters change significantly for different heart rates.

6.2.2 High frequency artifact addition for narrow bandwidth catheter-manometer systems.

Theoretically the frequency components of a blood pressure pulse should be within the bandwidth of the catheter-manometer system, as only these components can pass through the system without attenuation. However, the catheter-manometer system acts as a second order lowpass filter and the attenuation of the higher frequencies is determined by the roll-off properties of the filter. For the narrow bandwidth catheter-manometer system the corner frequency is lower than for the wide band catheter-manometer system and this would imply that a blood pressure signal measured by a wide bandwidth system should have higher frequency components of greater amplitude than those for a narrow bandwidth system, when measuring the same signal.

In section 5.2.1 the Fast Fourier transform of the double-peak pressure pulse recorded by the narrow bandwidth system suggested that the higher frequency components were more prominent than those recorded by a wide bandwidth system: frequencies components in the range of 17 to 30 Hz were found whereas for the wide bandwidth system these were not seen at all. This is shown in figure 5.20. Locating the exact range of accentuated frequency components was impossible to establish, since no true blood pressure signal was available to which the narrow bandwidth system recordings could be compared (the true blood pressure signal would have been measured by a Miller catheter-tip pressure transducer).

There is an indication that these frequencies are responsible for the extreme double peak of the pulse shown in Figure 5.25; it is suggested that they are not a true phenomenon of the patient's blood pressure but are artifacts of the patient-measuring system combination. Furthermore, the degree of the high frequency component addition is possibly determined by the bandwidth of the catheter-manometer system.

6.2.3 Heart rate and its effect on signal fidelity

An increase in heart rate increases the fundamental frequency of the blood pressure signal. This in turn results in a corresponding increase in the frequencies of the harmonics and it can be clearly seen in figure 5.32 that fewer harmonics are within the passband of the catheter-manometer system. Thus higher frequency components of the signal are attenuated by the low pass filter action of the system. This should result in attenuated waveforms with lower peak systolic and dp/dt values; however, with the addition of high frequency components in some measurements this effect is reversed and this explains the high rise in values of dp/dt maximum mentioned in 5.2.5.

6.2.4 Peak systolic and end diastolic blood pressure values

The peak systolic values measured by the narrow bandwidth system were generally higher (60 percent were higher, mean = 4 mmHg, range 0.1 - 5.9 mmHg) than those recorded by the wide bandwidth system. Although numbers are limited, this is an interesting finding as one would expect the opposite, i.e. peak systolic blood pressure values for wide bandwidth systems to be higher than those measured by narrow bandwidth systems. However, there is an indication that the high frequency artifacts and the lower damping factor of the low bandwidth system resulted in higher overshoot of the signal and thus the higher peak systolic measurements.

No apparent changes in the end diastolic values were observed for measurements using wide and narrow bandwidth systems.

6.2.5 Fourier Transforms

Comparing changes in the relative amplitudes of the harmonics of blood pressure waveform measured by wide and narrow bandwidth catheter-manometer systems was not possible for the reasons described in section 6.2.1. The Fourier transform was thus only used to identify the amplitude and the frequency of the harmonics of different blood pressure waveforms.

6.3 Catheter-manometer system models

It was found that the lumped parameter model of Bruner (1978) and the distributed model of Yeomanson and Evans (1983) did indeed accurately predict the frequency response characteristics of a catheter-manometer system for pressure tubing of length less than 600 mm; however, the model of Bruner showed large deviations from the measured frequency response parameters for pressure tubing exceeding approximately 800 mm. This deviation was reduced once different values for the Young's modulus of polyethylene were used. Furthermore, the calculated values were lower than the measured values which suggest that calculated values for compliance of the catheter-manometer system are indeed higher, as claimed by Latimer and Latimer (1969).

The model by Yeomanson and Evans did not show these deviations but the regular use of this model in a clinical context is limited as the frequency response calculations are very complex.

CHAPTER SEVEN

CONCLUSION AND RECOMMENDATIONS

7.1 Conclusion

The literature survey considered modelling, characterisation techniques and frequency response evaluation of catheter-manometer systems as well as physiological aspects of blood pressure and system requirements for accurate invasive blood pressure measurement.

The catheter-manometer system has been modelled as a second order system, whose frequency response is characterised by damped natural frequency and damping factor.

Frequency response requirements of catheter-manometer systems have been investigated by a number of researchers and it has been shown that the system should ideally have a bandwidth higher than 25 Hz and a damping factor of 0.6. For the purpose of waveform analysis however, the bandwidth of the catheter-manometer system should be higher than 200 Hz. Two methods (the transient and the steady state method) to determine these frequency response parameters have been widely used in the characterisation and assessment of catheter-manometer systems, or parts thereof. The steady state method is preferred because of its greater sensitivity.

For in vitro evaluation using the steady state method a pressure generator consisting of a vibration source, pressure chamber and compensating network was designed and constructed. This pressure generator complied with source impedance requirements for isolation of catheter-manometer system characteristics from those of the pressure generator and was incorporated into a measurement

system used for frequency response characterisation. Software was developed for a Personal Computer to acquire, manipulate and analyse frequency response data.

In vitro evaluation included the assessment of the damped natural frequencies and damping factors of cannulae, pressure tubing, stopcocks and flush devices (and combinations thereof).

It was found that all catheter-manometer systems tested are underdamped and their bandwidth is usually insufficient to transmit the blood pressure pulse without some loss in signal fidelity. Furthermore, investigations suggested that system compliance was the major source of error for incorrect blood pressure measurements. In vivo assessment of dynamic blood pressure measurement error was attempted by comparing two catheter-manometer systems, one with narrow bandwidth (15 Hz) and the other with a wider bandwidth (27 Hz). It was found that there was a distinct difference in the blood pressure waveform parameter measurements when using the two systems. Software was developed for frequency and time domain analysis.

In identifying the effects of system parameters on the frequency response of the catheter-manometer system and on the blood pressure pulse it is thus possible to recommend a system configuration that will comply with the requirements specified stated for accurate signal transmission.

7.2 Recommendations

7.2.1 General recommendations

Using catheter-manometer models to determine the frequency response of catheter-manometer systems is not recommended as the accuracy of the frequency response calculation depends on specific parameters normally not specified and/or supplied by the manufacturers.

The steady state method of catheter-manometer evaluation is recommended. The transient method can be used: however, extreme care must be observed when using this method as the results are subject to the measurement technique.

Furthermore, there are some general recommendations that will enhance the frequency response of catheter-manometer systems and thus the fidelity of the signal transmission.

- All connections between cannulae, stopcocks, flush devices and pressure tubing must be air-tight to prevent air bubbles entering the measurement system.
- The catheter-manometer system must be carefully debubbled.
- The pressure tubing and cannula must not be twisted or kinked.

7.2.2 Catheter-manometer system

7.2.2.1 Pressure tubing dimensions

For an optimal frequency response of pressure tubing it is recommended that the following properties and dimensions are adhered to:

- 1) Pressure tubing should not exceed 300 mm in length.
- 2) The lumen diameter should be in the range of 1.4 mm to 1.8 mm.
- 3) The radius ratio should be in the range of 0.45 to 0.55.
- 4) Stiff material should be used, such as polypropylene, Teflon or Teflon FEP.

7.2.2.2 Catheters

For an optimal frequency response of catheters the following are recommended:

- 1) Stopcocks and flush devices must have lumen diameters similar to that of the pressure tubing.
- 2) The number of stopcocks should be minimised.

7.2.2.3 Cannulae

It is recommended that:

- 1) Low compliance cannulae (Teflon) are used.
- 2) The cannula length does not exceed 5 cm.
- 3) The lowest possible gauge cannula is used, taking into account medical considerations.
- 4) Cannulae that include valves to prevent bleed back are not used.

7.3 Future work

It is recommended that future studies further investigate and quantify the measurement error for catheter-manometer systems used in vivo and establish the clinical significance of these errors, both in the time and frequency domains. This can only be achieved if the following conditions are met:

- use of a transducer-tip catheter to provide a reference signal and
- control of physiological conditions, e.g. heart rate kept constant by pacing.

It is further recommended that:

- the effects of transducer diaphragms and dome characteristics on the frequency response of catheter-manometer systems are investigated.

REFERENCES

- AAMI
1984
Spectramed Research Report
pp. 36-37, Spectramed, Bilthoven
- ANDERSON HR, BERGSTEN O.
1982
Blood pressure measurements and methods.
pp. 4-74, S&W Medico Teknik A/S, Albertslund
- ARDILL BL, FENTEM PH, WELLARD MJ.
July 1967
An electromagnetic pressure generator for testing the frequency
response of transducer and catheter systems.
pp. 19-21P, Physiological Society
- ASTHEIMER JP, DUTKEVICHTH D, SCHULTZ RO, YANKOWSKI AA.
1985
Data Manipulation
pp. II-5-2 - 25 In: Data Analysis in Asyst.
Macmillan Software Company, Rochester
- ATTINGER EO, SUGAWARA H, NAVARRO A, RICETTA A, MARLIN R.
1966
Pressure-flow relations in dog arteries.
Circulation Research, 19:230-245
- BENSON FA, HARRISON D.
1966
Electric circuit theory
pp. 78-112, Edward Arnold, London
- BERGEL DH.
1972
Cardiovascular fluid dynamics.
pp.11-49, Vol 1, Academic Press, London
- BERNOUW JC, VAN WIJK VAN BRIEVINGH RP, SCHMELTZ JW, HEETHAAR RM,
VAN DER WERF T, ZIMMERMAN ANE.
1983
Automatic electronic correction of catheter-manometer
characteristics in situ: physics and in vivo trials.
Adv. Cardiovasc. Phys., 5:177-192
- BIO-TEK
1981
Model 601A BP systems calibrator
pp.1-6, Bio-tek publication no. 06, Burlington

BOONZAIER DA.

1978

Resonance Artefact in intravascular blood-pressure measuring systems: A technique for on-line digital computer correction. South African Journal of Science, 74:250-55

BRUNER JMR.

1978

Handbook of blood pressure monitoring. pp. 1-89, PSG Publishing Company, Inc. Littleton, Massachusetts

BRUNER JMR, KRENIS LJ, KUNSMAN JM, SHERMAN AP.

1981a

Comparison of direct and indirect methods of measuring arterial blood pressure, part I. Medical Instrumentation, 15(1):11-21

BRUNER JMR, KRENIS LJ, KUNSMAN JM, SHERMAN AP.

1981b

Comparison of direct and indirect methods of measuring arterial blood pressure, part II. Medical Instrumentation, 15(2):97-101

BRUNER JMR, KRENIS LJ, KUNSMAN JM, SHERMAN AP.

1981c

Comparison of direct and indirect methods of measuring arterial blood pressure, part III. Medical Instrumentation, 15(3):162-188

BUECHE FJ.

1979

College Physics p.112, Schaum's Outline Series, McGraw-Hill, NY

BURATTINI R, BORGDORFF P, WESTERHOF N.

1987

Dynamics of the short-term regulation of the arterial pressure: frequency dependence and role of arterial compliance. Med. & Biol. Eng. & Comput., 25:277-283

CARO CG, PEDLEY TJ, SCHROTER RC, SEED WA.

1978

The mechanics of the circulation. pp.261-346, Oxford University Press, New York

CRUL JF.

1965

Measurement of arterial pressure. Acta Anaesthesiologica Scandinavica, 5:135-169.

DAMENSTEIN A, STOUT RL, WESSEL HU, PAUL MH.

1976

Electronic compensator for pressure waveform distortion by fluid-filled catheters. Medical and Biological Engineering, 3:186-98

- DiSTEFANO JJ, STUBBERUD AR, WILLIAMS IJ.
1967
Feedback and control systems.
pp.295-337, Schaums Outline Series, McGraw-Hill, NY
- FALSETTI HL, MATES RE, CARROLL RJ, GUPTA RL, BELL AC.
1974
Analysis and correction of pressure wave distortion in fluid-filled catheter systems.
Circulation, 49:165-72
- FOURIE PR, BADENHORST E, COETZEE AR.
1987
Drukometers in die kliniese en navorsingspraktyk
S Afr Med J., 71:651-654
- FOX F, MORROW DH, KACHER EJ, GILLELAND TH.
1978
Laboratory evaluation of pressure transducer domes containing a diaphragm.
Anesth. Analg., 57:67-76
- FRY DL.
1960
Physiologic recording by modern instruments with particular reference to pressure recording.
Physiol. Rev. 40:753-788
- GARDNER RM.
1981
Direct blood pressure measurement - Dynamic response requirements.
Anesthesiology 54:227-236
- GOLDMAN S.
1949
Transformation calculus and electrical transients.
Appendix C, Prentice-Hall, Englewood Cliffs, N.J.
- GOLDSTEIN S, KILLIP T.
1962
Comparison of direct and indirect arterial pressures in aortic regurgitation.
N. Engl. J. Med., 267:1121-24
- GOODFELLOW
1987
Goodfellow metals manual
pp.46-49, Goodfellows Metals Ltd, Cambridge
- GREINER LABORTECHNIK
1987
For medicine and research
pp. 89-93, Greiner labortechnik, Austria

GRIFFITHS M.

1981

Introduction to human physiology.
pp. 108-57, Macmillan Publishing Co., New York

HAMILTON WF, DOW P.

1939

An experimental study of the standing waves in the pulse
propagated through the aorta.
Am J Physiol, 125:48-59

HANSEN AT, WARBURG E.

1950

The theory of elastic liquid-containing membrane manometers.
Acta Physiol Scand 19:306

HASEGAWA M, RODBARD S.

1979

Effect of posture on arterial pressures, timing of the arterial
sounds and pulse velocities in the extremities.
Cardiology, 64:122-32

HÖK B.

1976

Dynamic calibration of manometer systems.
Medical and Biological Engineering, 5:193-198

JENNINGS RB, KROVETZ LJ.

1970

The use of a damping chamber and sine wave oscillator for optimal
frequency response in pressure recording.
IEEE Trans Ind Elec Con Inst 17:134-6

KROVETZ LJ, GOLDBLOOM SD.

1974a

Frequency content of intravascular and intracardiac pressures and
their time derivatives.
IEEE Trans. Biomed. Eng. 11:498-501

KROVETZ LJ, JENNINGS RB, GOLDBLOOM SD.

1974b

Limitation of correction of frequency dependent artefact in
pressure recordings using harmonic analysis.
Circulation, 50:992-7

KUO BJ.

1982

Automatic Control systems.
pp.554-654, Prentice-Hall, Eaglewood Cliffs., NJ

LADIN Z, TRAUTMAN E, TEPLICK R.

1983

Contribution of measurement system artifacts to systolic spikes.
Medical Instrumentation, 17(2):110-3

- LAM HY-F.
1979
Analog and digital filters
pp. 36-8, 1st ed. Prentice-Hall, Englewood Cliffs, NJ
- LASKEY WK, KUSSMAUL WG.
1987
Arterial wave relection in heart failure.
Circulation, 75(4):711-22
- LATIMER KE, LATIMER RD.
1969
Measurements of pressure-wave transmission in liquid filled tubes
used for intravascular blood pressure recording.
Medical and Biological Engineering, 7:143-68
- LINDEN RJ.
1959
Pressure Generators
J. Sci. Instrum., 36:137-139
- McDONALD DA.
1974
Blood Flow in Arteries.
pp.118-22, 2nd ed. Edward Arnold, London
- MELBIN J, SHOHR M.
1969
Evaluation and correction of manometer systems with two degrees
of freedom.
J. Appl. Physiol. 27(5):749-755
- MICROLINK
1986
Microlink - Hardware user manual
pp. 2.15-2.58, Biodata Ltd, Manchester
- MILLER GS, ZBILUT JP.
1983
Practical evaluation of catheter-transducer coupling systems for
artifact.
Heart & Lung, 12(2):156-61
- MILLS CJ, GABE IT, GAULT JH, MASON DT, ROSS J, BRAUNWALD E,
SHILLINGFORD JP.
1970
Pressure-flow relationship and vascular impedance in man.
Cardiovascular Research, 4:405-17
- MURGO JP, WESTERHOF N, GIOLMA JP, ALTOBELLI SA.
1981
Manipulation of ascending aorta pressure and flow wave
reflections with the valsalva maneuver: relationship to input
impedance.
Circulation, 63(1):122-132

MURGO JP, WESTERHOF N, GIOLMA JP, ALTOBELLI SA.
1980

Aortic input impedance in normal man: relationship to pressure waveforms.
Circulation, 62(1):105-116

MURRAY RHS, HOWE NA
1976

A calibration system for catheter transducer pressure measurement.
Biomedical Engineering, 5:180-2

NEWMAN DL, GREENWALD SE, BOWDEN NLR.
1979

An in vivo study of the total occlusion method for the analysis of forward and backward pressure waves.
Cardiovascular Research, 13:595-600

NOBLE FW.
1959

A hydraulic pressure generator for testing the dynamic characteristics of blood pressure manometers.
J. Lab. & Clin. Med., 54(6):897-902

O'ROURKE MF.
1968

Pressure wave transmission along the human aorta: Changes with age and in arterial disease.
Circ. Res., 23:567-576

O'ROURKE MF.
1970

Influence of ventricular ejection on the relationship between central aortic and brachial pressure pulse in man.
Cardiovascular Research, 4:291-300

O'ROURKE MF
1971

The arterial pulse in health and disease.
American Heart Journal, 82(5):687-702

O'ROURKE MF, AVOLIO AP.
1980

Pulsatile flow and pressure in human systemic arteries.
Circ. Res., 46(3):363-72

PASCARELLI EF, BERTRAND CA.
1964

Comparison of blood pressures in arms and legs.
N. Engl. J. Med. 270:693-98

PATEL DJ, MASON DT, ROSS J, BRAUNWALD E.
1965

Harmonic analysis of pressure pulses obtained from the heart and great vessels of man.
Am. Heart J., 69(6):785-94

PAUCA AL, MEREDITH JW.

1987

Possibility of A-V shunting upon cardiopulmonary bypass discontinuation

Anesthesiology, 67:91-94

RACAL

1987

Technical manual - store 7DS

pp. 17-20, Racal Recorders Limited, Southampton

RAGAN C, BORDLEY J.

1941

The accuracy of clinical measurements of arterial blood pressure. With a note on the auscultatory gap.

Bull. Johns Hopkins Hosp., 69:504-528

REMINGTON JW.

1960a

Unexplained features of the left ventricular pressure pulse.

Am. J. Physiol. 199(2):328-330

REMINGTON JW.

1960b

Contour changes of the aortic pulse during propagation.

Am. J. Physiol. 199(2):331-334

SHAPIRO GG, KROVETZ LJ

1970

Damped and undamped frequency responses of underdamped catheter-manometer systems.

American Heart Journal, 80(2):226-236

SHELTON CD, WATSON BW.

1968

A pressure generator for testing the frequency response of catheter/transducer systems used for physiological pressure measurements.

Phys. Med. Biol., 13(4):523-528

SHINNERS SM.

1980

Modern control system theory and application

pp.369-414, Addison-Wesley Publishing Company, London

SHINOZAKI T, DEANE R, MAZUZUAN J.

1980

The dynamic responses of liquid-filled catheter systems for direct measurements of blood pressure.

Anesthesiology 53:498-9

SIMONSEN AND WEEL

1972

Service manual for blood pressure amplifier BAP 001

p. 1-1, Albertslund

SMITH RN.

1978

Invasive pressure monitoring
American Journal of Nursing, 78(9):1514-21

SPIEGEL MR.

1968

Mathematical Handbook of formulas and tables.
pp.174-178, Schaums Outline Series, McGraw-Hill, NJ

STEGALL HF.

1967

A simple, inexpensive, sinusoidal pressure generator.
J. Appl. Physiol. 22(3):591-592

STERN DH, GERSON JI, ALLEN FB, PARKER FB.

1985

Can we trust the Direct Radial Artery Pressure immediately
following Cardiopulmonary bypass?
Anesthesiology, 62:557-561.

TAYLOR BC, ELLIS DM, DREW JM.

1986

Quantification and simulation of fluid-filled catheter/transducer
systems.
Medical Instrumentation 20(3):123-29

VAN BERGEN FH.

1954

Comparison of indirect and direct methods of measuring arterial
blood pressure.
Circulation, 10:481-90

VAN DER TWEEL T.

1957

Some physical aspects of blood pressure, pulse wave, and blood
pressure measurements.
Am. Heart J., 53(1):4-17

VIERHOUT RR, VENDRIK AJH.

1961

A hydraulic pressure generator for testing the dynamic
characteristics of catheters and manometers.
J. Lab. & Clin. Med., 58(2):330-3

VIERHOUT RR, VENDRIK AJH.

1964

On pressure generators for testing catheter manometer systems.
Phys. Med. Biol., 10(3):403-406

WESSELING KH, SETTELS JJ, VAN DER HOEVEN GMA, NIJBOER JA,
BUTIJN MWT, DORLAS JC.

1985

The effect of peripheral vasoconstriction on the measurement of
blood pressure in a finger.
Cardiovascular Research, 19:139-145

WILKINS DG, GREENBAUM R, GIBBS DF.

1972

Arterial pressure waveform recording: A clinical system.
Biomedical Engineering, August: 309-12

WOOD EH.

1956

Physical response requirements of pressure transducers for the reproduction of physiological phenomena.
Trans. American Institute of Electrical Engineers. I. Communications and Electronics 75:32-40

YAMAKOSHI K, KAMIYA A, SHIMAZU H, ITO H, TOGAWA T.

1983

Noninvasive automatic monitoring of instantaneous arterial blood pressure using the vascular unloading technique.
Med. & Biol. Eng. & Comput., 21:557-565

YEOMANSON CW, EVANS DH.

1983

The frequency response of external transducer blood pressure measurement systems: a theoretical and experimental study.
Clin. Phys. Physiol. Meas., 4(4):435-449.

APPENDIX A

BLOOD PRESSURE MEASUREMENT

CONTENTS

A1	Clinical aspects of blood pressure	A2
A1.1	Introduction	A2
A1.2	The pulsatility of the vascular system	A3
A1.3	The phases of the blood pressure pulse	A4
	Inotropic phase	A5
	Volume displacement phase	A6
	Diastole phase	A6
A1.3.1	Pressure pulse contour measured at sites further from the heart	A7
A2	Invasive blood pressure measurement technique	A12
A2.1	Introduction	A12
A2.2	Balancing and calibration of pressure transducer and catheter systems	A15
A2.3	Pressure measurement units	A17
A3	Advantages and risks of invasive blood pressure measurement	A18
A4	System requirements for invasive blood pressure measurement	A20
A4.1	Introduction	A20
A4.2	Review of system bandwidth requirements	A22
A4.3	General system requirements	A23
A4.3.1	Static accuracy	A23
A4.3.2	Dynamic accuracy	A24
A4.3.2.1	Noise	A25
A4.3.2.2	Dynamic response	A26
A4.3.3	Physiological reactance	A26
A4.4	The catheter-manometer requirements	A26
A4.5	Amplifier requirements	A28
A4.6	Response requirements for hard-copy records, display and storage systems	A30
A4.7	Ancillary requirements	A31

A1 Clinical aspects of blood pressure

The purpose of this appendix is to describe some important clinical aspects of blood pressure including: the generation of blood pressure, invasive measurement techniques, blood pressure units and blood pressure system requirements.

A1.1 Introduction

Oxygenated blood and vital nutrients must be supplied to organs and tissues for life to continue. Therefore, any obstruction of the blood flow to the vital organs or impediment of the pumping action of the heart may severely limit the function of the tissue or organ. It is this pumping action or ejection of a volume of blood (volume of blood per contraction - stroke volume) from the heart into the systemic circulation which is extremely important to monitor in critically ill patients. The stroke volume can vary from 70 ml/stroke to about 200 ml/stroke (Griffiths, 1981) and the mean pressure at which this blood volume is ejected into the systemic circulation is normally 100 mmHg.

The product of the stroke volume and the heart rate is the cardiac output and is thus defined as the volume of blood pumped out by either the left or right ventricle per minute. However, cardiac output is a measurement which is not easily attained in real time. Since peripheral resistance can be considered constant (Griffiths, 1981), blood flow is considered to be directly proportional to pressure and thus arterial blood pressure, in conjunction with parameters such as the heart rate, becomes the most convenient clinical indicator of cardiac performance.

A1.2 The pulsatility of the vascular system

The ejection of blood from the heart into the systemic circulation is pulsatile; however, the arterial walls are elastic and distend and recoil as the pressure within the arteries first increases and then decreases, thus producing a continuous but pulsatile blood flow.

The pressure pulse generated by the cardiac systole in the arterial tree travels more rapidly than the blood expelled (blood flow) from the left ventricle and reaches the peripheral arterioles 200 to 300 milliseconds after the onset of ventricular ejection. Blood flow velocity does not exceed 0.5 m/s, whereas the pressure pulse wave normally travels at 5 m/s, although velocities of up to 14 meters per second have been recorded (Remington, 1960a).

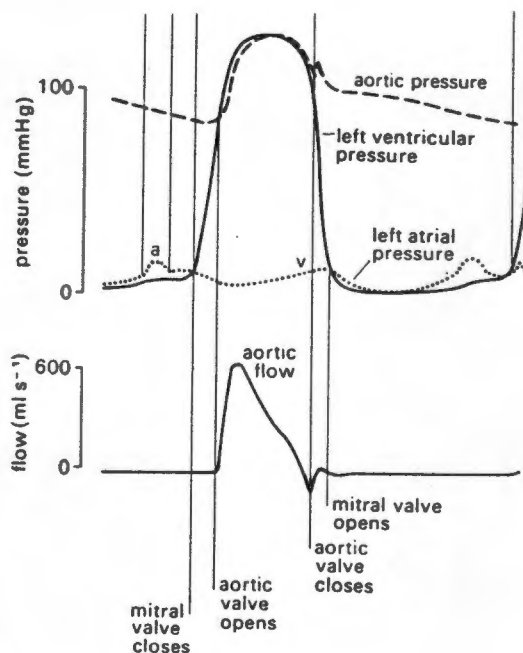


Figure A1.1

Blood pressure pulse and the corresponding blood flow (Caro et al, 1978).

The phase difference between the pressure and blood flow is about 60 degrees (Bruner, 1978) at the ascending aorta and figure A1.1 represents a typical relationship between blood pressure and blood flow.

A1.3 The phases of the blood pressure pulse

A typical arterial blood pressure pulse is shown in figure A1.2. It is convenient to divide this blood pressure pulse into three phases for the purpose of description. They are:

- the systolic phase (inotropic)
- the midsystolic phase (volume displacement), and
- the events of late systole and diastole (runoff and reflection)

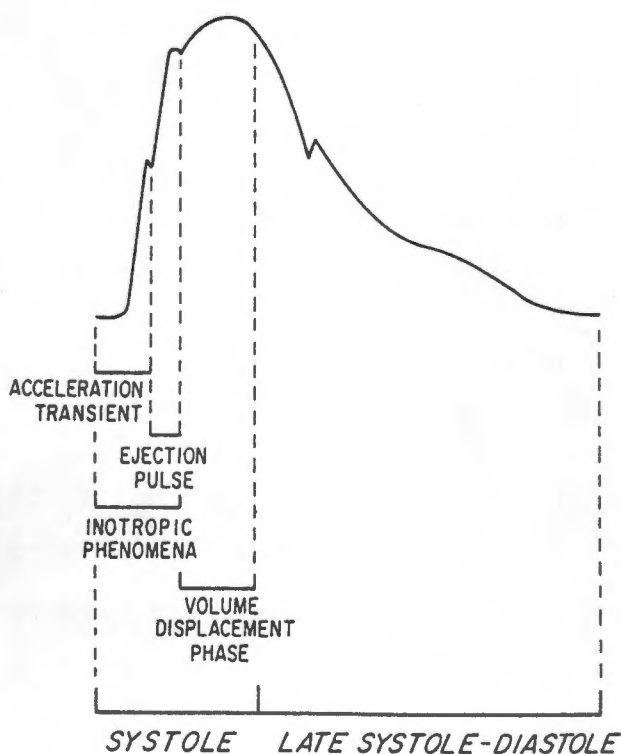


Figure A1.2

The phases of the pressure pulse (Bruner, 1978).

Inotropic phase

The brisk initial rise in the pressure pulse in the inotropic phase is associated with the sudden flow of blood into the aorta at the moment of aortic valve opening (Remington, 1960b; McDonald, 1974). Maximum acceleration of blood flow occurs at this instant (called the acceleration transient on the blood pressure pulse) and Mills et al (1970) agreed that the peak blood flow preceded the peak systolic blood pressure.

The systolic upstroke (anacrotic rise) in the pressure pulse continues to increase with the commencement of ejection of the stroke volume into the root of the ascending aorta. Bruner (1978) however, stated that the absolute height of the inotropic segment of the pressure pulse was also related to peripheral resistance and thus to arterial compliance and not necessarily to stroke volume alone.

The increase in volume in the aorta distends the aortic wall just distal to the aortic valve. The excess tension of the aortic wall in the first segment then displaces a small volume of blood into the next segment of the aorta and this serial transmission of the pressure pulse travels to the periphery, where it can be felt at various sites in the body.

The maximum amplitude (peak systole) and the rate (dp/dt) of the anacrotic rise in the inotropic phase thus depend on the rate of ejection and acceleration of blood into the aorta, on the state of the peripheral arteries and on the magnitude and timing of reflected pressure waves from the periphery (McDonald, 1974).

The duration of the anacrotic segment is about 30 milliseconds and the frequency components of this wave are in the range of 40 to 100 Hz (Bruner, 1978).

Volume displacement phase

The anacrotic rise ceases rather abruptly with a perceptible discontinuity, initiating the "shoulder" of the pressure pulse, which is the volume displacement phase of the cardiac cycle.

As ventricular emptying draws to a close, acceleration of flow assumes a negative value, as the pressure in the heart becomes lower than that in the ascending aorta and thus the aortic valve closes. This sharp deceleration of flow and aortic valve closure is indicated by the dicrotic notch. At the periphery however, the dicrotic notch is an artifact of reflection (McDonald, 1974; Bruner, 1978).

Diastole phase

A prolonged, ramplike decline in pressure continues through diastole to the beginning of the next systole. The diastolic ramp is not undisturbed, however, as defined undulations can be perceived. These are due to resonant waves in the great vessels and also to reflections of energy from the periphery.

A1.3.1 Pressure pulse contour measured at sites further from the heart.

The contour of the pressure pulse changes as it travels to the periphery (Attinger et al, 1966; O'Rourke, 1968; McDonald, 1974; Bruner, 1978; Bruner et al, 1981a). The changes in pressure waveforms have been ascribed to wave reflections from the periphery and damping within the arterial tree (Mills et al, 1970; Bruner et al, 1981a). Before describing how these changes to the pulse contour come about it will be worthwhile to review some of the physiological characteristics (peripheral impedance, wave reflection and resonance) of the circulatory system.

The effects of the physiological and physical characteristics of the circulatory system on the blood pressure pulse contour have been researched in detail by many workers (Bruner, 1978; Bruner et al, 1981a; McDonald, 1974; Burattini et al; 1987a, Hasegawa and Rodbard, 1979; Laskey and Kussman, 1987; O'Rourke, 1968; 1970; 1971 and 1980). This subject is controversial and many possible explanations have been published. The subject is beyond the scope of this thesis; however, the aim of this section is to provide the reader with a brief introduction to the fundamental characteristics of the circulatory system.

Generally, the purpose of the arterial tree is to accept hydraulic energy that is wholly pulsatile in nature and to transfer this energy to the periphery where it is dissipated as virtually steady flow through viscous resistance. This performance requirement is satisfied largely by the capacitance provided in the structure of the major vessels. In operational terms the highly capacitive receiving system allows pulsatile

emptying of the heart into a very low impedance. This means that the increase in pressure that follows a given increment of delivered volume is much less than it would be if the heart were required to empty into a non-elastic, purely resistive load. An element of inertance is introduced by the mass of the blood that is accelerated and decelerated. Inertial effects, however, are much less prominent than those related to capacitance.

Another characteristic is that the arterial tree behaves as though the heart is pumping into the bifurcation of two unlike and highly capacitive circuits connected in parallel (the vessels in the upper extremities and the head comprise one circuit and the vessels in the trunk and lower extremities comprise a second capacitive circuit). Therefore the pulse contours in the upper and lower extremities should be different. Pascarelli and Bertrand (1964) however, found that peak systolic, end diastolic and mean blood pressure measured simultaneously in the upper (brachial artery) and lower (femoral artery) extremities were similar (the patient was lying); however, the blood pressure pulse in the femoral artery started later than the pulse in the brachial artery. This concept was supported by Bruner (1978) and he suggested that pressures measured simultaneously in the upper and lower extremities are not in phase with each other. He stipulated without explanation however, that the peak systolic pressures in the lower extremities were higher than those of the upper extremities.

A further characteristic of the arterial tree is that there is progressive stiffening of the arterial tree towards the periphery; the visco-elastic behaviour of the vascular walls (at

the periphery there is a decrease in the mix of elastic fibers in favour of muscle in the walls) and the complex branching pattern of the arterial tree at the periphery result in an increase of the characteristic impedance (the impedance measured in the absence of reflections) which is not uniform but increases towards the periphery. Bruner et al (1981a) stated that the impedance at the periphery is resistive and about five times higher than the impedance in the aorta and the great vessels. This increase in impedance means that there will be a progressive increase in the amplitude of the pressure pulse as it travels distally. Hamilton and Dow (1939) found that despite the increase in peak systolic pressure, diastolic pressures at the arch of the aorta and at various peripheral points are essentially the same. Mean pressure also was virtually unchanged despite the great variation in pulse form and systolic pressure.

O'Rourke (1968) and Wesseling et al (1985) showed that age decreased the disparity between proximal and distal systolic blood pressures and this was ascribed to arterial degeneration. Furthermore, the difference between average systolic pressure and mean pressure is greater in the older age group than in the younger, again indicating a lack of resiliency in the arteries.

The marked impedance mismatch between the larger vessels and the periphery creates the opportunity for reflection of the blood pressure wave. Since the impedance changes occur at multiple distributed sites, reflections are blurred and overlapping. The latter is not the case, however, at the periphery. Here the discontinuity in impedance produces retrograde reflections of the pressure pulse, while pulse amplitude observed at a site close to the locus of reflection (the locus of this impedance mismatch

probably resides at the transition to the smaller arterioles less than 1 mm in diameter) is increased (Murgo et al, 1981).

Van Bergen (1954) observed that the systolic pressure pulse increased 20-30 mmHg with the compression of the brachial artery immediately distal to the indwelling needle. Newman et al (1979) and Murgo et al (1981), established that the blood pressure wave was indeed the summation of a forward pressure wave (heart generated) and a backward pressure wave (reflection), the vascular impedance of the peripheral network determining the magnitude of the reflected wave.

Furthermore the reflected pressure waves in the systemic arterial tree, supports oscillations and thus causes resonance in the arterial tree (the arterial tree is a resonant system with a natural frequency of 3-6 Hz). This results in a further increase of the peak systolic value and a narrowing of the pressure pulse (Bruner, 1978; Bruner et al, 1981a).

In effect then, the pressure pulse in a peripheral artery may be markedly different from the one observed closer to the heart. The major difference is the shortening of systole and the increase in peak systolic pressure the further away from the heart it is measured (Murgo et al, 1980). Figure A1.3 represents the change in pulse pressure as the site of measurement is moved away from the heart.

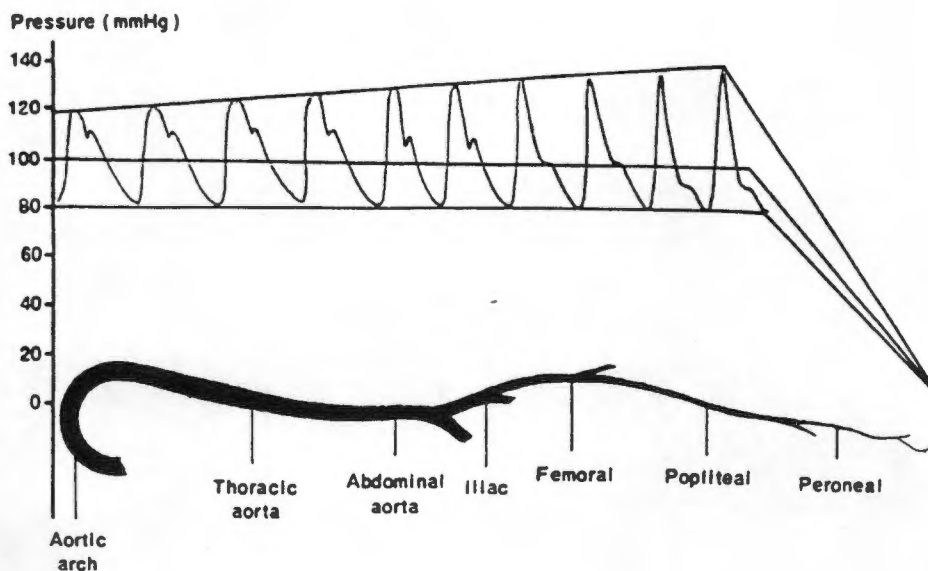


Figure A1.3

Differences in pulse pressure at several sites in the arterial system (Bruner, 1978).

A further consideration is the character of the pulse generated by cardiac ejection. A broad spectrum of frequencies is generated up to and including those perceivable as sound. It follows that this broad spectrum of frequencies may be acted upon in disparate ways by the highly non-homogenous transmission system. High frequency components of the pressure pulse travel faster than those of low frequency. These high frequency components tend to disappear in transit due to the frictional losses owing to fluid viscosity and non-elastic walls.

A2 Invasive blood pressure measurement technique

A2.1 Introduction

Blood pressure measurements are either non-invasive or invasive. In the most common non-invasive method, an artery is usually occluded by compressing an upper limb with an air-filled cuff at a pressure exceeding peak systolic pressure. As the cuff pressure is decreased, a sequence of mechanical phenomena (arterial wall movement or turbulence in blood flow) in the underlying artery are detected audibly or electronically - and correlated empirically to the measured cuff pressure.

This method usually is used for discrete blood pressure measurements. It is clinically safe and does not involve expensive equipment; however, continuous pressure measurement (monitoring) and waveform displays is not achieved.

Yamakoshi et al (1983), developed a non-invasive beat-to-beat blood pressure monitoring device based on the vascular unloading technique and found that the blood pressure recorded by the non-invasive method was in agreement with invasive arterial pressures. However, the manipulation of the equipment was difficult and large measurement errors occurred if the system was incorrectly used.

In the invasive method, a vessel is cannulated and the pressure within the vessel is measured via a fluid-column linked to an extracorporeal pressure measuring device (figure A2.1).

Comparative studies of direct and indirect blood pressure measurements have resulted in controversy and researchers have published a number of articles with greatly different and even contradicting results (Ragan and Bordley, 1941; Van Bergen, 1959; Goldstein and Killip, 1962; Bruner et al, 1981b, 1981c).

Recent studies confirm that direct measurements of systolic and diastolic pressure correlate rather poorly with indirect measurements. Bruner et al (1981c) concluded that direct blood pressure measurement and the indirect method (detection of flow beneath an occluding cuff) were different methodologies and thus no identical results could be expected.

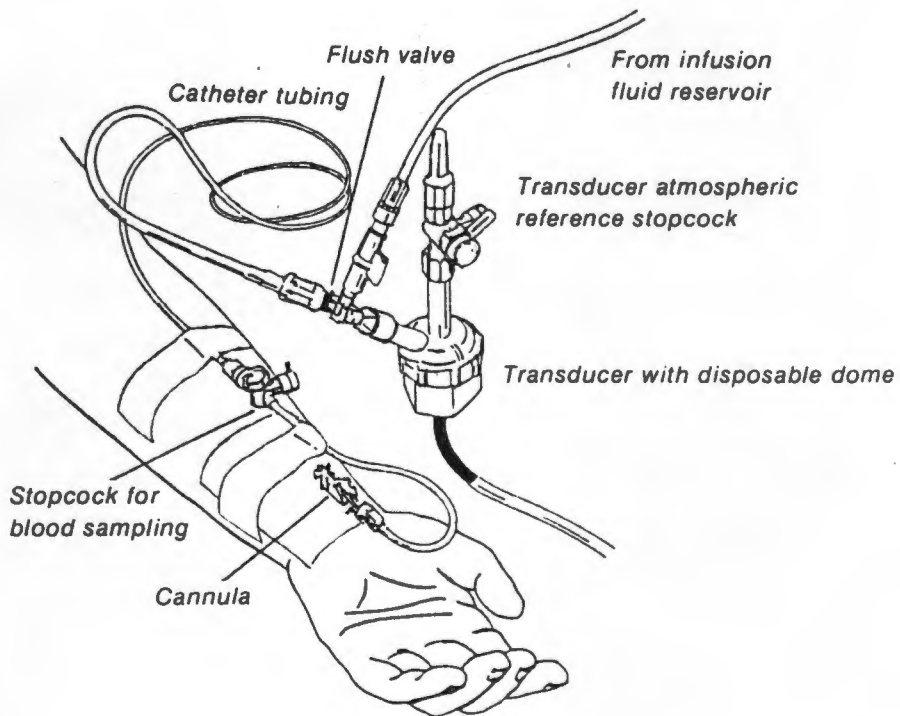


Figure A2.1

A recommended system for long-duration intravascular monitoring. A continuous flush valve allows a flow of 3 ml/h heparinized saline to prevent clotting (Smith, 1978).

The most common sites for arterial cannulation are the radial, brachial and femoral arteries (Smith, 1978). Catheters are generally inserted percutaneously, but a cutdown may also be done.

Of the three common sites the radial is the smallest and most anatomically stable. Usually it has a good collateral circulation and is used routinely for monitoring cardiac surgery patients. Van Bergen (1954) however, stated that reflection of the pressure pulse increased the systolic peak pressure at this measurement site and questioned the radial artery as the best site of pressure measurement.

Prior to insertion of the radial catheter, circulation to the hand is evaluated by assessing the circulation of the palmar arch by the Allen's test or by using a Doppler ultrasound device. The Allen's test consists of simultaneously compressing both the ulnar and the radial arteries for approximately one minute. During this time, the patient rapidly opens and closes his hand to promote exsanguination.

Approximately five seconds after release of one artery (usually the ulnar), there should be blushing of the extended hand due to capillary refilling. This reactive hyperemia indicates adequate circulation in the hand. If blanching occurs, palmar arch collateral circulation is inadequate and a radial catheter could lead to ischaemia of the hand.

A false positive may be obtained if the patient hyperextends his fingers or wrists during the Allen test (Smith, 1978).

After insertion of the cannula, the wrist of the patient is usually restrained in hyperextension to avoid kinking of the cannula and/or the catheter.

The transducer-amplifier system is then connected to the flushed catheter and pressure dome system and the system is balanced and calibrated as described in section A2.2.

The transducer transforms the hydraulic pressure energy to an electrical signal that is amplified, processed and displayed by an electronic monitoring system. This transformation requires a movement of a compliant membrane in the transducer.

A2.2 Balancing and calibration of pressure transducers and catheter systems

When a transducer-amplifier system is first set up, it must be balanced (zeroed) and calibrated. Because physiological pressures are measured relative to atmospheric pressure, the transducer must be adjusted to read zero when exposed to the pressure of room air and positioned at the level of the right atrium. Making this adjustment is known as balancing (Smith, 1978). If this is not done, then for each centimeter difference between the level of the right atrium and the transducer, there will be an error of about 2 mmHg in the reading.

The exact method used for balancing a system varies for the different makes of equipment, but there are certain basic common points (Murray and Howe, 1976; Smith, 1978), listed below:

1. Connect the transducer to the pressure amplifier and turn the power on.
2. Fill the transducer dome with sterile I.V. solution, using the recommended setup technique.
3. Turn the stopcock on one port of the transducer so that it is open to air and adjust the level of the transducer so that this port is at midaxillary line or at the level of the right atrium of the patient.

4. Allow the recommended warm-up time for the transducer-amplifier combination (usually not longer than 3 minutes).
5. Adjust the amplifier so that the reading is at zero (or "baseline").

Calibration is done to check and adjust the visual and numerical display of the pressure on the monitor so that it truly reflects the pressure being exerted on the transducer.

There are a number of devices available which are used to apply a known pressure to the measurement system and these range from the common mercury sphygmomanometer to electronic calibration devices. The method used in static (dc) calibration of the system is listed below:

1. Randomly apply known pressures to the transducer (e.g. 80 mmHg, 100 mmHg and 120 mmHg).
2. If the pressure reading on the monitor differs that of the test device, adjust the monitor calibration knob (This calibration knob may be on the monitor or on the blood pressure module).
3. Calibrate the system when it is initially set up for each patient and recalibrate if the transducer is changed or if there is some doubt as to the accuracy of the pressure read-out.

A2.3 Pressure measurement units

The units, used in clinical practice, viz. the millimeter of mercury (mmHg) or centimeter of water (cm H₂O), differ from the internationally approved (SI) units. The SI unit for pressure is given as the Pascal (Pa) and is defined as a force of 1 Newton per square meter.

In the modern medical texts, pressures are often expressed in Pascal, and are sometimes given in parallel in mmHg or Torr. In table A2.1 conversion factors for these pressure units are given.

$$\begin{aligned} 1 \text{ mmHg} &= 133.3 \text{ Pascal (Pa)} = 0.133 \text{ k Pascal} = 1.36 \text{ cmHg} \\ 1 \text{ Pascal} &= 0.0075 \text{ mmHg} = 1 \text{ Torr} \end{aligned}$$

e.g.

$$1 \text{ atm} = 101.3 \text{ kPa} = 101.3 \text{ kTorr} = 759.7 \text{ mmHg}$$

Table A2.1

Conversion table for pressure units

Most clinical pressure measurements are made with respect to atmospheric pressure, which is assigned a value of zero pressure; i.e. gauge pressure, rather than absolute pressure, is used.

A3 Advantages and risks of invasive blood pressure measurement.

Invasive (direct) blood pressure measurement has a number of advantages over the non-invasive method. These are summarized and listed below;

- Better accuracy than the non-invasive method
- Availability of beat-to-beat measurements
- Availability of hard-copy time course recording
- Availability of true mean pressures
- Possibility of measurements at specific internal sites
- Better recording fidelity during rapid changes of pressure.

There are however a number of risks and subsequent disadvantages are involved with the invasive method.

The major risks associated with direct vascular monitoring are sepsis, bleeding back and thromboembolic phenomena.

To prevent sepsis, care must be taken to sterilise any instrumentation that is in contact with the patient. The use of disposable transducers and tubing is the recommended option, but usually at an increased cost (especially with the current rate of exchange).

Bleed-back occurs when the patient's blood pressure at the measurement site is higher than the counteracting pressure of the flush solution. This may occur when the equipment that is used to apply pressure to the flushing unit (or drip) fails or when there is some type of leak in the pressure-monitoring system, such as

when a cracked or warped pressure dome is used.

Clotting of pressure lines occurs whenever flushing of the pressure lines is inadequate. This may increase the risk of thrombosis and decrease the fidelity of the pressure recording due to a negative effect on damping.

A4 System requirements for invasive blood pressure measurement

A4.1 Introduction

Medical therapy is often based on the absolute value of a blood pressure measurement. Inaccurate or false values may lead to inappropriate therapy which may be detrimental to the patient's health. It is thus important and necessary that certain equipment requirements for the accurate measurement of blood pressure be established and adhered to.

Before the pressure monitoring equipment requirements are investigated in detail, it is important to establish the fundamental requirements of any system used to record a blood pressure pulse.

In the pressure measurement system, the overall gain (the ratio of system output to input amplitude at any given frequency) is the product of the gain of the individual components: the catheter-manometer system (cannula, pressure tubing, stopcock and transducer), the amplification stage and the recorder stage, and thus the lowest bandwidth of any component mentioned will be the maximum bandwidth of the entire system.

For an ideal system, the overall gain should be linear (constant over all frequencies of interest), bearing in mind that output equals voltage and the input equals pressure, i.e. the displayed value of pressure equals the applied pressure at all the frequencies of interest. Similarly the phase response of the entire system is the sum of the individual phase responses of the components. An ideal system should have a linear phase response and therefore no phase distortion, as linear phase response

implies a constant time delay irrespective of frequency. All frequency components of the waveform are delayed equally and waveform shape is therefore preserved. Ideal amplitude and phase responses are displayed in figure A4.1.

In the non-ideal case, the amplitude and phase responses produce non-linearities which alter the pressure pulse waveform. In order to quantify these changes it is necessary to have a true reference signal i.e. a signal obtained by a system with ideal / near ideal characteristics. The time delays of the recorded signals can in many physiological applications be tolerated; however, for comparative studies this delay may be unacceptable.

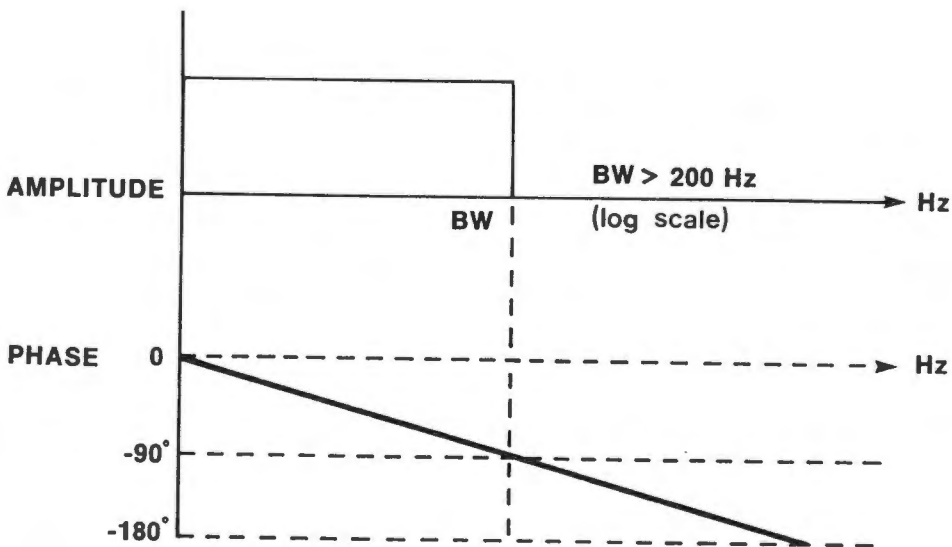


Figure A4.1

Ideal amplitude and phase response for blood pressure measurement systems.

A4.2 Review of system bandwidth requirements

Otto Frank in 1903 was the first to establish criteria for recording pressure waveforms with adequate fidelity. Since 1946 extensive research has been conducted into dynamic response, the theoretical formulation of catheter-manometer systems and the frequency content of blood pressure waveforms (Fry, 1960; McDonald, 1974; Bruner et al, 1981a; Andersen and Bergsten, 1982; Yeomanson and Evans, 1983). Bruner (1978) stated the frequency content for the inotropic phase (section A1.3) of the blood pressure pulse measured in the ascending aorta, had frequency components in the range of 40-100 Hz. Krovetz and Goldbloom (1974), employing harmonic analysis of blood pressures recorded at various sites with catheter-tip manometers, found frequencies of 15-19 Hz even in the brachial artery pulse. The frequency components of the volume displacement phase of the blood pressure pulse were in the range of 3 - 5 Hz.

Bruner et al (1981a) stated that the criteria for good signal reproduction, required that the resonant frequency of catheter-manometer systems was at least five times higher than the highest frequency deemed significant in the blood pressure signal.

For accurate recording and reproduction of the inotropic phase of any blood pressure, the frequency response of the catheter-manometer system would thus have to be very high (> 200 Hz).

However, it has been established that catheter-manometer systems with bandwidth lower than 200 Hz can be used to record blood pressure waveforms (Bruner, 1978). No consensus on the minimum frequency response for adequate blood pressure recording has yet been obtained. Wood (1956) observed that a system of 6 Hz was

adequate in recording blood pressure, while Bruner (1978) stated that 20-25 Hz was needed.

In the characterisation of catheter-manometer system requirements, Krovetz et al, (1974) stated that the important parameter is that of frequency bandwidth alone, e.g. "flat to 16 Hz" or "flat to the 10th harmonic of the fundamental pressure waveform frequency". However, the two main parameters (accepted in medical literature) to characterise a catheter-manometer system response are the damped natural frequency and the damping factor.

A4.3 General system requirements

Before the catheter-manometer system requirements for accurate blood pressure measurement are investigated, the concepts of static accuracy, dynamic accuracy and physiological reactance are discussed. Furthermore, monitoring and engineering terminology is listed in the glossary and will guide the reader in following sections.

A4.3.1 Static Accuracy

Static accuracy is the ability of the pressure measuring instrument to record extremely slow varying (with time) events. Static accuracy implies two qualities: stability and uniqueness. Stability implies that there should be no base line drift, no calibration drift and no change in gain factor of the equipment. Uniqueness indicates that the system will respond uniquely to any statically applied signal. The property of hysteresis exhibited

by some recording systems is an example of the lack of uniqueness in static response.

The methods for testing uniqueness and stability are identical and constitute applying a progressively changing signal to the input of the recording equipment. The output is recorded (either on a strip chart recorder, magnetic tape recorder or digital display) and is then compared to the input signal. For uniqueness a line (output/input) is obtained upon which all the points will lie that represent the system response to the different input signals. If these lines are superimposable the requirement of stability is met. If however the slopes of the lines are different, the gain of the system has drifted. If the origins are different but slopes are the same, the base line has drifted.

Although the foregoing discussion pertains to the behaviour of the pressure measurement system itself, the act of reading or recording may introduce error. This error is usually referred to as recording error and is often random in nature.

A4.3.2 Dynamic Accuracy

Dynamic accuracy of a recording system is the fidelity with which the response of the system will simulate the dynamic signal being measured. The dynamic accuracy of a system is governed by the noise level of the system and by the dynamic response of the system.

A4.3.2.1 Noise

The term noise is used to describe a time-varying signal that arises from various sources that are not directly related to the physiological event being measured. Noise is commonly divided into three categories; electrical noise, mechanical noise and thermal noise.

Electrical noise (which arises in electronic amplification components and occasionally from the organism) and thermal noise are not common problems in blood pressure measurement techniques. However, transducers are affected by mechanical noise (which arises from vibrations in the recording equipment) and if the noise has the same periodicity as that of the signal being measured, the recorded pressure fidelity will be affected. This however is not a common problem.

A4.3.2.2 Dynamic response

Dynamic response of a recording system may be determined experimentally by driving it with a known changing input and observing its response. This driving force signal may be either a sinusoidal waveform or a step pulse. The graphic display of the amplitude and the phase of the response of the system compared to an input sinusoidal wave of constant amplitude is called the frequency response curve. It is intuitively clear that constant amplitude response for a given bandwidth indicates the measurement system's ability to accurately follow changing physiological phenomena provided the significant frequency components fall within the systems bandwidth.

A4.3.3 Physiological reactance

Physiological reactance is defined as the undesirable effect of the recording system on the physiological parameter being recorded. It occurs if the presence of a sensing probe of the recording instrument so alters the structure of the vessel that the pressure that is recorded bears little relationship to the original pressure at that site. This effect can be observed with the presence of a large cannula in a small artery.

A4.4 Catheter-manometer requirements

Optimal pressure measurement of the applied pressure is obtained if:

- the physiological reactance (section A4.3.3) is at its minimum, and
- the pressure is measured at the source (Fry, 1960).

These points imply that the transducer dimensions have to be at a minimum and that the transducer must be as close to the applied pressure. However, cost and practical reasons of construction prohibit the general use of this type of transducer (catheter-tip).

Extracorporeal transducers larger than the catheter-tip are thus coupled to the blood pressure source via a cannula and a fluid-filled catheter.

Most transducers currently in use for pressure monitoring measure the displacement of a mechanical diaphragm due to applied pressure. This displacement is converted, either by a capacitive,

Most transducers currently in use for pressure monitoring measure the displacement of a mechanical diaphragm due to applied pressure. This displacement is converted, either by a capacitive, resistive or inductive circuit, to an electrical signal. The catheter-manometer system (cannula and catheter) should be able to detect an applied pressure and convert it into the analogue electrical signal, without degenerating the signal quality. The bandwidth of the cannula and catheter should be higher (by a factor of 5) than the highest significant frequency component of the blood pressure pulse (Bruner, 1978) for high accuracy applications.

Furthermore, transducer requirements (as set by the Association for the Advancement of Medical Instrumentation - AAMI and Andersen and Bergsten, 1982) are listed in table A4.1.

■ Linearity	-	\pm 2% error for pressure range of - 20 to 250 mmHg.
■ Hysteresis	-	\pm 2% error for pressure range of - 20 to 250 mmHg
■ Temperature coefficient of sensitivity	-	\pm 0.05 mV/cmHg/ $^{\circ}$ C for temp. range of 15 to 40 $^{\circ}$ C
■ Temperature coefficient at zero pressure	-	\pm 0.3 mmHg/ $^{\circ}$ C for temp. range of 15 to 40 $^{\circ}$ C
■ Pressure measurement range	-	- 20 to 400 mmHg

Table A4.1

Transducer requirements for accurate blood pressure measurement (Andersen and Bergsten, 1982; AAMI, 1984).

A4.5 Amplifier requirements

In the amplification of blood pressure signals, three basic types of electronic amplifiers are commonly used: (a) carrier, (b) direct coupled and (c) chopper amplifier (Fry, 1960).

Carrier amplifiers are used where high gain with high amplifier stability is necessary or where certain reactance type transducers are used. The disadvantage of the carrier amplifier is the increased complexity of operation and a signal to noise ratio that is some what poorer than that which can be achieved in the direct coupled amplifiers.

Direct coupled amplifiers are used where a lower gain is acceptable and where the signal from the transducer is directly coupled to the amplifier. The advantage of the direct coupled amplifier is its simplicity and high signal to noise ratio. However, at high attenuation of the input signal the amplifier becomes unstable.

The chopper amplifier is a compromise between the above-mentioned and therefore permits both high gain and stability. The major disadvantage of this amplifier is a limited linearity for the frequencies used in blood pressure amplification.

The blood pressure amplifiers used in practice are normally combinations of the above mentioned amplifiers so that optimal gain, stability, signal to noise ratio and linearity are obtained.

More recently advanced digital electronic systems have enhanced the electronic signal processing capabilities. Digital filters and signal analysis algorithms are routine components of

presently used blood pressure measurement systems. A detailed discussion of this field would be beyond the scope of this thesis.

Blood pressure amplifier requirements may thus be generally given as:

- Dynamic accuracy - (Appendix A4.3.2)
- Linearity - < 2% error for 0-200 Hz
- High gain stability - < $7\mu\text{V}/^\circ\text{C}$ (15-40 $^\circ\text{C}$)
- High signal to noise ratio - > 70 dB
- Large bandwidth - > 200 Hz

A4.6 Response requirements for hard-copy records, display and storage systems

The recording systems used for the display and/or storage of pressure measurements may be classified into three different groups; the direct writer, the optical recorder/display and the electromagnetic storage system.

The direct writer (strip chart with either thermal, inkjet or dot matrix plotting devices) has the advantage that it displays a hard copy of the pressure waveform almost instantaneously; however, the response of the writing mechanism of some of the direct writers are limited and the paper costs high.

The optical recorder/display which is used generally consists of a cathode ray tube and/or photographic film record (latter requires processing); this has a high frequency response. Cathode ray tubes and appropriate electronic circuits can be constructed so that linearity is obtained. The advantage of this system is that multi-channel representation is possible at reduced cost and without the loss in bandwidth.

Electromagnetic, laser optical and electronic storage systems can be constructed with very high frequency responses. The electronic circuitry may be digital and specific filtering circuits guarantee high frequency response.

The summarised requirements are the same as for the amplifier and are listed below;

- Dynamic accuracy - (Appendix A4.3.2)
- Linearity - < 2% error for 0-200 Hz
- High gain stability - < 7 μ V/°C (15-40 °C)
- High signal to noise ratio - > 70 dB
- Large bandwidth - > 200 Hz

A4.7 Ancillary requirements

In addition to the frequency response requirements specified for the catheter-manometer, amplifier and recording/display system, ancillary requirements for blood pressure measurement equipment has been stipulated by AAMI and is listed in table A4.2.

■ Null offset or unbalance	-	± 75 mmHg
■ Fluid isolation		
■ Pressure measurement range	-	-20 to 400 mmHg
■ Electrical leakage	-	10 μ A for 220 Volts (50 Hz)
■ Operating Temperature	-	-15 to 40 °C

Table A4.2

Ancillary system requirements for blood pressure measurement equipment (AAMI, 1984).

APPENDIX B

MODELLING AND CHARACTERISATION OF THE CATHETER-MANOMETER SYSTEM

CONTENTS

B1	Introduction	B2
B1.1	The distributed parameter model	B2
B1.1.1	Fry (1960) model	B2
B1.1.1.1	Terminal mechanical impedance of the pressure dome	B3
B1.1.1.2	Characteristic fluid impedance of the cannulae and pressure tube	B5
B1.1.1.3	Dynamic response of the catheter manometer model.	B6
B1.1.2	Model by Andersen and Bergsten (1982)	B9
B1.1.3	Model by Yeomanson and Evans (1983)	B12
B1.2	The lumped parameter model	B17
B2	Fundamentals of second-order systems	B23
B2.1	Relationship between damping factor and overshoot	B27

B1 Introduction

To investigate the magnitude and relationship of influences that determine the behaviour of catheter-manometer systems, many researchers have either devised lumped or distributed parameter models such as those discussed in chapter 2. These models enable us to relate numerous variables and the effects they have on the behaviour of the system. In particular, the models relate the variables that influence the frequency response of the catheter-manometer systems.

B1.1 The distributed parameter model

B1.1.1 Fry (1960) model

The mathematical derivation of equations for the distributed parameter catheter-manometer model formulated by Fry is beyond the scope of this thesis and may be found in literature on transmission line theory (Goldman, 1949). The sections below will however, briefly describe the relationship of fluid dynamic parameters and catheter impedances on the system response.

The catheter-manometer system model is described in terms of two parameters: one describing the physical properties of the pressure chamber, Z_T , called the terminal mechanical impedance and the other describing the physical properties of the catheter system (cannula and pressure tubing) called the characteristic fluid impedance, Z_o . Both Z_T and Z_o are complex numbers having a real and an imaginary part; therefore, each is represented by both magnitude and phase.

B1.1.1.1 Terminal mechanical impedance of the pressure dome

Fry stated that the catheter-manometer system was a second order system which had three components describing its response. These are acceleration, velocity and displacement and are proportional to three types of forces: inertia, friction and elasticity, respectively.

These forces can be represented on a vector diagram as shown in figure B1.1. Since the inertial and elasticity forces are opposite in direction they are replaced by a resultant vector, a reactive force.

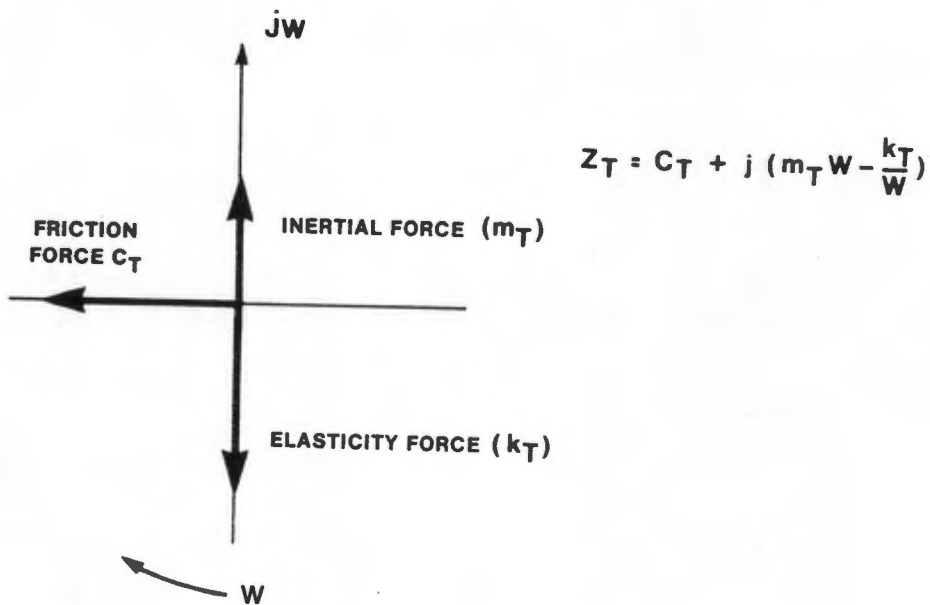


Figure B1.1

Vector diagram relating the forces acting on a second order system. m_T represents the inertial and k_T and c_T the elasticity and friction force respectively.

m_T is the coefficient of mass representing the inertial force per unit acceleration of the moving element (the membrane and transducer diaphragms) in the pressure chamber, k_T is the pressure-mass coefficient of the elasticity force per unit fluid displaced into the pressure chamber and c_T is the coefficient of friction representing the frictional force per unit mass flow into the pressure chamber.

The pressure-mass coefficient, k_T , in a liquid-filled system, is predominantly determined by the pressure-volume coefficient of the pressure chamber which is in turn determined by the elastic properties of the pressure dome membrane and the transducer diaphragm. Since k_T is the rate of change of pressure per unit change of mass in the pressure chamber, it is equal to the reciprocal of (the product of fluid density and the chamber volume and the sum of fluid compressibility and the pressure dome chamber distensibility).

Thus k_T is equal to the total pressure-volume coefficient of the gauge chamber, k_v , divided by the fluid density, i.e.,

$$k_T = k_v / \rho. \quad (B1.1)$$

The terminal mechanical impedance, Z_T , is given by the equation B1.2.

$$Z_T = c_T + j(m_T \omega - k_T / \omega) \quad (B1.2)$$

where ω is the angular frequency in radians per second,

Equation B1.2 is derived such that the rotating vector representing the sinusoidal pressure acting on the pressure

chamber is equal to the vector product of Z_T times the sinusoidal flow in and out of the pressure chamber, i.e. the amplitude (length) of the pressure vector is equal to the amplitude of the flow vector times the amplitude of Z_T and the phase angle difference between the pressure and the flow is the angle of Z_T . Therefore, the impedance Z_T , relates the pressure in the pressure chamber to the flow of fluid into and out of the chamber.

B1.1.1.2 Characteristic fluid impedance of the cannulae and pressure tube

The characteristic fluid impedance of the catheter (cannulae and pressure tubing) is given by equation B1.3 (Fry, 1960; McDonald, 1974).

$$Z_o = [(m_o w - j c_o) k_o / w]^{\frac{1}{2}} \quad (B1.3)$$

The distributed mass flow inertance, m_o , of the catheter fluid is the pressure drop per unit length per unit mass flow acceleration and is given approximately by the expression

$$m_o \approx 1/\pi r^2 \quad (B1.4)$$

where r is the inner or lumen radius of the catheter. The distributed coefficient of frictional resistance which is the pressure drop per unit length per unit mass flow is approximated from Poiseuille's law by the expression (McDonald, 1974).

$$c_o \approx 8\nu/\pi r^4 \quad (B1.5)$$

where ν is the time average of the fluid kinematic viscosity, and as before r is the lumen radius of the catheter.

The distributed coefficient of elastance of the catheter, k_0 is defined as the fluid mass increase per unit increase of pressure per unit length of the catheter. Again, this represents the reciprocal of (the product of the fluid density and volume of fluid per unit length and the sum of fluid compressibility and catheter distensibility).

B1.1.1.3 Dynamic response of the catheter-manometer model.

In formulating the amplitude and phase response of this catheter-manometer model, the following approach is taken:

Any sinusoidal function of time may be represented in complex number notation by the projection on the x axis of a vector rotating at the same frequency as the sinusoidal function. The sinusoidal pressure in the pressure chamber can be represented by the complex number P_r (a rotating vector) and the pressure applied to the opening of the catheter by another rotating vector P_i which will have a different magnitude and will lead P_r in phase (figure B1.2). The pressure vectors P_i and P_r are the products of mass flow and the characteristic and terminal impedances respectively.

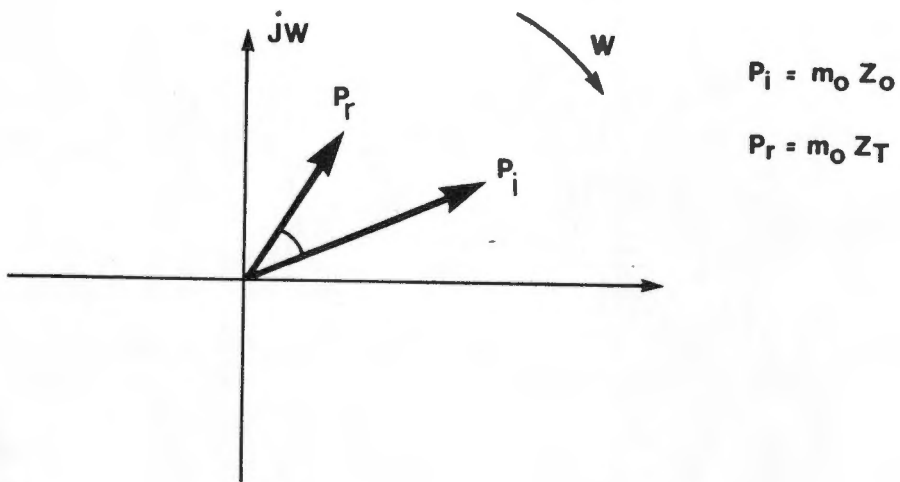


Figure B1.2

Vectors representing P_i and P_r in a catheter-manometer system.

Since the mass flow in and out of the pressure chamber equals the mass flow in and out of the catheter, the following relationship exists:

$$\frac{P_i}{Z_0} = \frac{P_r}{Z_T} \tag{B1.6}$$

where P_r is the dome pressure, P_i is the input pressure at the catheter tip,

Assuming that the applied pressure is sinusoidal and m_T and c_T (usually they are) are small compared to k_T one may omit m_T and c_T and thus obtain a simpler approximation for the frequency response of the catheter-manometer system:

$$\frac{P_r}{P_i} = \frac{k_T}{j\omega(Z_T \cosh \Phi l + Z_o \sinh \Phi l)} \quad (\text{B1.7})$$

where l is the catheter length and Φ the propagation constant which is derived from Z_o and given as:

$$\Phi = \left[\frac{j c_o \omega - m_o \omega^2}{k_o} \right]^{\frac{1}{2}} \quad (\text{B1.8})$$

A plot of the magnitude of the ratio given in equation B1.7 versus frequency would be the amplitude response curve for the catheter system. Similarly, a plot of the angle of the ratio of equation B1.7 versus frequency is the phase response of the system.

If the distributed elastance of the catheter, k_o is very high, then the flow through the catheter to and from the pressure chamber will tend to move as a unit and little excess fluid mass will be stored in the catheter. In this simplified model the catheter-manometer system may be viewed as a bar of liquid, l units long, sliding in a viscous sleeve in the lumen of the catheter. Expanding the transfer function given in equation B1.7 in series and taking the limit as k_o approaches infinity and m_T and c_T approaches zero, the transfer function simplifies to:

$$\frac{P_r}{P_i} = \frac{k_T}{(k_T - m_o l \omega^2) + j \omega c_o l} \quad (\text{B1.9})$$

B1.1.2 Model by Andersen and Bergsten (1982)

In the distributed catheter-manometer model of Andersen and Bergsten (1982) described in section 2.2.1, the system parameters that determined the frequency response were represented by electrical elements (figure B1.3).

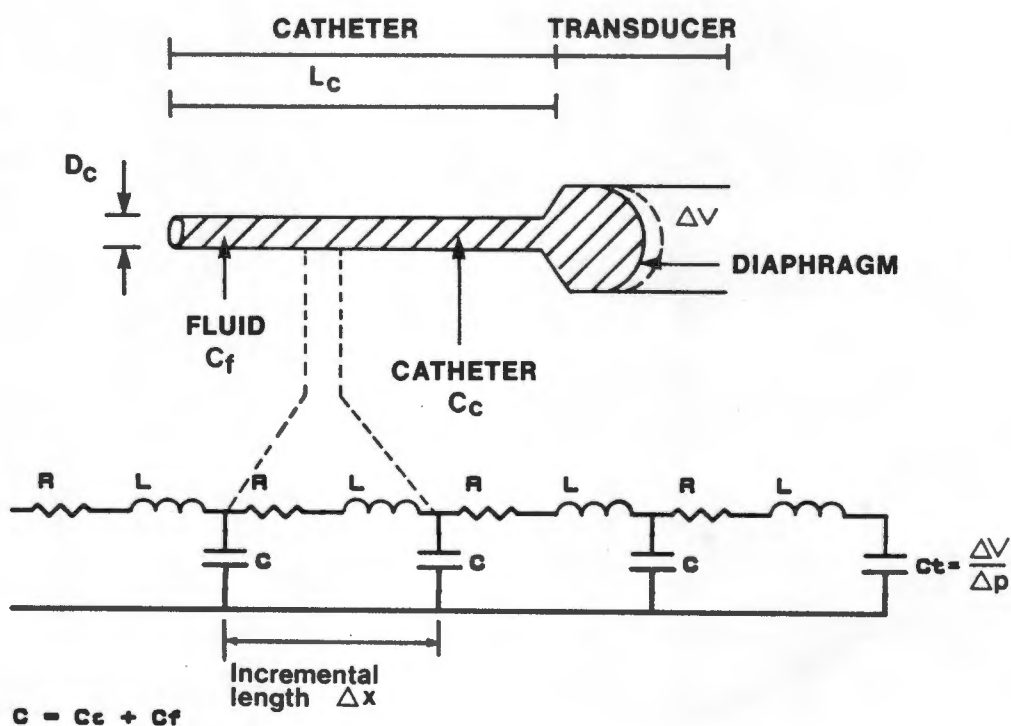


Figure B1.3

The electrical analogue model described by Andersen and Bergsten (1982). The pressure chamber has a compliance C_t . The compliance of the catheter is C_c and that of the fluid is given by C_f . The lumen diameter of the catheter is given by D_c and its length by L_c . In the electrical analogue R is the resistance per unit length related to the viscosity of the fluid and L is the inductance per unit length representing the inertia of the fluid. C is the catheter and fluid compliance.

The fluid dynamic analogies of the electrical parameters that are shown in figure B1.3 are given below:

The resistance related to the viscosity of the fluid in the catheter is given by:

$$R = \frac{8 \cdot l \cdot v}{r^4} \quad (\text{B1.10})$$

where l is the catheter length, v the fluid viscosity and r the lumen radius of the catheter.

The inertia of the fluid is given by:

$$L = \frac{\rho \cdot l}{r^2} \quad (\text{B1.11})$$

where ρ is the density of the fluid and r is the lumen radius of the catheter.

The compliance C , is given as:

$$C = \left(\frac{2.5 \cdot \pi \cdot r^3}{4 \cdot E \cdot t_w} + k_w \cdot \pi \cdot r^2 \right) \cdot l \quad (\text{B1.12})$$

where E is the Young's modulus for the catheter material, t_w the thickness of the catheter wall and k_w is the compressibility of water.

Values for compliance of catheters and transducers diaphragms were calculated by Andersen and Bergsten using equation B1.12 and are given in table B1.1.

Catheter type	C_c (mm ³ / mmHg / m)
PE50	2 x 10 ⁻⁴
Cournaud 6F	2.5 x 10 ⁻⁴
Cournaud 8F	15.0 x 10 ⁻⁴
Transducer type	C_t (mm ³ / mmHg / m)
AME, AE40	3 x 10 ⁻⁴
HP 1290A	20 x 10 ⁻⁴
Statham P23	4 x 10 ⁻⁴

Table B1.1

Values for compliance of selected catheters and transducers (Andersen and Bergsten, 1982).

Andersen and Bergsten stated that this model was a simple second-order system with one degree of freedom and presented without derivation the resonant frequency as:

$$f_p = \frac{1}{2 \cdot L \cdot (C_t + C/3)^{\frac{1}{2}}} \quad (\text{B1.13})$$

and the damping factor by,

$$\beta = \frac{(C_t + CR/3)}{(2 \cdot (L \cdot (C_t + C/3))^{\frac{1}{2}})^{\frac{1}{2}}} \quad (\text{B1.14})$$

B1.1.3 Model by Yeomanson and Evans (1983)

Yeomanson and Evans also presented a distributed model of the catheter-manometer system in terms of electrical parameters that had fluid dynamic analogies. Their model is schematically represented in figure B1.4 and is treated as a transmission line whose characteristic impedances are shown.

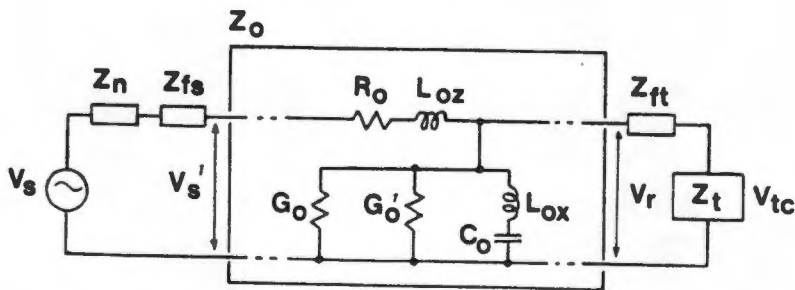


Figure B1.4

R_o is the resistance per unit length due to the fluid viscosity. L_{oz} is the inductance per unit length corresponding to the axial inertia of the mass of the liquid, C_o the capacitance per unit length representing the compliance of the manometer line walls and the filling fluid, G_o is the conductance per unit length and G_o' is the conductance per unit length due to the inelastic behaviour of the fluid. L_{ox} represents the inductance per unit length representing the radial inertia of the fluid and the catheter wall (Yeomanson and Evans, 1983).

Energy losses arising from the inelastic behaviour of water are negligible in comparison with those arising from other mechanisms and for compliances and wall losses encountered in typical manometer lines the effect of the radial inertia of the fluid and wall can be ignored.

The catheter forms part of the coupling between the transducer impedance Z_t , and the vascular system which has a high compliance. The latter is modelled as a zero impedance voltage source, V_s . At both ends of the pressure tubing are Luer fittings, of a small impedance Z_{fs} and Z_{ft} , one of which is connected to a needle or cannula, impedance Z_n . The phase velocity of pressure waves in the components of the measurement system other than in the catheter can thus be regarded to have lumped impedances in the electrical analogue.

Using the electrical analogue circuit in figure B1.4, the voltage across the terminating impedance, Z_r (equation B1.21), of a transmission line of length l which is driven by an voltage source V_s is given by Benson and Harrison (1966) as:

$$V_r = V_s / [\cosh \Phi l + (Z_o / Z_{term}) \sinh \Phi l] \quad (B1.15)$$

where

$$Z_r = Z_t + Z_{ft} \quad (B1.16)$$

and where the characteristic impedance Z_o , is given by

$$Z_o = [(R_o + j\omega L_{oz}) / (G_o + j\omega C_o)]^{1/2} \quad (B1.17)$$

and Φ is the propagation constant of the line. The constant is expressed by

$$\Phi = [(R_o + j\omega L_{oz})(G_o + j\omega C_o)]^{1/2} \quad (B1.18)$$

In the electrical analogue, shown in figure B1.4, the input voltage of the transmission line is modified by the impedance of the cannulae and the luer fittings (Z_n and Z_{fs}) and is given by

$$V_{s'} = V_s (Z_{in} / (Z_{in} + Z_n + Z_{fs})) \quad (B1.19)$$

where $V_{s'}$ is the source voltage minus the voltage drop across the luer fitting and cannula. Z_{in} is the input impedance of the line.

$$Z_{in} = Z_0 \cdot (Z_r \cosh \Phi l + Z_0 \sinh \Phi l) / (Z_r \sinh \Phi l + Z_0 \cosh \Phi l) \quad (B1.20)$$

Similarly for the terminating impedance, which is the sum of the impedance of the transducer diaphragm and the catheter luer fitting, an equation relating these impedances can be written. Therefore

$$Z_r = (Z_{tc} + Z_{td}) + Z_{ft} \quad (B1.21)$$

where Z_{tc} and Z_{td} are the impedance of the pressure dome port and pressure dome respectively.

An equation (B1.22) can thus be found that represents actual recorded pressure or voltage across Z_{tc} .

$$V_{tc} = \frac{V_{s'}}{\cosh \Phi l + (Z_0/Z_r) \cdot \sinh \Phi l} \cdot \frac{Z_{tc}}{Z_{tc} + Z_{td} + Z_{fc}} \quad (B1.22)$$

The amplitude response of the measurement system is obtained by the magnitude of the ratio of output/input, i.e. $|V_{tc}/V_s'|$. Associated with the amplitude response there is also a phase response. The phase lag $\phi(\omega)$ of the pressure at the transducer relative to the source may be written in terms of real and imaginary components of the complex argument of equation B1.22 and is given in equation B1.23.

$$\phi(\omega) = -\arctan(V_{imag}/V_{real}) \quad (B1.23)$$

Furthermore, Yeomanson and Evans (1983) devised a method by which they were able to calculate the characteristic impedance by using the equations given by McDonald (1974) for the determination of rigid, fluid filled tubes (equation B1.24).

$$Z_{rigid} = (v_c a^2 l / \pi r^4 M_{10}(a)) / (\sin \epsilon_{10}(a) + j \cos \epsilon_{10}(a)) \quad (B1.24)$$

where the catheter has a length l and a lumen radius of r .

and

$$a = r(\omega p / v)^{1/2} \quad (B1.25)$$

where p is the fluid density, v is the coefficient of viscosity and a is a dimensionless quantity that characterises the oscillatory flow in a rigid tube. M_{10} and ϵ_{10} are related to the amplitude and phase components of zero and first order complex Bessel functions of a . These series expressions are listed in the table B1.2 and used in the calculation of the characteristic impedance and the frequency response of rigid tubes in chapter 5.

α	M'_{10}/α^2	ϵ_{10}	α	M'_{10}/α^2	ϵ_{10}	α	M'_{10}/α^2	ϵ_{10}	α	M'_{10}/α^2	ϵ_1
0.00	0.1250	90.00	2.50	0.0855	44.93	5.00	0.0302	18.65	7.50	0.0147	11.87
0.05	0.1250	89.98	2.55	0.0837	43.88	5.05	0.0297	18.43	7.55	0.0146	11.78
0.10	0.1250	89.90	2.60	0.0819	42.86	5.10	0.0292	18.23	7.60	0.0144	11.70
0.15	0.1250	89.79	2.65	0.0802	41.86	5.15	0.0287	18.02	7.65	0.0142	11.61
0.20	0.1250	89.62	2.70	0.0784	40.90	5.20	0.0282	17.83	7.70	0.0140	11.53
0.25	0.1250	89.40	2.75	0.0767	39.96	5.25	0.0278	17.63	7.75	0.0139	11.45
0.30	0.1250	89.14	2.80	0.0750	39.05	5.30	0.0273	17.44	7.80	0.0137	11.37
0.35	0.1250	88.83	2.85	0.0734	38.17	5.35	0.0269	17.26	7.85	0.0136	11.29
0.40	0.1250	88.47	2.90	0.0717	37.32	5.40	0.0264	17.08	7.90	0.0134	11.21
0.45	0.1249	88.07	2.95	0.0701	36.50	5.45	0.0260	16.90	7.95	0.0133	11.14
0.50	0.1249	87.61	3.00	0.0685	35.70	5.50	0.0256	16.73	8.00	0.0131	11.06
0.55	0.1248	87.11	3.05	0.0670	34.93	5.55	0.0252	16.56	8.05	0.0130	10.98
0.60	0.1248	86.57	3.10	0.0655	34.18	5.60	0.0248	16.39	8.10	0.0128	10.91
0.65	0.1247	85.97	3.15	0.0640	33.46	5.65	0.0244	16.23	8.15	0.0127	10.84
0.70	0.1246	85.33	3.20	0.0626	32.77	5.70	0.0240	16.07	8.20	0.0125	10.77
0.75	0.1244	84.65	3.25	0.0612	32.09	5.75	0.0237	15.91	8.25	0.0124	10.70
0.80	0.1243	83.91	3.30	0.0598	31.45	5.80	0.0233	15.76	8.30	0.0122	10.63
0.85	0.1240	83.14	3.35	0.0585	30.82	5.85	0.0230	15.61	8.35	0.0121	10.56
0.90	0.1238	83.32	3.40	0.0572	30.22	5.90	0.0226	15.46	8.40	0.0120	10.49
0.95	0.1235	81.45	3.45	0.0559	29.64	5.95	0.0223	15.32	8.45	0.0119	10.42
1.00	0.1232	80.55	3.50	0.0547	29.08	6.00	0.0220	15.18	8.50	0.0117	10.36
1.05	0.1228	79.60	3.55	0.0535	28.53	6.05	0.0216	15.04	8.55	0.0116	10.29
1.10	0.1224	78.61	3.60	0.0523	28.01	6.10	0.0213	14.90	8.60	0.0115	10.22
1.15	0.1219	77.59	3.65	0.0512	27.51	6.15	0.0210	14.77	8.65	0.0114	10.16
1.20	0.1213	76.53	3.70	0.0501	27.02	6.20	0.0207	14.63	8.70	0.0112	10.10
1.25	0.1207	75.44	3.75	0.0490	26.55	6.25	0.0204	14.50	8.75	0.0111	10.04
1.30	0.1200	74.31	3.80	0.0480	26.10	6.30	0.0201	14.38	8.80	0.0110	9.97
1.35	0.1193	73.16	3.85	0.0470	25.66	6.35	0.0199	14.25	8.85	0.0109	9.91
1.40	0.1185	71.98	3.90	0.0460	25.24	6.40	0.0196	14.13	8.90	0.0108	9.85
1.45	0.1176	70.77	3.95	0.0451	24.83	6.45	0.0193	14.01	8.95	0.0107	9.79
1.50	0.1166	69.54	4.00	0.0441	24.43	6.50	0.0191	13.89	9.00	0.0106	9.73
1.55	0.1156	68.30	4.05	0.0432	24.05	6.55	0.0188	13.77	9.05	0.0104	9.68
1.60	0.1144	67.03	4.10	0.0424	23.68	6.60	0.0185	13.66	9.10	0.0103	9.62
1.65	0.1133	65.76	4.15	0.0415	23.32	6.65	0.0183	13.54	9.15	0.0102	9.56
1.70	0.1120	64.47	4.20	0.0407	22.98	6.70	0.0181	13.43	9.20	0.0101	9.51
1.75	0.1107	63.18	4.25	0.0399	22.64	6.75	0.0178	13.32	9.25	0.0100	9.45
1.80	0.1093	61.89	4.30	0.0391	22.32	6.80	0.0176	13.21	9.30	0.0099	9.40
1.85	0.1078	60.59	4.35	0.0384	22.00	6.85	0.0173	13.11	9.35	0.0098	9.34
1.90	0.1063	59.30	4.40	0.0376	21.70	6.90	0.0171	13.00	9.40	0.0097	9.29
1.95	0.1047	58.02	4.45	0.0369	21.40	6.95	0.0169	12.90	9.45	0.0096	9.24
2.00	0.1031	56.74	4.50	0.0362	21.11	7.00	0.0167	12.80	9.50	0.0096	9.18
2.05	0.1015	55.47	4.55	0.0355	20.84	7.05	0.0165	12.70	9.55	0.0095	9.13
2.10	0.0998	54.22	4.60	0.0349	20.56	7.10	0.0163	12.60	9.60	0.0094	9.08
2.15	0.0980	52.98	4.65	0.0342	20.30	7.15	0.0161	12.50	9.65	0.0093	9.03
2.20	0.0963	51.77	4.70	0.0336	20.05	7.20	0.0159	12.41	9.70	0.0092	8.98
2.25	0.0945	50.57	4.75	0.0330	19.80	7.25	0.0157	12.31	9.75	0.0091	8.93
2.30	0.0927	49.39	4.80	0.0324	19.55	7.30	0.0155	12.22	9.80	0.0090	8.88
2.35	0.0909	48.24	4.85	0.0319	19.32	7.35	0.0153	12.13	9.85	0.0089	8.84
2.40	0.0891	47.11	4.90	0.0313	19.09	7.40	0.0151	12.04	9.90	0.0088	8.79
2.45	0.0873	46.01	4.95	0.0308	18.86	7.45	0.0149	11.95	9.95	0.0088	8.74
2.50	0.0855	44.93	5.00	0.0302	18.65	7.50	0.0147	11.87	10.00	0.0087	8.69

Table B1.2

Bessel functions (McDonald, 1974).

B1.2 The lumped parameter model

In section 2.2.2, the catheter-manometer system was regarded as analogous to a simple second-order system consisting of a mass (the effective mass of the fluid in the probe) suspended from a spring (the gauge diaphragm and pressure dome chamber) which is viscously damped by a dash pot (the viscous resistance of the fluid in the probe lumen) as shown in figure 2.5 and repeated in figure B1.5.

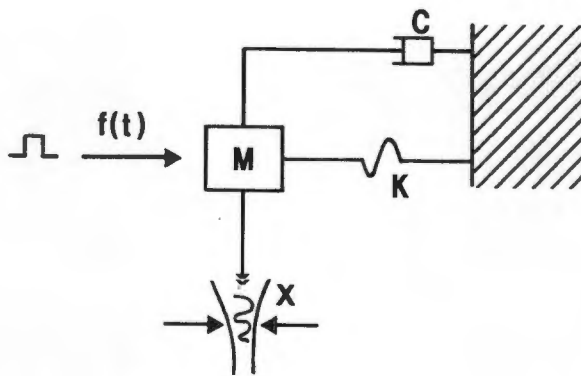


Figure B1.5

The mechanical analogue model where the mass M , is restrained by a spring K and a viscous dashpot, C (Fry, 1960).

The pressure applied to the system becomes the force applied to the mass, and the response of the system becomes the displacement of the mass. The spring, like the diaphragm, yields to an applied pressure. Thus the mass of fluid in the catheter shifts towards the pressure chamber until the spring tension increases sufficiently to equal the applied force. The mass overshoots somewhat due to its momentum and oscillations occur at the damped natural frequency. If the system was ideal, these oscillations

would continue unchanged at a constant frequency; however the frictional or damping properties of the fluid in the catheter attenuate these oscillations.

Mathematically this system is represented by:

$$f(t) = M \frac{d^2x}{dt^2} + C \frac{dx}{dt} + Kx \quad (B1.26)$$

where M is the mass of the system, C the friction coefficient and K is the spring constant.

The pressure that is recorded at the pressure chamber is proportional to the displacement x and the applied pressure would be indicated by f(t). Taking equation B1.26 and setting $f(t) = A \cos wt$ where A is the amplitude of the pressure and w is the angular frequency in radians/second, x can be solved for by integrating equation B1.26 (Spiegel, 1968) and is given in equation B1.27 (Fry, 1960).

$$x = \left[F e^{-Ct/2M} \cos \left[\left[\frac{K}{M} - \frac{C^2}{4M^2} \right]^{\frac{1}{2}} \cdot t - \phi \right] \right] + \left[\frac{A \cos (wt - \phi)}{(K - Mw^2)^2 + (wC)^2} \right] \quad (B1.27)$$

F and ϕ represent arbitrary constants determined from the initial conditions of the catheter-manometer model and the applied forces.

In a case of a sudden stepwise pressure change, F is proportional to the magnitude of the sudden change in pressure. Under these circumstances the transient term represents a sinusoidal wave of initial amplitude F that is attenuated exponentially with time

determined by the value of C and M. The frequency of these oscillations can be derived from equation B1.27 and is given in B1.28

$$w_d = \sqrt{(K/M - C^2/4M^2)} \quad (B1.28)$$

where w_d is called the damped natural frequency of the system.

The ratio $C/2M$ is a damping coefficient and as its value increases, the damped natural frequency becomes smaller. When the value of the radical becomes zero, there will be no oscillations and C_c then said to be critically damped. From equation B1.28, the critical damping is given by

$$C_c = 2\sqrt{KM} \quad (B1.29)$$

where K is the spring stiffness and M is the mass.

The undamped natural frequency of the system would be the frequency of the free oscillations if the system were frictionless; that is if C were equal to zero. The undamped natural frequency is then given by

$$w_n = \sqrt{(K/M)} \quad (B1.30)$$

The negative exponential value in equation B1.27, causes the complete term (the first bracketed term) to approach zero with time. Thus after a short period of time x may only be determined by the right hand (bracketed) part of equation B1.27. This part of the equation is the steady-state response of the system and has an amplitude r_a , given as;

$$r_a = A/\sqrt{[(K-Mw^2)^2 + (wC)^2]} \quad (B1.31)$$

and the response will lag the driving force with an angle of

$$\theta = \tan^{-1} [Cw/K - Mw^2] \quad (B1.32)$$

r_a in equation B1.31 may be expressed as a force if it is multiplied by K . The force amplitude ratio can be obtained if the force is divided by A and it follows that both equation B1.31 and B1.32 then represent the magnitude and the angle respectively of the complex number represented by equation B1.9 where K is equivalent to k_T , M to $m_o \cdot l$ and C to $c_o \cdot l$.

A plot of the above mentioned parameters will yield gain and response curves, as shown in figure B1.6 and B1.7 respectively, for various values of damping factor as a function of normalised frequency.

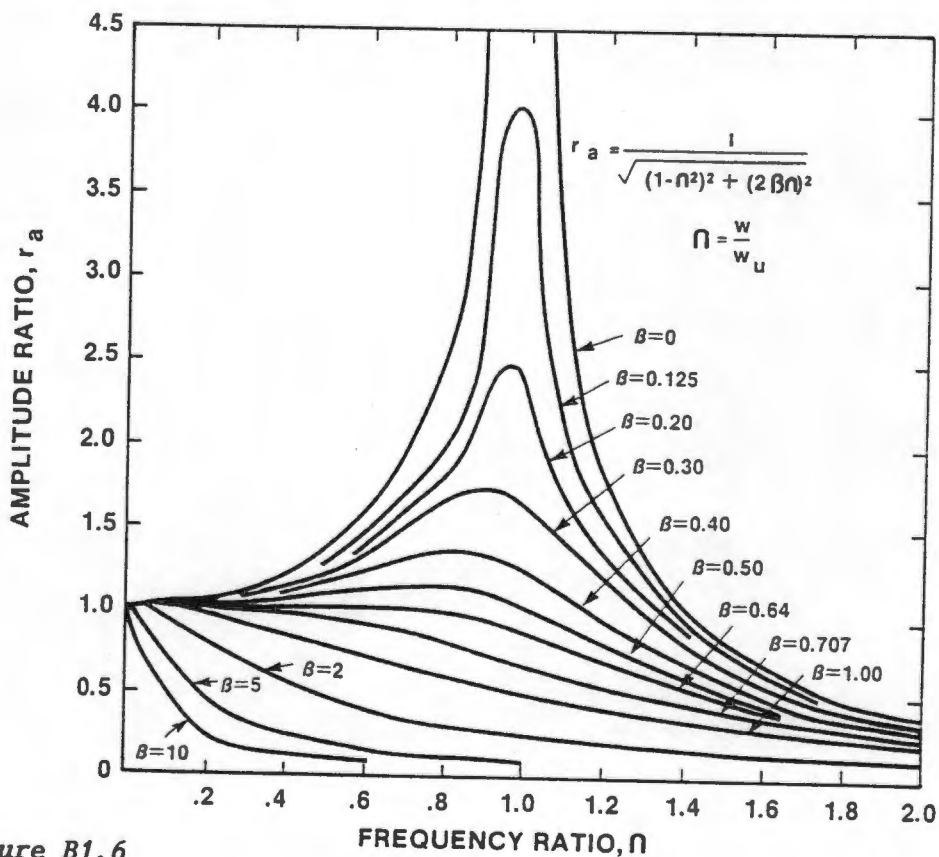


Figure B1.6

The amplitude ratio of a second order catheter-manometer system as a function of normalised frequency and damping ratio, β (Fry, 1960).

In describing catheter-manometer systems it is useful to describe the system constants in the form of dimensionless ratios. The frequency is expressed as a normalised frequency, Ω , which is the ratio of driving frequency, w , to the undamped natural frequency, w_n .

$$\Omega = w/w_n \quad (B1.33)$$

Similarly the damping is expressed as the damping ratio or damping factor, β . This is the ratio of the actual damping to the critical damping and is given by:

$$\beta = C/C_c \quad (B1.34)$$

Thus using the dimensionless ratios, equations B1.31 and B1.32 become

$$r_a = 1/\sqrt{[(1-\Omega^2)^2 + (2\beta\Omega)^2]} \quad (B1.35)$$

and

$$\theta = \tan^{-1} [2\beta\Omega/(1-\Omega^2)] \quad (B1.36)$$

From figure B1.6 it can be noted that for systems with a damping ratio higher than 0.707, the amplitude response does not initially rise to a maximum value but only with an increase of frequency. The frequency at which this maximum value of the amplitude ratio occurs is called the resonant frequency. An expression for the resonant frequency can be obtained by using equation B1.31 and setting the derivative of the equation with respect to w equal to zero,

$$w_p = \sqrt{(k/M - C^2/2M^2)} \quad (B1.37)$$

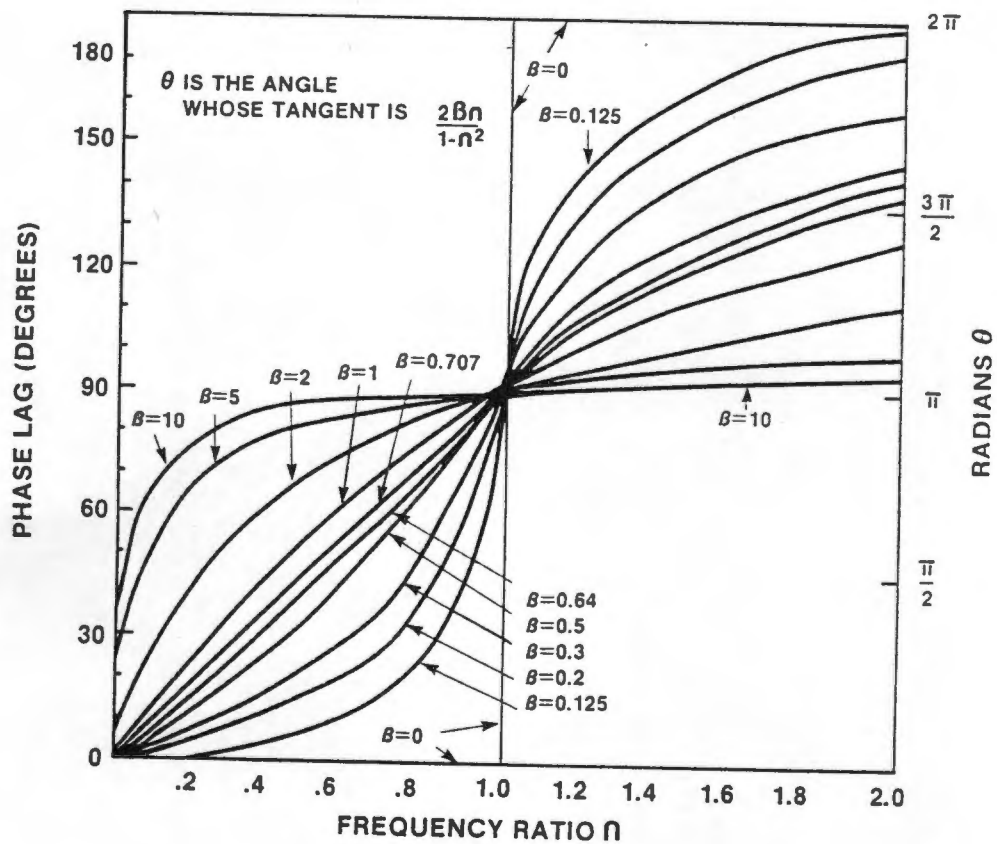


Figure B1.7

The phase-response as a function of normalised frequency and damping ratio (Fry, 1960).

B2 Fundamentals of second-order systems

In the spring-force system, energy is stored and is represented by

$$f(t) = K \cdot y(t) \quad (\text{B2.1})$$

where K is the spring constant. If the two systems are combined, a linear translational motion friction C , exists as shown in figure B2.1 and given as

$$f(t) = C \frac{dy(t)}{dt} \quad (\text{B2.2})$$

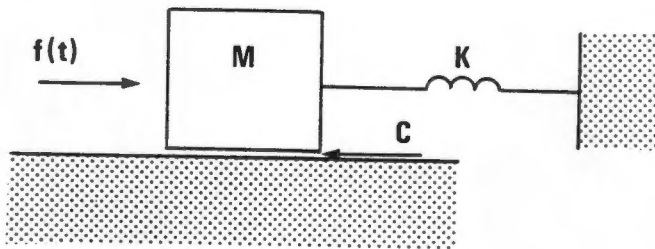


Figure B2.1

Force-mass-friction system.

This force is rewritten as

$$f(t) = M \frac{d^2y(t)}{dt^2} + C \frac{dy(t)}{dt} + Ky(t) \quad (\text{B2.3})$$

Divide both sides by M

$$\frac{d^2y(t)}{dt^2} + \frac{C}{M} \frac{dy(t)}{dt} + \frac{K}{M} y(t) = 1/M \cdot f(t) \quad (B2.4)$$

This differential equation describes the dynamic relationship between the input $f(t)$ and the output $y(t)$. Taking the Laplace transformation on both sides of the equation and assuming zero initial conditions,

$$(s^2 + C/M s + K/M) \cdot Y(s) = 1/M \cdot F(s) \quad (B2.5)$$

therefore $G(s)$

$$G(s) = \frac{Y(s)}{F(s)} = \frac{1/M}{s^2 + C/M s + K/M} \quad (B2.6)$$

In control systems theory this equation is of the form of

$$s^2 + 2\beta w_n s + w_n^2 = w_n^2$$

where β is the damping factor, w_n the undamped natural frequency and βw_n the damping coefficient. Thus $\beta w_n = C/2M$ (the damping coefficient) and the characteristic equation is

$$s = C/2m \pm j\sqrt{(K/M - C^2/4M^2)} \quad (B2.7)$$

and the damped natural frequency

$$w_d = \sqrt{(K/M - C^2/4M^2)} \quad (B2.8)$$

The undamped natural frequency of this second order system is

$$\omega_n = \sqrt{K/M} \quad (B2.9)$$

The resonant frequency of the second order system is determined by equation B2.6. Substitute $j\omega$ for s and normalize the equation to obtain:

$$\frac{Y(j\omega)}{F(j\omega)} = \frac{1}{[(1-\omega^2/\omega_n^2) + j2\beta(\omega/\omega_n)]^{\frac{1}{2}}} \quad (B2.10)$$

Differentiate B2.10 and set to zero.

The maximum point in figure B2.2 is thus the maximum amplitude at resonance and ω_p is the frequency at which it occurs.

$$M_p = \frac{1}{2\beta\sqrt{1-\beta^2}} \quad (B2.11)$$

and

$$\omega_p = \omega_n \cdot \sqrt{1-2\beta^2} \quad (B2.12)$$

The bandwidth of the second order system is then calculated as follows;

Set equation B2.10 equal to 0.707 and solve (normalise the frequency, $\Omega = \omega/\omega_n$),

$$M(\omega) = \frac{Y(\omega)}{F(\omega)} = \frac{1}{[(1-\omega^2)+j2\beta(\omega)]^{\frac{1}{2}}} = 0.707 \quad (\text{B2.13})$$

$$M(\omega) = \frac{Y(\omega)}{F(\omega)} = \frac{1}{[(1-\omega^2)+4\beta^2(\omega)]^{\frac{1}{2}}} = 0.707 \quad (\text{B2.14})$$

$$[(1-\omega^2)+4\beta^2(\omega)]^{\frac{1}{2}} = \sqrt{2}$$

$$\omega^2 = (1-2\beta^2) \pm \sqrt{(4\beta^4 - 4\beta^2 + 2)}$$

therefore, bandwidth

$$\text{BW} = \omega_n \cdot [(1-2\beta^2) \pm \sqrt{(4\beta^4 - 4\beta^2 + 2)}]^{\frac{1}{2}} \quad (\text{B2.15})$$

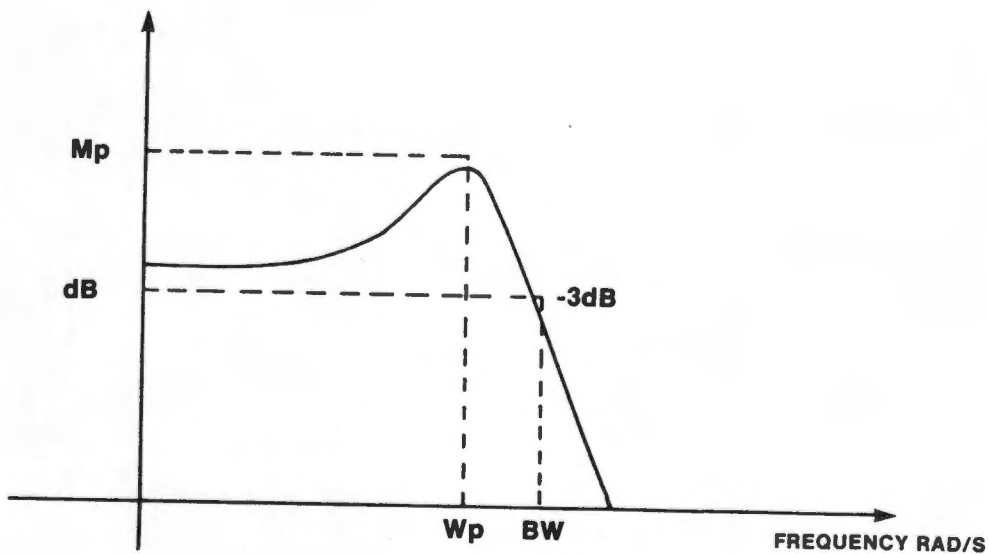


Figure B2.2

Peak resonance, resonant frequency and bandwidth for a second order system.

B2.1 Relationship between damping factor and gain at resonance

$$M_p = 1/2\beta\sqrt{(1-\beta^2)} \quad (\text{B2.16})$$

$$(1/M_p)^2 = 4\beta^2(1-\beta^2) = 4\beta^2 - 4\beta^4 \quad (\text{B2.17})$$

$$- (1/M_p)^2 = 4\beta^2 - 4\beta^4 - 1 + 1 \quad (\text{B2.18})$$

factorise

$$1 - (1/M_p)^2 = (2\beta^2 - 1)(2\beta^2 - 1) \quad (\text{B2.19})$$

and solve for β

$$2\beta^2 = 1 \pm \sqrt{(1 - (1/M_p)^2)} \quad (\text{B2.20})$$

and therefore

$$\beta = \left[\frac{1 - \sqrt{(1 - (1/M_p)^2)}}{2} \right]^{\frac{1}{2}} \quad (\text{B2.21})$$

APPENDIX C

PRESSURE GENERATOR AND COMPENSATION NETWORK DESIGN AND CONSTRUCTION

CONTENTS

C1	Pressure generator construction and evaluation	C2
C2	Electronic compensation network for the pressure generator	C9
C2.1	Network analysis in the frequency domain	C9
C2.2	Phase-lag compensation	C12
C2.3	Pole-zero cancellation compensator	C15
C2.4	Circuit design of pole-zero compensator	C18
C2.4.1	Summation circuit	C20
C2.4.2	Non-inverting circuit	C21
C2.4.3	The integrator	C23
C2.4.4	The printed circuit board	C25
C3	Equipment set up of in vitro testing	C26
C3.1	Pressure tubing and stopcocks	C27
C3.2	Cannulae testing	C28

C1 Pressure generator construction and evaluation

The pressure generator first used was essentially that depicted in figure C1.1.

A function generator (HP 3314A) with a constant amplitude output up to a frequency of 2 MHz was used to drive a speaker via a transistorised power stage. The power stage was an amplifier with a flat frequency response of DC to 400 hertz (-3 dB). The amplitude variation was less than 1 percent for this frequency range.

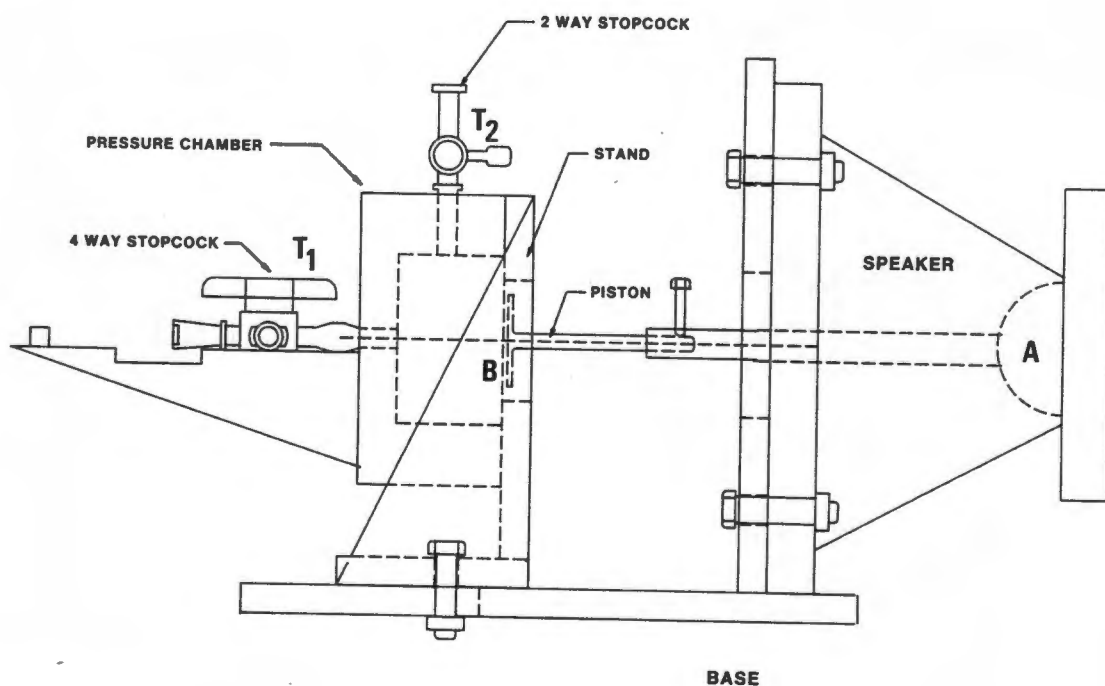


Figure C1.1

A lateral view of the pressure generator (model A). The oscillator is a 5 Watt loudspeaker (diameter $3 \frac{1}{2}$ inch) connected by a piston to a mylar diaphragm (0,12 mm in thickness) of the pressure chamber.

The output of the amplification stage is connected to a loudspeaker system (4 Ohm). A perspex disk (A) was designed and glued over the central dome of the speaker. A modified surgical needle (piston) was glued to both the perspex disk and on to the mylar diaphragm. Care was taken that the needle was placed at the center of the mylar diaphragm, using the perspex disk (B).

The pressure chamber in figure C1.1 has a volume of 21.17 cm³. The internal surfaces were given a smooth finish to facilitate removal of air bubbles. Two stopcocks (T₁ and T₂) were glued into the openings of the chamber as indicated. A groove was machined at the top of the pressure chamber as this assisted in the removal of air trapped in the chamber. The loudspeaker and the pressure chamber were rigidly mounted on a base plate. This minimized vibrations and thus artifact and unwanted reflections in the chamber.

The material used to construct the pressure chamber had to be rigid and perspex of thickness 10 mm was used.

Before the pressure generator was tested to determine its frequency response, the pressure chamber was cleaned and flushed with 90 percent alcohol to ensure that the inside of the pressure chamber was clean.

A reference pressure transducer (AME AE840) was connected to stopcock T₁ (figure C1.1) and the chamber was filled with physiological saline (0.9 percent) at 25 °C, to a pressure of 100 mmHg. Air bubbles were removed by tapping the chamber and releasing them via stopcock T₂. The signal generator was used in either automatic sweep mode or manual mode to produce a constant amplitude sine wave (500 mV peak to peak) with a frequency range of 0 - 100 hertz. This output signal activated the speaker and

thus the membrane. The pressure variations recorded by the reference transducer were measured and displayed by an oscilloscope (Kikusui COM 7101A) and by the digital multi-meter (HP 3435A). The frequency response results is presented in table C1.1. The test was repeated for a mean pressure in the chamber of 60 mmHg, 80 mmHg, 120 mmHg and 140 mmHg.

Mean pressure in chamber	Resonant frequency	Flat Frequency Range
60 mmHg	69 Hz	9 - 43 Hz
80 mmHg	65 Hz	7 - 41 Hz
100 mmHg	58 Hz	9 - 40 Hz
120 mmHg	55 Hz	7 - 34 Hz
140 mmHg	49 Hz	11 - 31 Hz

Table C1.1

Resonant frequency (f_p) and the range for which the amplitude response of the pressure chamber was constant at different mean pressures. Flat frequency range is for amplitude responses with gains less than ± 1.5 dB relative to the input.

From the results obtained it was clear that the test equipment was not linear at the lower frequencies (1-6 Hz). The increase in fluid pressure in the chamber also produced nonlinearities and the explanation for this was that the material and construction were not rigid enough to prevent vibrations. Furthermore, there existed movement between the speaker and the pressure chamber, resulting in unmatched forces being applied to the membrane. For frequencies ranging between 9 and 40 Hz (at 100 mmHg mean pressure), the system had a flat frequency response (within 3 dB;

the output was normalised to the input at 1Hz). Considering that tests had to be performed on Swan Ganz catheters (which are known for their low bandwidth) and the requirement that the test equipment have a bandwidth five times higher than the system tested, it was decided that the existing pressure generator had to be improved.

The construction was modified and the problem of nonlinearity at lower frequencies was solved partially. The modification included a re-designed base plate and speaker stand stand as indicated in the construction details in Appendix D (drawing 1). The improved responses are listed in table C1.2 .

Mean pressure in chamber	Resonant frequency	Flat Frequency Range
60 mmHg	109 Hz	1 - 75 Hz
80 mmHg	105 Hz	1 - 71 Hz
100 mmHg	97 Hz	2 - 68 Hz
120 mmHg	93 Hz	3 - 64 Hz
140 mmHg	88 Hz	4 - 54 Hz

Table C1.2

Improved frequency response of the pressure chamber.

Although the requirements for the pressure generator were met, testing was limited to a peak fluid pressure of 60 to 100mmHg. Once the fluid pressure was increased beyond this, the recorded signal waveform was distorted. It appeared that the speaker was unable to match the force produced in the chamber. Furthermore

the test frequency was in the audio range of the speaker, resulting in excessive noise. The speaker was thus replaced by an vibration generator.

Tests were repeated and the results are given in table C1.3. The detailed construction plan for the second pressure generator (model B) is given in appendix D (drawing D1 to D6) and the vibration generator and pressure chamber are shown in figure C1.2.

Pressure in chamber	Resonant frequency	Flat Frequency Range
60 mmHg	122 Hz	1 - 78 Hz
80 mmHg	112 Hz	1 - 75 Hz
100 mmHg	105 Hz	1 - 76 Hz
120 mmHg	100 Hz	1 - 64 Hz
140 mmHg	91 Hz	1 - 59 Hz

Table C1.3

Improved frequency response of the pressure chamber at different pressures (model B).

Investigation of table C1.3 and the appropriate frequency response results (figure C1.3) indicated that the pressure generator had a bandwidth response that was sufficient to test catheter-manometer systems (resonant frequency at 105 Hz). However, the amplitude response up to the frequency of 105 Hz was not constant, and electronic compensation was necessary to correct the amplitude gain.

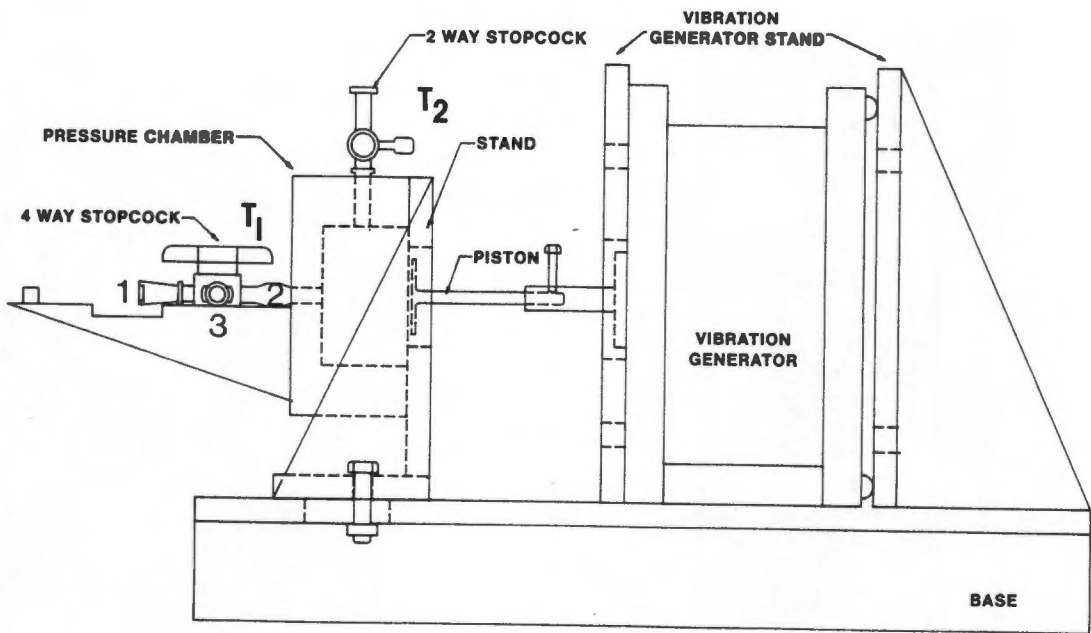


Figure C1.2

The final form of the pressure generator with the vibration generator as the source of movement for the membrane.

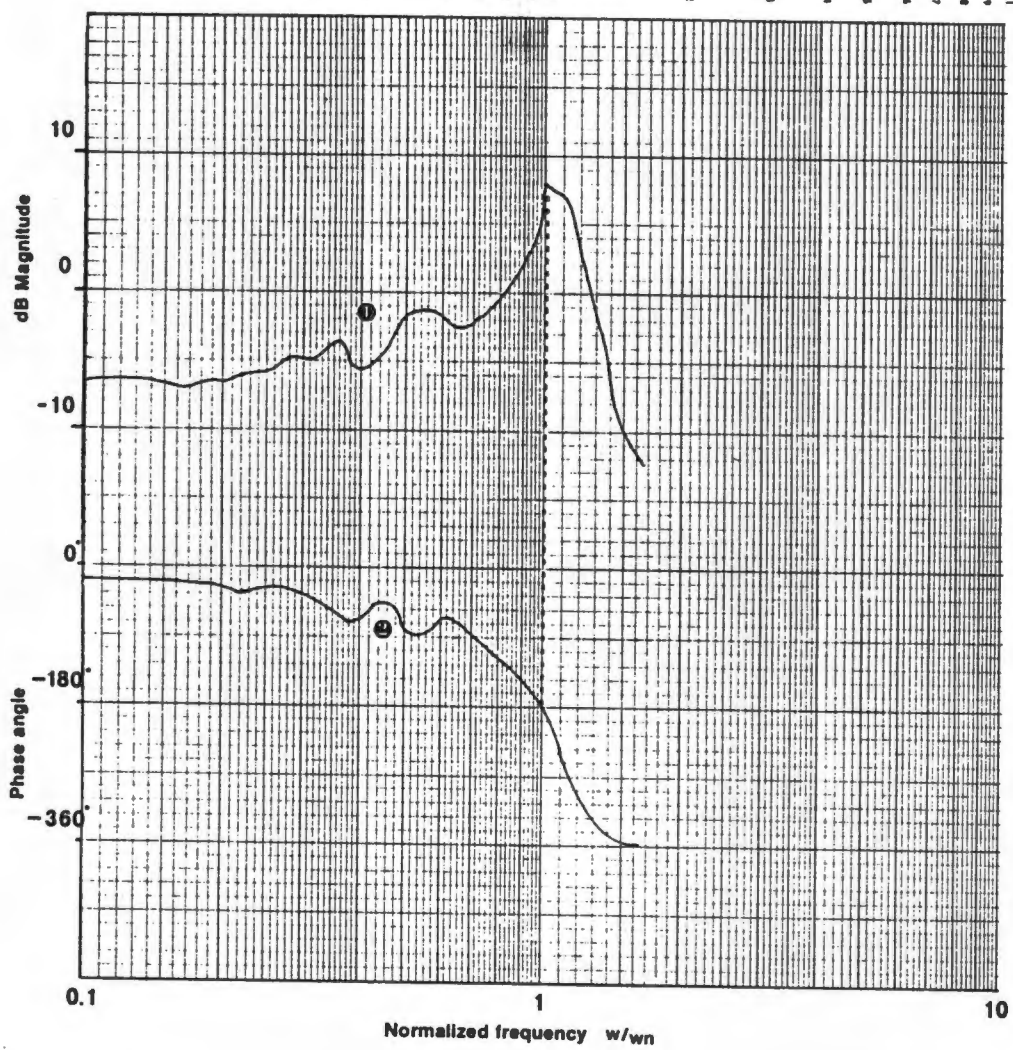


Figure C1.3

Frequency response of the catheter-manometer test equipment.

C2 Electronic compensation network for the pressure generator

An appropriate electronic compensation network will ensure that the variation in amplitude response up to a frequency of 105 Hz will be reduced and that the system is stabilised, thus fulfilling the requirement mentioned in section 4.2.1. Before a detailed discussion on the compensation network is given, a brief introduction to network analysis in the frequency-domain is presented.

C2.1 Network analysis in the frequency domain

The availability of existing analytical tools in the frequency domain is the primary motivation for the analysis of linear control systems in this domain. The starting point of the frequency domain analysis of electronic control systems is the transfer function, which is defined as the ratio of the frequency transform of the output of a system to the frequency transform of the input. The system is assumed to be at rest prior to excitation, and all initial values are assumed to be zero when determining the transfer function. Figure C2.1 represents a block diagram of a simple linear system.

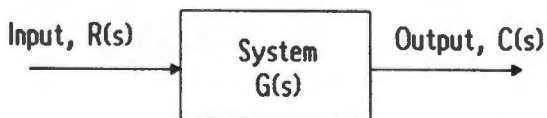


Figure C2.1

Block diagram of a simple linear system.

For a single-loop feedback control system, the closed-loop transfer function is written as (Shinners, 1980)

$$M(s) = \frac{C(s)}{R(s)} = \frac{G(s)}{1 + G(s)H(s)} \quad (C2.1)$$

and under the sinusoidal steady state, $s = j\omega$ (Shinners, 1980). A general block diagram of a single-loop feedback system is given in figure C2.2.

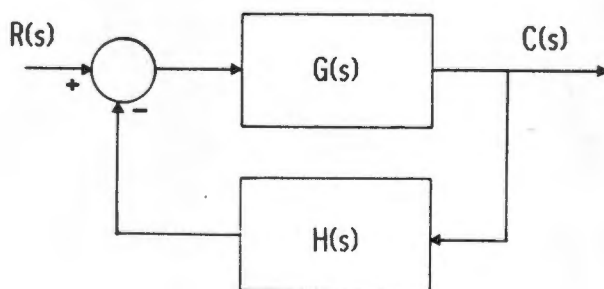


Figure C2.2

General block diagram of a single-loop feedback system.

Equation C2.1 implies that the output of a single-loop feedback system depends on the feedback transfer function $H(s)$ and on the direct transfer function $G(s)$, provided $G(s)H(s) \gg 1$. Use is made of this characteristic in the feedback control system.

In designing a control system the open loop transfer function $G(s)$ and the feedback path gain $M(s)$ must be known. $H(s)$, the feedback transfer function can then be calculated and the appropriate electronic network, represented by $H(s)$, can be constructed.

In the analysis of the feedback control system, the determination of the performance characteristics and the system stability is of utmost importance. Thus, we are interested in the location of the characteristic equation roots which are the poles of the closed-loop transfer function.

The resonant frequency of the uncompensated pressure generator was 105 Hz (table C1.3 and figure C1.3). The peak resonance amplitude, M_p was equal to 14.5 dB (measured relative to the "flat" gain and taken as 0 dB). This value was calculated by taking the peak voltage at resonance, thus

$$M_p = 20 \log V_{\text{peak}}$$

and $V_{\text{peak}} = 5.35$ Volts, therefore $M_p = 14.5$ dB.

The damping factor β and the peak resonance M_p are related to each other by the following equation (Kuo, 1982):

$$M_p = \frac{1}{2\beta\sqrt{1-\beta^2}} \quad (C2.2)$$

It is important to note that M_p is a function of β only, whereas w_p is a function of β and w_n .

w_p is the resonant frequency and w_n is the natural undamped frequency.

$$w_p = w_n\sqrt{1-2\beta^2} \quad (C2.3)$$

The undamped natural frequency (ω_n) for the pressure generator is thus equal to 109 Hz or 685 rad/s ($\omega_n = 2\pi f_0$). From equation C2.3, $\beta = 0.1$ (equation is derived in appendix B2.1).

In figure C2.3 the poles are represented schematically in the s -plane. The pressure generator becomes unstable for high frequencies, the boundary of instability being at that point where the poles (represented by X) moves to the right side of the imaginary axis.

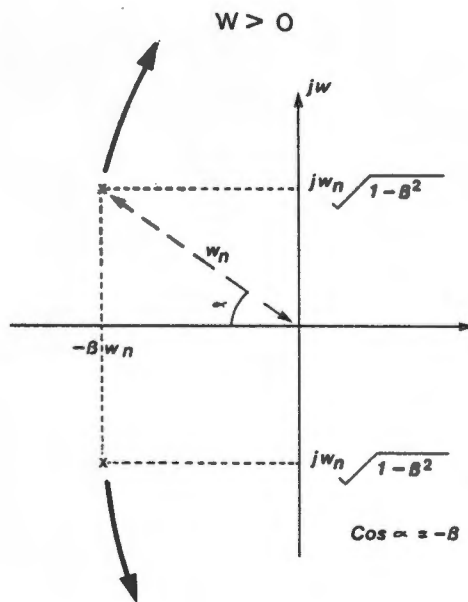
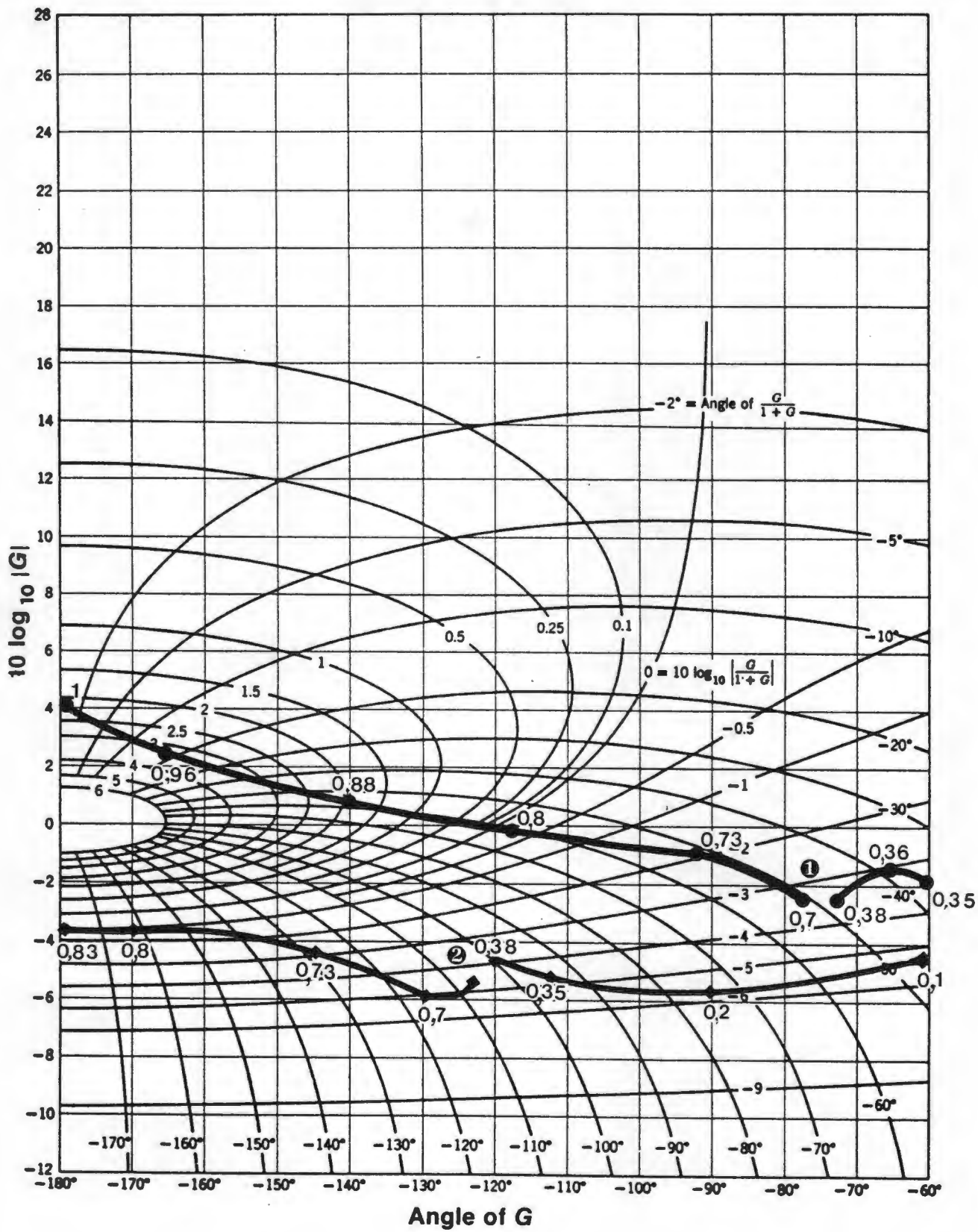


Figure C2.3

Characteristic roots (represented by the poles) of $G(s)$ and the expected plot of $G(s)$ for higher frequencies.

C2.2 Phase-lag compensation

From the frequency response plots (figure C1.3) a phase-lag compensation network was designed using the Nichols Chart given in figure C2.4.



Nichols chart

Figure C2.4

The frequency response plots of the pressure generator and phase-lag compensator represented on a Nichols chart. Points 1. and 2. correspond to those on figure C1.3.

The solid fat line (figure C2.4) represents the frequency response of the pressure generator without compensation, while the thin solid line represents the frequency response of the compensated circuit. The phase lag was designed to be 50° (from the Nichols Chart) and $\alpha = 10$, where

$$\alpha = \frac{\text{pole}}{\text{zero}}$$

The circuit was constructed and tested; however, the amplitude response (figure C2.5) was not improved satisfactorily and a pole-zero cancellation technique was designed.

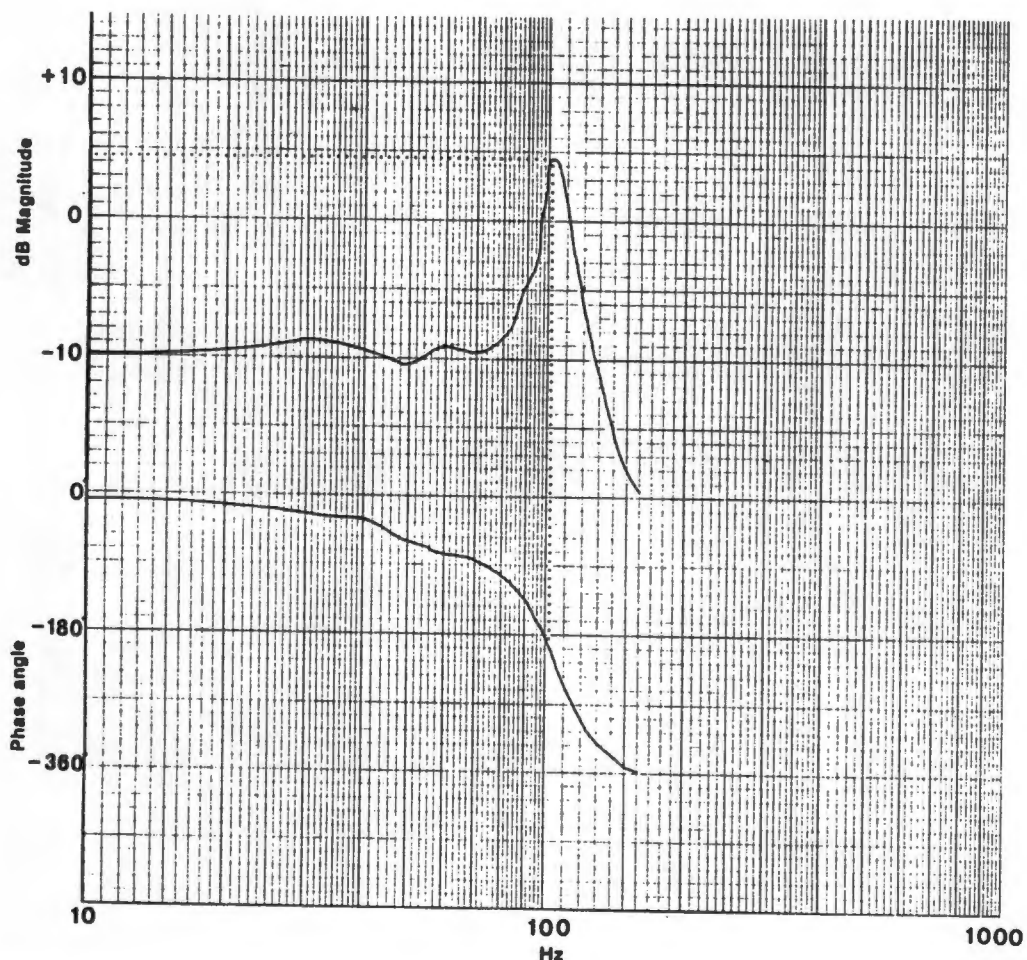


Figure C2.5

Amplitude and phase response of the pressure generator and phase-lag compensator.

C2.3 Pole-zero cancellation compensator

For easy construction and realisation of the compensation network, a second order biquad control system design (Lam, 1979) was chosen. The closed-loop transfer function is given by (Kuo, 1982)

$$\frac{V_o(s)}{V_i(s)} = \frac{s^2 + 2\beta\omega_n s + \omega_n^2}{(s + b)^2} \quad (C2.4)$$

This equation introduces two zeros on or near the existing poles. These tend to cancel the effect of the poles; however, two poles are created with this control circuit and it is important that they are at a frequency that is at least three times higher than the resonant frequency of the open-loop transfer function. The latter design is critical as it ensures that the effect of the introduced poles does not influence the response significantly (Shinners, 1980).

In this design the poles were placed at a frequency 5 times higher than that of the zeros ($b = 3500$ in equation C2.4) and is shown in figure C2.6.

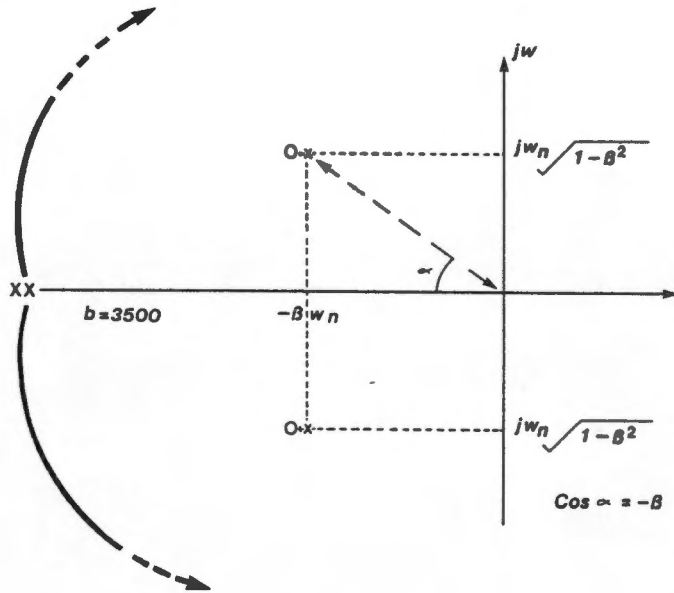


Figure C2.6

Characteristic roots of $G(s)$ and the expected plot of $G(s)$ for higher frequencies of the pressure generator and pole-zero compensator.

Equation C2.4 must be rearranged and written in terms of $V_o(s)$, the output voltage, so that an electrical circuit can be designed. Thus equation C2.4 reduces to equation C2.5.

$$V_o(s) \cdot [(s + b)^2] = V_i(s) \cdot [s^2 + 2\beta w_n s + w_n^2]$$

therefore

$$V_i(s) \cdot [s^2 + 2\beta w_n s + w_n^2] - V_o(s) \cdot [2bs + b^2] = V_o(s) \cdot s^2$$

and

$$V_i(s) \left[1 + \frac{2\beta w_n}{s} + \frac{w_n^2}{s^2} \right] - V_o(s) \left[\frac{2b}{s} + \frac{b^2}{s^2} \right] = V_o(s) \quad (C2.5)$$

This transfer function given in equation C2.5 is realised in figure C2.7.

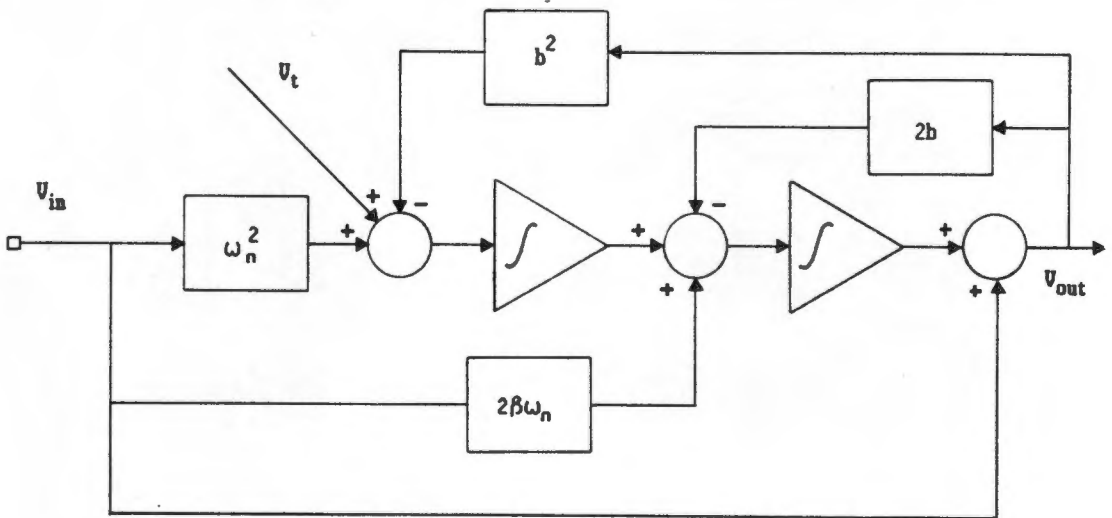


Figure C2.7

Block diagram of the pole-zero compensator.

To obtain a larger degree of freedom in the circuit adjustment, it was decided to design the feedback circuit in such a manner as to be able to vary the damping factor β and the undamped natural frequency ω_n independently (figure C2.8). It is thus possible to "move" the zeros of the compensation network in the left hand plane in figure C2.6.

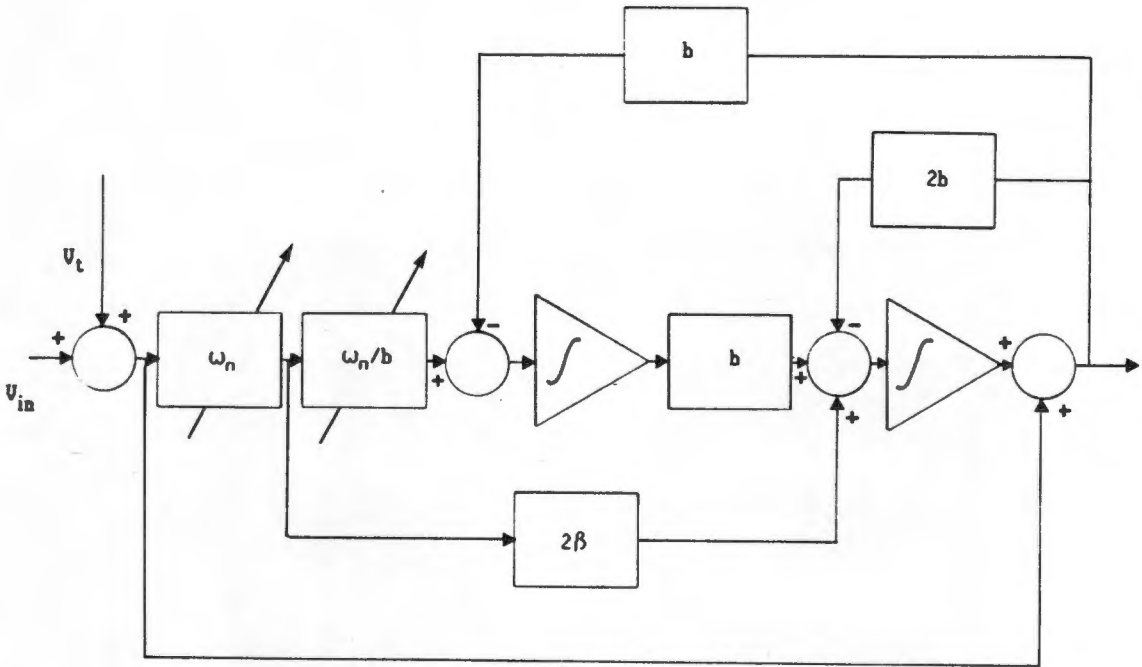


Figure C2.8

Block diagram of the variable pole-zero compensator. Note that the adjustment of the undamped natural frequency, ω_n , must occur simultaneously (in both blocks) and thus a dual potentiometer must be used, to manually adjust ω_n .

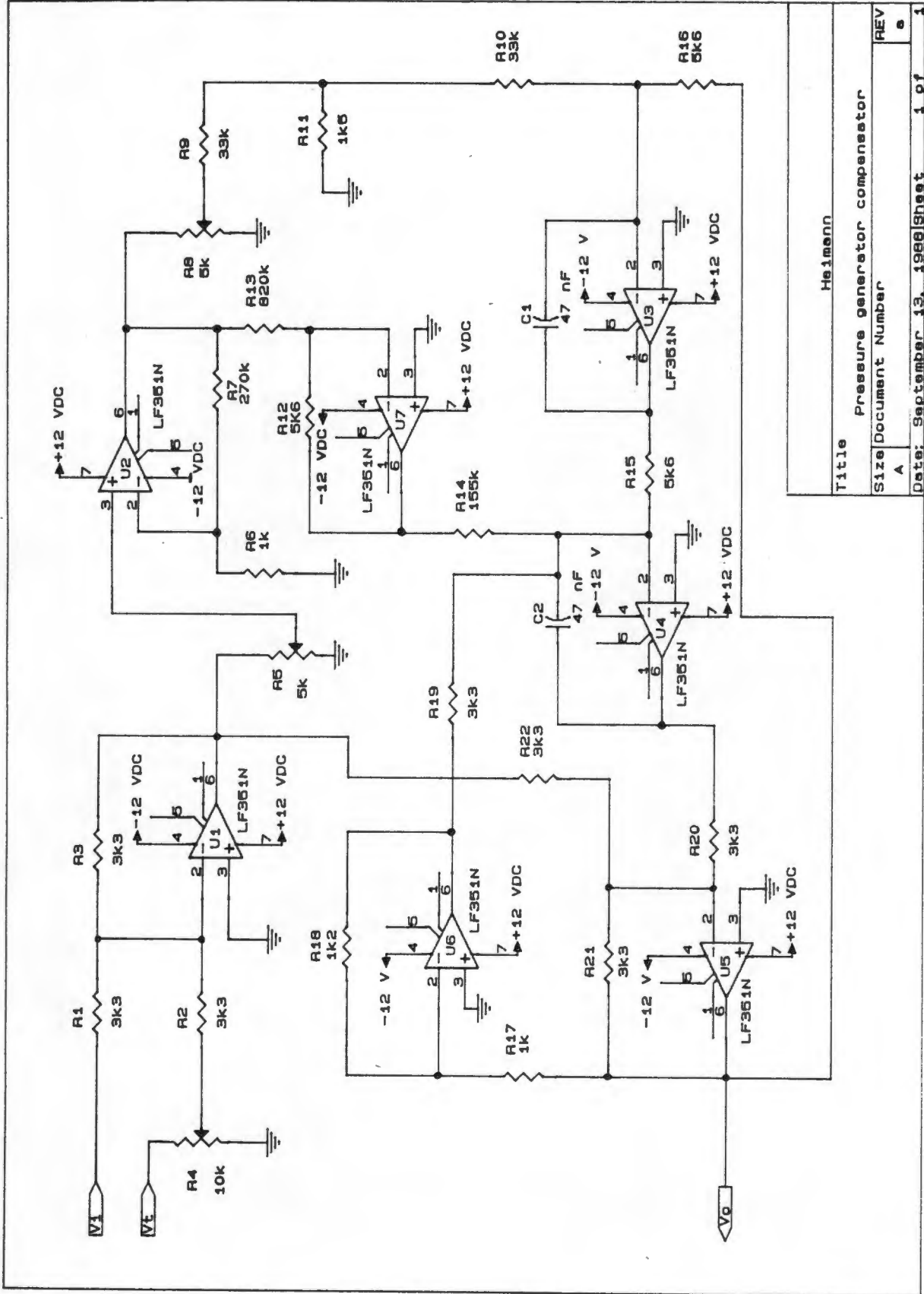
This will ensure that optimum compensation of the closed-loop transfer function is established. The block diagram of the controller is thus given in figure C2.8.

The component values are calculated in section C2.4.

C2.4 Circuit design of pole-zero compensator

From the block diagram in figure C2.8, the circuit in figure C2.9 can be developed. Each section represents a parameter shown in figure C2.8 (summation, ω_n , $\int \omega_n/b$ and b).

The individual sections of the circuits are developed in sections C2.4.1 to C2.4.3.



Title		Heilmann	
Size		Pressure generator compensator	
Document Number		REV	
A		e	
Date: September 13, 1988		Sheet 1 of 1	

Figure C2.9

Electronic circuit of compensator.

C2.4.1 Summation circuit

A circuit representation of the basic summation circuit is given in figure C2.10.

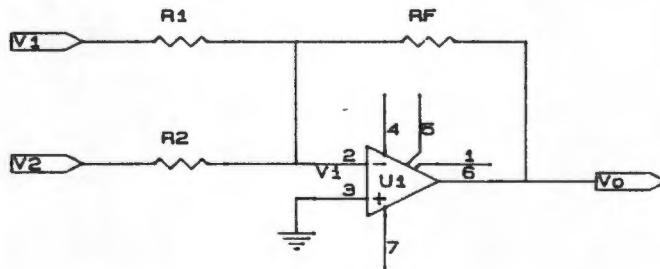


Figure C2.10

The summation circuit.

In this circuit the input resistance of the amplifier is very high ($> 5 \text{ M}\Omega$), the sum of the input currents are equal and opposite in direction to the feedback current or

$$\frac{V_2 - v_i}{R_2} + \frac{V_1 - v_i}{R_1} = \frac{V_o - V_i}{R_F} \quad (\text{C2.6})$$

The gain of the operational amplifier is very large and thus $v_i = V_o/\text{gain}$ is very small in comparison to V_1 , V_2 and V_o and can be neglected. Equation C2.6 reduces to equation C2.7,

$$V_o = - \left[\frac{R_F}{R_2} V_2 + \frac{R_F}{R_1} V_1 \right] \quad (\text{C2.7})$$

and the output of the amplifier circuit is the weighted sum of

the inputs. This circuit is used for the summing operations of the compensator.

The input voltage of the signal generator V_i , and that of the feed-back circuit V_t (figure C2.9), are in the range of ± 1.5 volts. To keep the current through the resistors low, R_1 , R_2 and R_3 are chosen to be 3k3 ohm. The gain in this section is unity and the quiescent current is 450 μ A. Similarly, R_{20} , R_{21} and R_{22} are calculated using equation C2.6 and C2.7. The gain in this stage is likewise unity and the current passing through the resistors is 450 μ A.

C2.4.2 Non-inverting circuit

In figure C2.11, the input signal is applied to the non-inverting (+) terminal and a fraction of the output signal is fed back to the inverting (-) terminal. Here R_1 and R_F constitute a voltage divider across the output voltage.

$$v_a = \frac{R_1}{R_1 + R_F} v_o \quad (C2.8)$$

and

$$A_F = \frac{v_o}{v_a} = \frac{R_1 + R_F}{R_1} \quad (C2.9)$$

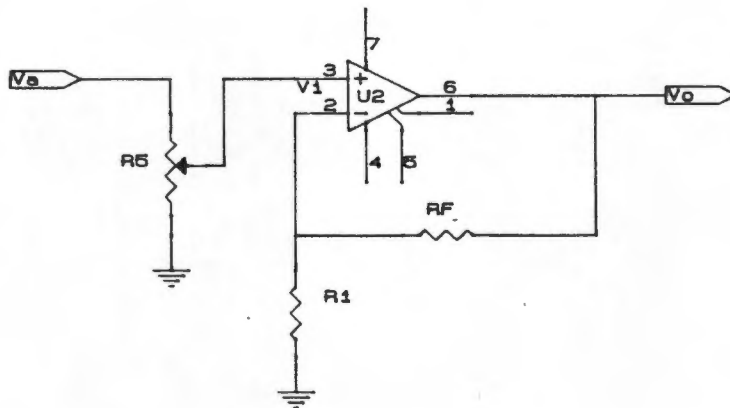


Figure C2.11

The non-inverting amplifier

The output of this circuit is in phase with the input and the input resistance is very high, while the output resistance is very low. The result is that the source is not "loaded" by the amplifier and the amplifier is not affected by other loads. ω_n was calculated as 685 rad/s and thus a non-inverting amplifier was designed to represent this value.

The resistors R_6 and R_7 represent those in figure C2.9 and therefore:

$$\left[\frac{R_6 + R_7}{R_6} \right] \times 0.5 = \omega_n$$

where the factor 0.5 is derived from the center setting of the variable resistor R_5 (5k Ω). R_6 becomes 1k Ω and R_7 , 270k Ω .

C2.4.3 The integrator

In figure C2.12, the feedback element is a capacitor C. For the op-amp, $v_i \approx 0$, $i_i \approx 0$ and the sum of the currents into the node n is:

$$; \quad \frac{v_1}{R_1} + C \frac{dv_o}{dt} = 0 \quad (C2.10)$$

Integrating each term with respect to time and solving.

$$v_o = - \frac{1}{R_1 C} \int v_1 dt \quad (C2.11)$$

and the device acts as an integrator.

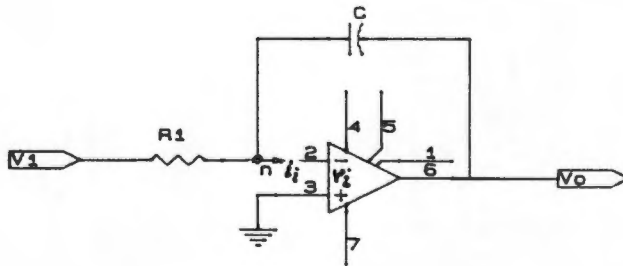


Figure C2.12

The integrator.

Calculating the values for the integrator in figure C2.9, $b = 3500$ and $w_n = 685$, thus

$$0.5 \times \frac{1}{C_1 R_{10}} = \frac{w_n}{b} = 195.7 \times 10^{-3} \quad (C2.12)$$

and C_1 is 47 nF and R_{10} , 33k Ω . R_8 , R_9 and R_{11} are calculated to be 5k Ω , 33k Ω and 1k5 respectively.

Similarly the values are calculated for the second integrator.

Table C2.1 lists the component values for the entire circuit in figure C2.9.

Resistors		Capacitors	
R1	= 3k3	C1	= 47 nF (tant)
R2	= 3k3	C2	= 47 nF (tant)
R3	= 3k3		
R6	= 1k	Variable resistors	
R7	= 270k	R4	= 10k
R9	= 33k		dual pot
R10	= 33k	R5	= 5k
R11	= 1k5	R8	= 5k
R12	= 5k6		
R13	= 820k	IC	
R14	= 155k	U1 - U7	= LF351N
R15	= 5k6		
R16	= 5k6		
R17	= 1k		
R18	= 1k2		
R19	= 3k3		
R20	= 3k3		
R21	= 3k3		
R22	= 3k3		

Table C2.1

Component list. All resistors are $\frac{1}{4}$ W (5% tolerance).

C2.4.4 The printed circuit board

A printed circuit board was designed with the appropriate software (Smartwork Version 2.1) and constructed. The design of the printed circuit is given in figure C2.13.

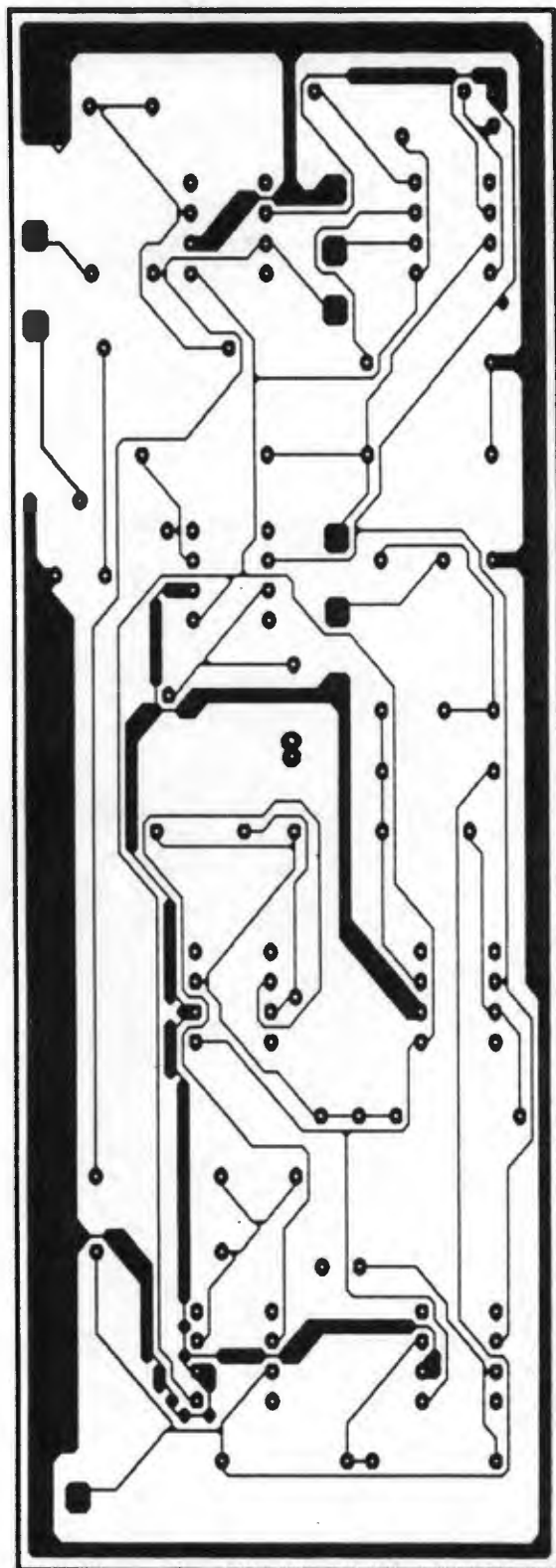


Figure C2.13

The printed circuit board layout

C3 Equipment set up for in vitro testing

This procedure is listed in points 1 to 4 below (refer to figure C3.1).

1. Open stopcock T_2 and stopcock T_1 (path 1 and 3 open) so that the saline can enter the pressure chamber. Air trapped in the pressure chamber escapes via stopcock T_2 .
2. Tap the chamber until no air bubbles are visible.
3. Close stopcock T_2 and open stopcock T_1 (path 1, 2 and 3 open) and remove air from the stopcock.
4. Disconnect the flushing device by closing stopcock T_1 (path 1 and 3 open).

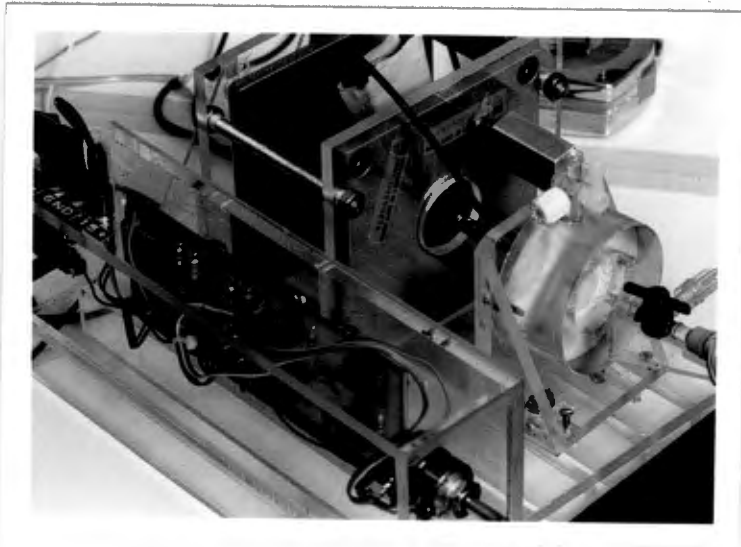


Figure C3.1

Pressure generator system

C3.1 Pressure tubing and stopcocks

The catheter-manometer system that is being tested is connected to the 3 way stopcock (T_1) as described in section 4.3.3. It is important to ensure that:

- The Luer connectors are fitted tightly so that no air may enter the system under test.
- The connectors and fittings are made from transparent material to assist the researcher in detecting any trapped air bubbles.

The system under test is then flushed as described in points 5 to 8 below:

5. The catheter-manometer system to be tested is flushed by opening stopcock T_1 (path 2 and 3 open) and stopcock T_2 .
6. Stopcock T_2 is closed and stopcock T_1 (path 1, 2 and 3 open) is opened.
7. The saline bag is then elevated to give a mean pressure reading of 100 mmHg.
8. Stopcock T_1 is changed so that path 1 and 3 are open.

The system is ready for testing and the function generator is turned on. The output signal is displayed on an oscilloscope and results are recorded. An example of the results i.e. input vs. output signal is given in figure 4.11.

C3.2 Cannulae testing

The frequency response tests performed on cannulae are similar to those mentioned in section C3.1. Points 1 and 2 are the same; however a stopcock with a rubber dome is attached to stopcock T_1 . The cannula is inserted into this rubber stop, and the needle is removed. Point 3, mentioned above, is followed so that saline is flushed out of the cannula.

To prevent the thin polyethylene tube of the cannula from being deformed during frequency response testing, a cannula sliding device (design details in Appendix D, drawing D7), shown in figure C3.2 is attached to the pressure chamber.

The procedure of flushing the cannula tube is described in the points 8 to 10 below;

8. Connect the flush device to stopcock T_2 and flush with saline through the pressure chamber.
9. Connect the cannula. Special care has to be taken to prevent air from being introduced into the system.
10. Follow points 5, 6 and 7.

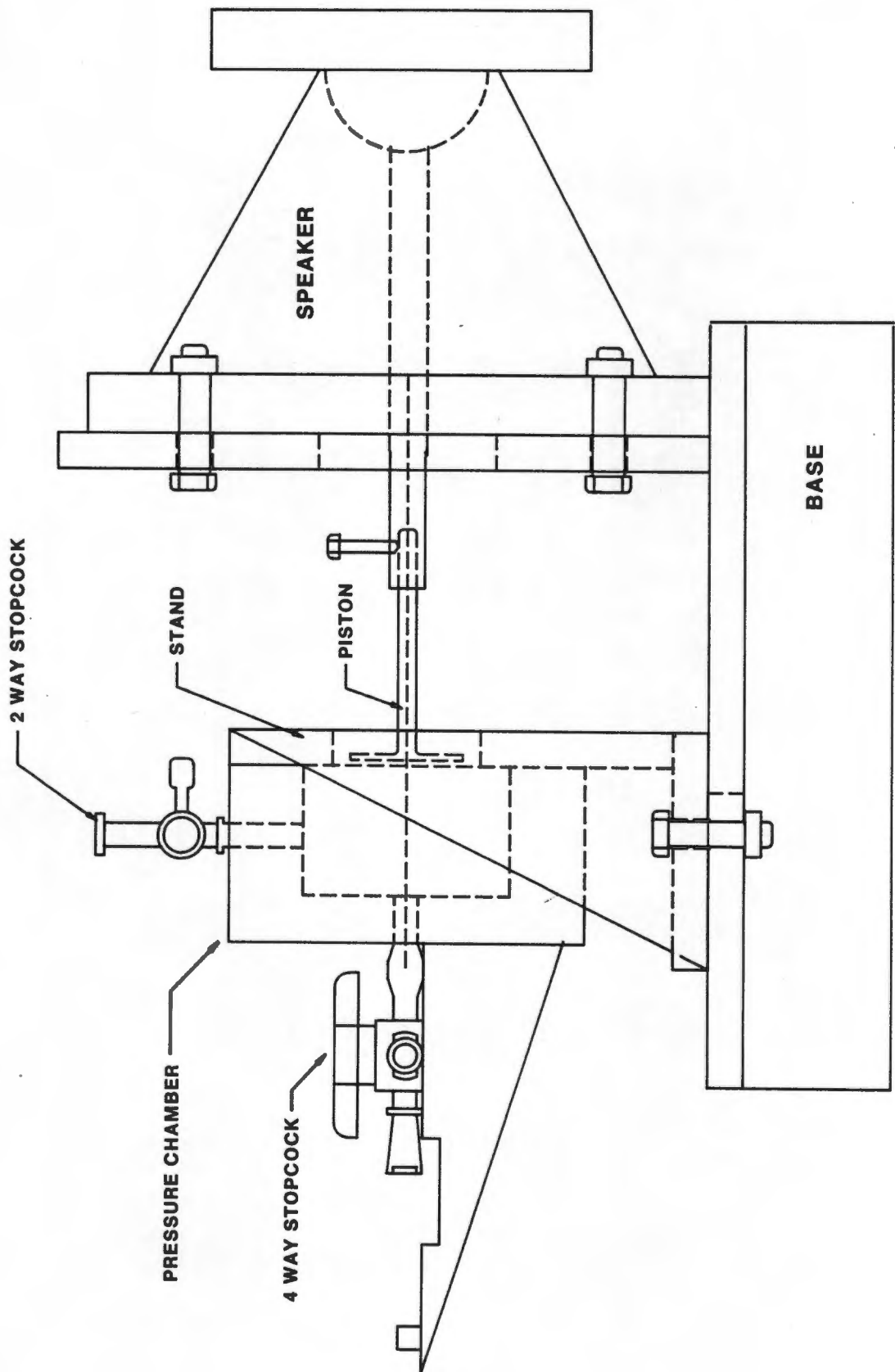


Figure C3.2

Cannula sliding device

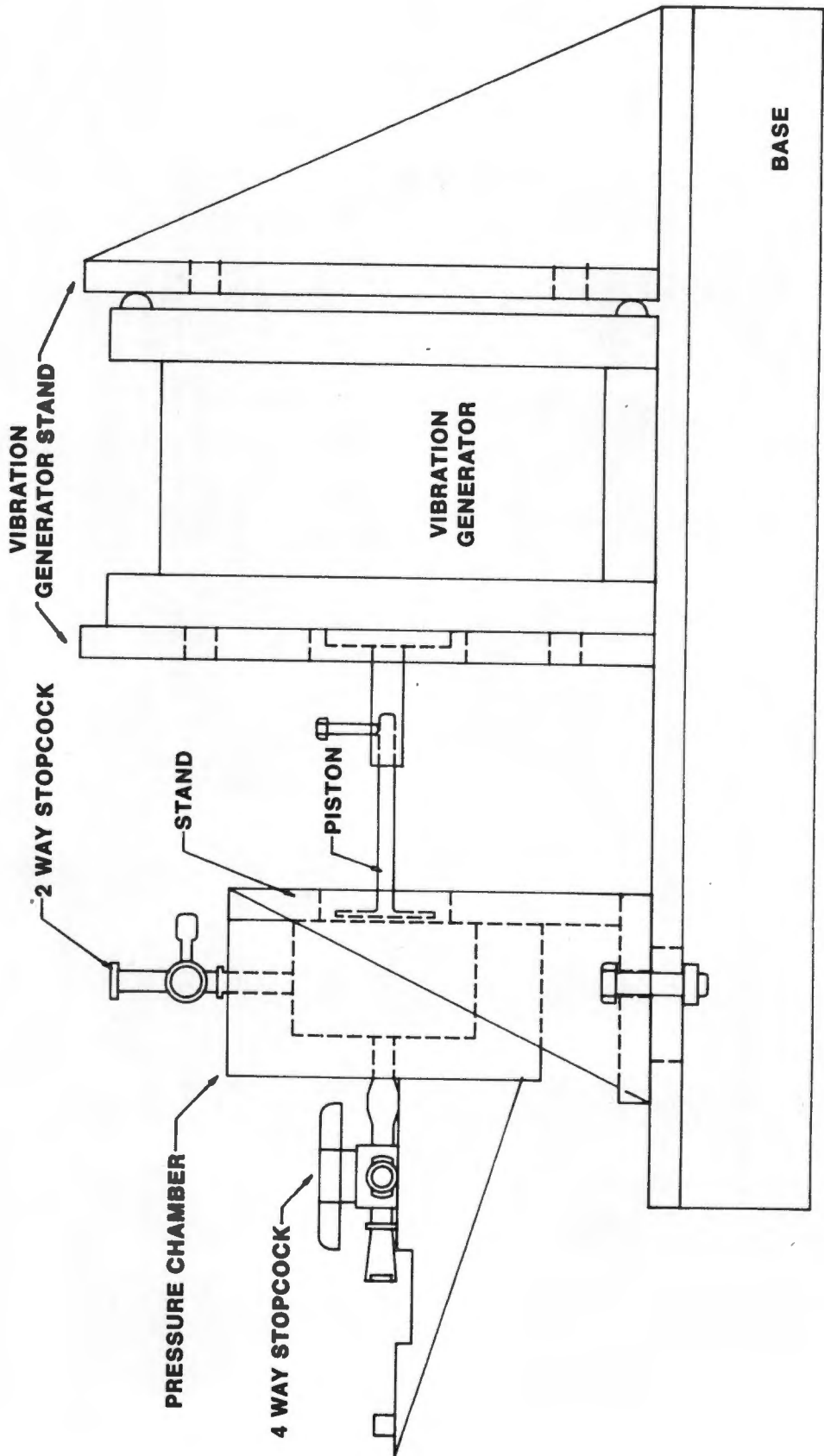
APPENDIX D

CONSTRUCTION PLAN FOR TEST EQUIPMENT



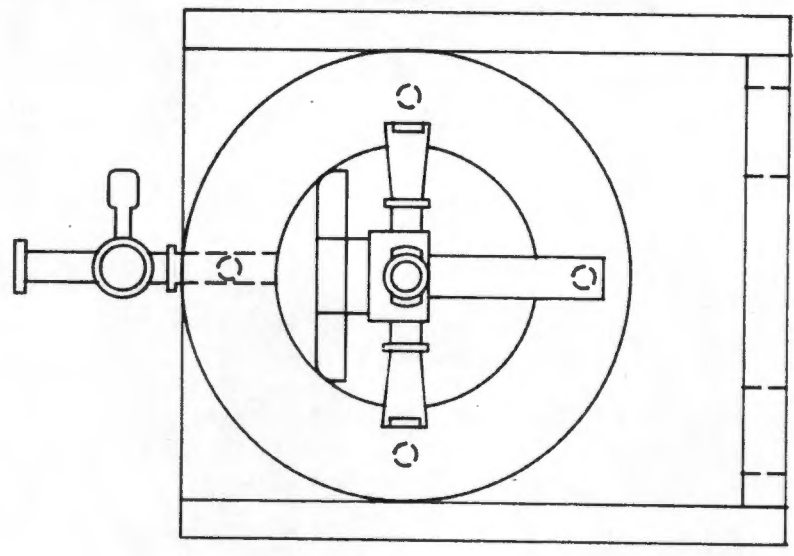
Drawing D1

Assembled catheter-manometer frequency response tester (model A)

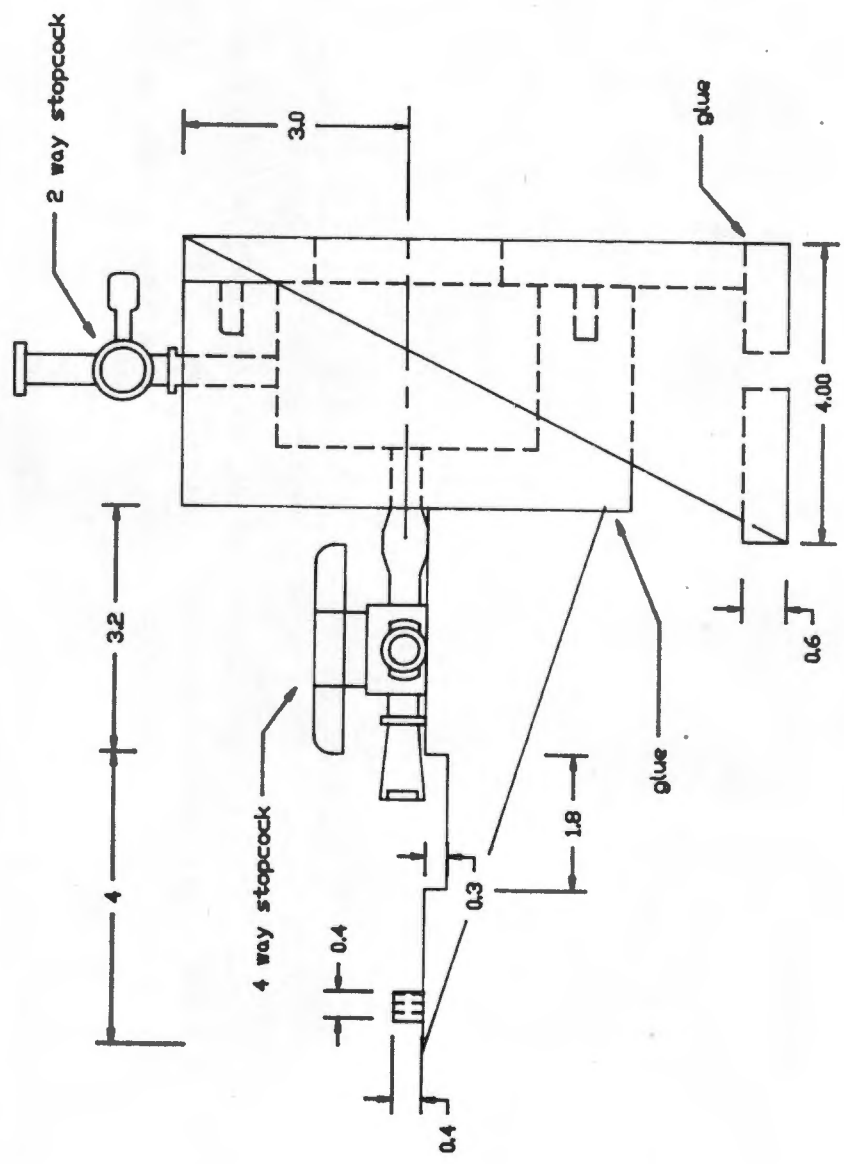


Drawing D2

Assembled catheter-manometer frequency response tester (model B)



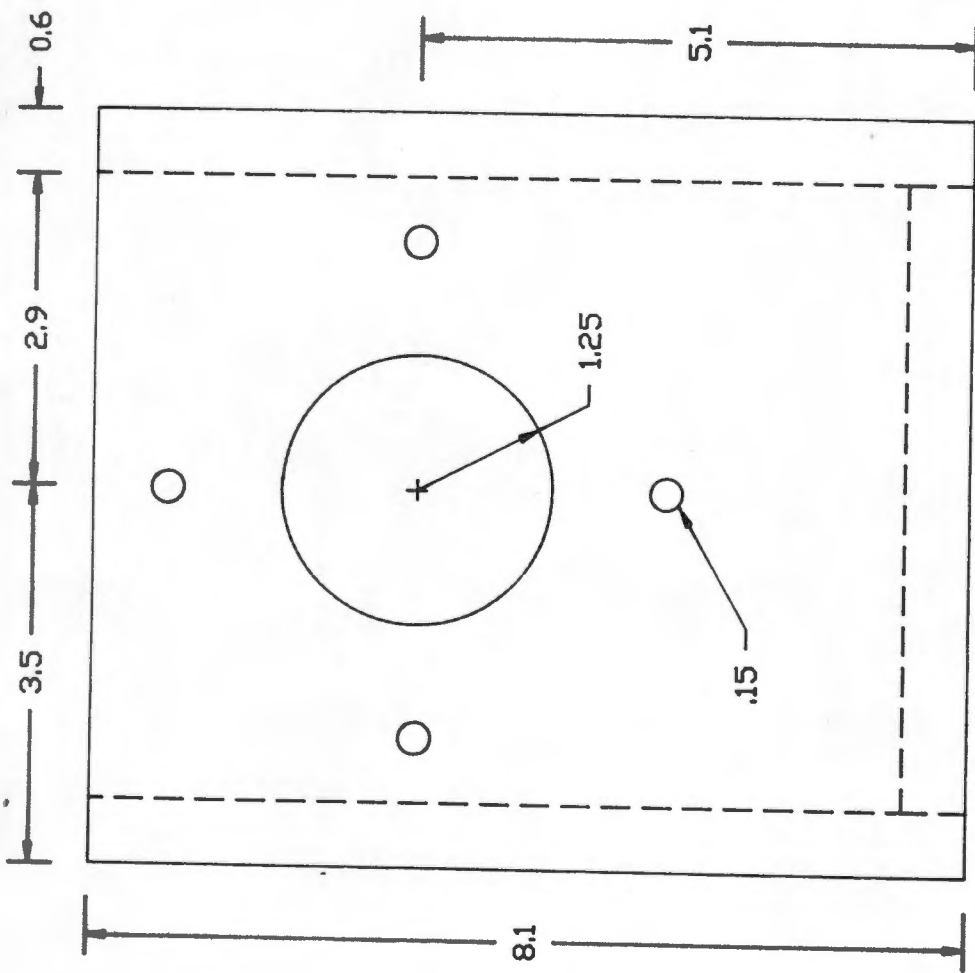
Pressure Chamber (reverse)



Assembled Pressure Chamber (side)

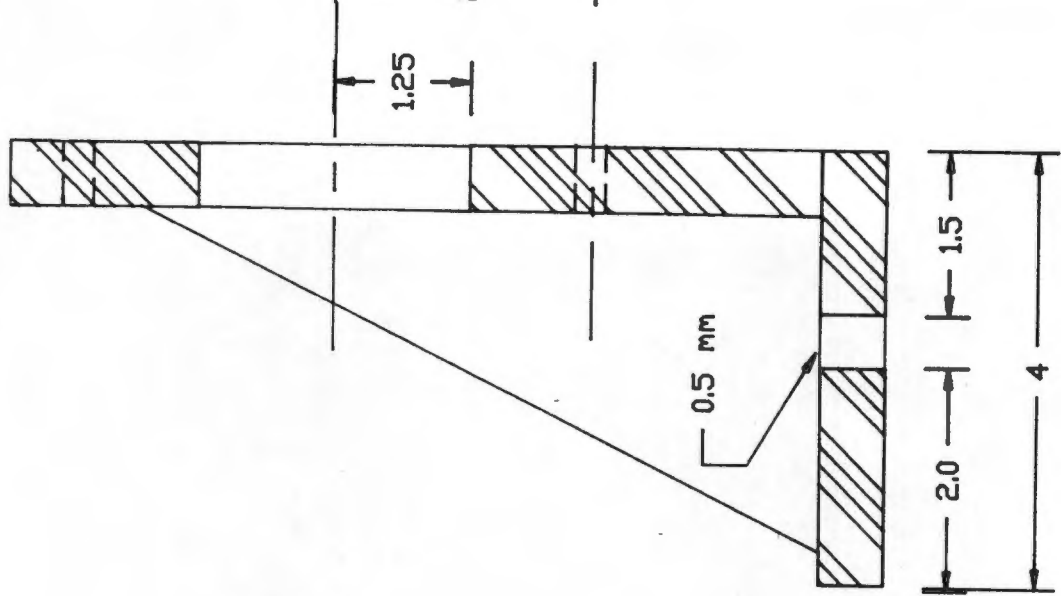
Drawing D3

Assembled pressure chamber



Note: 4 x 3 mm holes

Stand (front)



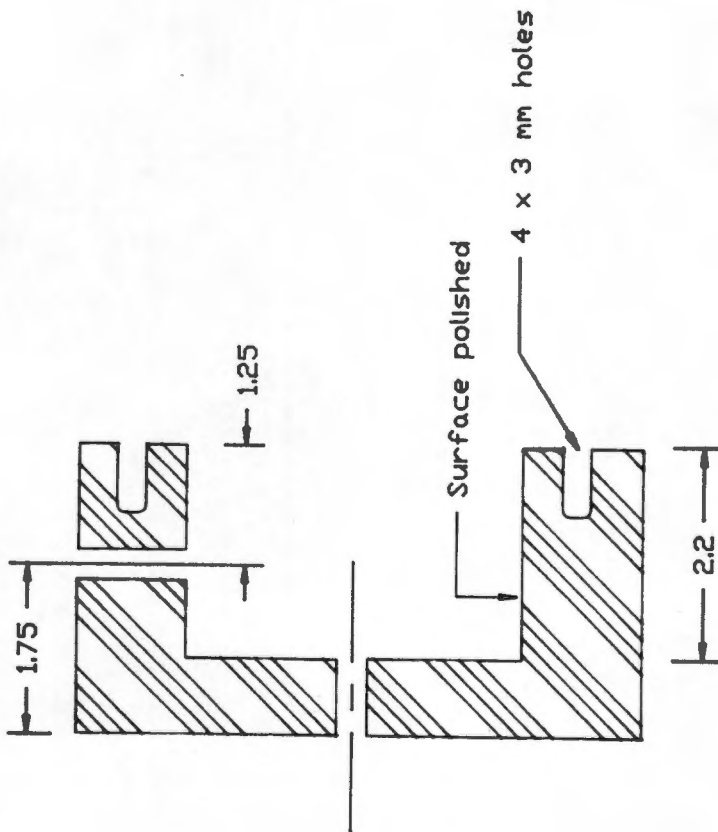
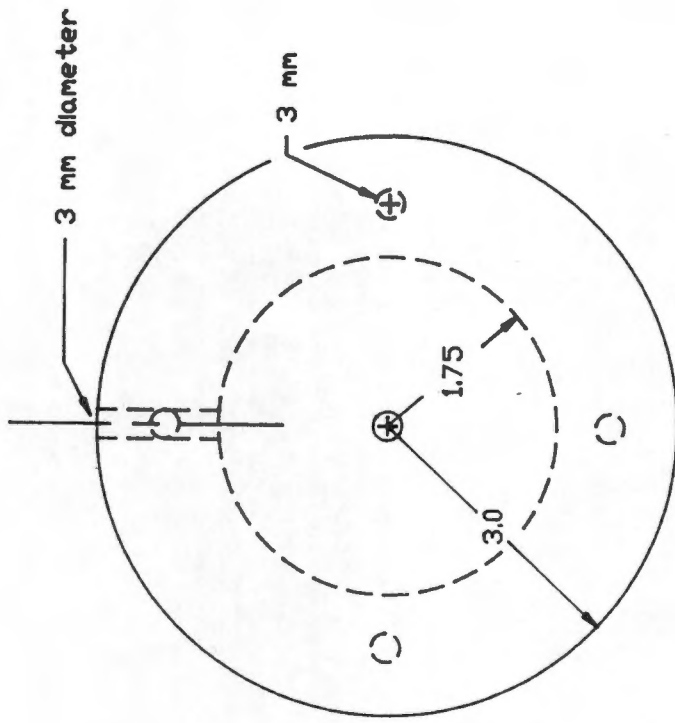
Stand (side)

Drawing D4

Stand

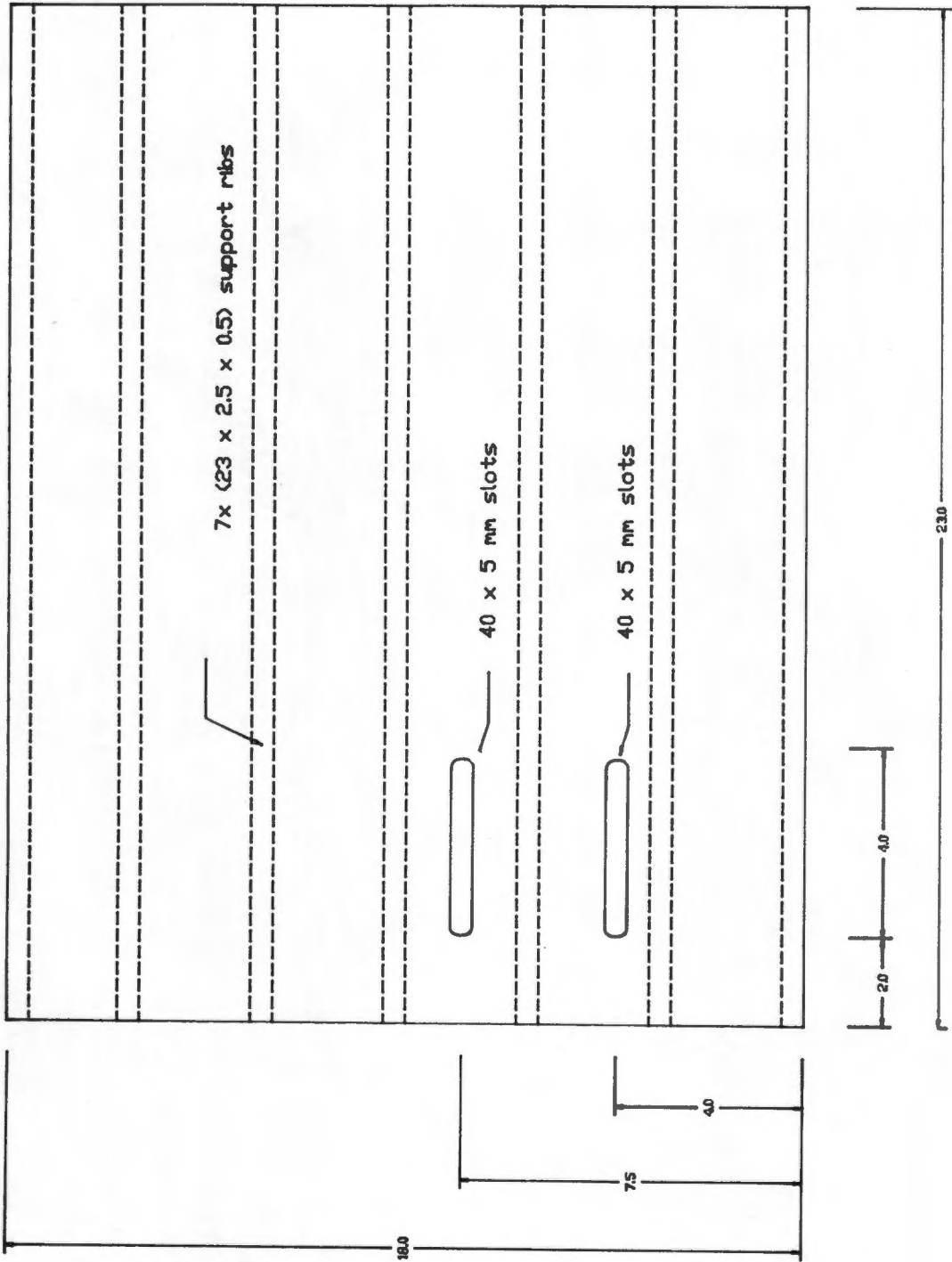
Drawing D5

Pressure chamber



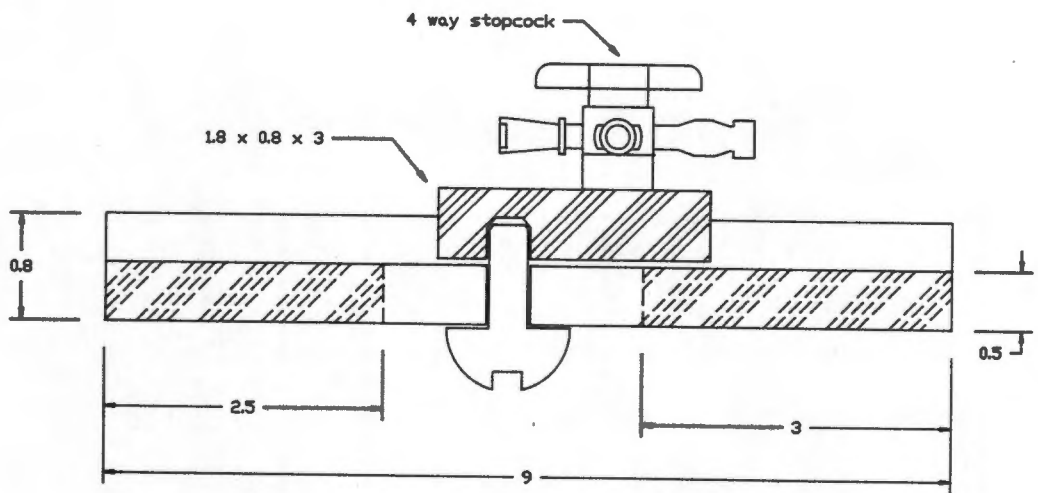
Pressure chamber (side)

Pressure chamber (reverse)



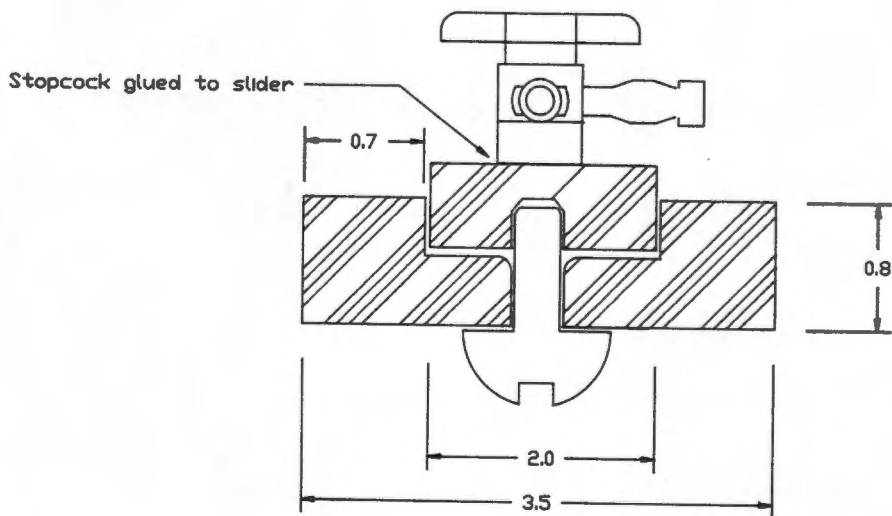
Drawing D6

Base



Drawing D7(a)

Cannula sliding device - side view



Drawing D7(b)

Cannula sliding device - front view

APPENDIX E

SOFTWARE OPERATION

CONTENTS

E1	Guidelines on the operation of MEAS.THE	E2
E1.1	Getting started	E2
E1.2	Main menu functions	E6
E1.2.1	Manual data entry (version 1.00)	E6
E1.2.1.1	The array editor	E10
E1.2.2	File access, frequency response calculations and hard copy presentation.	E13
E1.2.2.1	Data retrieval from diskette	E13
E1.2.2.2	Resonant frequency and damping factor calculations	E21
E1.3	MEAS.THE (version 1.25)	E22
E1.3.1	Automated data entry	E22
E1.3.2	Reading data from diskette	E23
E1.3.3	Data viewing	E23
E1.3.4	Resonant frequency and damping factor calculations	E25
E1.3.5	Hard copy presentation	E25
E2	Guidelines on the operation of ANAL.THE	E26
E2.1	Getting started	E26
E2.2	Main menu functions	E27
E2.2.1	Opening, data sampling and diskette access routines for ANAL.THE	E27
E2.2.2	The array scroller	E35
E2.2.3	The analysis routines	E39
E3	Examples of hardcopy presentation	E52

E1 Guidelines on the operation of MEAS.THE

E1.1 Getting started

The micro-computer is booted with PC Dos or MSDOS (Version 2.01 or later). At the A> prompt, the ASYST master diskette is placed into drive "A", the diskette containing the program MEAS.THE and into drive "B". The procedure listed below must then be followed:

- 1) Type [A:] Asyst and <return>
- 2) At the OK prompt, type Load B:Cath1.the and <return>
- 3) Again the OK prompt appears, then type Main and <return>

Replace the ASYST master disk with the working diskette (data diskette). The opening/main menu of the program will then appear on the screen as shown in figure E1.1.

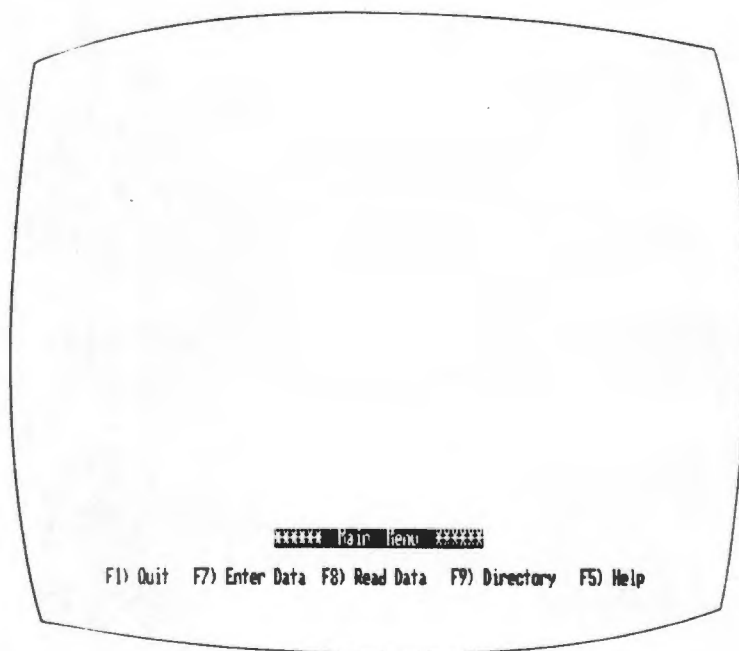


Figure E1.1

The opening menu of the program. The function menu, at the base of the screen, will remain active throughout the program.

The main function keys are then activated (table E1.1); however, any error encountered in this process will be displayed and the system will be restarted automatically. In the system restart, the number stack is cleared and the interrupts are reset, thus enabling the software the access to Asyst commands. Not clearing the number stack would tentatively prohibit any further use of Asyst commands, as the identity of the entry at the top of the number stack would be unknown. An error leaves a random entry at the top of the number stack with a corresponding random flag, either true or false, on the symbol stack. A false flag would prevent defining a function to a function key (Astheimer et al, 1985).

Figure E1.2 represents the key to the box diagrams used for the flow-charts while the flow-diagram of the main subroutine of MEAS.THE is given in figure E1.3.

- F1 quits the program and returns the user to Dos
- F5 calls the help menu
- F7 calls the data acquisition routines
- F8 calls the data read subroutines
- F9 calls the Directory

Table E1.1

Active function keys for the Main Menu

Explanation of function keys

(1) Function key F1

The process may be terminated elegantly and the user is returned to DOS. Verification of this function prevents unplanned exits from the program.

(2) Function key F5

Main Help Menu is displayed.

(3) Function key F7

Calls the data entry routines. These routines are discussed in section E1.2.1 and by the flow-chart in figure E1.4.

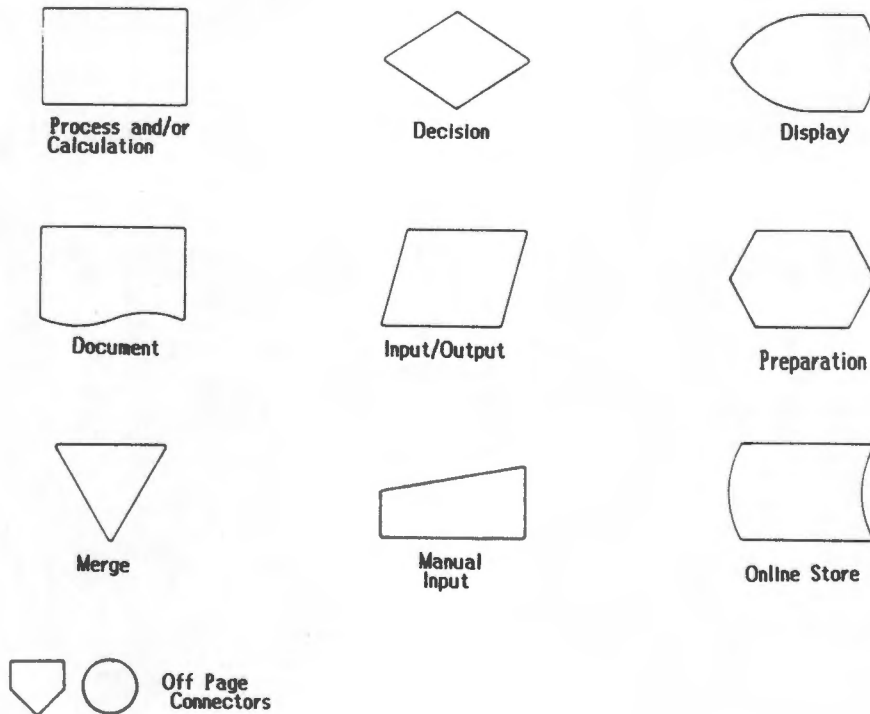


Figure E1.2

Key to the box diagrams used in the flowcharts.

(4) Function key F8

Calls the data reading subroutines (section E1.2.2.1) and the flowchart is given in figure E1.7.

(5) Function key F9

Displays the directory of the diskette in drive "A":

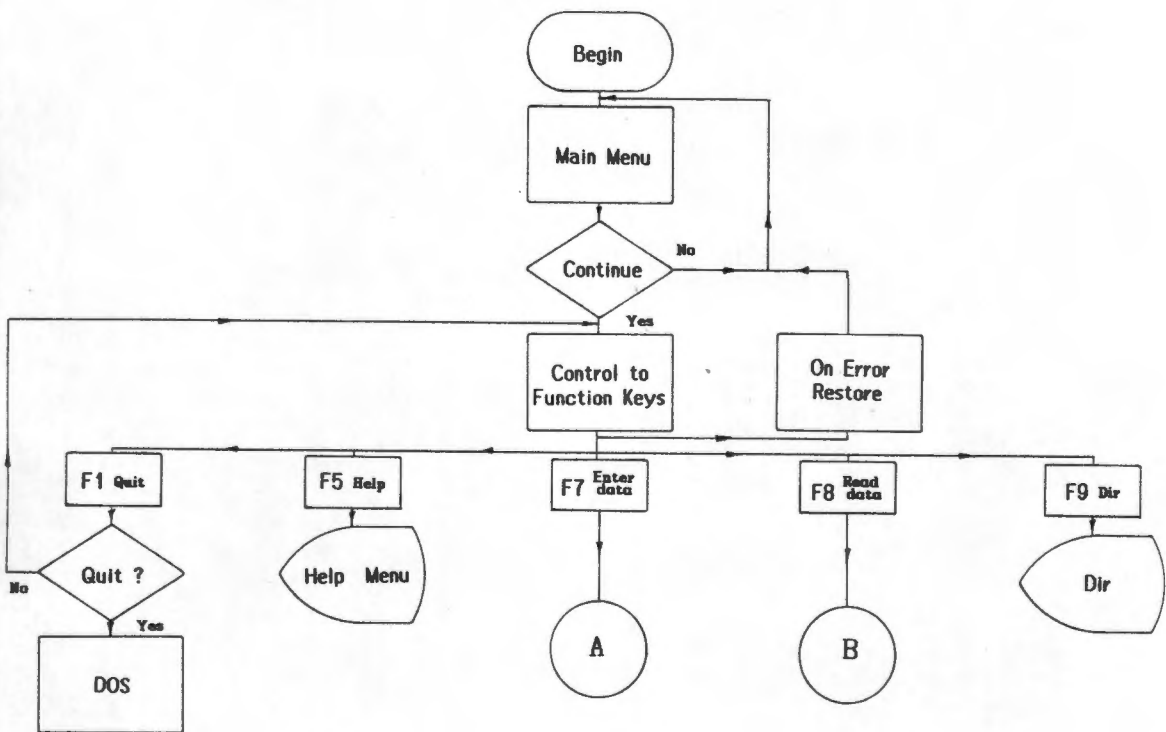


Figure E1.3

Flow-diagram of the main subroutine of MEAS.THE

E1.2 Main menu functions

E1.2.1 Manual data entry (Version 1.00)

The lower section of the screen is reserved for the display of menus. The functions displayed in the function key flow diagram in figure 4.13 correspond to the active keys listed in table E1.2.

Selecting function key F7 (Enter data, in figure E1.1), the data enter menu is displayed. Function keys F7, F8 and F9 are deactivated and function keys F2 and F5 are activated for the functions listed below. Function key F6 is defined but remains inactive until the Read.data.key subroutine (Appendix F1) which activates F6 is called. The active function keys are now:

- F1 quits the program and returns the user to DOS
- F2 reads data manually/automatically
- F5 calls the help menu
- F6 Saves the data

Table E1.2

Active function keys for the Data Entry Menu

Explanation of function keys

(1) Function key F1

The process may be terminated elegantly and the user is returned to DOS. Verification of this function prevents unplanned exits from the program.

(2) Function key F5

Data Entry Help Menu is displayed.

(3) Function key F2

Calls the array editor for manual data entry.

(4) Function key F6

Saves the data entries.

The flowchart of the data entry subroutines is shown in figure E1.4.

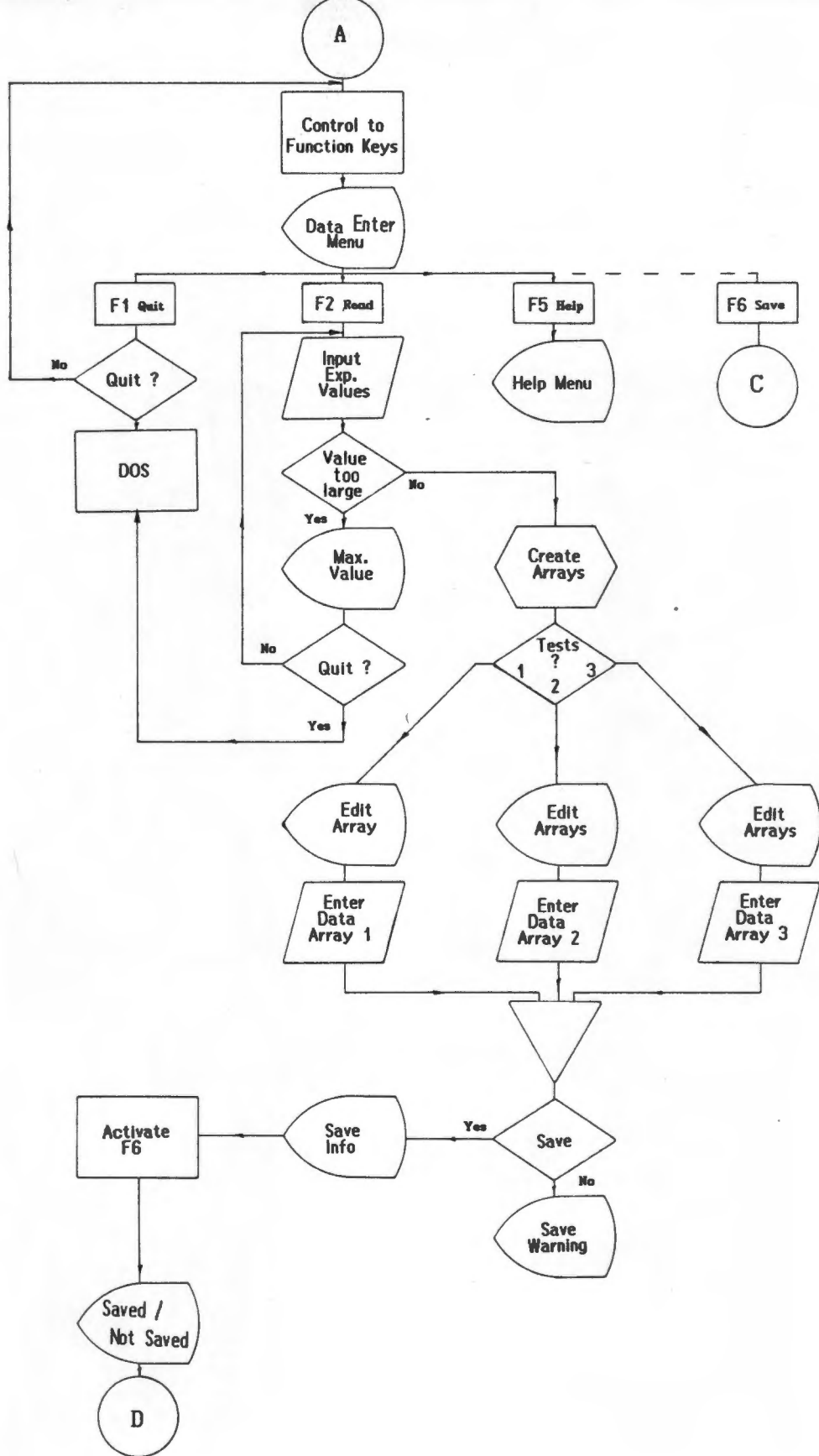


Figure E1.4

The flow-chart for the data entry subroutines.

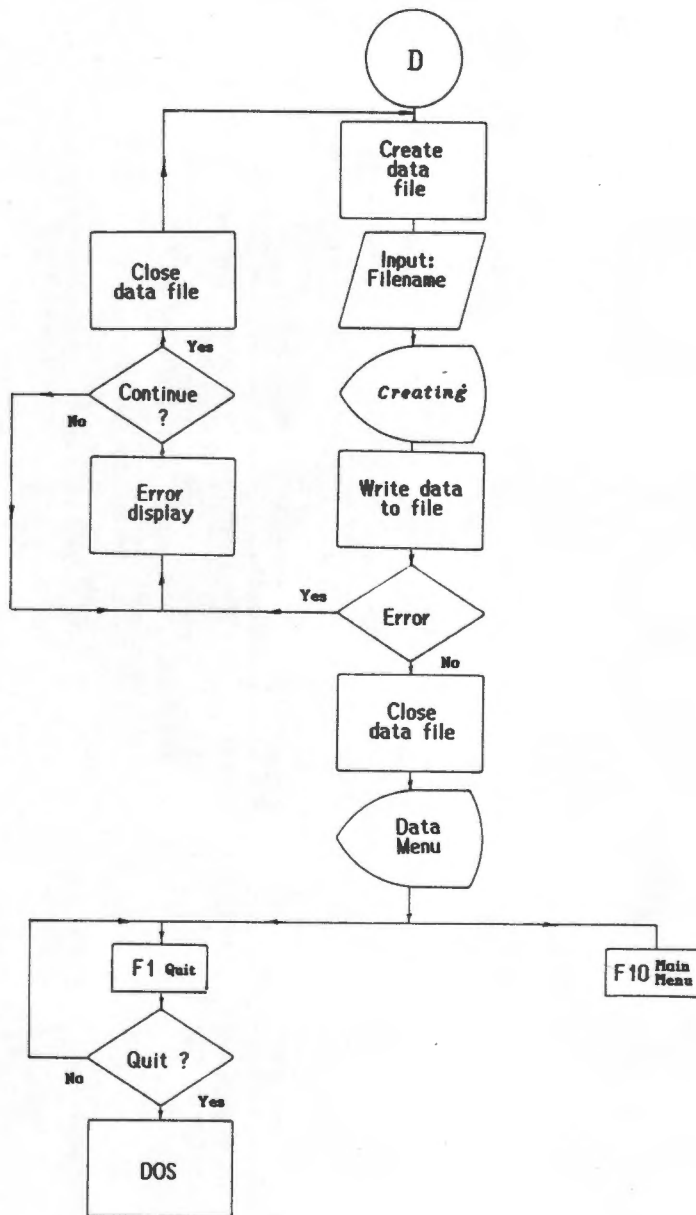


Figure E1.4 (continued)

The flow-chart for the data entry subroutines.

E1.2.1.1 The array editor

F2 clears the screen and prompts the user to define the array editor. The array editor is required in the data acquisition process, but before it is initialised, certain parameters must be defined. The program will require the input of the parameters listed below;

- a) Title of the experiment
- b) Experiment identification number
- c) Catheter material and make
- d) Internal diameter of catheter
- e) How many tests for this experiment <3>
- f) Data pairs in this experiment <15>

Parameters a) to d) are used to enhance the user friendliness and are not essential parameters for the program; e) and f) however, are important parameters and their default values (indicated between the < > brackets) may be changed. The parameter in (e) indicates the number of repeated tests for one particular catheter-manometer system. The maximum number and default value is three. The parameter listed in (f) indicates the number of measurement samples in one test (the number of corresponding frequency and amplitude entries). The default value is fifteen and the maximum value is thirty.

Parameters (a) to (d) are stored in strings (maximum of 15 characters) and parameters (e) and (f) in arrays. The characters entered into the strings are used to identify the data and are not important to any calculations. The parameters entered in the arrays are compared with allowable values and verified.

Errors are displayed with the maximum and minimum permissible values. The process may be terminated if an error is located by pressing Y at the "Quit" prompt. A N reply enables the experiment parameters to be re-entered.

Data arrays (the entries are real numbers) with the dimensions defined by the entered parameters are created and the array editor is displayed (Figure E1.5). Data is then entered.

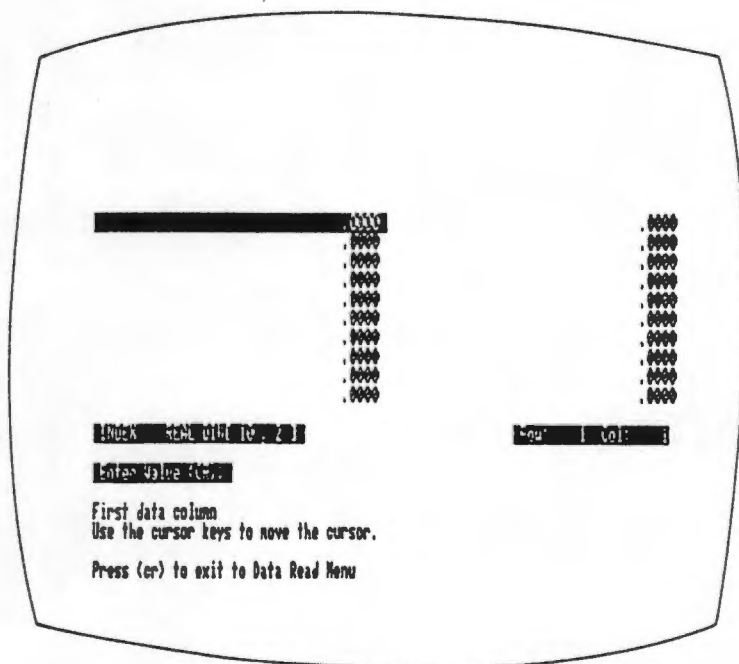


Figure E1.5

The array editor. The first and second column represent the frequency (Hz) and the corresponding amplitude gain in decibel (dB) value for a catheter-manometer system respectively.

Data pairs (amplitude gain in decibels and the corresponding frequency) which is manually recorded from the dB meter and signal generator respectively, are then entered into the columns using the control keys (their functions for the array editing are displayed in table E1.3).

Pressing the <return> key once will save the present data in the array editor. The INS key allows the current entry, at the cursor position, to be replaced by a new value.

Key	Function
Arrow up	Moves cursor up one position
Arrow down	Moves cursor down one position
Arrow left	Moves cursor left one position
Arrow right	Moves cursor right one position
Home	Moves cursor to upper left element
Pg Up	Moves cursor to upper right element
End	Moves cursor to lower left element
Pg Dn	Moves cursor to lower right element
Del	Exits the array editor
Ins	Allows new entries

Table E1.3

Control keys of the array editor

Selecting the <return> key once more, the array editor will become inactive and the user may save the data by selecting function key F6. The user is warned that the present data is lost if the saving process is not done before new data is entered. The program prompts the user for a file name and creates a data file on the default drive "A", which can be changed to the "B" or "C" drive. If any error is encountered during the creation of the data file, the software will close the file and thus enable the user to retain his entered data.

The data menu is displayed if the data was successfully saved. F10 is then activated which calls the Main Menu, deactivates F2, F5 (Data Entry Help Menu) and F6.

E1.2.2 File access, frequency response calculations and hard copy presentation.

E1.2.2.1 Data retrieval from diskette

The Read Data key (F8 in the Main Menu) prompts the Data Read Menu to appear (figure E1.6) and activates the function keys in table E1.4.

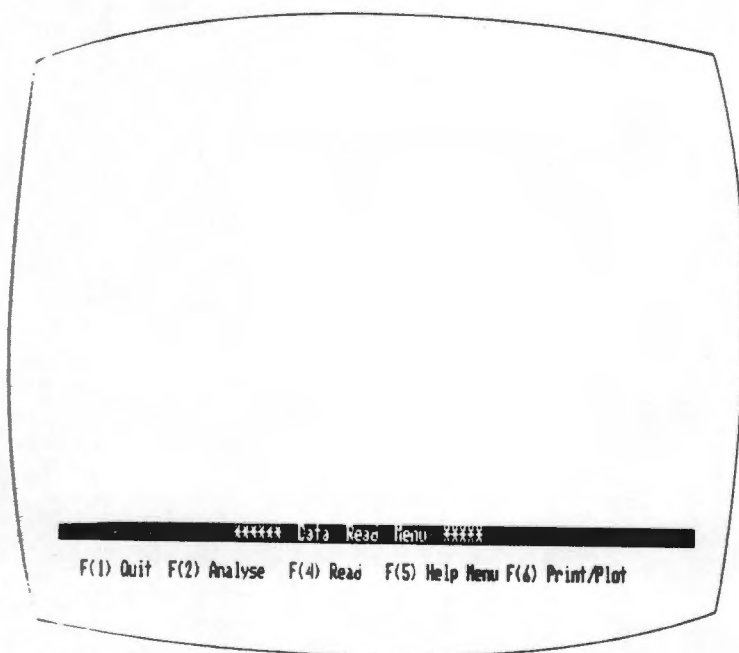


Figure E1.6

The read data menu of MEAS.THE. The function keys correspond to the action listed in table E1.4

- F1 quits the program and returns the user to Dos
- F2 does analysis of the data
- F4 reads data file
- F5 calls the help menu
- F6 calls the printer/plotter menu

Table E1.4

Active function keys for the Data Read Menu

Explanation of function keys

Function key F4

Selecting F4, a filename is requested (the input may be any word of eight characters and an extension of three characters). The file is opened and the data stored in the file is transferred to the stack in array format. Any error encountered will be displayed and the file will be closed. This action will again enable the user to continue without rebooting the system. On successfully reading a data file, the read menu will be displayed.

Function key F2

Selecting F2 will analyse the data that is currently on the stack (the last file that was called from diskette).

The software will establish the values for the experiment parameters (these have been saved as strings in the data file) and will then clear the operational stack. The resonant

frequency, the mean value of the recorded pressure (this value is required for the calculation of the damping factor) and the damping factor of each test is thereafter calculated. The mathematical mean and variance of the results are derived and displayed. The flow-diagram is given in figure E1.7.

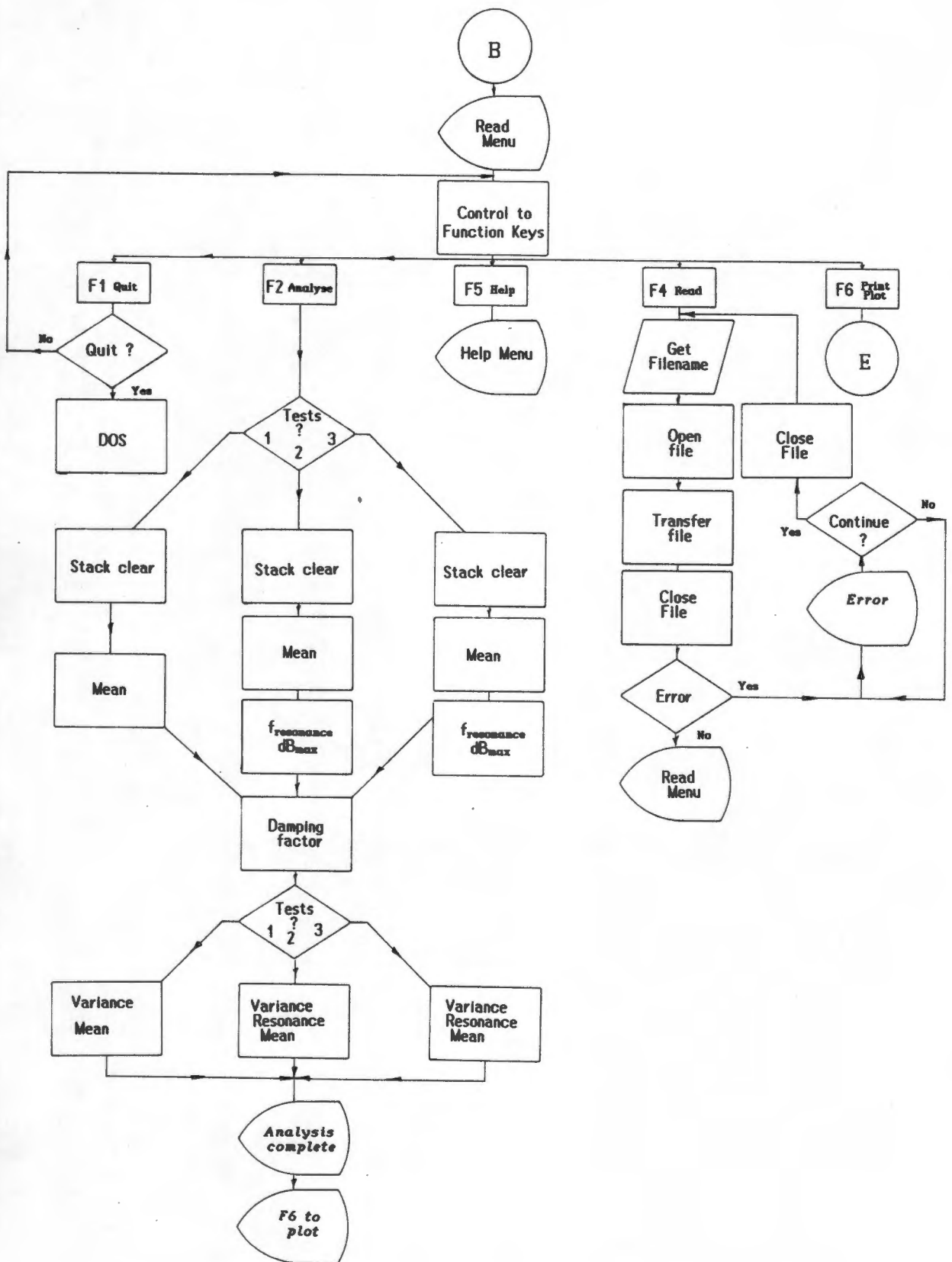


Figure E1.7

Flow-chart for the data read and data analysis subroutines.

Function key F6

Pressing F6 will display the printing menu (figure E1.8) and activate the printer and plotter function keys listed in table E1.5.

- | |
|---|
| <ul style="list-style-type: none">■ F2 Displays all the traces■ F3 Displays the mean trace■ F4 Prints a report■ F5 Calls Help Menu■ F6 Plots a mean trace■ F7 Plots all traces |
|---|

Table E1.5

Active function keys for the Printing Menu

Explanation of function keys

Function Key F2 and F3

Function keys F2 (displays all the traces) and F3 (displays the mathematical mean) will display the frequency vs. the amplitude trace in graphics mode. This display mode is used to present the trace in an elegant manner. This is achieved by fitting the data with an appropriate axis and annotation. The screen area (in graphics mode) of the visual display unit (VDU) or monitor is positioned in the upper right hand side of the screen to allow for the print menu to be displayed on the same screen. This display is shown in figure E1.9.

Function key F6 and F7

F6 (mean trace) and F7 (individual traces) analogously plot the traces as mentioned above on A4 size paper.

The plotting area, plotter speed (cm/sec) and the plotter pen colours are defined by the software. The plotter is initialised by the software and the data transmission occurs at a baud rate of 4800. The user acknowledges the end of the plotting procedure by pressing the <return> key.

Function key F4

Function key F4 activates the printer and will formulate a report that consists of the original test data and the calculated results.

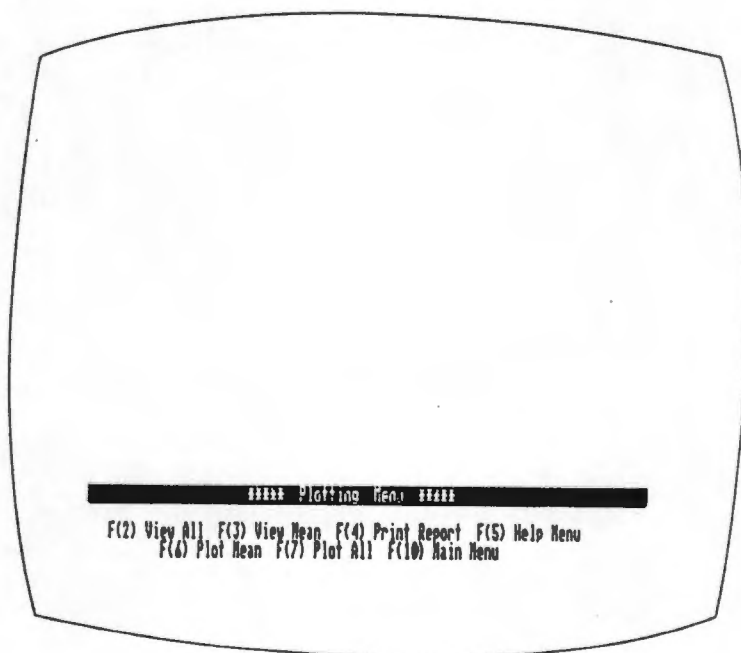


Figure E1.8

Printer and Plotting Menu

The user acknowledges that the printer is switched to the ready state, by typing a "Y" at the prompt. The output is then directed to the printer. The control of the micro computer is returned to the console once the printing process has been completed.

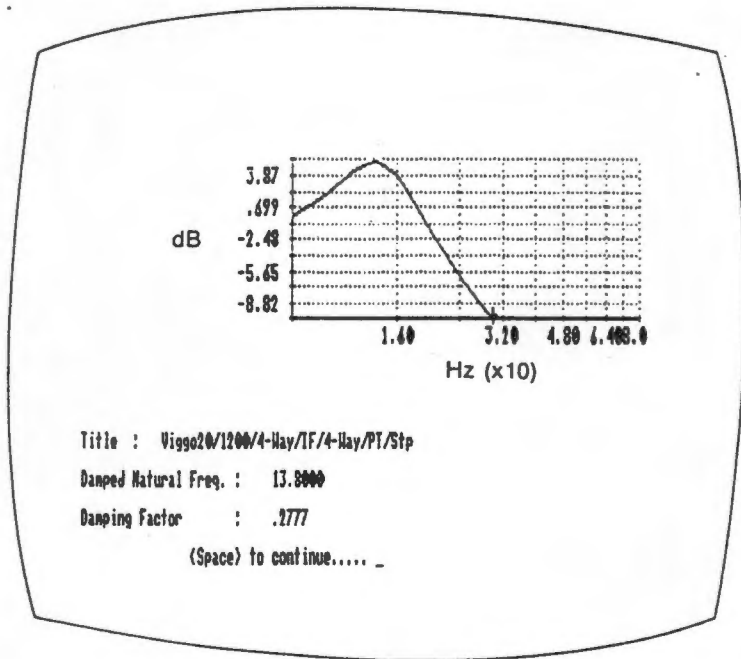


Figure E1.9

Amplitude response plot for average value of n number of tests.

The user again acknowledges the end of the printing process by pressing the <return> key. The present active function keys are then replaced by F7 and F8 (active function keys in the Main Menu) as the active function keys.

The flow diagram of the subroutines are given in figure E1.10.

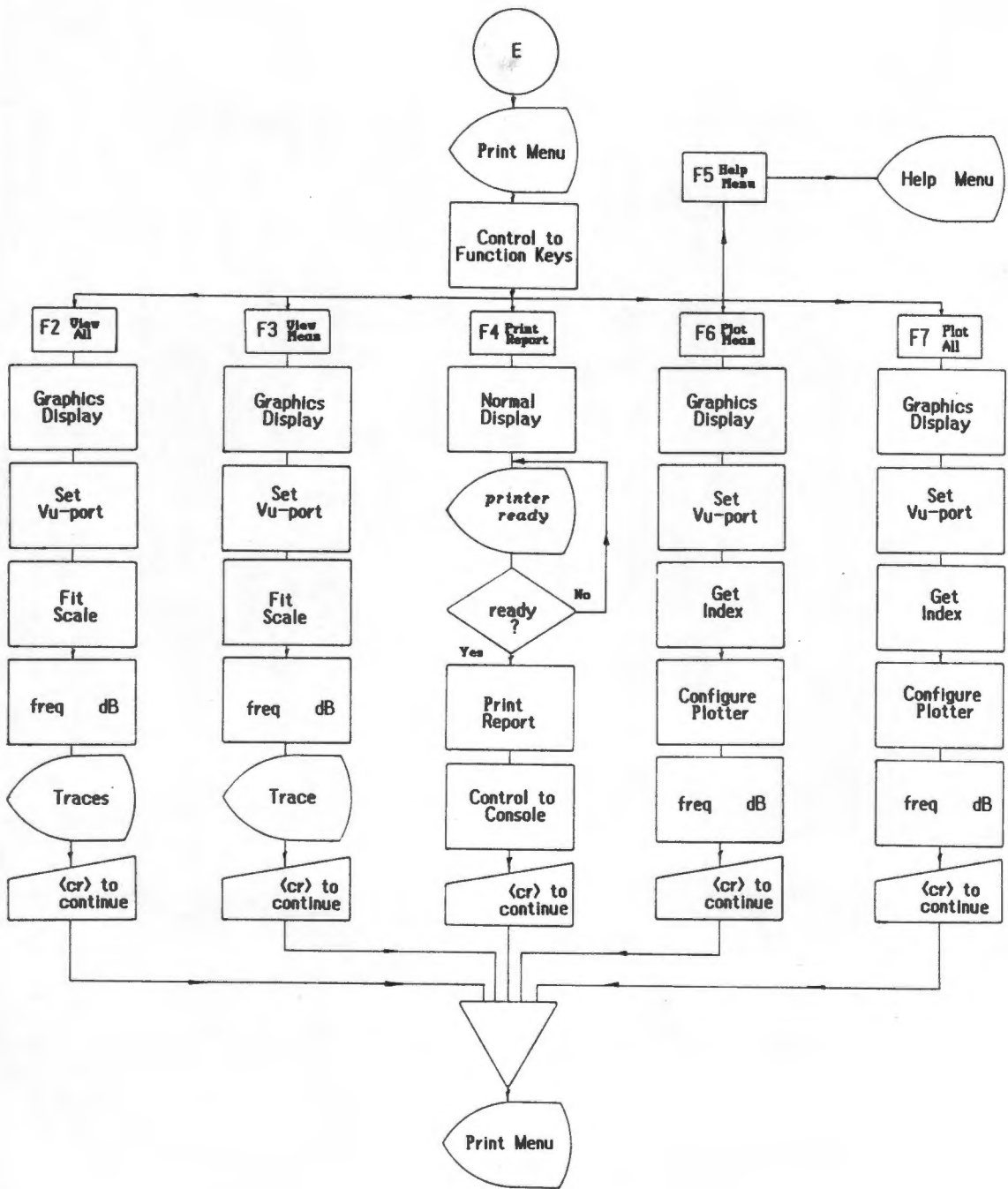


Figure E1.10

The flowchart for the printing routines.

E1.2.2.2 Resonant frequency and damping factor calculations

Function key F2, will activate the frequency response and damping factor calculations. The damping factor and resonant frequency of each data array (corresponding to an individual test) will be calculated. The variance and the mean of the results will be displayed and will give the user an idea of the fidelity of result. The results are displayed on the screen, and/or a hard copy may be produced.

The program may be exited at any stage by selecting F1. The program questions this command with a Yes/No option and will return the user to Dos, if positively answered.

Help Menus are available to the user throughout the program.

E.1.3 MEAS.THE (Version 1.25)

This version of MEAS.THE very similar to version 1.00 however, the data entry procedure is automated and thus the data calculation section is modified.

E1.3.1 Automated data entry

An identical opening menu to that of Version 1.00 (figure E.1) is displayed after the program is activated. The function flow chart is the same as in Version 1.00; however, on selecting the data read key F7, the following prompts are displayed:

- a) Title of the experiment
- b) Experiment identification number
- c) Catheter material and make
- d) Internal diameter of catheter
- e) How many tests for this experiment <3>

Similar to version 1.00, parameters (a) to (d) are non essential parameters for the program; however, parameter (e) determines the number the in vitro frequency response test is repeated. The default value is three.

The sampling of amplitude response data (amplitude and the corresponding frequency) is activated after a display message by selecting function key F2. The display message will remind the user to prepare the MICROLINK to send information to the computer. A <return> will immediately start the sampling process.

The sampling process parameters (i.e. sampling rate 1 kHz, and number of samples 10 000) may be changed permanently in the

software or temporarily after the program has been activated. The sampling process is discussed in detail in section E2.2.1. From the defined parameters, the sampling period is 10 seconds, after which a message indicates the completion of the process. The user then may choose to either save the data, view the data or sample a new set of data. Saved data is removed from the number stack and stored as a real array in a file that is set by default to the current drive (the A drive). Again the user may sample a new set of data or continue to the data calculation phase.

1.3.2 Reading data from diskette

Reading of stored data is identical to that of version 1.00 which was discussed in section E1.2.2.1.

E1.3.3 Data viewing

The saved data may be viewed. The viewing process is controlled by a scroller. The user thus may scroll and manipulate the scroll window with the keys as shown in Table E1.6. The scrolling may be halted at any time by selecting the <return> key once. The segment of data currently displayed on the screen relative to the complete data array is indicated by the arrows at the lower border of the scroll window - see figure E2.4. The indices (the index value of the first and last data value displayed on the screen) of the scroll window are given at the base of the scroll window. The numbers allow the user to establish an exact position within the data array.

Key	Function
Arrow up	Increases data point increment by a factor of two - faster scrolling
Arrow down	Decreases data point increment by a factor of two - slower scrolling
Arrow left	Scrolls the display window backwards
Arrow right	Scrolls the display window forwards
Home	Moves the display window to the beginning of the data
End	Moves the display window to the end of the data
Pg Up	Increases the horizontal expansion factor by two. Eight is the max.
Pg Dn	Decreases the horizontal expansion factor by two. One is the min.

Table E1.6

Scroll control keys. A bell is sounded whenever the data increment or expansion factor cannot be increased or decreased.

Following the data scrolling by another <return> key, two vertical marker bars appear in the scroll window and these may be moved within the displayed segment of data by the function keys listed in table E1.7.

By pressing the <return> key for a second time once a particular amplitude response is marked, its indices (the start and end points of the pulse within the data array) are stored. The user has the option of marking either one, three or five amplitude responses.

Key	Function
Arrow up	Increases the mark increment by a factor of two - number of data points that the marker jumps at each strike of the left or right arrow key.
Arrow down	Decreases the mark increment by a factor of two - number of data points that the marker jumps at each strike of the left or right arrow key.
Arrow left	Moves the active mark to the left
Arrow right	Moves the active mark to the right
Home	Displays the horizontal and vertical coordinate on the screen
End	Makes left mark active
Pg Dn	Makes right mark active

Table E1.7

Marker-bar control keys

E1.3.4 Resonant frequency and damping factor calculations

Damping factor and resonant frequency calculations in MEAS.THE (Version 1.25) are different from Version 1.00 in so far that the new version of the program first calculates the positive peak value and period (T) of each oscillation. These results are then used to calculate the resonant frequency and damping factor, as in Version 1.00.

E1.3.5 Hard copy presentation

This section is the same as version 1.00.

E2 Guidelines on the operation of ANAL.THE

E2.1 Getting started

To activate the program, the micro-computer is booted with any DOS Version higher than Version 2.01. The following steps are then taken to load ANAL.THE;

- 1) At the A> prompt place the Asyst master diskette into drive "A", and the diskette containing the program ANAL.THE into drive "B".
- 2) Change the control to the B drive
- 3) At the B> prompt, type; ANAL and <return>
- 4) At the OK prompt, type; Load Cath11.the and <return>
- 5) At the second OK prompt, type Main followed by a <return>

The program is loaded and compiled and the configuration of the A/D card will be done automatically; however, should the user have a different system to that described in section 5.3, the system start and configuration must be done manually. The method is described in points 1 to 4 below.

- 1) Place the ASYST master disk in drive "A" and the disk containing the ANAL.THE file into drive "B".
- 2) At the A> prompt, type Asyst followed by <return>
- 3) Type Load B:Config.hpb at the OK prompt followed by <return>

The program will direct a few questions to the user, which have to be answered in accordance to the system used. The end of the configuration process of the system is marked by the return of the OK prompt.

- 4) Then type Load B:Cath11.the

E2.2 Main Menu functions

E2.2.1 Opening, data sampling and diskette access routines of ANAL.THE

Following the correct configuration procedure described in the previous section, the Opening Menu of ANAL.THE is displayed (figure E2.1).

The left hand side of the screen is reserved as the information table. The lower left window of the information table displays the active function keys that may be chosen to activate a given procedure.

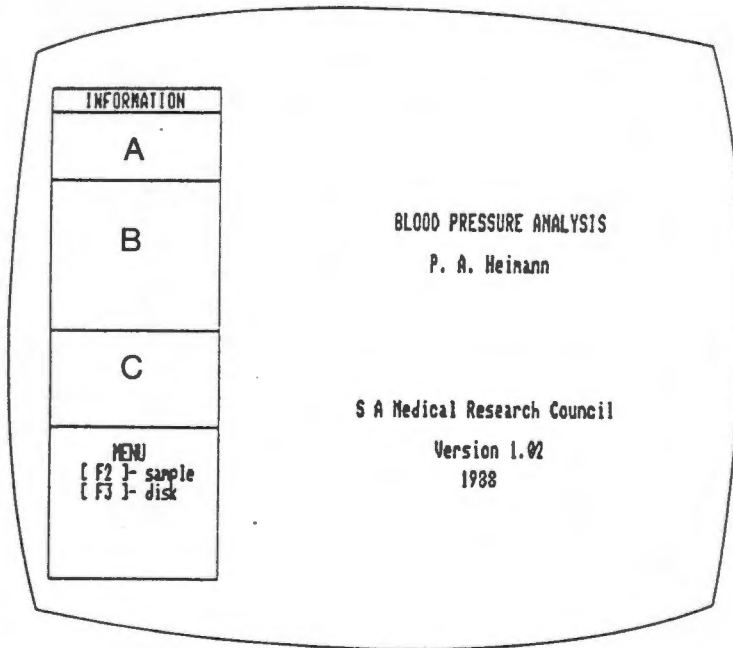


Figure E2.1

The opening menu of the program. The left hand side of the screen is reserved as the information table. Window A displays a header message for the graphics, window B displays user instructions and C is the interaction window. Window D displays the current menu as shown.

The flowchart of the main menu is represented in figure E2.2 and the function keys, listed below, are assigned to control and start the procedures ascribed to them.

- | |
|---|
| <ul style="list-style-type: none">■ F2 Samples data from Microlink■ F3 Reads a file from diskette■ F10 Quit |
|---|

Table E2.1

Active function keys for the Data Read Menu

Any error encountered will be displayed and the system restarted for the reasons described in section E1.1.

Explanation of Function Keys

Function Key F2

Function key F2 starts the configuration and sampling procedure. The configuration process is performed before the actual data transfer and defines the address structure for the micro-computer to communicate with the MICROLINK.

(i) High speed clock configuration process

The configuration process is started by sending a `Send.Interface.Clear` (pulses the IFC line on the current bus) signal on the GPIB. This command initialises the bus and makes the sender of the latter command the controller. The micro-computer establishes itself as the controller (`me.talker`) and

addresses the high speed clock board (in the MICROLINK with a primary address 3 and secondary address 0) as the receiver of information by the command MK.HSC LISTNER. The high speed clock, addressed as a listener, expects two data bytes defining the clock speed and interval. These will be interpreted as follows;

Data Byte One

- Bits 0 - 2 are interpreted as the number which determines the basic rate of the clock. This basic rate is one of seven that is in a geometric series, increasing by a factor of ten. This is displayed in table E2.2. The smallest basic clock unit (for the A/D conversion in the MICROLINK) is 1 microsecond, but the final clock speed will be determined by the fastest rate at which data bytes can be transferred to the computer controlling the process. The maximum rate of data transfer in the HP VECTRA is 20 kbytes/sec (or a clock speed of 50 μ sec).

Bit pattern	Decimal	Clock
000	0	1 μ sec
001	1	10 μ sec
010	2	100 μ sec
011	3	1 msec
100	4	10 msec
101	5	100 msec
110	6	1 sec

Table E2.2

The 7 clock rates and bit patterns to select the clock speed.

- Bit 3 of the data byte is the high speed clock enable bit. This bit must be set to a 1 for the clock to be used.
- Bit 4 of the data byte is the synchroniser flag bit. This bit is set to a 0 as this greatly simplifies synchronisation of the external and internal triggers.
- Bits 5,6 and 7 are not used.

Data byte two

- This eight bit number is interpreted as the number of basic clock units between each sample, i.e. the clock can be programmed to wait between 1 and 255 of the clock cycles between each analogue to digital conversion (clock interval time).

The actual clock speed and the clock interval time are set by entering an integer on the top of the number stack and sending this information to the high speed clock by the commands, 12 stack.talk (byte one) and 1 stack.talk (byte two).

The integer, 12, is calculated from table E2.2 and represents a clock rate of 10 milli seconds (binary 100). Bit 3 is set to a 1 and thus the integer number equals 12 (binary 1100). The second number (byte two) is set to 1 and thus the time interval between each sample is 10 milli seconds or the sampling rate is 100 Hz. The configuration process of the high speed clock is discontinued by the command unlisten.

Analogue to digital converter configuration

The micro-computer re-establishes itself as the controller and addresses the A/D card (primary address 3 and secondary address 1) in a similar method to that described for the high speed clock. The micro-computer then selects the channels (the A/D card has 32 input channels) which have to be sampled by sending a data byte to the A/D card.

The interpretation of the bits of this data byte is as follows;

Bit	Meaning
0	Skip flag - skip a channel
1	Return flag
2-6	Channel number as a binary code
7	Not used

Selecting channel 0 requires a data byte with the value 2 (no skip flag, thus a 0 for bit 0 and a 1 for a return flag after the channel defined in bits 2 to 6, which in this case is 0).

The controller (the micro-computer) there after relinquishes the control by sending the unlisten command and the A/D card is ready to transfer data if addressed.

(ii) Data Transfer

Data transfer from the A/D card to the micro-computer is established by the subroutine `data.collect` (Appendix F). The micro-computer is defined as the listener (receiver of data) while the A/D card is defined as the sender. Data transmission starts once an external trigger is received by the MICROLINK or by the internal trigger, which is sent to the MICROLINK by the computer after a defined time delay (this time delay acts as a time out procedure and prevents the micro-computer from being

inactive for long periods of time). A 100 milli second time delay was defined because no external trigger was available and thus the actual sampling process commenced with a small delay as soon as F2 was pressed.

One thousand data samples are read to the number stack and transferred to an array.

The end of the sampling process is displayed and the communication with the MICROLINK ended.

The user has the option of saving the data on diskette or using the data without saving. On exit from the saving routine, the function key F2 will be allocated to a stack buffer. This enables the user to define a other process to function key F2. Pressing function key F1 (escape), the latter process is removed from the stack buffer and the original routine for F2 will be active. This allows the user to move within the program structure and simplifies the control of the program.

Function key F3

Data can be read from diskette by typing F3. The micro-computer will prompt a filename (a word of eight characters with/without an extension of three characters). The file will be read and the data transferred to an array.

Function key F3 is then placed onto a separate stack buffer (not the same stack buffer as for function key F2) for later use as described above.

The View Menu is displayed and the number of pulses to be analysed is prompted. The default value is three. This number is used to define the multi-dimension array that is to hold the numerical data.

Function key F10

Function key F10 provides the user with an elegant method of terminating the program. The user is verified on his decision.

The flowchart is given in figure E2.2.

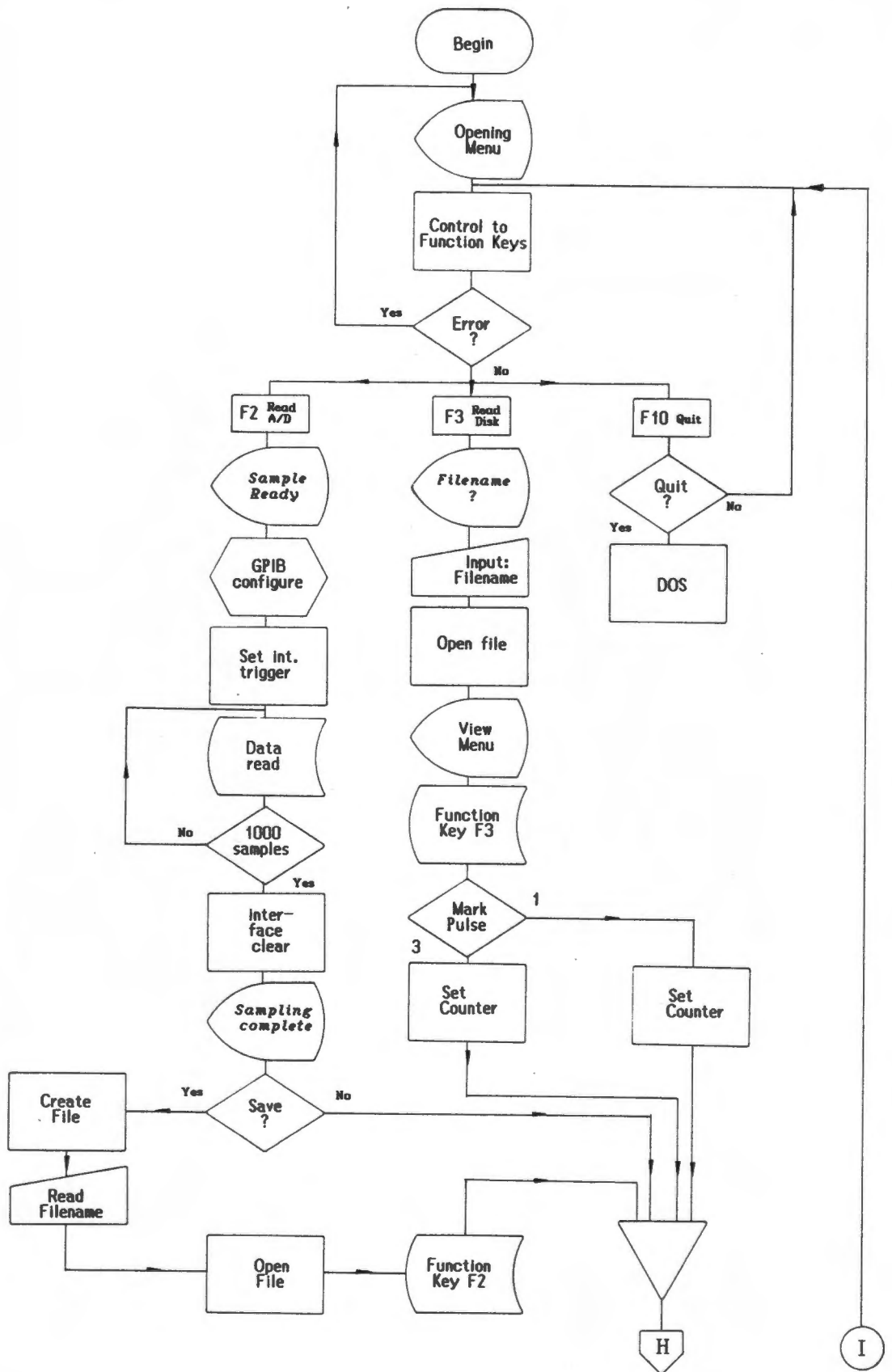


Figure E2.2

Flow-chart for the main subroutine for ANAL.THE

E2.2.2 The array scroller

With the display of the View Menu, the controls of the function keys are changed, thus leaving F6, F4 and F1 active. Function key F2 and F3 are inactive and thus striking these keys will elicit no response.

The flowchart of the view menu is given in figure E2.3.

Explanation of the function keys

Function key F4

This key activates the scroller and the keys required to manipulate the scrolling process. The keys are given in table E2.3.

Key	Function
Arrow up	Increases data point increment by a factor of two - faster scrolling
Arrow down	Decreases data point increment by a factor of two - slower scrolling
Arrow left	Scrolls the display window backward
Arrow right	Scrolls the display window forward
Home	Jumps the display window to the beginning of the data
End	Jumps the display window to the end of the data
Pg Up	Increases the horizontal expansion factor by two. Eight is the max.
Pg Dn	Decreases the horizontal expansion factor by two. One is the min.

Table E2.3

Scroll control keys

The scrolling may be halted at any time by depressing the <return> key once. The segment of data currently displayed on the screen relative to the complete data array is indicated by the

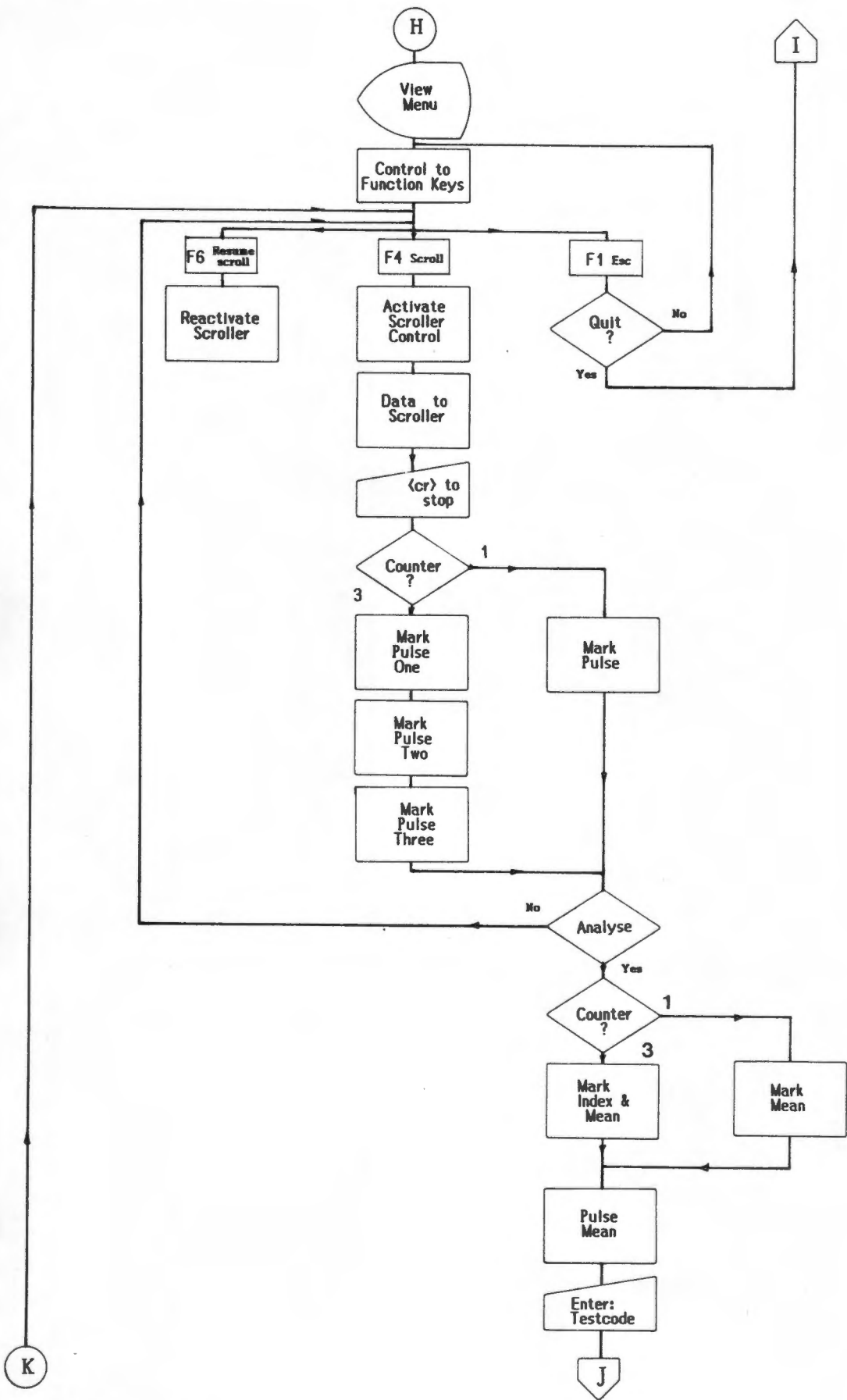


Figure E2.3

Flowchart of the view menu

arrows at the lower border of the scroll window - see figure E2.4. The indices (the index value of the first and last data value displayed on the screen) of the scroll window are given at the base of the scroll window. The numbers allow the user to establish an exact position within the data array.

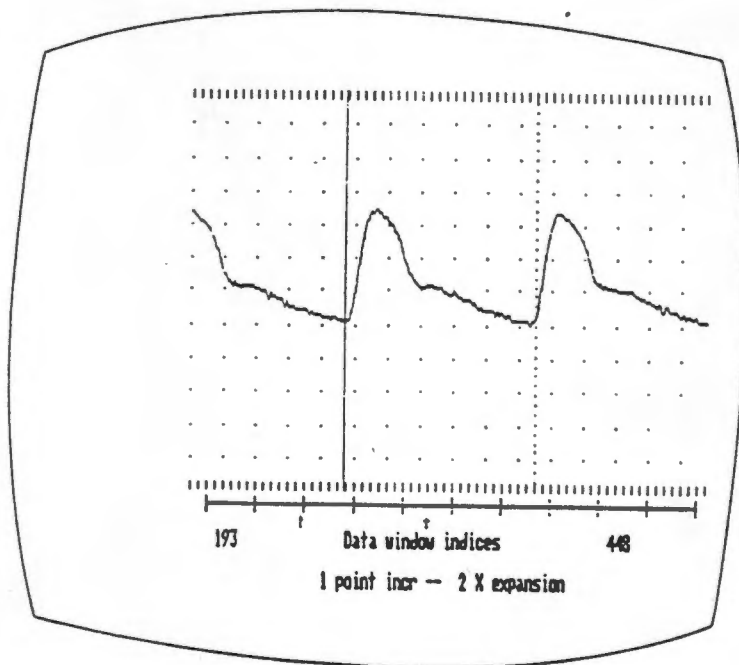


Figure E2.4

The scroll window of the program. The background matrix is used as a timing assistance - the time interval between two dots is 0.2 seconds.

Once the data scrolling was stopped by the <return> key, two vertical marker bars appear in the scroll window and these may be moved within the displayed segment of data by the function keys listed in table E2.4.

By depressing the <return> key for a second time once a particular pulse is marked, its indices (the begin and end index of the pulse within the data array) are stored. The user has the option of marking either one, three or five pulses. The default is set to three pulses. This option was created as to smooth out transient irregularities.

Key	Function
Arrow up	Increases the mark increment by a factor of two - number of data points that the marker jumps at each strike of the left or right arrow key.
Arrow down	Decreases the mark increment by a factor of two - number of data points that the marker jumps at each strike of the left or right arrow key.
Arrow left	Moves the active mark to the left
Arrow right	Moves the active mark to the right
Home	Displays the horizontal and vertical coordinate on the screen
End	Makes left mark active
Pg Dn	Makes right mark active

Table E2.4

Marker-bar control keys

The software establishes if the user wants the marked pulses analysed (by a message on the input/output window) and requires an input. The program will continue automatically to the next lower level, the analysis level, if (Yes) is typed.

Function key F6

This key activates the scroller without the option of marking a pulse or if the control of the scroller has been relinquished after the pulses had been marked.

Function key F1

Drops the current defined function keys and reinstates the function keys described for the main menu.

E2.2.3 The analysis routines

The analysis menu is displayed and the function keys defined in table E2.5 are placed onto the stack buffer. New function keys are activated and are listed below. The flowchart representing these routines is given in figure E2.5.

- | |
|--|
| <ul style="list-style-type: none">■ F1 Escape■ F7 Time analysis■ F8 Print■ F9 Frequency analysis■ F10 Quit |
|--|

Table E2.5

Active function keys for the Analysis Menu

Explanation of the function keys

Function key F1

Reinstates function keys defined in Section E2.2.

Function key F10

Terminates the program

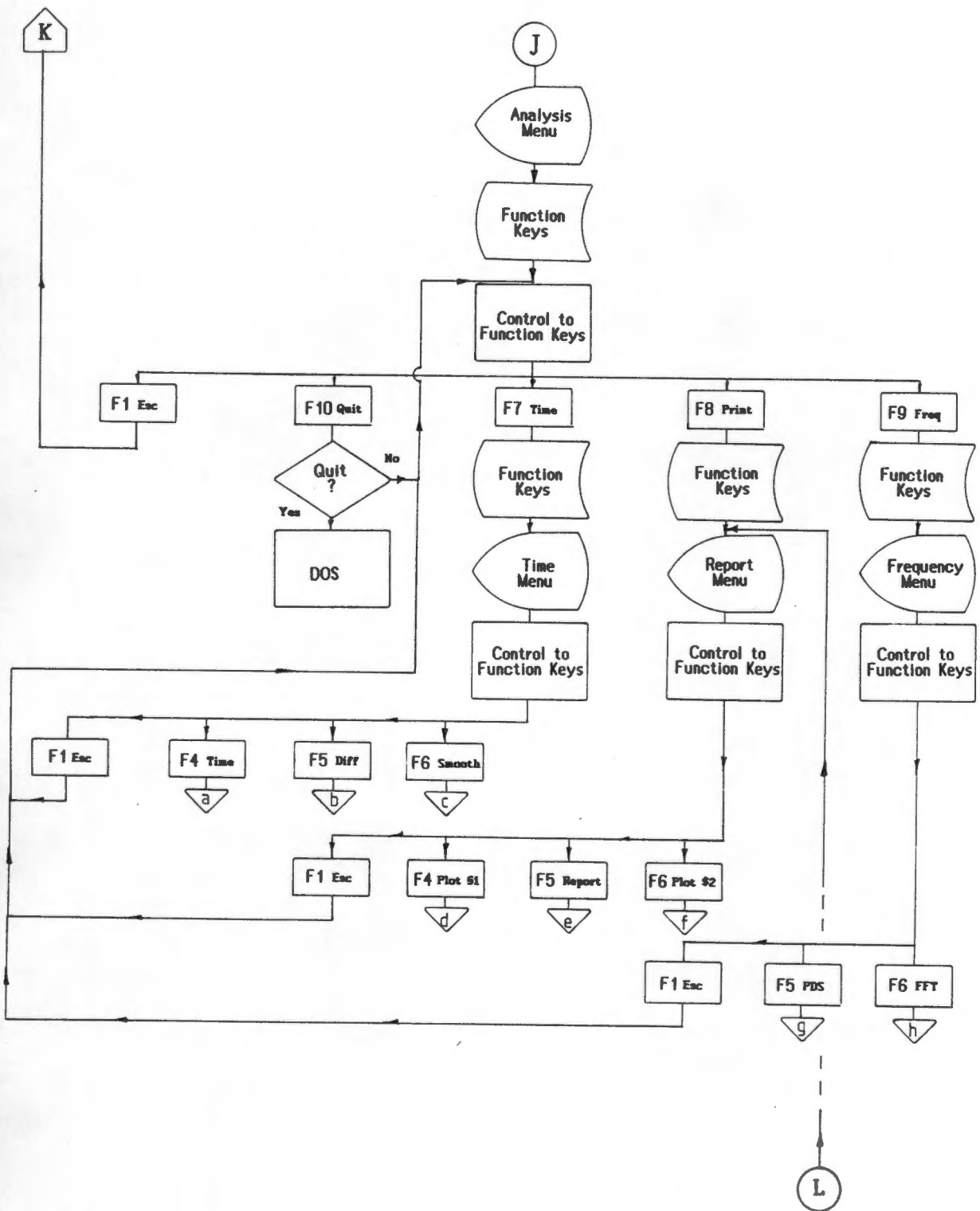


Figure E2.5

Flowchart for the analysis menu

Function key F7

Pressing this function key, the function keys listed under section E2.2.2 are placed on the stack buffer and the time menu (figure E2.6) is displayed. Ensuing active function keys are listed in table E2.6 and the flow chart is given in figure E2.7.

■ F1	Escape
■ F4	Time analysis
■ F5	Differentiate waveform
■ F6	Filter waveform
■ F10	Quit

Table E2.6

Active function keys for the time analysis

The user may escape to the analysis menu or continue with the time analysis. Selecting F4, the instruction window (figure E2.1) displays user information. The user must then mark sections of the blood pressure pulse (see Chapter A section 1.3) which is displayed with the control keys defined in table E2.7 as follows:

- 1) The end of the anacrotic wave
- 2) The end of the predicrotic wave
- 3) The start of the dicrotic wave
- 4) The dicrotic notch

Manual marking, by an expert in blood pressure waveform recognition, of the above mentioned components of the recorded blood pressure pulse was preferred to that by an automated

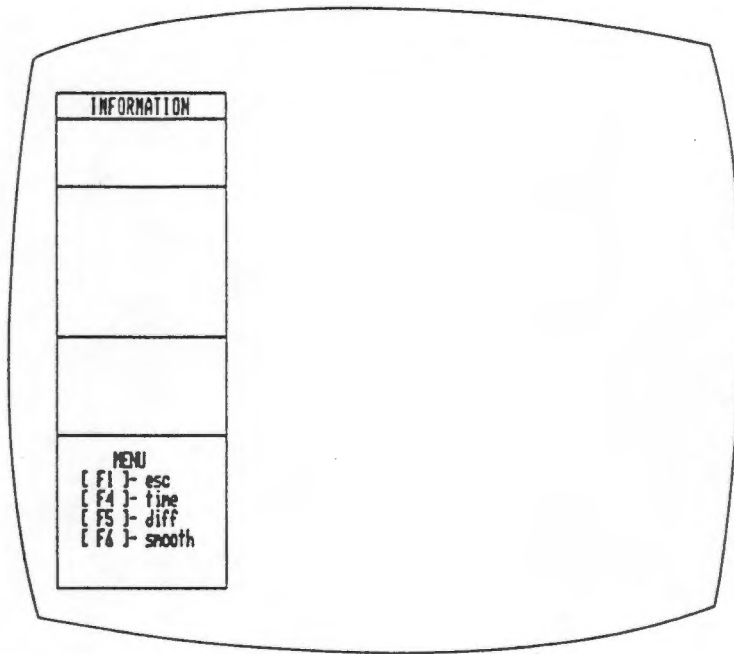


Figure E2.6

Screen display for the time menu

marking process in the software, as the variations of the blood pressure waveforms were excessive.

The peak systolic pressure, end diastolic pressure and the mathematical mean pressure however, were calculated automatically.

Function key F5 differentiates the blood pressure waveform and calculates the maximum value for the differentiated anacrotic wave (dp/dt maximum). Furthermore, a routine will establish if the maximum dp/dt value obtained was that of double peak blood pressure wave. If so, the user will be informed that the dp/dt

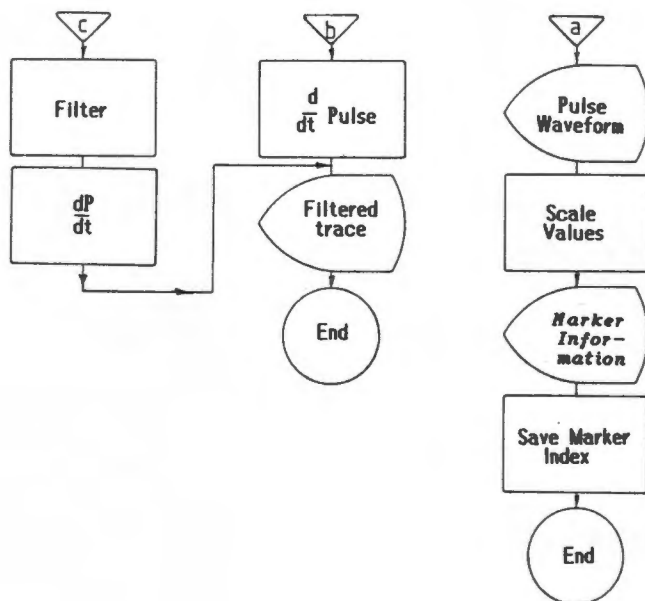


Figure E2.8

Flowchart of the time analysis program

value possibly is incorrect and the user may confirm his answer by pressing F6. This routine will activate the low-pass filter (default value: -3dB at 30 Hz) and the sampled data will be filtered (the double peak will be eliminated) before the differentiation process. The magnitude of the dp/dt value will be reduced for this filtered signal however, corresponding peaks for the filtered and non-filtered differentiated traces will indicate that the original dp/dt value was correct (see figure E2.9 in the lower trace). The program automatically determines this and proceeds without changing the dp/dt value and the original dp/dt values will be stored.

Key	Function
Arrow down	Allows motion of both marker lines with arrow keys
Arrow left	Moves either or both marker lines to the left
Arrow right	Moves either or both marker lines to the right
Home	Displays the x and y coordinates of the active marker on the screen
Pg Up	Sets the distance increment with which the arrow keys will move the marker Press once: min. increment value Press 4 times: max. increment value
Pg Dn	Activates right marker line only
End	Activates left marker line only
Del	Removes marker lines and inhibits the action of the control keys
Ins	Data between the two marker lines will be replotted in the current screen

Table E2.7

Editor-marker control keys

If the peaks do not correspond, the program will calculate the dp/dt value of the non-filtered, differentiated signal at the corresponding time instant for which the filtered, differentiated signal had its maximum dp/dt value. The initial dp/dt value is discarded and the new value is stored.

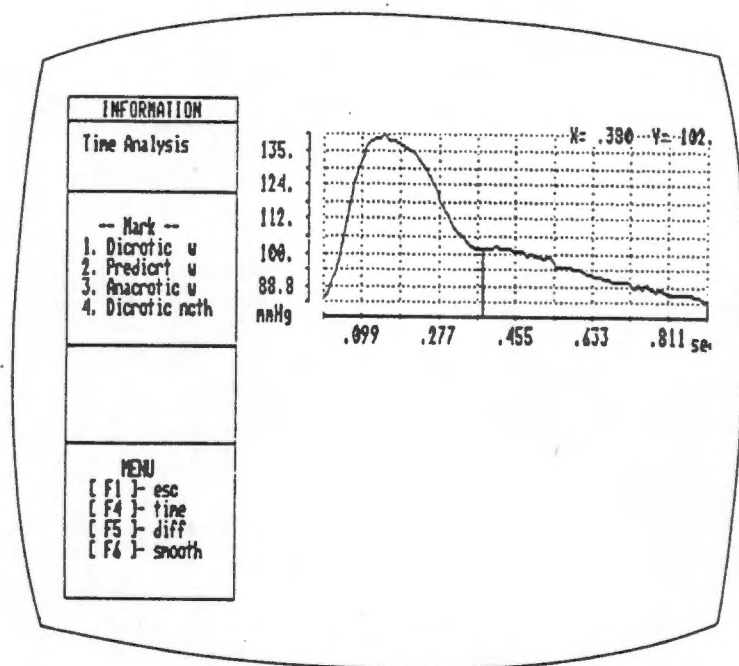


Figure E2.8

Time analysis information window. The blood pressure waveform and the marker bars are displayed.

This procedure may also necessary if the recorded data is extremely 'noisy'.

The graphical representation of the results is indicated on the screen (as shown in figure E2.10).

Depressing F1 will return the user to the analysis menu.

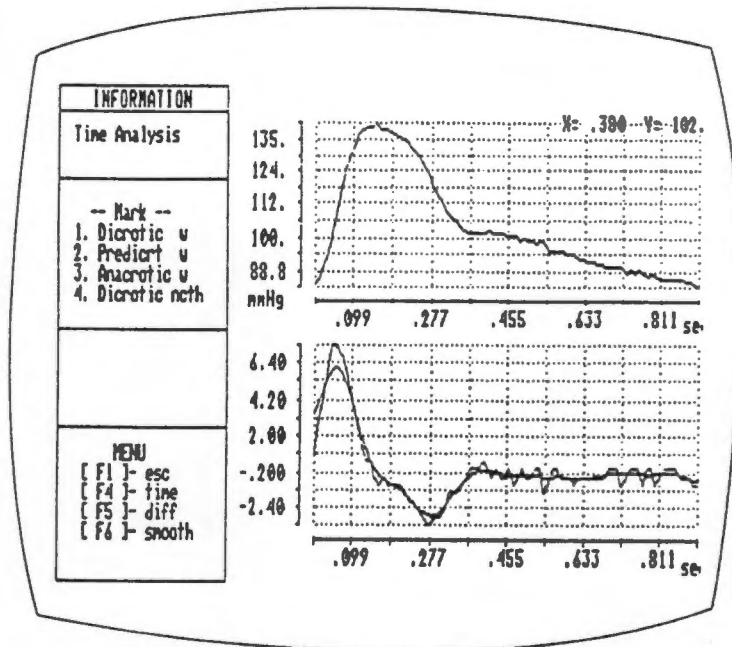


Figure E2.9

Screen display of the time analysis results. The upper trace represents the un-filtered blood pressure waveform. The lower trace displays the filtered and un-filtered differentiated traces.

Function Key F9

Selecting function key F9, the frequency domain analysis menu (figure E2.10) will be displayed and the function keys listed in table E2.8 will be activated.

■	F1	Escape
■	F5	Power density spectrum
■	F6	Fast Fourier transform
■	F10	Quit

Table E2.8

Active function keys for the frequency domain analysis

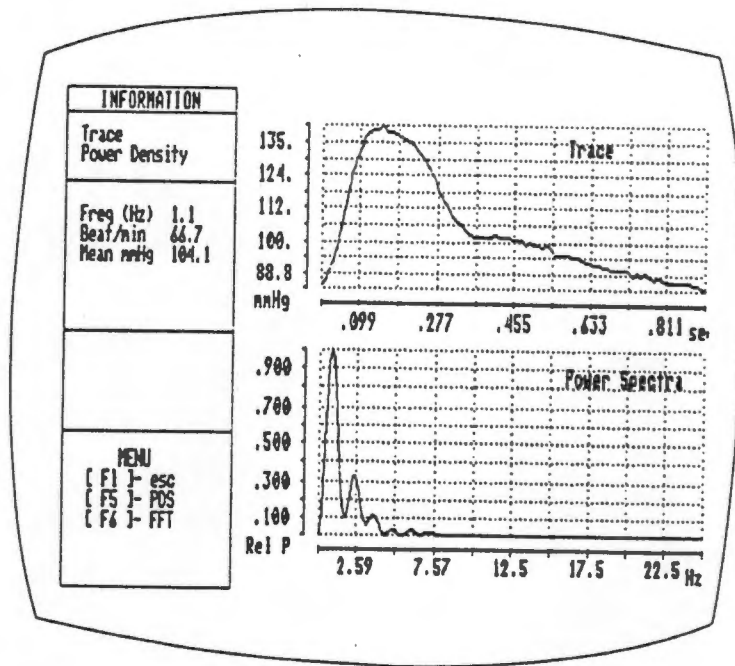


Figure E2.10

Frequency analysis menu and a Power Density Spectra display

F6 will calculate the Fast Fourier Transform of the blood pressure waveform, while F5 will calculate the Power Density Spectrum of the signal. Fast Fourier Transforms and harmonic analysis results are shown in figure E2.11.

The flowchart of the frequency domain analysis is given in figure E2.12 and F1 returns the user to the analysis menu.

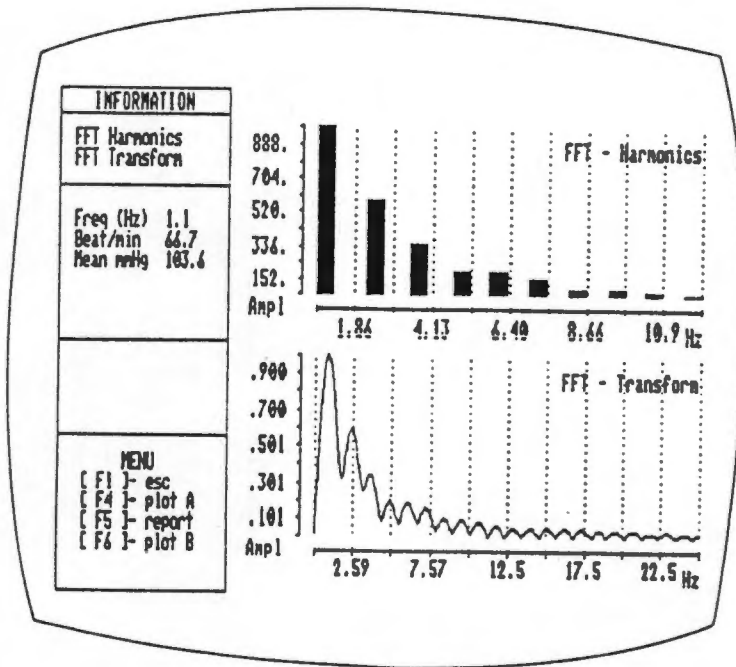


Figure E2.11

Screen display for frequency domains results

Function key F8

Hard copies of the results may be made by selecting function key F8. Table E2.9 lists the active function keys while in figure E2.13 the flowchart of the printer routines is given.

■	F1	Escape
■	F4	Plot page #1
■	F5	Print report
■	F6	Plot page #2

Table E2.9

Active function keys for the printer routines

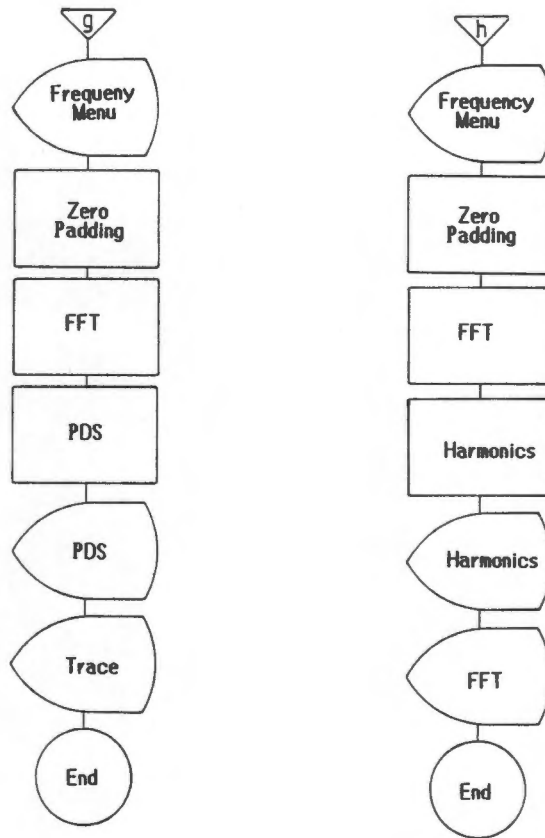


Figure E2.12

Flow chart of the frequency domain subroutines.

The in/out window will indicate the status of the printer and the plotter. An example of a report (function key F5) is shown in Figure E2.14, while selecting function key F4 and F6 will produce a page of results as given in Appendix E3.

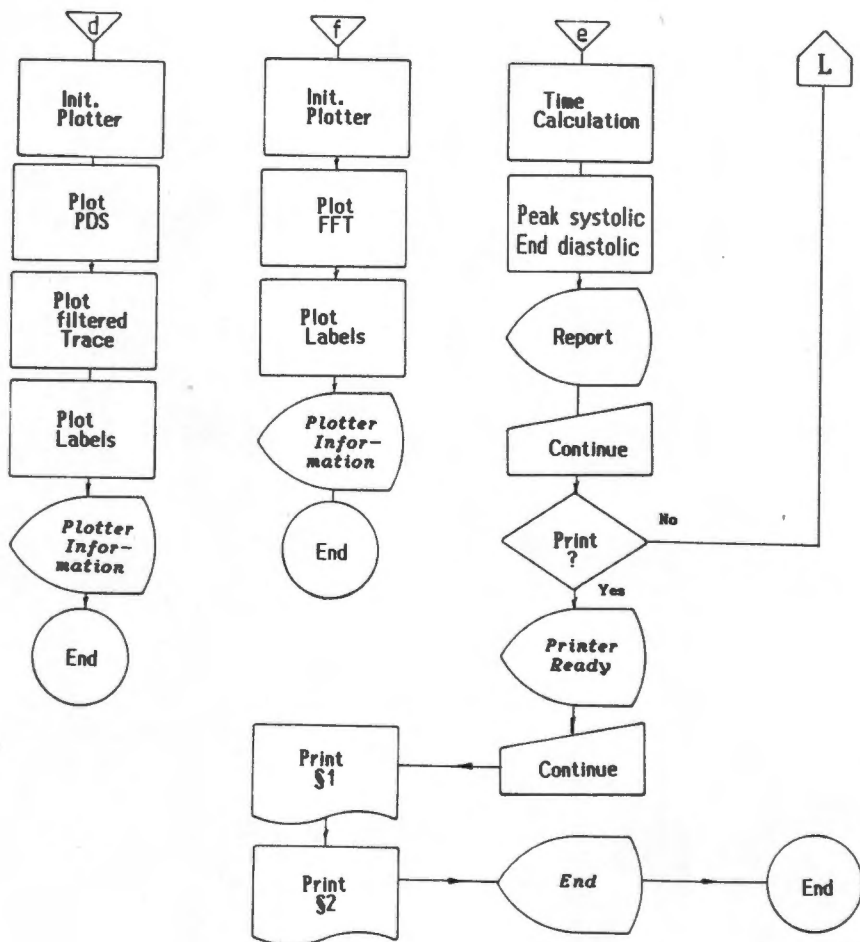


Figure E2.13

Flowchart of the printer routines.

ANALYSIS RESULTS

Predicrotic wave was marked

Filename : NU12068	Beats/min	66.67
Date : 06/14/88	Mean Pressure	103.58
Time : 14:06:13.94	dp/dt max	.00
Catheter : 00004	End Diastolic Pressure	1.35

Timing Results (seconds)

Wave/Event	Duration	Delay
Aortic wave	.14	--
Predicrotic wave	.20	.14
Dicrotic wave	.04	.34

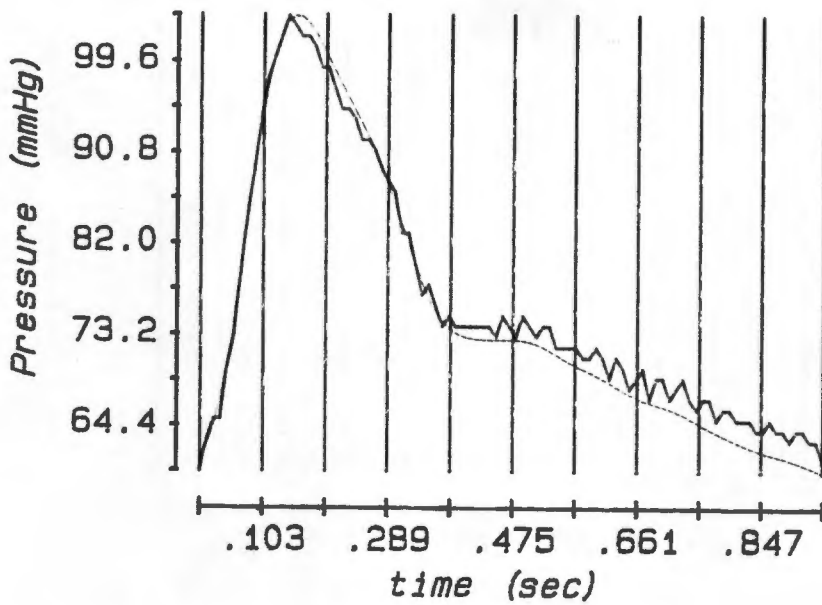
Event	Delay	Pressure (mmHg)
Systolic pulse	.16	137.58
Diastolic pulse	--	85.00
Dicrotic notch	.38	102.00

To continue - (space)

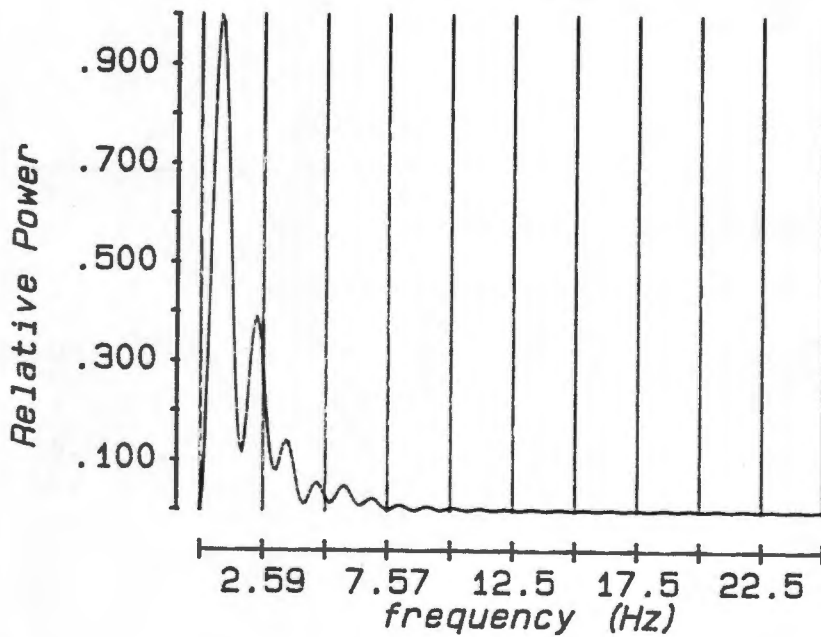
Figure E2.14

Example of a report of the time analysis screen page.

E3 Example of the hard-copy presentation.



a) Pulse shape



b) Power Spectra

Figure a: Pulse Characteristics

Beats/min	-	63.8
Systolic Peak Pressure (mmHg)	-	101.7
Diastolic Pressure (mmHg)	-	60.0
Mean Pressure (mmHg)	-	76.2
dp/dt maximum	-	261.1

Figure b: Power Density Characteristics

Maximum Signal Power at (Hz)	-	.9
------------------------------	---	----

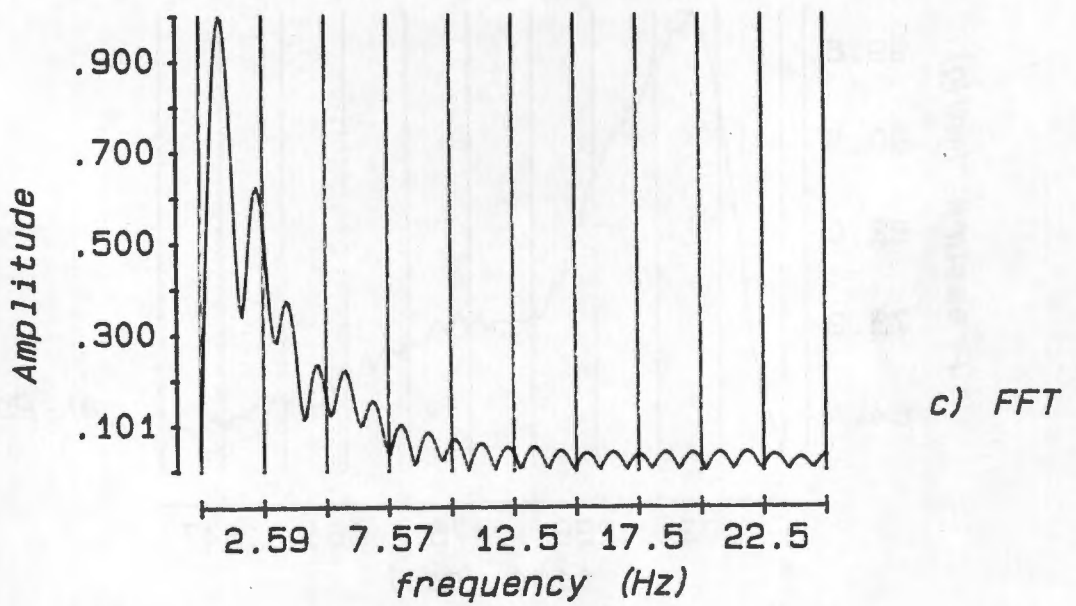
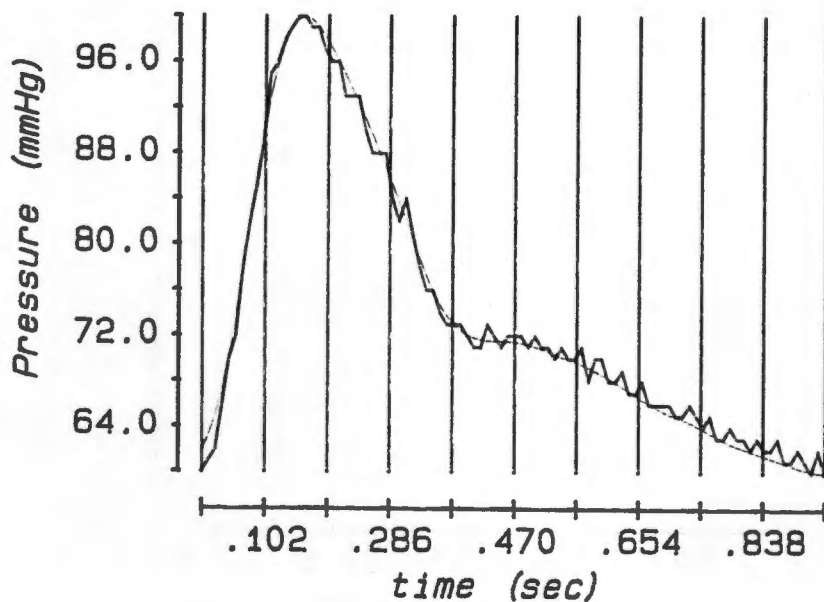


Figure c: Fast Fourier Transforms

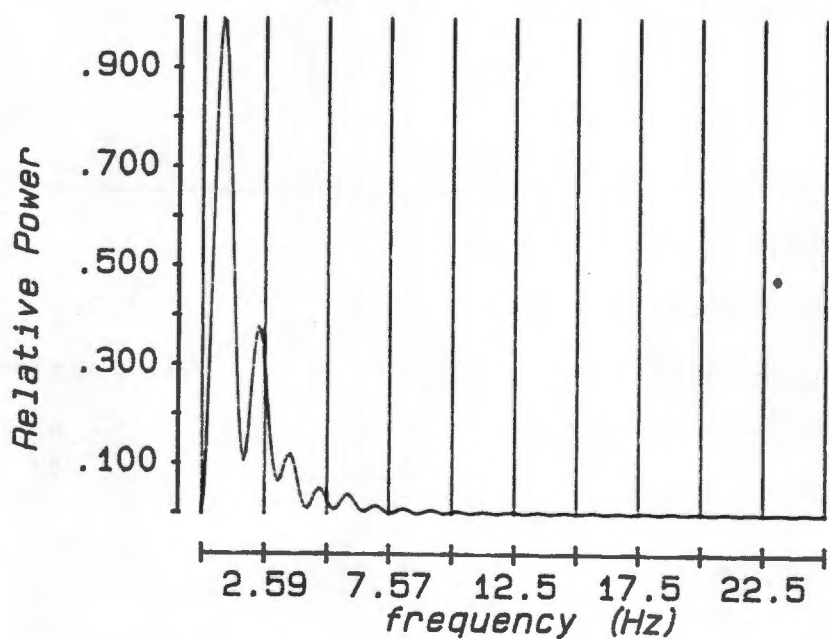
Harmonics at	Herz	Rel	Amplitude
	.88		1.00
	2.34		.62
	3.52		.37
	4.79		.23
	5.86		.22
	6.93		.15
	8.11		.10
	9.18		.08
	10.16		.07

Percentage decrease of Amplitude in successive Harmonics calculated from the highest relative Amplitudes

38. 25. 14. 1. 7. 5.



a) Pulse shape



b) Power Spectr

Figure a: Pulse Characteristics

Beats/min	-	64.5
Systolic Peak Pressure (mmHg)	-	98.7
Diastolic Pressure (mmHg)	-	60.0
Mean Pressure (mmHg)	-	74.1
dp/dt maximum	-	734.1

Figure b: Power Density Characteristics

Maximum Signal Power at (Hz)	-	.9
------------------------------	---	----

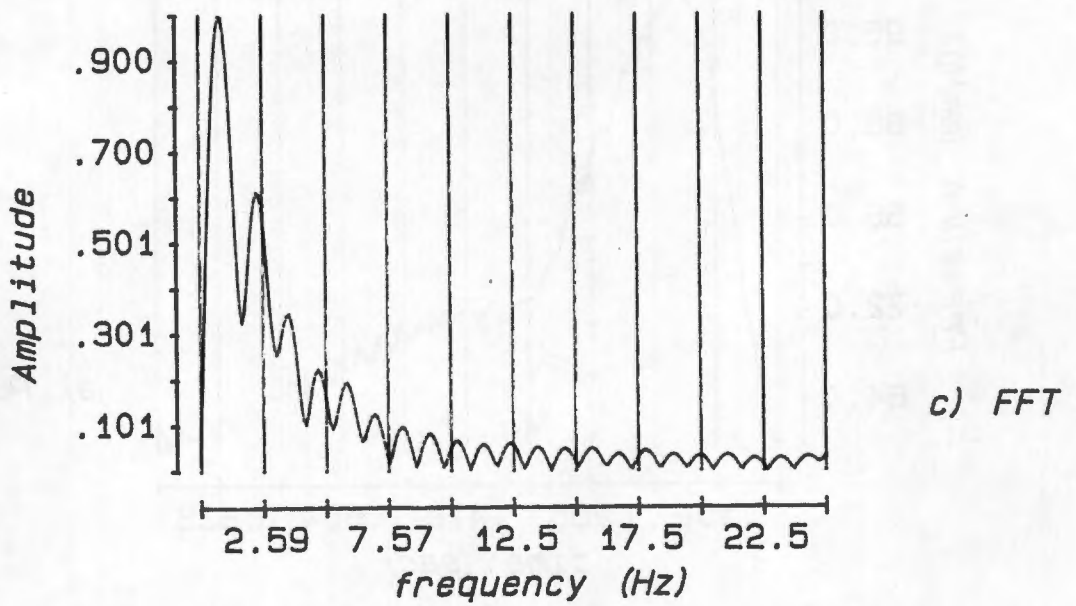


Figure c: Fast Fourier Transforms

Harmonics	at	Herz	Rel	Amplitude
		.88		1.00
		2.34		.61
		3.61		.35
		4.79		.22
		5.96		.19
		7.03		.13
		8.11		.10
		9.28		.08
		10.35		.07

Percentage decrease of Amplitude in successive Harmonics calculated from the highest relative Amplitudes

39. 27. 12. 3. 7. 3.

APPENDIX F

PROGRAM LISTING

CONTENTS

F1.1	Program listing of MEAS.THE	F2
F1.2	Program listing of ANAL.THE	F24

Appendix F1.1

Listing of program: MEAS.THE

CATHETER AND PRESSURE TUBING ANALYSING PROGRAM

P.A. HEIMANN

This program is designed to receive data manually from the keyboard, plot and analyse it. The data must be real. The entered data can be stored on disk. Stored data can be retrieved and analysed. Analysis include; Least Square Fit Damping calculations, Frequency response calculation , Mean and variance calculations.

Results can be viewed, printed and/or plotted

Version 1.00
February 1988
Cape Town

Variable definitions

INTEGER SCALAR MAXPAIRS
REAL SCALAR MAXSETS
20 MAXPAIRS :=
2 MAXSETS :=

REAL DIM[MAXPAIRS] ARRAY NEW.INDEX
REAL DIM[MAXPAIRS] ARRAY XVALUE
REAL DIM[MAXPAIRS] ARRAY XVALUE1
REAL DIM[MAXPAIRS] ARRAY XVALUE2
REAL DIM[MAXPAIRS] ARRAY XVALUE3
REAL DIM[MAXPAIRS] ARRAY TEST1
REAL DIM[MAXPAIRS] ARRAY TEST2
REAL DIM[MAXPAIRS] ARRAY TEST3
REAL DIM[MAXPAIRS , MAXSETS] ARRAY INDEX
DIM[3] ARRAY HOLDIT

REAL SCALAR DEVIATION1
REAL SCALAR DEVIATION2
REAL SCALAR DEVIATION3
REAL SCALAR TOP
REAL SCALAR MANY

SCALAR #PAIRS
SCALAR DAMP.ONE
SCALAR DAMP.TWO
SCALAR DAMP.THREE
SCALAR DAMPING.FACTOR
SCALAR TOP.FREQUENCY
SCALAR TOP.FREQUENCY.ONE
SCALAR TOP.FREQUENCY.TWO
SCALAR TOP.FREQUENCY.THREE

14 STRING FILENAME
30 STRING MAKE
30 STRING IND
35 STRING TITLE
25 STRING #EXP

Window size definitions

0 0 1 79 WINDOW {TOPLINE}
2 0 2 70 WINDOW {TWOLINE}
16 0 16 79 WINDOW {DESCRIB}
18 0 18 79 WINDOW {DNF}
20 0 20 79 WINDOW {DF}
24 0 24 79 WINDOW {BOTLINE}
22 0 22 79 WINDOW {MENULINE}
23 0 23 79 WINDOW {MENULINE2}
14 25 20 55 WINDOW {INFO}
10 0 20 79 WINDOW {SHOW.DIR}

Set screen area, axis, tick and spacing

: DATA.VU
.270 .500 VUPOINT.ORIG
.730 .450 VUPOINT.SIZE
HORIZONTAL AXIS.FIT.OFF
VERTICAL AXIS.FIT.OFF
.180 .210 AXIS.ORIG
.800 .740 AXIS.SIZE
.025 .008 TICK.SIZE
.5 .8 TICK.JUST
;

Set plotting area

: DATA.VU.SET
XVALUE SUB[1 , #PAIRS]
NEW.INDEX SUB[1 , #PAIRS]
OVER
OVER WORLD.COORDS
[]MIN/MAX VERTICAL WORLD.SET
[]MIN/MAX HORIZONTAL WORLD.SET
[]MIN SWAP []MIN SWAP WORLD.COORDS AXIS.POINT
HORIZONTAL LOGARITHMIC
;

Clear Function keys of current function

```
: CLEAR.FKEYS
  133 0 DO
    I FUNCTION.KEY.DOES NOP
  LOOP
;
```

Set colour and position of Function keys on screen

```
: HELP.MESSAGE.DISPLAY
  NORMAL.DISPLAY SCREEN.CLEAR
  {SHOW.DIR}
  0 BACKGROUND 14 FOREGROUND
;
```

Main Menu

```
: MAIN.MENU
  {DEF}
  SCREEN.CLEAR
  {MENULINE}
  SCREEN.CLEAR 27 SPACES
  2 BACKGROUND 0 FOREGROUND
  ." ***** Main Menu *****"
  {BOTLINE}
  CURSOR.OFF
  SCREEN.CLEAR INTEN.ON 6 SPACES
  1 BACKGROUND 15 FOREGROUND
  ." F1) Quit F7) Enter Data "
  ." F8) Read Data F9) Directory F5) Help "
;
```

Plotting Menu

```
: GRAPH.MENU
  NORMAL.DISPLAY {DEF} SCREEN.CLEAR
  {DF} SCREEN.CLEAR 2 BACKGROUND 0 FOREGROUND
  22 SPACES
  ." ***** Plotting Menu *****"
  {MENULINE} SCREEN.CLEAR 1 BACKGROUND 15 FOREGROUND
  3 SPACES
  ." F(2) View All F(3) View Mean F(4) Print Report F(5) Help Menu
  {MENULINE2} SCREEN.CLEAR 1 BACKGROUND 15 FOREGROUND
  10 SPACES
  ." F(6) Plot Mean F(7) Plot All F(10) Main Menu
  CURSOR.OFF
;
```

Help Menu

```
: GRAPH.HELP
  HELP.MESSAGE.DISPLAY
    CR 22 SPACES
    ." ***** Help Menu ***** "
    CR 7 SPACES
    ." F(2) plot's all the data traces on screen. F(3) plots the " CR
    7 SPACES
    ." mean value on the screen. You are permitted to toggle between " CR
    7 SPACES
    ." F(2) and F(3). F(4) prints a detailed report for one file. " CR
    7 SPACES
    ." F(5) plots the mean data trace and F(6) plots all traces in " CR
    7 SPACES
    ." different colours. " CR CR 7 SPACES
    ." Type <Space> to return to 'Plot Menu' "
  CURSOR.OFF
  PCKEY ?DROP DROP
  GRAPH.MENU
```

This routine displays the results on the screen

```
: SHOW.SPECS
  {DF} SCREEN.CLEAR
  3 SPACES
  ." Damping Factor : " 2 SPACES DAMPING.FACTOR .
  {DNF} SCREEN.CLEAR
  3 SPACES
  ." Damped Natural Freq. : " 2 SPACES TOP.FREQUENCY .
  {DESCRIB} SCREEN.CLEAR
  3 SPACES
  ." Title : " 2 SPACES TITLE "TYPE
```

User instruction

```
: TO.CONTINUE
  {MENULINE}
  20 SPACES
  ." <Space> to continue..... "
  BELL PCKEY
  ?DROP
  DROP
  GRAPH.MENU
```

These routines plot the mean values of the traces

```
: PLOTT1
    TEST1
    NEW.INDEX :=
;

: PLOTT2
    TEST1
    TEST2 +
    2 /
    NEW.INDEX :=
;

: PLOTT3
    TEST1
    TEST2 +
    TEST3 +
    3 /
    NEW.INDEX :=
;

: ADD.CATH
    GRAPHICS.DISPLAY
    DATA.VU
    VUPORT.CLEAR
    DATA.VU.SET
    XY.AXIS.PLOT
    MANY 1 =
    IF PLOTT1
    ELSE
    MANY 2 =
    IF PLOTT2
    ELSE
    MANY 3 =
    IF PLOTT3
    THEN
    THEN
    THEN
    NEW.INDEX SUB[ 1 , #PAIRS ]
    XVALUE SUB[ 1 , #PAIRS ] SWAP
    XY.DATA.PLOT
    OUTLINE
    SHOW.SPECS
    TO.CONTINUE
;
```

These routines plot the individual traces

```
: PLOT1
    XVALUE1 SUB[ 1 , #PAIRS ]
    TEST1 SUB[ 1 , #PAIRS ]
    2 COLOR
    XY.DATA.PLOT
;
```

```
: PLOT2
  PLOT1
  XVALUE2 SUB[ 1 , #PAIRS ]
  TEST2 SUB[ 1 , #PAIRS ]
  3 COLOR
  XY.DATA.PLOT
```

;

```
: PLOT3
  PLOT1
  PLOT2
  XVALUE3 SUB[ 1 , #PAIRS ]
  TEST3 SUB[ 1 , #PAIRS ]
  4 COLOR
  XY.DATA.PLOT
```

;

```
: PLOT.SAVED.GRAPH
  GRAPHICS.DISPLAY
  DATA.VU
  VUPORT.CLEAR
  DATA.VU.SET
  1 COLOR
  XY.AXIS.PLOT
  MANY 1 =
  IF
  PLOT1
  ELSE
  MANY 2 =
  IF
  PLOT2
  ELSE
  MANY 3 =
  IF
  PLOT3
  THEN
  THEN
  THEN
  OUTLINE
  SHOW.SPECS
  TO.CONTINUE
```

;

These routines represent analysis calculations

```
: DAMPING
  20 /
  10 SWAP **
  2 **
  INV 1 SWAP
  -
  SQRT 1 SWAP -
  2 /
  SQRT
  DAMPING.FACTOR :=
```

;

```

: AVER1
  STACK.CLEAR
  XVALUE1 XVALUE :=
  TEST1
  DUP
  NEW.INDEX :=
  XVALUE SUB[ 1 , #PAIRS ]
  NEW.INDEX SUB[ 1 , #PAIRS ]
  1 SET.#.OPTIMA
  5 SET.#.POINTS
  LOCAL.MAXIMA
  DAMPING
  REAL TOP :=
  XVALUE [ TOP ]
  TOP.FREQUENCY :=
;

```

```

: AVER2
  STACK.CLEAR
  XVALUE1 XVALUE2 +
  2 /
  XVALUE :=
  TEST1 TEST2 +
  2 /
  DUP
  NEW.INDEX :=
  XVALUE SUB[ 1 , #PAIRS ]
  NEW.INDEX SUB[ 1 , #PAIRS ]
  1 SET.#.OPTIMA
  5 SET.#.POINTS
  LOCAL.MAXIMA
  DAMPING
  REAL TOP :=
  XVALUE [ TOP ]
  TOP.FREQUENCY :=
;

```

```

: AVER3
  STACK.CLEAR
  XVALUE1 XVALUE2 + XVALUE3 +
  3 /
  XVALUE :=
  TEST1 TEST2 + TEST3 +
  3 /
  DUP
  NEW.INDEX :=
  XVALUE SUB[ 1 , #PAIRS ]
  NEW.INDEX SUB[ 1 , #PAIRS ]
  1 SET.#.OPTIMA
  5 SET.#.POINTS
  LOCAL.MAXIMA
  DAMPING
  REAL TOP :=
  XVALUE [ TOP ]
  TOP.FREQUENCY :=
;

```

Report printing routines

: AVERAGE

CR CR

." Mean " CR

." Frequency dB "

CR

." _____ "

CR

#PAIRS 1 + 1 DO

 NEW.INDEX [I]

 XVALUE [I]

 . 18 ?COL - SPACES . CR

 LOOP

 CR CR CR

." _____ "

CR

." The Damped Natural Frequency in (Hz) is " TOP.FREQUENCY . CR CR

." The damping factor " DAMPING.FACTOR .

CR

." _____ "

CR

;

: HOW.PRINT1

CR CR

." Test 1 " CR

." Frequency dB "

CR

." _____ "

CR CR

#PAIRS 1 + 1 DO

 TEST1 [I]

 XVALUE1 [I]

 . 19 ?COL - SPACES . CR

 LOOP

;

: HOW.PRINT2

CR CR

." Test 2 " CR

." Frequency dB "

CR

." _____ "

CR CR

#PAIRS 1 + 1 DO

 TEST2 [I]

 XVALUE2 [I]

 . 19 ?COL - SPACES . CR

 LOOP

;

```

: HOW.PRINT3
  CR CR
  ."      Test 3      "
  CR
  ." Frequency      dB  "
  CR
  ." _____ "
  CR CR
  #PAIRS 1 + 1 DO
  TEST3 [ | ]
  XVALUE3 [ | ]
  . 19 ?COL - SPACES . CR
  LOOP

```

```

: REPORT
  NORMAL.DISPLAY SCREEN.CLEAR
  {MENULINE} SCREEN.CLEAR
  5 SPACES
  2 BACKGROUND 0 FOREGROUND
  ." Report Printing "
  {BOTLINE} SCREEN.CLEAR
  1 BACKGROUND 15 FOREGROUND
  ." <cr> when printer ready ... " BELL
  PCKEY
  ?DROP
  SCREEN.CLEAR
  OUT>PRINTER
  18 SPACES ." Catheter Analysis " CR CR
  ." _____ "
  CR CR
  6 SPACES ." Date: " .DATE 9 SPACES ." Time: " .TIME CR
  6 SPACES ." Experiment name: " TITLE "TYPE CR
  6 SPACES ." Experiment No. : " #EXP "TYPE CR
  6 SPACES ." Make: " MAKE "TYPE 19 SPACES ." ID : " IND "TYPE CR
  CR
  ." _____ "
  CR

```

```

MANY 1 =
IF HOW.PRINT1
  AVERAGE
ELSE

```

```

MANY 2 =
IF HOW.PRINT1
  HOW.PRINT2
  CR CR CR CR CR CR CR CR CR CR CR
  AVERAGE
ELSE

```

```

MANY 3 =
  IF HOW.PRINT1
    HOW.PRINT2
    CR CR CR CR CR CR CR CR CR CR CR
    HOW.PRINT3
    AVERAGE
  THEN
  THEN
  THEN
  CONSOLE
  CR ." Press any key to continue."
  PCKEY ?DROP DROP
  SCREEN.CLEAR
  GRAPH.MENU
;

```

Plotter control subroutines

```

: PLOTTER.INFORMATION
  STACK.CLEAR
  {DEF} NORMAL.DISPLAY
  SCREEN.CLEAR
  {BOTLINE}
  3 SPACES 1 BACKGROUND 15 FOREGROUND
  ." Plotter must be ready ..... type any key " BELL
  PCKEY
  ?DROP DROP
;

```

```

: GIVE.DESCRPTION
  10. SLANT
  1 COLOR
  NORMAL.COORDS
  0.018 0.6 POSITION
  " dB" LABEL
  0.40 0.07 POSITION
  " Frequency x 10 (Hz)" LABEL
;

```

```

: SCREEN2.VIEW
  PLOTTER.INFORMATION
  GRAPHICS.DISPLAY
  HP7440
  DATA.VU
  VUPORT.CLEAR
  DATA.VU.SET
  1 COLOR
  XY.AXIS.PLOT
  GIVE.DESCRPTION
;

```

: NUMBER.OF.PLOTT

MANY 1 =

IF PLOTT1

ELSE

MANY 2 =

IF PLOTT2

ELSE

MANY 3 =

IF PLOTT3

THEN

THEN

THEN

1 COLOR

OUTLINE

CURSOR.OFF

;

: NUMBER.OF.PLOT

MANY 1 =

IF PLOT1

ELSE

MANY 2 =

IF PLOT2

ELSE

MANY 3 =

IF PLOT3

THEN

THEN

THEN

1 COLOR

OUTLINE

CURSOR.OFF

;

: TO.PLOT.AVERAGE

SCREEN2.VIEW

STACK.CLEAR

DATA.VU

VUPORT.CLEAR

DATA.VU.SET

NUMBER.OF.PLOTT

NEW.INDEX SUB[1 , #PAIRS]

XVALUE SUB[1 , #PAIRS] SWAP

XY.DATA.PLOT

GRAPH.MENU

;

: TO.PLOT.ALL

SCREEN2.VIEW

STACK.CLEAR

DATA.VU

VUPORT.CLEAR

DATA.VU.SET

NUMBER.OF.PLOT

GRAPH.MENU

;

This section presents the opening banner of the program

```
: BANNER
  GRAPHICS.DISPLAY
  CURSOR.OFF
  {TOPLINE} SCREEN.CLEAR
  20 SPACES
  ." Catheter Data Analysis Program "
  {TWOLINE}
  28 SPACES
  ." P. A. Heimann "
  {MENULINE} 27 SPACES
  ." <Space> to continue ... "
  PCKEY ?DROP DROP
  NORMAL.DISPLAY
;
```

Subroutine that define the control of function keys

```
: GRAPH.KEYS
  F3 FUNCTION.KEY.DOES PLOT.SAVED.GRAPH
  F2 FUNCTION.KEY.DOES ADD.CATH
  F4 FUNCTION.KEY.DOES REPORT
  F6 FUNCTION.KEY.DOES TO.PLOT.AVERAGE
  F7 FUNCTION.KEY.DOES TO.PLOT.ALL
  F5 FUNCTION.KEY.DOES GRAPH.HELP
;
```

This routine controls the printing of the file

```
: ANSWER.PRINT
  SCREEN.CLEAR
  GRAPH.KEYS
  GRAPH.MENU
  INTERPRET.KEYS
;
```

Data read Menu

```
: DATA.MENU
  {BOTLINE}
  SCREEN.CLEAR 3 SPACES
  1 BACKGROUND
  15 FOREGROUND
  ." F1) Quit  F6) Save Data  F10) Main Menu "
  CURSOR.OFF
;
```

File management routines

: CREATE.DATA.FILE

FILE.TEMPLATE

4 COMMENTS

INTEGER DIM[3] SUBFILE

REAL DIM[MAXPAIRS] SUBFILE

6 TIMES

END

CR ." Name of file to create ? "

"INPUT FILENAME " :=

FILENAME DEFER> FILE.CREATE

;

: WRITE.DATA.FILE

FILENAME DEFER> FILE.OPEN

TITLE 1 >COMMENT

MAKE 2 >COMMENT

IND 3 >COMMENT

#EXP 4 >COMMENT

#PAIRS HOLDIT [1] :=

MAXSETS HOLDIT [2] :=

MANY HOLDIT [3] :=

1 SUBFILE HOLDIT ARRAY>FILE

2 SUBFILE XVALUE1 ARRAY>FILE

3 SUBFILE XVALUE2 ARRAY>FILE

4 SUBFILE XVALUE3 ARRAY>FILE

5 SUBFILE TEST1 ARRAY>FILE

6 SUBFILE TEST2 ARRAY>FILE

7 SUBFILE TEST3 ARRAY>FILE

FILE.CLOSE

ONERR:

{BOTLINE} SCREEN.CLEAR

." Can't open file.... <Space> to continue. " BELL PCKEY ?DROP DROP

?FILE.OPEN IF FILE.CLOSE THEN

;

: STORE.DATA

{BOTLINE}

SCREEN.CLEAR

1 BACKGROUND

15 FOREGROUND

CREATE.DATA.FILE

CR ." Creating - " FILENAME "TYPE

WRITE.DATA.FILE

DATA.MENU

INTERPRET.KEYS

;

Data read menu

```
: DATA.READ.MENU
{DEF} SCREEN.CLEAR CURSOR.OFF
{MENULINE} SCREEN.CLEAR 2 BACKGROUND 0 FOREGROUND
22 SPACES
." ***** Data Read Menu *****"
{BOTLINE}
SCREEN.CLEAR 1 BACKGROUND 15 FOREGROUND 3 SPACES
." F(1) Quit F(2) Analyse F(4) Read F(5) Help Menu "
." F(6) Print/Plot "
```

These subroutines control the data reading process

```
: GET.SAVED.FILE
FILENAME DEFER> FILE.OPEN
1 COMMENT> TITLE :=
5 SUBFILE TEST1 FILE>ARRAY
2 COMMENT> MAKE :=
6 SUBFILE TEST2 FILE>ARRAY
3 COMMENT> IND :=
7 SUBFILE TEST3 FILE>ARRAY
4 COMMENT> #EXP :=
1 SUBFILE HOLDIT FILE>ARRAY
HOLDIT [ 1 ] #PAIRS :=
HOLDIT [ 2 ] MAXSETS :=
HOLDIT [ 3 ] MANY :=

2 SUBFILE XVALUE1 FILE>ARRAY
3 SUBFILE XVALUE2 FILE>ARRAY
4 SUBFILE XVALUE3 FILE>ARRAY
FILE.CLOSE
ONERR:
{BOTLINE} SCREEN.CLEAR
." Can't open file.... <Space> to continue ." BELL PCKEY ?DROP DROP
?FILE.OPEN IF FILE.CLOSE THEN
```

```
: GET.FILENAME
{BOTLINE} SCREEN.CLEAR 1 BACKGROUND 15 FOREGROUND
2 SPACES
CR ." Filename of data file: " "INPUT
FILENAME :=
GET.SAVED.FILE
DATA.READ.MENU
```

These subroutines determine variance, mean and frequency response

```
: FULL.TEST1
  XVALUE1 SUB[ 1 , #PAIRS ]
  TEST1 SUB[ 1 , #PAIRS ]
    1 SET.#.OPTIMA
    5 SET.#.POINTS
    LOCAL.MAXIMA
      DAMPING
      DAMPING.FACTOR
      DAMP.ONE :=
    REAL TOP :=
    XVALUE1 [ TOP ]
  TOP.FREQUENCY.ONE :=
  NEW.INDEX SUB[ 1 , #PAIRS ]
  TEST1 SUB[ 1 , #PAIRS ] -
  WITHOUT.FREQUENCIES VARIANCE
  DEVIATION1 :=
```

```
;
: FULL.TEST2
  FULL.TEST1
  XVALUE2 SUB[ 1 , #PAIRS ]
  TEST2 SUB[ 1 , #PAIRS ]
    1 SET.#.OPTIMA
    5 SET.#.POINTS
    LOCAL.MAXIMA
      DAMPING
      DAMPING.FACTOR
      DAMP.TWO :=
    REAL TOP :=
    XVALUE2 [ TOP ]
  TOP.FREQUENCY.TWO :=
  NEW.INDEX SUB[ 1 , #PAIRS ]
  TEST2 SUB[ 1 , #PAIRS ] -
  WITHOUT.FREQUENCIES VARIANCE
  DEVIATION2 :=
```

```
;
: FULL.TEST3
  FULL.TEST1
  FULL.TEST2
  XVALUE3 SUB[ 1 , #PAIRS ]
  TEST3 SUB[ 1 , #PAIRS ]
    1 SET.#.OPTIMA
    5 SET.#.POINTS
    LOCAL.MAXIMA
      DAMPING
      DAMPING.FACTOR
      DAMP.THREE :=
    REAL TOP :=
    XVALUE3 [ TOP ]
  TOP.FREQUENCY.THREE :=
  NEW.INDEX SUB[ 1 , #PAIRS ]
  TEST3 SUB[ 1 , #PAIRS ] -
  WITHOUT.FREQUENCIES VARIANCE
  DEVIATION3 :=
```

```

: MEAN.MAX.FULL
MANY 1 =
IF FULL.TEST1
DAMP.ONE DAMPING.FACTOR :=
ELSE
MANY 2 =
IF FULL.TEST2
DAMP.TWO DAMP.ONE + 2 /
DAMPING.FACTOR :=
ELSE
MANY 3 =
IF FULL.TEST3
DAMP.ONE DAMP.TWO + DAMP.THREE
+ 3 / DAMPING.FACTOR :=
THEN
THEN
THEN
;

```

These routines display results on the screen

```

: ANALYSIS.DISPLAY1
NORMAL.DISPLAY
CR 15 SPACES
." RESULTS "
CR
CR
5 SPACES
." TEST ONE: DAMPING " DAMP.ONE . 2 SPACES ." DNF " TOP.FREQUENCY.ONE .
2 SPACES ." VARIANCE: " DEVIATION1 . CR
;

: ANALYSIS.DISPLAY2
5 SPACES
." TEST TWO: DAMPING " DAMP.TWO . 2 SPACES ." DNF " TOP.FREQUENCY.TWO .
2 SPACES ." VARIANCE: " DEVIATION2 . CR
;

: ANALYSIS.DISPLAY3
5 SPACES
." TEST THREE: DAMPING " DAMP.THREE . 2 SPACES ." DNF " TOP.FREQUENCY.THREE .
2 SPACES ." VARIANCE: " DEVIATION3 . CR
;

: ANALYSIS.DISPLAY
5 SPACES
." MEAN : DAMPING " DAMPING.FACTOR . 2 SPACES ." DNF "
TOP.FREQUENCY . CR
CR CR
STACK.CLEAR
;

```

```

: WHICH.ANALYSIS.DISPLAY
  MANY 1 =
    IF ANALYSIS.DISPLAY1
    ELSE
      MANY 2 =
        IF ANALYSIS.DISPLAY1
        ANALYSIS.DISPLAY2
        ELSE
          MANY 3 =
            IF ANALYSIS.DISPLAY1
            ANALYSIS.DISPLAY2
            ANALYSIS.DISPLAY3
            THEN
              THEN
                THEN
                  ANALYSIS.DISPLAY
;

```

Main analysis program

```

: MEAN.MAX
  MANY
  MANY 1 =
    IF AVER1
    ELSE
      MANY 2 =
        IF AVER2
        ELSE
          MANY 3 =
            IF AVER3
            THEN
              THEN
                THEN
                  STACK.CLEAR
                  MEAN.MAX.FULL
                  WHICH.ANALYSIS.DISPLAY
                  STACK.CLEAR
                  {BOTLINE}
                  SCREEN.CLEAR
                  1 BACKGROUND 15 FOREGROUND
                  3 SPACES
                  ." Analysis completed .... Press <F6> "
;

```

Subroutine preventing unwanted exit

```

: XY.BYE
  {DEF}
  SCREEN.CLEAR
  {BOTLINE}
  4 BACKGROUND 15 FOREGROUND
  SCREEN.CLEAR 10 SPACES
  BELL ." Quit ? ... (Y/N) "
  PCKEY ?DROP 89 = IF BYE THEN
  MAIN.MENU
;

```

Help menu text 1

```
: MAIN.HELP
  HELP.MESSAGE.DISPLAY
  CR 20 SPACES
  ." ***** Main Help Menu ***** "
  CR CR 7 SPACES
  ." To enter data, type F(7). To read data from disk, type " CR
  7 SPACES
  ." F(8). At any stage in the program F(1) can be typed. F(10) " CR
  7 SPACES
  ." will always return you to the Main Menu. " CR
  CR 13 SPACES
  ." Type any key to return to Main Menu "
  PCKEY ?DROP DROP
  MAIN.MENU
```

Help menu text 2

```
: CATH.HELP
  HELP.MESSAGE.DISPLAY
  CR 22 SPACES
  ." ***** Help Menu ***** "
  CR CR 7 SPACES
  ." Function keys are represented by <F(x)> . Adding new data to " CR
  7 SPACES
  ." be analysed, the correct function key must be selected. This " CR
  7 SPACES
  ." will introduce the insert mode. The first vertical column is " CR
  7 SPACES
  ." the frequency and the second vertical column is the dB value " CR
  CR 7 SPACES
  ." A value may be changed despite a wrong entry by pressing the " CR
  7 SPACES
  ." <INS> key twice. " CR CR
  13 SPACES
  ." Press any key to return to the Data Read Menu .."
  PCKEY ?DROP DROP
  DATA.READ.MENU
```

Control to function keys

```
: READ.KEYS
  F1 FUNCTION.KEY.DOES XY.BYE
  F2 FUNCTION.KEY.DOES MEAN.MAX
  F4 FUNCTION.KEY.DOES GET.FILENAME
  F5 FUNCTION.KEY.DOES CATH.HELP
  F6 FUNCTION.KEY.DOES ANSWER.PRINT
```

```
: READ.DATA.FILE  
  READ.KEYS  
  DATA.READ.MENU  
  INTERPRET.KEYS  
;
```

Warning message

```
: HAS.DATA.SAVED  
  {BOTLINE} SCREEN.CLEAR  
  4 BACKGROUND  
  15 FOREGROUND  
  3 SPACES  
  ." Warning: Data has not been saved on disk !!! - Save (F6) "  
  INTERPRET.KEYS  
;
```

Automated saving routine

```
: DECIDE.DATA.SAVE  
  PCKEY CR ?DROP 89 = IF BYE THEN  
    HAS.DATA.SAVED  
  PCKEY CR ?DROP 63 = IF CATH.HELP THEN  
    HAS.DATA.SAVED  
  PCKEY CR ?DROP 64 = IF STORE.DATA THEN  
    STORE.DATA  
;
```

User instruction

```
: INTO.ARRAY  
  INTEN.ON  
  BELL  
  ." Use the cursor keys to move the cursor. "  
  CR CR  
  ." Press <cr> to exit to Data Read Menu "  
  ARRAY.EDIT.WORDS  
  INSERT  
;
```

Control routines for the array editor

```
: PREPARE
  TEST1 0 * TEST1 :=
  TEST2 0 * TEST2 :=
  TEST3 0 * TEST3 :=
  XVALUE1 0 * XVALUE1 :=
  XVALUE2 0 * XVALUE2 :=
  XVALUE3 0 * XVALUE3 :=
;

: ED.DATA
  PREPARE
  STACK.CLEAR
  MANY 1 =
  IF INDEX SUB[ 1 , #PAIRS ; 1 , MAXSETS ] ARRAY.EDIT
    ." First data column " CR
    INTO.ARRAY
    INDEX XSECT[ ! , 1 ]
    XVALUE1 :=
    INDEX XSECT[ ! , 2 ]
    TEST1 :=
  ELSE
    MANY 2 =
    IF INDEX SUB[ 1 , #PAIRS ; 1 , MAXSETS ] ARRAY.EDIT
      ." First data column " CR
      INTO.ARRAY
      INDEX XSECT[ ! , 1 ]
      XVALUE1 :=
      INDEX XSECT[ ! , 2 ]
      TEST1 :=
    INDEX SUB[ 1 , #PAIRS ; 1 , MAXSETS ] ARRAY.EDIT
      ." Second data column " CR
      INTO.ARRAY
      INDEX XSECT[ ! , 1 ]
      XVALUE2 :=
      INDEX XSECT[ ! , 2 ]
      TEST2 :=
    ELSE
      MANY 3 =
      IF INDEX SUB[ 1 , #PAIRS ; 1 , MAXSETS ] ARRAY.EDIT
        ." First data column " CR
        INTO.ARRAY
        INDEX XSECT[ ! , 1 ]
        XVALUE1 :=
        INDEX XSECT[ ! , 2 ]
        TEST1 :=
      INDEX SUB[ 1 , #PAIRS ; 1 , MAXSETS ] ARRAY.EDIT
        ." Second data column " CR
        INTO.ARRAY
        INDEX XSECT[ ! , 1 ]
        XVALUE2 :=
        INDEX XSECT[ ! , 2 ]
        TEST2 :=
      INDEX SUB[ 1 , #PAIRS ; 1 , MAXSETS ] ARRAY.EDIT
        ." Third data column " CR
```

```

        INTO.ARRAY
        INDEX XSECT[ ! , 1 ]
        XVALUE3 :=
        INDEX XSECT[ ! , 2 ]
        TEST3 :=
    THEN
    THEN
    THEN

    DATA.MENU
    DECIDE.DATA.SAVE
;

: REDMAT
{DEF} SCREEN.CLEAR
." Title of experiment " "INPUT TITLE " := CR CR
." Experiment identification number ? " "INPUT #EXP " := CR CR
." What is the catheter material and name ? " "INPUT MAKE " := CR
." What is the internal diameter ? " "INPUT IND " := CR CR
." How many Frequency scans in this test ? " #INPUT
MANY :=
CR
BEGIN
." Number of data pairs in this set ? " #INPUT
IF #PAIRS :=
ELSE GRAPHICS.DISPLAY {MENULINE} HOME ." Press F1" EXIT
THEN
#PAIRS MAXPAIRS >
IF ." Maximum #pairs allowable is " MAXPAIRS
-1 0 FIX.FORMAT MAXPAIRS .
-1 2 SCI.FORMAT FALSE
ELSE TRUE
THEN
UNTIL
ED.DATA
;

```

Data Reading Menu

```

: PREDATA.MENU
{DEF}
NORMAL.DISPLAY
SCREEN.CLEAR
{MENULINE}
SCREEN.CLEAR 22 SPACES
2 BACKGROUND
0 FOREGROUND
." ***** Data Entering Menu *****"
{BOTLINE}
SCREEN.CLEAR 7 SPACES
1 BACKGROUND
15 FOREGROUND
." F1) Quit F2) Enter Data / Save F5) Help F10) Main Menu "
CURSOR.OFF
{DEF}
;

```

Control to function keys

```
: DATA.KEYS
  F1 FUNCTION.KEY.DOES XY.BYE
  F2 FUNCTION.KEY.DOES REDMAT
  F5 FUNCTION.KEY.DOES CATH.HELP
  F6 FUNCTION.KEY.DOES STORE.DATA
;
```

Automatic data enter routines

```
: ENTER.DATA
  {BOTLINE} SCREEN.CLEAR
  DATA.KEYS
  PREDATA.MENU
  INTERPRET.KEYS
  {DEF}
;
: SHOWD
  NORMAL.DISPLAY
  {DEF} SCREEN.CLEAR
  DATA.READ.MENU
  {SHOW.DIR}
  SCREEN.CLEAR
  0 BACKGROUND 14 FOREGROUND
  DIR A:
;
```

This routine defines the function keys for the Main Menu

```
: PLOT.KEYS
  F1 FUNCTION.KEY.DOES XY.BYE
  F7 FUNCTION.KEY.DOES ENTER.DATA
  F8 FUNCTION.KEY.DOES READ.DATA.FILE
  F9 FUNCTION.KEY.DOES SHOWD
  F5 FUNCTION.KEY.DOES MAIN.HELP
;
```

Main Program

```
: MAIN
  CLEAR.FKEYS
  BANNER
  PLOT.KEYS
  MAIN.MENU
  F10 FUNCTION.KEY.DOES MAIN.MENU
  INTERPRET.KEYS
ONERR: NORMAL.DISPLAY {DEF} SCREEN.CLEAR
  {MENULINE}
  4 BACKGROUND 15 FOREGROUND 4 SPACES
  ." Unrecoverable error - <ctrl-Break> to restart."
  BELL PCKEY ?DROP DROP BYE
;
```

Listing of program: ANALTHE

BLOOD PRESSURE ANALYSIS PROGRAM

P.A. HEIMANN

The program gives the user the option to define the GPIB bus for data sampling, (the sample rate may be changed in the program) or reading data from disk. The data may be scrolled and individual pulses marked.

Analysis includes Fourier transforms, Power Density Spectra and time domain analysis.

Results may be plotted (for PDS and time plot) and/or a report printed.

The system is configured, however the user may change the configuration by loading CONFIG.HPB.

To run the program, type MAIN after the OK prompt.....

F1 - escape to previous menu

F10 - quit

Version 1.25

April 1988

Cape Town

Variable definitions

ECHO.OFF
INTEGER SCALAR START.INDEX
INTEGER SCALAR START.INDEX.ONE
INTEGER SCALAR START.INDEX.TWO
INTEGER SCALAR START.INDEX.THREE
INTEGER SCALAR END.INDEX.ONE
INTEGER SCALAR END.INDEX.TWO
INTEGER SCALAR END.INDEX.THREE
INTEGER SCALAR END.INDEX
INTEGER SCALAR NEW.INDEX
INTEGER SCALAR INDEX.NUMBER
INTEGER SCALAR INDEX.NUMBER.ONE
INTEGER SCALAR PAD.NUMBER
INTEGER SCALAR INCREMENTS
INTEGER SCALAR DATA.POINTS

REAL SCALAR OMEGA
REAL SCALAR TOP
REAL SCALAR SAMPLE.RATE
REAL SCALAR FREQUENT
REAL SCALAR BEAT
REAL SCALAR PULSE.MEAN
REAL SCALAR PULSE.NUMBER
REAL SCALAR SYSTOLIC
REAL SCALAR DIASTOLIC
REAL SCALAR OBEN
REAL SCALAR MANY
REAL SCALAR XSYSTOL
REAL SCALAR HALF
REAL SCALAR ANACROTIC
REAL SCALAR DICROTIC
REAL SCALAR PRECROTIC
REAL SCALAR DICROTIC.NOTCH
REAL SCALAR DICROTIC.PRESSURE
REAL SCALAR LINE.POINTER
REAL SCALAR END.SYSTOLIC
REAL SCALAR DP/DT.MAX
REAL SCALAR PDS.MAX
REAL SCALAR DIFFERENCE
REAL SCALAR ELEMENTS
REAL SCALAR ELEMENT1
REAL SCALAR ELEMENT2
REAL SCALAR ELEMENT4
REAL SCALAR ELEMENT5
REAL SCALAR ELEMENT6

14 STRING FILENAME
14 STRING CODES
1000 DATA.POINTS :=
1024 INDEX.NUMBER :=
1024 NEW.INDEX :=
1024 ELEMENT4 :=
0.01 SAMPLE.RATE :=

INTEGER DIM[DATA.POINTS] ARRAY DATA.IN
INTEGER DIM[INDEX.NUMBER] ARRAY PULSE.TO.ANAL
INTEGER DIM[NEW.INDEX] ARRAY PADDING
INTEGER DIM[NEW.INDEX] ARRAY PADDED
REAL DIM[200] ARRAY PULSE1.ADD
REAL DIM[200] ARRAY PULSE2.ADD
REAL DIM[200] ARRAY PULSE3.ADD
REAL DIM[200] ARRAY PULSE4.ADD
REAL DIM[200] ARRAY PULSE5.ADD
REAL DIM[200] ARRAY PULSE.ADDED
REAL DIM[10] ARRAY LINE.POSITION
REAL DIM[10] ARRAY HARMONICS
REAL DIM[10] ARRAY AMPLITUDES
REAL DIM[NEW.INDEX] ARRAY YVALUE
REAL DIM[INDEX.NUMBER] ARRAY XVALUE
REAL DIM[INDEX.NUMBER] ARRAY XVALUE.ONE
REAL DIM[ELEMENT4] ARRAY FOURIER

GPIB configuration

3 GPIB.DEVICE MK
3 GPIB.DEVICE MK.HSC
0 SECONDARY.ADDRESS
3 GPIB.DEVICE MK.AN
2 SECONDARY.ADDRESS
3 GPIB.DEVICE MK.AN1632
1 SECONDARY.ADDRESS

Set screen area, axis, tick and spacing

: DATA.VU
HORIZONTAL AXIS.FIT.OFF
VERTICAL AXIS.FIT.OFF
.180 .210 AXIS.ORIG
.800 .740 AXIS.SIZE
.025 .008 TICK.SIZE
.5 .8 TICK.JUST
;

Set window location

: DATA.VU.ONE
.270 .500 VUPOINT.ORIG
.730 .450 VUPOINT.SIZE
DATA.VU
;

: DATA.VU.TWO
.270 .010 VUPOINT.ORIG
.730 .490 VUPOINT.SIZE
DATA.VU
;

: BOTTOM.LEFT
18 2 23 19 SET.WINDOW
;

: MIDDLE.LEFT
13 2 16 19 SET.WINDOW
;

: UPPER.LEFT
6 2 11 19 SET.WINDOW
;

: TOP.LEFT
2 2 3 19 SET.WINDOW
;

: INTERACTIVE.WINDOW
14 2 16 19 SET.WINDOW
;

```
: BOTTOM.RIGHT
  24 25 24 34 SET.WINDOW
;
```

Set window frame

```
: TECHNICAL.DISPLAY
  UPPER.LEFT
  -1. 1. FIX.FORMAT
  .* Freq (Hz) " FREQUENT . CR
  .* Beat/min " BEAT . CR
  .* Mean mmHg " PULSE.MEAN . CR
  CURSOR.OFF
  -1. 4. FIX.FORMAT
;
```

```
: MENU.DISP
  BOTTOM.LEFT SCREEN.CLEAR
  .* MENU" CR
  .* [ F2 ]- sample" CR
  .* [ F3 ]- disk" CR
;
```

```
: VIEW.MENU
  BOTTOM.LEFT SCREEN.CLEAR
  .* MENU"CR
  .* [ F1 ]- esc" CR
  .* [ F4 ]- scroll" CR
  .* [ F6 ]- resume"
  CURSOR.OFF
;
```

```
: ANALYSIS.MENU
  BOTTOM.LEFT SCREEN.CLEAR
  .* MENU"CR
  .* [ F1 ]- esc" CR
  .* [ F7 ]- time" CR
  .* [ F8 ]- print" CR
  .* [ F9 ]- freq" CR
;
```

```
: FREQUENCY.MENU
  BOTTOM.LEFT SCREEN.CLEAR
  .* MENU"CR
  .* [ F1 ]- esc" CR
  .* [ F5 ]- PDS" CR
  .* [ F6 ]- FFT" CR
;
```

```
: TIME.MENU
  BOTTOM.LEFT SCREEN.CLEAR
  .* MENU"CR
  .* [ F1 ]- esc" CR
  .* [ F4 ]- time" CR
  .* [ F5 ]- diff" CR
  .* [ F6 ]- smooth" CR
;
```

```

: PRINT.MENU
  BOTTOM.LEFT SCREEN.CLEAR
  ."      MENU"CR
  ." [ F1 ]- esc" CR
  ." [ F4 ]- plot A" CR
  ." [ F5 ]- report" CR
  ." [ F6 ]- plot B"
;

: RETURN.INFORMATION
  INTERACTIVE.WINDOW SCREEN.CLEAR
  ." [ F1 ] Main Menu" CR
  CURSOR.OFF
;

```

Window screen control routine

```

: SIDE.VIEW
  .0 .0 VUPOINT.ORIG
  .25 .95 VUPOINT.SIZE
  SCREEN.CLEAR
  OUTLINE
  .0 .31 VUPOINT.ORIG
  .25 .50 VUPOINT.SIZE
  OUTLINE
  .0 .51 VUPOINT.ORIG
  .25 .90 VUPOINT.SIZE
  OUTLINE
  NORMAL.COORDS
  .23 .95 POSITION
  " INFORMATION" LABEL
  CURSOR.OFF
;

```

Clear Function keys of current function

```

: CLEAR.FKEYS
  133 0 DO
    I FUNCTION.KEY.DOES NOP
  LOOP
;

```

User information

```

: BEGIN.READ.INFORMATION
  INTERACTIVE.WINDOW
  ." Reading ...."
  CURSOR.OFF
;

```

```

: END.READ.INFORMATION
  INTERACTIVE.WINDOW
  ." Completed !!"
  BELL
  2000 MSEC.DELAY
  CURSOR.OFF
;
: WAITING
  INTERACTIVE.WINDOW SCREEN.CLEAR
  ." Running .... "
  CURSOR.OFF
;

```

Opening banner and screen displays

```

: HEADING.DISPLAY
  NORMAL.COORDS
  .42 .73 POSITION
  " BLOOD PRESSURE ANALYSIS" LABEL
  .49 .65 POSITION
  " P. A. Heimann" LABEL
  .35 .35 POSITION
  " S A Medical Research Council " LABEL
  .50 .27 POSITION
  " Version 1.02 " LABEL
  .55 .21 POSITION
  " 1988 " LABEL
;
: REPORTING.MENU
  {DEF} NORMAL.DISPLAY SCREEN.CLEAR
  20 SPACES
  ." ANALYSIS RESULTS "
  CR
;
: MARK.INFORMATION
  UPPER.LEFT
  ." Mark end of .. " CR
  ." 1. Anachr t w " CR
  ." 2. Predicrt w " CR
  ." 3. Dichrt w " CR
  ." 4. Dichrtic ncth " CR
  CURSOR.OFF
;

```

User instruction

```

: PLOTTER.INFORMATION
  MIDDLE.LEFT SCREEN.CLEAR
  ." Ready ..? " CR BELL
  ." <space> " CR
  PCKEY
  ?DROP DROP
;

```

Plotter control routines

```
: PLOT.LABELS
  GRAPHICS.DISPLAY HP7440
  15 SLANT
  NORMAL.COORDS
  .2 .985 POSITION
  " SIGNAL ANALYSIS -- TEST NO "LABEL
  .65 .985 POSITION FILENAME LABEL
  .425 .33 POSITION
  " frequency (Hz) "LABEL
  .43 .66 POSITION
  " time (sec) "LABEL
  90 LABEL.DIR
  .185 .42 POSITION
  " Relative Power "LABEL
  .185 .77 POSITION
  " Pressure (mmHg) "LABEL
  0 LABEL.DIR
  .77 .75 POSITION
  " a) Pulse shape "LABEL
  .77 .44 POSITION
  " b) Power Spectra "LABEL
```

;

```
: PLOT.LABELS.TWO
  GRAPHICS.DISPLAY HP7440
  15 SLANT
  NORMAL.COORDS
  .43 .66 POSITION
  " frequency (Hz) "LABEL
  90 LABEL.DIR
  .185 .77 POSITION
  " Amplitude "LABEL
  0 LABEL.DIR
  .80 .75 POSITION
  " c) FFT "LABEL
```

;

Clear Function keys of current function

```
: REMOVE.KEYS
  F4 FUNCTION.KEY.DOES NOP
  F5 FUNCTION.KEY.DOES NOP
  F6 FUNCTION.KEY.DOES NOP
```

;

Plotting subroutines

```
: TO.PLOTTER.TWO
  STACK.CLEAR
  PLOTTER.INFORMATION
  GRAPHICS.DISPLAY
  HP7440
  1 COLOR
    XVALUE SUB[ ! , HALF ]
  FOURIER SUB[ ! , HALF ]
  DUP 1 SET.#.OPTIMA 3 SET.#.POINTS LOCAL.MAXIMA
  SWAP DROP /
    5.5 7 PLOTTER.SIZE
  DATA.VU.ONE
  XY.AUTO.PLOT
  PLOT.LABELS.TWO
  GRAPHICS.DISPLAY
  SIDE.VIEW
  END.READ.INFORMATION
  RETURN.INFORMATION
```

```
;
: TO.PLOTTER
  STACK.CLEAR
  PLOTTER.INFORMATION
  GRAPHICS.DISPLAY
  HP7440
  1 COLOR
    XVALUE SUB[ ! , HALF ]
    YVALUE SUB[ ! , HALF ]
  XY.DATA.FIT
  5.5 7 PLOTTER.SIZE
  DATA.VU.TWO
  XY.AXIS.PLOT
  2 COLOR
    XY.DATA.PLOT
  DATA.IN SUB[ START.INDEX , INDEX.NUMBER ] DUP
  XVALUE.ONE SUB[ ! , INDEX.NUMBER ] SWAP
  XY.DATA.FIT
  1 COLOR DATA.VU.ONE
  XY.AXIS.PLOT
  2 COLOR
  XY.DATA.PLOT
  3 COLOR
  DATA.IN SUB[ START.INDEX , INDEX.NUMBER ]
  SMOOTH
  XVALUE.ONE SUB[ ! , INDEX.NUMBER ] SWAP
  XY.DATA.FIT
  XY.DATA.PLOT
  PLOT.LABLES
  GRAPHICS.DISPLAY
  SIDE.VIEW
  END.READ.INFORMATION
  RETURN.INFORMATION
```

Time domain analysis routines

```
: NO.PRE.WAVE
  ." No Predicrotic wave was marked "
  LINE.POSITION [ 5 ] LINE.POSITION [ 1 ] - DICROTIC :=
  LINE.POSITION [ 1 ] LINE.POINTER :=
  0 LINE.POSITION [ 3 ] :=
```

```
: PRE.WAVE
  ." Predicrotic wave was marked "
  LINE.POSITION [ 5 ] LINE.POSITION [ 3 ] - DICROTIC :=
  LINE.POSITION [ 3 ] LINE.POINTER :=
```

```
: FIND.DIASTOLE
  IF DATA.IN [ 1 ] MIN DIASTOLIC :=
  ELSE DATA.IN [ 1 ] DIASTOLIC :=
  THEN
```

Result representation

```
: REPORT.PRESENT
-1. 2. FIX.FORMAT
  CR
  ."
  ." _____ " CR
  ." | Filename : " FILENAME "TYPE 9 SPACES ." | Beats/min " 15 SPACES BEAT . CR
  ." | Date      : " .DATE 9 SPACES ." | Mean Pressure " 12 SPACES PULSE.MEAN . CR
  ." | Time      : " .TIME 6 SPACES ." | dp/dt max " 15 SPACES DP/DT.MAX 60 * . CR
  ." | Patient   : " CODES "TYPE CR
  ." _____ " CR
  CR
  ." Timing Results (seconds) " CR
  ." _____ " CR
  ." | Wave/Event | Duration | Delay | " CR
  ." _____ " CR
  ." | Anacrotic wave | " 5 SPACES ANACROTIC . 13 SPACES ." | " 12 SPACES ." -- " CR
  ." | Predicrotic wave | " 5 SPACES PRECROTIC . 13 SPACES ." | " 10 SPACES LINE.POSITION [ 1 ] . CR
  ." | Dicrotic wave | " 5 SPACES DICROTIC . 13 SPACES ." | " 10 SPACES LINE.POINTER . CR
  ." _____ " CR
  ." | Event | Delay | Pressure (mmHg) | " CR
  ." _____ " CR
  ." | Systolic pulse | " 5 SPACES XSYSTOL . 13 SPACES ." | " 4 SPACES SYSTOLIC . CR
  ." | Diastolic pulse | -- | " 5 SPACES DIASTOLIC . CR
  ." | Dicrotic notch | " 5 SPACES LINE.POSITION [ 7 ] . 13 SPACES ." | " 5 SPACES LINE.POSITION [ 8 ] . CR
  ." _____ " CR
-1. 4. FIX.FORMAT
```

```
: LINE.FEEDS
  44 1 DO
  CR
  LOOP
```

```
: LINE.FEEDS.TWO
  28 1 DO
  CR
  LOOP
```

```
: HARMONICS.PRINT
  ELEMENT6 1 DO
  HARMONICS [ 1 ]
  40 SPACES . AMPLITUDES [ 1 ] 10 SPACES . CR
  LOOP
```

Printer control and print routines

```
: PRINT.REPORT
  TOP.LEFT SCREEN.CLEAR
  ." Printer "
  MIDDLE.LEFT SCREEN.CLEAR
  INTERACTIVE.WINDOW SCREEN.CLEAR
  ." <cr> when " CR
  ." ready " CR BELL
  PCKEY
  ?DROP
  SCREEN.CLEAR
  OUT>PRINTER
  LINE.FEEDS
  10 SPACES
  ." _____ " CR CR CR
5. 1. FIX.FORMAT
10 SPACES ." Figure a: Pulse Characteristics " CR CR
21 SPACES ." Beats/min - " 3 SPACES BEAT . CR
21 SPACES ." Systolic Peak Pressure (mmHg) - " 3 SPACES SYSTOLIC . CR
21 SPACES ." Diastolic Pressure (mmHg) - " 3 SPACES DIASTOLIC . CR
21 SPACES ." Mean Pressure (mmHg) - " 3 SPACES PULSE.MEAN . CR
21 SPACES ." dp/dt maximum (mmHg/min) - " 3 SPACES DP/DT.MAX 60 * . CR CR CR
10 SPACES ." Figure b: Power Density Characteristics " CR CR
21 SPACES ." Maximum Signal Power at (Hz) - " 3 SPACES PDS.MAX . CR
-1. 4 FIX.FORMAT
INTERACTIVE.WINDOW SCREEN.CLEAR
CONSOLE
  ." Insert " CR
  ." New Page "
  3000 MSEC.DELAY
  CURSOR.OFF
  SCREEN.CLEAR
PLOTTER.INFORMATION
OUT>PRINTER
LINE.FEEDS.TWO
10 SPACES
  ." _____ " CR CR
```

6. 2. FIX.FORMAT

```
10 SPACES ." Figure c: Fast Fourier Transforms " CR CR
21 SPACES ." Fundamental Frequency (Hz) - " 3 SPACES FREQUENT . CR CR
21 SPACES ." Harmonics at Herz - Rel Amplitude " 3 SPACES CR CR
HARMONICS.PRINT CR CR
```

-1. 0 FIX.FORMAT

```
10 SPACES ." Percentage decrease of Amplitude in successive Harmonics " CR
10 SPACES ." calculated from the highest relative Amplitudes " CR CR
```

```
14 SPACES AMPLITUDES [ 1 ] AMPLITUDES [ 2 ] - 100 * .
3 SPACES AMPLITUDES [ 2 ] AMPLITUDES [ 3 ] - 100 * .
3 SPACES AMPLITUDES [ 3 ] AMPLITUDES [ 4 ] - 100 * .
3 SPACES AMPLITUDES [ 4 ] AMPLITUDES [ 5 ] - 100 * .
3 SPACES AMPLITUDES [ 5 ] AMPLITUDES [ 6 ] - 100 * .
3 SPACES AMPLITUDES [ 6 ] AMPLITUDES [ 7 ] - 100 * . CR
```

MIDDLE.LEFT SCREEN.CLEAR

-1. 4. FIX.FORMAT

CONSOLE

;
: DECIDE.TO.PRINT

15 SPACES ." To continue - <space> "

PCKEY

DROP ?DROP

GRAPHICS.DISPLAY

SIDE.VIEW MIDDLE.LEFT SCREEN.CLEAR

." Print (Y/N) " BELL CR

PCKEY

?DROP 89 = IF PRINT.REPORT THEN

PRINT.MENU

INTERPRET.KEYS

Time domain analysis

: TIME.CALCULATION

LINE.POSITION [1] ANACROTIC :=

LINE.POSITION [3] LINE.POSITION [1] - PRECROTIC :=

LINE.POSITION [7] DICROTIC.NOTCH :=

LINE.POSITION [8] DICROTIC.PRESSURE :=

LINE.POSITION [3] LINE.POSITION [1] - DIFFERENCE :=

DIFFERENCE 0 =

IF NO.PRE.WAVE

ELSE

PRE.WAVE

THEN

DATA.IN SUB[START.INDEX , INDEX.NUMBER]

SMOOTH

1 SET.#.OPTIMA

3 SET.#.POINTS

LOCAL.MAXIMA

SYSTOLIC :=

OBEN :=

XVALUE.ONE [OBEN] XSYSTOL :=

DATA.IN SUB[START.INDEX , INDEX.NUMBER]

1 SET.#.OPTIMA

3 SET.#.POINTS

```
LOCAL.MINIMA
  FIND.DIASTOLE
    SYSTOLIC DICROTIC.PRESSURE / END.SYSTOLIC :=
    YVALUE SUB[ ! , HALF ]
      1 SET.#.OPTIMA
      3 SET.#.POINTS
    LOCAL.MAXIMA
```

```
      SWAP SAMPLE.RATE NEW.INDEX * 1 SWAP / *
      PDS.MAX :=
      REPORT.PRESENT
    DECIDE.TO.PRINT
```

```
;
: REPORTING
  NORMAL.DISPLAY
  REPORTING.MENU
  TIME.CALCULATION
  PCKEY ?DROP DROP
  GRAPHICS.DISPLAY
```

Control to function keys

```
: PRINT.KEYS
  F4 FUNCTION.KEY.DOES TO.PLOTTER
  F5 FUNCTION.KEY.DOES REPORTING
  F6 FUNCTION.KEY.DOES TO.PLOTTER.TWO
```

```
;
: REPORT
  PRINT.MENU
  STORE.FUNCTION.KEYS
  PRINT.KEYS
  INTERPRET.KEYS
  ONESCAPE: RESTORE.FUNCTION.KEYS REMOVE.KEYS ANALYSIS.MENU
```

Routines to normalise frequency

```
: RATIONAL
  YVALUE SUB[ ! , HALF ]
    1 SET.#.OPTIMA
    5 SET.#.POINTS
  LOCAL.MAXIMA
  YVALUE [ 1 ]
  MAX
  ELEMENT1 :=
  YVALUE SUB[ ! , HALF ] ELEMENT1 /
  YVALUE SUB[ ! , HALF ] :=
```

```

: SCALE
  XVALUE []RAMP
  NEW.INDEX SAMPLE.RATE * 1 SWAP /
  OMEGA :=
  XVALUE OMEGA *
  DUP []SIZE ELEMENT2 :=
  XVALUE SUB[ ! , ELEMENT2 ] :=
;

```

```

: SCALE.ONE
  STACK.CLEAR
  XVALUE.ONE []RAMP
  XVALUE.ONE SAMPLE.RATE *
  DUP
  XVALUE.ONE :=
  STACK.CLEAR
;

```

Frequency domain representation

```

: DISPLAY.POWER.DENSITY
  STACK.CLEAR
  SCALE
  GRAPHICS.DISPLAY
  SIDE.VIEW FREQUENCY.MENU TOP.LEFT
  ." Trace " CR
  ." Power Density "
  DATA.VU.TWO
  RATIONAL
  YVALUE SUB[ ! , HALF ]
  XVALUE SUB[ ! , HALF ] SWAP
  XY.AUTO.PLOT
  NORMAL.COORDS
  .7 .85 POSITION " Power Spectra " LABEL
  .957 .05 POSITION " Hz " LABEL
  .04 .16 POSITION " Rel P " LABEL
  STACK.CLEAR
  SCALE.ONE
  XVALUE.ONE SUB[ ! , INDEX.NUMBER ]
  DATA.IN SUB[ START.INDEX , INDEX.NUMBER ]
  DATA.VU.ONE
  XY.AUTO.PLOT
  NORMAL.COORDS
  .7 .85 POSITION " Trace " LABEL
  .957 .05 POSITION " sec " LABEL
  .05 .16 POSITION " mmHg " LABEL
  CURSOR.OFF
  UPPER.LEFT TECHNICAL.DISPLAY
;

```

Zero padding routines

```
: ZERO.PADDING
  STACK.CLEAR
  0 PADDING :=
    DATA.IN SUB[ START.INDEX , INDEX.NUMBER ] DUP MEAN -
    PADDING SUB[ ! , INDEX.NUMBER ]
    :=
    PADDING SUB[ ! , NEW.INDEX ]
;
```

```
: DO.PADDING
  ZERO.PADDING
  WAITING
  FFT
  ZMAG ABS 2 **
  INDEX.NUMBER / DUP
  []SIZE
  ELEMENTS :=
    YVALUE SUB[ ! , ELEMENTS ] :=
    ELEMENTS 4 /
  HALF :=
  INTERACTIVE.WINDOW SCREEN.CLEAR
  DISPLAY.POWER.DENSITY
;
```

Fourier analysis routines

```
: DO.FOURIER
  STACK.CLEAR
  XVALUE SUB[ ! , HALF ]
  FOURIER SUB[ ! , HALF ]
  DUP
  1 SET.#.OPTIMA
  3 SET.#.POINTS
  LOCAL.MAXIMA
  SWAP DROP
  DATA.VJ.TWO
  XY.AUTO.PLOT
;
```

```
: PLOT.DATA
  STACK.CLEAR
  GRAPHICS.DISPLAY SIDE.VIEW ANALYSIS.MENU
  TOP.LEFT
  ." FFT Harmonics " CR
  ." FFT Transform "
  TECHNICAL.DISPLAY
  ZERO.PADDING
  WAITING
  FFT
  ZMAG DUP
  []SIZE
  ELEMENT4 :=
  INTERACTIVE.WINDOW SCREEN.CLEAR
```

```

FOURIER SUB[ ! , ELEMENT4 ] :=
FOURIER SUB[ ! , HALF ]
  10 SET.#.OPTIMA
  3 SET.#.POINTS
  LOCAL.MAXIMA
[ ]SIZE ELEMENT6 :=
SAMPLE.RATE NEW.INDEX *
  1 SWAP /
  3 ROLL * DUP HARMONICS SUB[ ! , ELEMENT6 ] := SWAP
DUP DUP [ ]MAX / AMPLITUDES SUB[ ! , ELEMENT6 ] :=
DATA.VU.ONE
GRID.OFF
XY.AUTO.BAR
NORMAL.COORDS
  .7 .85 POSITION " FFT - Harmonics " LABEL
  .957 .05 POSITION " Hz " LABEL
  .05 .16 POSITION " Ampl " LABEL
DATA.VU.TWO
DO.FOURIER
NORMAL.COORDS
  .7 .85 POSITION " FFT - Transform " LABEL
  .957 .05 POSITION " Hz " LABEL
  .05 .16 POSITION " Ampl " LABEL
CURSOR.OFF

```

Control to function keys

```

: FREQUENCY.ANALYSIS.KEYS
  F5 FUNCTION.KEY.DOES DO.PADDING
  F6 FUNCTION.KEY.DOES PLOT.DATA

```

Digital filtering routines

```

: DIFF.SMOOTH
  STACK.CLEAR
  SCALE.ONE
  XVALUE.ONE SUB[ ! , INDEX.NUMBER ]
  DATA.IN SUB[ START.INDEX , INDEX.NUMBER ]
  DIFFERENTIATE.DATA
  SMOOTH
  DUP 1 SET.#.OPTIMA 3 SET.#.POINTS LOCAL.MAXIMA
  DP/DT.MAX := DROP
  XY.DATA.PLOT
  NORMAL.COORDS
  .957 .05 POSITION " sec " LABEL
  CURSOR.OFF

```

```
: DIFF
  STACK.CLEAR
  SCALE.ONE
  XVALUE.ONE SUB[ ! , INDEX.NUMBER ]
  DATA.IN SUB[ START.INDEX , INDEX.NUMBER ]
  DIFFERENTIATE.DATA
  DATA.VU.TWO
  XY.AUTO.PLOT
;
```

Scroller control routines

```
: TIME.SCROLL
  STACK.CLEAR
  GRAPHICS.DISPLAY SIDE.VIEW TIME.MENU TOP.LEFT
  ." Time Analysis "
  MARK.INFORMATION
  SCALE.ONE
  XVALUE.ONE SUB[ ! , INDEX.NUMBER ]
  DATA.IN SUB[ START.INDEX , INDEX.NUMBER ]
  DATA.VU.ONE
  XY.AUTO.PLOT
  NORMAL.COORDS
  .957 .05 POSITION " sec " LABEL
  .05 .16 POSITION " mmHg " LABEL
  0. LINE.POSITION :=
  LINE.POSITION
  READOUT>ARRAY
  NORMAL.COORDS
  .7 .95 READOUT>POSITION
  WORLD.COORDS
  ARRAY.READOUT
;
```

Control to function keys

```
: TIME.ANALYSIS
  F4 FUNCTION.KEY.DOES TIME.SCROLL
  F5 FUNCTION.KEY.DOES DIFF
  F6 FUNCTION.KEY.DOES DIFF.SMOOTH
;
```

Main frequency domain analysis routine

```
: FREQUENCY.DOMAIN
  STORE.FUNCTION.KEYS
  FREQUENCY.MENU
  FREQUENCY.ANALYSIS.KEYS
  INTERPRET.KEYS
  ONESCAPE: RESTORE.FUNCTION.KEYS REMOVE.KEYS ANALYSIS.MENU
;
```

Main time domain analysis routine

```
: TIME.DOMAIN
  STORE.FUNCTION.KEYS
  TIME.MENU
  TIME.ANALYSIS
  INTERPRET.KEYS
  ONESCAPE: RESTORE.FUNCTION.KEYS REMOVE.KEYS ANALYSIS.MENU
;
```

Control to function keys

```
: ANALYSIS.KEYS
  F1 FUNCTION.KEY.DOES ESCAPE
  F7 FUNCTION.KEY.DOES TIME.DOMAIN
  F8 FUNCTION.KEY.DOES REPORT
  F9 FUNCTION.KEY.DOES FREQUENCY.DOMAIN
;
```

Main analysis routine

```
: DO.ANALYSIS
  GRAPHICS.DISPLAY
  BOTTOM.LEFT SCREEN.CLEAR
  SIDE.VIEW ANALYSIS.MENU
  STORE.FUNCTION.KEYS
  ANALYSIS.KEYS
  INTERPRET.KEYS
  ONESCAPE: RESTORE.FUNCTION.KEYS REMOVE.KEYS VIEW.MENU
;
```

User instruction

```
: NAME.TEST
  MIDDLE.LEFT SCREEN.CLEAR
  ." Test code ?" CR
  "INPUT CODES " :=
;
```

Timing control routines

```
: FIND.INDEX
  END.INDEX.ONE DUP END.INDEX :=
  START.INDEX.ONE DUP START.INDEX := --
  INDEX.NUMBER :=
  INDEX.NUMBER SAMPLE.RATE *
  DUP 1 SWAP / FREQUENT :=
  60 SWAP / BEAT :=
;
```

```

: FIND.INDEXES
  END.INDEX.ONE START.INDEX.ONE - INDEX.NUMBER.ONE :=
  INDEX.NUMBER.ONE INDEX.NUMBER :=
  , INDEX.NUMBER SAMPLE.RATE *
  DUP 1 SWAP / FREQUENT :=
  60 SWAP / BEAT :=
  DATA.IN SUB[ START.INDEX.ONE , INDEX.NUMBER ]
  DATA.IN SUB[ START.INDEX.TWO , INDEX.NUMBER ] +
  DATA.IN SUB[ START.INDEX.THREE , INDEX.NUMBER ] + 3 /
  DATA.IN SUB[ START.INDEX , INDEX.NUMBER ] :=
;

```

Scroller control routines

```

: MARK.AVERAGE.PULSE
  PULSE.NUMBER 1 =
  IF FIND.INDEX
  ELSE
    PULSE.NUMBER 3 =
    IF FIND.INDEXES
    THEN
  THEN
    DATA.IN SUB[ START.INDEX , INDEX.NUMBER ]
    MEAN PULSE.MEAN :=
    NAME.TEST
  DO.ANALYSIS
;

```

```

: DECIDE.TO.ANALYSE
  MIDDLE.LEFT SCREEN.CLEAR
  ." To continue" CR
  ." <space>" CR
  PCKEY
  DROP ?DROP
  MIDDLE.LEFT SCREEN.CLEAR
  ." Analyse (Y/N) " BELL CR
  PCKEY
  ?DROP 89 = IF MARK.AVERAGE.PULSE THEN
  MIDDLE.LEFT SCREEN.CLEAR
  VIEW.MENU
  INTERPRET.KEYS
;

```

```

: RESUME.SCROLLING
  RESUME.SCROLL
;

```

```

: MARK.PULSE
  PCKEY ?DROP DROP
  RESUME.SCROLLING
  PCKEY ?DROP DROP
  SCROLL.READOUT
;

```

```
: PULSE.ONE
  SCROLL.READOUT
    ?SCROLL.MARK.INDICES
  END.INDEX.ONE :=
  START.INDEX.ONE :=
;
```

```
: PULSE.TWO
  MARK.PULSE
    ?SCROLL.MARK.INDICES
  END.INDEX.TWO :=
  START.INDEX.TWO :=
;
```

```
: PULSE.THREE
  MARK.PULSE
    ?SCROLL.MARK.INDICES
  END.INDEX.THREE :=
  START.INDEX.THREE :=
;
```

Display data routines

```
: VIEW.DATA
  DATA.IN
  GRAPHICS.DISPLAY
  DEF.SCROLL.PICTURE
  1 ARRAY.SCROLL
  PCKEY ?DROP DROP
  PULSE.NUMBER 3 =
  IF PULSE.ONE PULSE.TWO PULSE.THREE
  ELSE
  PULSE.NUMBER 1 =
  IF PULSE.ONE
  THEN
  THEN
  DECIDE.TO.ANALYSE
;
```

```
: MARK.THREE.PULSES
  3 PULSE.NUMBER :=
;
```

Control to function keys

```
: VIEW.KEYS
  F1 FUNCTION.KEY.DOES ESCAPE
  F4 FUNCTION.KEY.DOES VIEW.DATA
  F6 FUNCTION.KEY.DOES RESUME.SCROLLING
;
```

Scroll marker routines

```
: HOW.MANY.PULSES
  1 PULSE.NUMBER :=
  MIDDLE.LEFT SCREEN.CLEAR
  ." 3 Pulses (Y/N) " BELL CR
  PCKEY
  ?DROP 89 = IF MARK.THREE.PULSES THEN
  MIDDLE.LEFT SCREEN.CLEAR
  VIEW.KEYS
```

File manager routines

```
: GET.SAVED.FILE
  FILENAME DEFER> FILE.OPEN
  1 COMMENT> FILENAME " :=
  1 SUBFILE DATA.IN FILE>ARRAY
  FILE.CLOSE

: READ.FROM.DISK
  MIDDLE.LEFT SCREEN.CLEAR
  ." Read File ? " CR BELL "INPUT
  FILENAME " :=
  GET.SAVED.FILE
  BOTTOM.LEFT SCREEN.CLEAR
  VIEW.MENU
  STORE.FUNCTION.KEYS
  HOW.MANY.PULSES
  INTERPRET.KEYS
  ONESCAPE: RESTORE.FUNCTION.KEYS MENU.DISP

: WRITE.DATA.FILE
  FILENAME DEFER> FILE.OPEN
  FILENAME 1 >COMMENT
  1 SUBFILE DATA.IN ARRAY>FILE
  FILE.CLOSE

: CREATE.DATA.FILE
  FILE.TEMPLATE
  1 COMMENTS
  INTEGER DIM[ DATA.POINTS ] SUBFILE
  1 TIMES
  END
  MIDDLE.LEFT SCREEN.CLEAR
  ." Filename ?"
  CR
  "INPUT FILENAME " :=
  FILENAME DEFER> FILE.CREATE
```

```
: STORE.TO.DISK
  CREATE.DATA.FILE
    MIDDLE.LEFT SCREEN.CLEAR
    ." Creating "
  WRITE.DATA.FILE
    STORE.FUNCTION.KEYS
    MIDDLE.LEFT SCREEN.CLEAR
    BOTTOM.LEFT SCREEN.CLEAR
  VIEW.MENU
  VIEW.KEYS
  INTERPRET.KEYS
  ONESCAPE: RESTORE.FUNCTION.KEYS MENU.DISP
;
```

User interaction

```
: CONTINUE.TO.VIEW
  MIDDLE.LEFT
  SCREEN.CLEAR
  CR
  ." <Space> "CR
  ." to continue .. "
  PCKEY
  ?DROP DROP
  MIDDLE.LEFT SCREEN.CLEAR
  ." Save (Y/N) " BELL CR
  PCKEY ?DROP 89 = IF STORE.TO.DISK THEN
  VIEW.MENU
  VIEW.KEYS
  INTERPRET.KEYS
;
```

A/D Converter configuration routines

```
: CONVERTER.SETUP
  SEND.INTERFACE.CLEAR
  ME TALKER
  MK.HSC LISTENER
  12 STACK.TALK
  1 STACK.TALK
  UNLISTEN
  ME TALKER
  MK.AN1632 LISTENER
  2 STACK.TALK
  UNLISTEN
;
```

Sampling routines

```
: SCOOP
  1000 1 DO
    STACK.LISTEN
    STACK.LISTEN
    SWAP 256 * +
    DATA.IN [ 1 ] :=
    LOOP
;

: DATA.COLLECT
  ME LISTENER
  MK.AN1632 TALKER
  GROUP.EXECUTE.TRIGGER
  SCOOP
  SEND.INTERFACE.CLEAR
;

: READ.IN.DATA
  MIDDLE.LEFT
  BEGIN.READ.INFORMATION
  STACK.CLEAR
  100 MSEC.DELAY
  CONVERTER.SETUP
  DATA.COLLECT
  DATA.IN 0.0385 *
  DATA.IN :=
  END.READ.INFORMATION
  CONTINUE.TO.VIEW
;
```

Subroutine preventing unwanted exit

```
: XYQUIT
  MIDDLE.LEFT SCREEN.CLEAR
  ." Quit (Y/N) " CR
  PCKEY
  ?DROP 89 = IF BYE THEN
  MENU.DISP
;
```

Control to function keys

```
: MAIN.KEYS
  F2 FUNCTION.KEY.DOES READ.IN.DATA
  F3 FUNCTION.KEY.DOES READ.FROM.DISK
  F10 FUNCTION.KEY.DOES XYQUIT
;
```

Main program

```
: MAIN
  CLEAR.FKEYS
  GRAPHICS.DISPLAY
  MAIN.KEYS
  HEADING.DISPLAY
  SIDE.VIEW BOTTOM.LEFT MENU.DISP
  INTERPRET.KEYS
ONERR: NORMAL.DISPLAY {DEF} SCREEN.CLEAR
      ." Unrecoverable error - <ctrl-Break> to restart."
      BELL PCKEY ?DROP DROP BYE
;
```

APPENDIX G

RESULTS LISTING

CONTENTS

G1	Introduction	G2
G2	In vitro results	G3
G2.1	Index of pressure tubing tested	G3
G2.1.1	Damped natural frequency and damping factors for different pressure tubing systems tested.	G4
G2.2	Damped natural frequency and damping factor for pressure tubing connected to stopcocks and flush devices.	G7
G2.3	Index of cannulae tested	G8
G2.3.1	Damped natural frequency and damping factors for cannulae tested.	G9
G2.4	Damped natural frequency and the damping factors for catheter-manometer systems.	G10
G2.5	Damped natural frequency and the damping factors of Swan Ganz catheters.	G13
G3	In vivo results	G14
G3.1	Data file index	G14
G3.2	Heart rate, dp/dt maximum and mean blood pressure for seven patients under-going surgery	G15
G3.3	Peak systolic pressure, diastolic pressure and time delays in blood pressure waveforms	G16
G3.4	Frequency domain analysis	G17
G4	Calculated frequency responses for catheter-manometer systems.	G19

G1 Introduction

The in vitro results for the frequency response evaluation and system parameter analysis for catheter-manometer systems are given in section G2. The data listed were obtained by both the manual and automated data acquisition procedures. The mean values given are calculated from five measurement readings.

In vivo catheter-manometer evaluation, which includes frequency and time domain analysis, is given in section G3.

The calculated frequency response of catheter-manometer models is given in section G4.

G2 IN VITRO RESULTS

G2.1 Index of pressure tubing tested

ID	Length (mm)	Type	Lumen diameter	Outer diameter	Radius ratio
A	300	PE	1.49	3.22	0.462
B	300	PE	1.41	2.98	0.473
H	300	PE	1.53	3.33	0.459
I	300	PE	1.53	3.12	0.490
J	300	PE	1.44	3.08	0.467
C	300	T	1.47	2.35	0.625
G	300	T	1.39	2.27	0.612
E*	400	PE	1.66	3.32	0.5
E*	600	PE	1.66	3.32	0.5
E*	900	PE	1.66	3.32	0.5
E*	1000	PE	1.66	3.32	0.5
D	1200	PE	1.56	3.22	0.484
E	1200	PP	1.66	3.32	0.5
K	1200	PP	1.68	3.18	0.528
L	1200	PP	1.44	2.56	0.562
F	1500	PP	1.53	2.47	0.619

Table G2.1

Table of pressure tubing evaluated. Dimensions are in millimetres. The materials are listed under the column heading "Type".

PE = Polyethylene, PP = Polypropylene, T = Teflon

E cut down from E to length as shown.*

G2.1.1 Damped natural frequency and damping factors for
different pressure tubing systems.

ID	Damped natural frequency			Damping factor		
	range	SD	mean	range	SD(x10 ⁻²)	mean
A	41.9-46.8	± 2.28	44.2	0.14-0.16	± 0.60	0.15
B	37.1-41.6	± 1.55	38.7	0.16-0.19	± 1.10	0.18
C	39.6-43.3	± 1.33	41.9	0.16-0.17	± 0.40	0.16
H	43.9-49.4	± 1.98	45.6	0.13-0.17	± 1.30	0.15
I	44.8-47.8	± 1.06	45.8	0.14-0.16	± 0.74	0.15
J	38.6-42.7	± 1.36	40.8	0.15-0.18	± 1.04	0.16
G	37.5-39.3	± 0.61	38.4	0.21-0.26	± 1.75	0.24
D	17.8-21.7	± 1.38	19.6	0.20-0.23	± 1.12	0.22
E	19.3-20.2	± 0.38	19.7	0.19-0.22	± 1.02	0.20
K	19.5-23.4	± 1.26	21.4	0.18-0.19	± 0.45	0.19
L	14.3-17.2	± 0.93	15.6	0.24-0.25	± 0.44	0.25
F	10.5-15.0	± 1.52	12.9	0.20-0.22	± 0.74	0.21

Table G2.2

Damped natural frequency f_d (Hz) and damping factor for pressure tubing.

ID	Damped natural frequency			Damping factor		
	range	SD	mean	range	SD(x10 ⁻²)	mean
A	39.7-44.2	± 1.76	42.1	0.14-0.17	± 0.71	0.16
B	35.9-40.0	± 1.36	38.4	0.17-0.19	± 0.72	0.18
C	37.7-43.8	± 1.97	40.5	0.16-0.17	± 0.44	0.17
H	42.6-44.6	± 0.80	43.4	0.13-0.17	± 1.42	0.15
I	44.0-46.9	± 1.01	45.1	0.14-0.16	± 0.74	0.15
J	37.5-42.8	± 1.96	40.6	0.16-0.18	± 0.94	0.17
G	36.1-38.4	± 0.93	37.3	0.23-0.26	± 1.23	0.24
D	16.7-21.6	± 1.77	19.0	0.21-0.23	± 0.82	0.22
E	18.1-19.4	± 0.40	18.8	0.19-0.22	± 1.22	0.20
K	19.0-21.3	± 1.01	19.8	0.19-0.21	± 0.73	0.20
L	12.7-15.2	± 0.91	14.3	0.24-0.26	± 0.71	0.25
F	10.5-15.1	± 1.53	12.9	0.20-0.22	± 0.74	0.21

Table G2.3

Damped natural frequency f_d (Hz) and damping factor for pressure tubing coiled around an 8 cm diameter cylinder.

ID	Damped natural frequency			Damping factor		
	range	SD	mean	range	SD($\times 10^{-2}$)	mean
A	40.7-45.6	± 2.16	43.2	0.15-0.16	± 0.41	0.16
B	36.5-40.0	± 1.11	38.4	0.17-0.19	± 0.79	0.18
C	39.4-43.8	± 1.60	41.1	0.16-0.17	± 0.44	0.16
H	42.6-45.8	± 1.17	43.8	0.13-0.17	± 1.44	0.15
I	44.4-47.8	± 1.25	45.4	0.14-0.16	± 0.74	0.15
J	37.7-41.8	± 1.56	40.0	0.15-0.18	± 1.23	0.17
G	36.3-38.8	± 0.91	37.6	0.23-0.26	± 1.43	0.24
D	17.9-20.7	± 1.32	19.0	0.20-0.23	± 1.11	0.22
E	18.8-20.2	± 0.62	19.3	0.19-0.22	± 1.14	0.20
K	18.7-21.7	± 1.17	20.1	0.19-0.21	± 0.71	0.20
L	12.8-15.7	± 1.13	14.7	0.24-0.26	± 0.60	0.25
F	10.5-15.0	± 1.52	12.9	0.20-0.22	± 0.69	0.21

Table G2.4

Damped natural frequency f_d (Hz) and damping factor for pressure tubing coiled around an 15 cm diameter cylinder.

ID	Damped natural frequency			Damping factor		
	range	SD	mean	range	SD($\times 10^{-2}$)	mean
A	43.6-46.8	± 1.23	44.9	0.14-0.15	± 0.41	0.15
B	38.9-41.4	± 0.81	40.2	0.16-0.19	± 1.74	0.19
C	39.6-44.3	± 1.54	41.7	0.15-0.17	± 0.55	0.16
H	44.0-49.1	± 1.79	46.6	0.13-0.17	± 1.46	0.15
I	45.6-48.0	± 0.91	46.4	0.14-0.16	± 0.69	0.15
J	39.8-42.8	± 1.19	41.0	0.15-0.17	± 0.71	0.16
G	38.4-40.9	± 0.98	39.6	0.21-0.25	± 1.41	0.23
D	18.7-20.6	± 0.70	20.0	0.20-0.23	± 0.89	0.22
E	19.6-21.7	± 0.77	20.8	0.19-0.21	± 0.78	0.20
K	21.3-23.5	± 0.79	22.4	0.17-0.19	± 0.76	0.19
L	13.8-16.8	± 1.10	15.7	0.23-0.25	± 0.71	0.24
F	10.5-15.0	± 1.52	12.9	0.19-0.21	± 0.67	0.20

Table G2.5

Damped natural frequency f_d (Hz) and damping factor for pressure tubing twisted through 720° around its longitudinal axis.

Length (mm)	f_d (Hz)			β		
	range	mean	SD	range	mean	SD(β)
300	38.7-46.5	42.4	± 2.56	0.14-0.16	0.15	± 0.71
400	36.6-42.0	39.2	± 1.85	0.16-0.19	0.18	± 1.04
600	21.8-26.1	23.8	± 2.14	0.17-0.19	0.18	± 0.69
900	18.4-23.3	22.1	± 1.85	0.17-0.19	0.18	± 0.74
1000	18.4-22.0	19.8	± 1.20	0.18-0.19	0.18	± 0.43
1200	19.3-20.2	19.7	± 1.20	0.19-0.22	0.20	± 1.04

Table G2.6

Damped natural frequency and damping factor for: Polyethylene pressure tubing (ID = "E"). Internal diameter 1.66 mm and 0.82 mm wall thickness. Standard deviation for damping factor ($\times 10^{-2}$). Boiled saline.

Length (mm)	f_d (Hz)			β		
	range	mean	SD(f_d)	range	mean	SD(β)
300	36.1-42.5	38.8	± 2.26	0.15-0.16	0.15	± 0.40
400	33.7-38.8	36.8	± 1.84	0.17-0.19	0.18	± 0.74
600	19.8-23.9	21.4	± 1.44	0.18-0.19	0.18	± 0.39
900	18.5-22.0	20.2	± 1.12	0.18-0.20	0.19	± 0.72
1000	17.5-18.8	18.0	± 0.47	0.19-0.20	0.19	± 0.58
1200	16.8-17.5	17.2	± 0.27	0.20-0.23	0.22	± 1.01

Table G2.7

Damped natural frequency and damping factor for: Polyethylene pressure tubing (ID = "E"). Internal diameter 1.66 mm and 0.82 mm wall thickness. Standard deviation for damping factor ($\times 10^{-2}$). Non-boiled saline.

G2.2 Damped natural frequency and damping factors for pressure tubing connected to stopcocks and flush devices.

In the tables listed below the ID refers to the pressure tubing tested in section G2.1.1. The pressure tubing was connected in series with a 3-way stopcock and an intraflow/flush device (the stopcock was connected between the pressure tube and flush device). The saline was boiled and debubbled and cooled to 25 °C.

ID	Damped natural frequency			Damping factor		
	range	SD	mean	range	SD(x10 ⁻²)	mean
A	29.4-30.1	± 0.22	29.8	0.22-0.24	± 0.68	0.23
C	26.7-28.0	± 0.50	27.5	0.28-0.30	± 0.55	0.29
I	26.8-27.4	± 0.24	27.1	0.28-0.30	± 0.79	0.29
G	30.5-31.3	± 0.26	30.9	0.23-0.26	± 1.04	0.25
E	16.1-17.0	± 0.34	16.6	0.19-0.20	± 0.38	0.19
K	14.9-16.5	± 0.53	15.9	0.18-0.19	± 0.43	0.19
L	14.9-15.7	± 0.40	15.3	0.28-0.30	± 0.61	0.29
F	11.5-12.9	± 0.48	12.3	0.31-0.35	± 1.37	0.32

Table G2.8

Damped natural frequency f_d (Hz) and damping factor for catheter systems.

G2.3 Index of cannulae tested

Cannulae ID	Size gauge	Lumen diameter	Wall Thickness
19	18	0.99	0.18
18	18	0.97	0.19
20	20	0.75	0.26
17	20	0.79	0.17
24	20	0.77	0.15
21	20	0.70	0.16
25	20	0.39	0.16
16	22	0.62	0.11
15	22	0.59	0.16
14	24	0.46	0.12
23	24	0.48	0.12
13	26	0.47	0.11

Table G2.9

Cannulae characteristics. The dimensions are in millimetres. The material is Teflon.

G2.3.1 Damped natural frequency and damping factors of cannulae tested.

ID	Damped natural frequency			Damping factor		
	range	SD	mean	range	SD(x10 ⁻²)	mean
19	56.3-56.8	± 0.17	56.6	0.11-0.12	± 0.41	0.12
18	45.3-46.0	± 0.27	45.6	0.10-0.11	± 0.38	0.10
20	48.9-50.3	± 0.47	49.7	0.17-0.18	± 0.65	0.18
17	42.8-43.9	± 0.39	43.3	0.11-0.12	± 0.44	0.12
24	41.2-43.1	± 0.73	42.3	0.22-0.24	± 0.79	0.23
21	50.1-51.2	± 0.36	50.6	0.17-0.18	± 0.41	0.17
25	34.4-36.8	± 1.06	35.1	0.15-0.16	± 0.39	0.16
16	52.6-53.5	± 0.32	52.9	0.30-0.33	± 1.41	0.32
15	45.3-46.1	± 0.30	45.8	0.19-0.20	± 0.38	0.19
14	28.1-29.6	± 0.53	28.6	0.25-0.27	± 0.71	0.26
23	43.3-44.9	± 0.58	44.3	0.23-0.25	± 0.55	0.24
13	25.1-28.8	± 1.40	27.7	0.41-0.44	± 1.03	0.43

Table G2.10

Damped natural frequency f_d (Hz) and damping factor range for cannulae not pressurized externally.

ID	Damped natural frequency			Damping factor		
	range	SD	mean	range	SD(x10 ⁻²)	mean
19	57.1-57.7	± 0.22	57.3	0.11-0.12	± 0.40	0.11
18	45.5-46.4	± 0.34	46.1	0.09-0.11	± 0.57	0.10
20	49.0-50.3	± 0.42	49.8	0.17-0.18	± 0.37	0.17
17	43.2-43.9	± 0.25	43.6	0.10-0.12	± 0.71	0.11
24	42.9-44.0	± 0.40	43.4	0.22-0.23	± 0.40	0.22
21	50.1-51.9	± 0.60	50.9	0.16-0.18	± 0.59	0.17
25	35.1-37.4	± 0.83	36.3	0.15-0.16	± 0.39	0.15
16	53.0-54.8	± 0.69	53.4	0.31-0.33	± 1.14	0.32
15	45.0-48.1	± 1.18	46.5	0.18-0.19	± 0.38	0.19
14	28.3-31.2	± 1.13	29.9	0.25-0.27	± 0.71	0.26
23	43.8-46.0	± 0.81	45.1	0.23-0.25	± 0.65	0.24
13	25.1-28.8	± 1.40	27.7	0.41-0.44	± 1.03	0.43

Table G2.11

Damped natural frequency f_d (Hz) and damping factor for cannulae pressurized by 100 mmHg externally.

G2.4 Damped natural frequency and the damping factors for catheter-manometer systems.

Damped natural frequency and damping factor were tested for combinations of: (1) cannulae and (2) flush device, stopcock and pressure tubing. For both (1) and (2), only the systems with the highest resonant frequency (tables G2.2 and G2.10) were considered.

The system and cannulae ID's in table G2.12-14 indicate the selections from table G2.5 and the system from table G2.12 respectively.

Sys ID	Cannula ID			
	20	21	16	23
A	25.5 (± 0.68)	27.0 (± 1.01)	24.4 (± 0.94)	22.5 (± 0.89)
G	25.8 (± 0.75)	26.2 (± 1.16)	26.5 (± 1.48)	20.0 (± 0.90)
E	15.6 (± 0.41)	16.3 (± 0.54)	17.9 (± 0.75)	15.6 (± 0.25)
L	14.5 (± 0.25)	14.4 (± 0.43)	13.8 (± 0.49)	12.9 (± 0.85)
F	12.0 (± 0.83)	12.4 (± 0.92)	11.5 (± 0.58)	11.4 (± 0.65)

Table G2.12a

Damped natural frequency f_d (Hz) for catheter-manometer systems. The saline was boiled and used at 25 °C. Standard deviation in brackets.

Sys ID	Cannulae ID			
	20	21	16	23
A	0.17 (± 0.72)	0.15 (± 1.31)	0.24 (± 1.96)	0.28 (± 1.38)
G	0.19 (± 0.70)	0.15 (± 1.04)	0.28 (± 1.28)	0.27 (± 1.33)
E	0.22 (± 1.39)	0.22 (± 1.03)	0.27 (± 1.35)	0.30 (± 0.96)
L	0.29 (± 0.55)	0.26 (± 1.11)	0.29 (± 0.97)	0.32 (± 0.84)
F	0.33 (± 1.26)	0.33 (± 1.04)	0.31 (± 1.56)	0.34 (± 1.69)

Table G2.12b

Damping factor β for catheter-manometer systems. The saline was boiled and used at 25 °C. Standard deviation ($\times 10^{-2}$) in brackets.

Sys ID	Cannulae ID			
	20	21	16	23
A	23.7 (± 0.49)	24.9 (± 0.41)	22.0 (± 0.74)	20.3 (± 0.65)
G	23.3 (± 0.55)	25.5 (± 0.29)	23.4 (± 0.72)	21.2 (± 1.55)
E	14.7 (± 0.19)	15.6 (± 0.14)	14.8 (± 0.27)	14.3 (± 0.32)
L	12.9 (± 0.26)	14.0 (± 0.29)	12.8 (± 0.35)	11.8 (± 0.44)
F	11.1 (± 0.51)	11.7 (± 0.48)	10.6 (± 0.43)	10.6 (± 0.28)

Table G2.13a

Damped natural frequency f_d (Hz) for catheter-manometer systems. The saline was not boiled and used at 25 °C. Standard deviation in brackets.

Sys ID	Cannulae ID			
	20	21	16	23
A	0.18 (± 0.39)	0.19 (± 0.36)	0.27 (± 0.66)	0.32 (± 0.79)
G	0.20 (± 1.04)	0.19 (± 1.01)	0.29 (± 0.71)	0.30 (± 0.84)
E	0.24 (± 0.67)	0.23 (± 0.66)	0.29 (± 0.78)	0.32 (± 0.80)
L	0.30 (± 1.03)	0.29 (± 0.65)	0.31 (± 1.37)	0.32 (± 0.77)
F	0.35 (± 0.62)	0.35 (± 0.44)	0.33 (± 0.39)	0.37 (± 0.66)

Table G2.13b

Damping factor β for catheter-manometer systems. The saline was not boiled and used at 25 °C. Standard deviation ($\times 10^{-2}$) in brackets.

Sys ID	Cannulae ID			
	20	21	16	23
A	24.1 (± 1.10)	25.8 (± 1.16)	23.2 (± 0.84)	20.7 (± 1.03)
G	24.5 (± 0.95)	24.9 (± 1.17)	25.6 (± 1.29)	19.5 (± 1.44)
E	14.3 (± 0.33)	15.3 (± 0.41)	15.2 (± 0.37)	14.4 (± 0.78)
L	13.8 (± 0.50)	13.7 (± 0.60)	12.9 (± 0.69)	11.8 (± 0.54)
F	11.3 (± 0.56)	11.5 (± 0.97)	10.6 (± 0.29)	10.5 (± 0.41)

Table G2.14a

Damped natural frequency f_d (Hz) for catheter-manometer systems. The saline was boiled and used at 37 °C. Standard deviation in brackets.

Sys ID	Cannulae ID			
	20	21	16	23
A	0.17 (± 0.71)	0.16 (± 0.67)	0.25 (± 1.37)	0.29 (± 1.04)
G	0.20 (± 1.08)	0.17 (± 0.71)	0.29 (± 1.38)	0.28 (± 1.53)
E	0.23 (± 0.65)	0.24 (± 0.68)	0.29 (± 0.68)	0.32 (± 0.39)
L	0.29 (± 0.98)	0.27 (± 0.40)	0.31 (± 0.96)	0.35 (± 3.51)
F	0.33 (± 1.04)	0.34 (± 1.00)	0.32 (± 0.66)	0.34 (± 1.67)

Table G2.14b

Damping factor β for catheter-manometer systems. The saline was boiled and used at 37 °C. The standard deviation ($\times 10^{-2}$) is given in brackets.

G2.5 Damped natural frequency and the damping factors of Swan Ganz catheters.

Sys ID	prox orifice β	prox orifice f_d	dis orifice β	dis orifice f_d
A	0.23 (± 1.17)	9.3 (± 0.20)	0.37 (± 1.19)	9.2 (± 0.19)
B	0.19 (± 1.03)	11.3 (± 0.24)	0.22 (± 1.38)	10.4 (± 0.12)

Table G2.15

Mean values and standard deviations for damped natural frequency f_d (Hz) and damping factor β (standard deviation for damping $\times 10^{-2}$) for Swan Ganz catheters (7F). Saline is boiled and measurements are taken at 25 °C.

Sys ID	prox orifice β	prox orifice f_d	dis orifice β	dis orifice f_d
A	0.22 (± 1.01)	6.2 (± 0.20)	0.29 (± 0.89)	5.7 (± 0.08)
B	0.27 (± 0.79)	8.4 (± 0.12)	0.32 (± 1.12)	7.5 (± 0.12)

Table G2.16

Mean values and standard deviations for damped natural frequency f_d (Hz) and damping factor β (standard deviation for damping $\times 10^{-2}$) for Swan Ganz catheters (5F). Saline is boiled and measurements are taken at 25 °C.

G3 IN VIVO RESULTS

G3.1 Data file index

File Number	Sex	Age	Operation
NVSL.005 NVLL.025	M	56	CB
NVSL.026 NVLL.036 NVSL.056 NVLL.046	F	40	MV
NVSL.009 NVLL.019	F	18	MV
NVSL.047 NVLL.057 NVSL.007 NVLL.017	M	18	MV/AV
NVSL.027 NVLL.037	M	45	MV
NVSL.067 NVLL.077	F	37	MV
NVSL.098 NVLL.088	M	43	CB
NVSL.128 NVLL.138	M	55	MV

Table G3.1

Patient index table listing age, sex and type of operation.

MV = mitral valve replacement

AV = aortic valve replacement

CB = coronary bypass

G3.2 Heart rate, dp/dt maximum and mean blood pressure for seven patients under-going cardiac surgery.

File Number	rate (bpm)	dp/dt max (mmHg/sec)	Mean (mmHg)
NVSL.005	65	534.2	93
NVLL.025	78	364.2	91
NVSL.026	77	439.1	91
NVLL.036	74	409.0	90
NVSL.056	77	407.0	85
NVLL.046	88	341.2	89
NVSL.009	65	1129.2	74
NVLL.019	64	414.0	76
NVSL.047	100	402.4	82
NVLL.057	130	253.3	83
NVSL.007	100	328	85
NVLL.017	98	365.8	82
NVSL.027	103	334.6	82
NVLL.037	87	447.1	86
NVSL.067	140	178.0	66
NVLL.077	117	298.0	67
NVSL.098	105	685.7	82
NVLL.088	103	712.7	81
NVSL.128	109	711.0	68
NVLL.138	107	749.5	66

Table G3.2

Average values for heart rate, dp/dt maximum and mean blood pressure

G3.3 Peak systolic pressure, end diastolic pressure and time delays in blood pressure waveforms.

File Number	peak systolic (mmHg)	end diastolic (mmHg)	systolic (s)	dicrotic (s)
NVSL.005	116.9	73.0	0.16	0.35
NVLL.025	112.5	74.4	0.12	0.30
NVSL.026	115.5	83.0	0.13	0.33
NVLL.036	109.6	76.0	0.10	0.24
NVSL.056	109.6	70.0	0.13	0.30
NVLL.046	109.1	75.0	0.11	0.30
NVSL.009	98.7	60.0	0.16	0.33
NVLL.019	101.7	60.0	0.15	0.42
NVSL.047	116.8	69.0	0.10	0.28
NVLL.057	113.6	60.3	0.16	0.29
NVSL.007	112.8	72.0	0.12	0.30
NVLL.017	111.9	66.0	0.10	0.26
NVSL.027	110.4	76.0	0.12	0.29
NVLL.037	118.3	72.1	0.16	0.29
NVSL.067	87.6	54.0	0.14	0.23
NVLL.077	97.9	53.0	0.12	0.21
NVSL.098	118.3	49.7	0.09	0.35
NVLL.088	118.2	50.0	0.10	0.33
NVSL.128	115.0	41.0	0.09	0.33
NVLL.138	111.2	41.0	0.08	0.35

Table G3.3

Average values for peak systolic, end diastolic pressures and the time delay in seconds for the onset of peak systolic pressure and the dicrotic notch.

G3.4 Frequency domain analysis

The harmonic number and the subsequent relative amplitude (the fundamental has a nominal amplitude of one) are given in the tables listed below.

The file number of each patient is given and refers to the patient index, table G3.1. Furthermore, the term in brackets refers to the frequency at which the harmonic occurs.

File No	Relative amplitude (frequency)			
	1	2	3	4
NVSL.005	0.53 (2.4)	0.36 (3.6)	0.20 (4.8)	0.23 (6.0)
NVLL.025	0.51 (2.8)	0.37 (4.3)	0.20 (5.8)	0.22 (7.1)
NVSL.015	0.59 (3.1)	0.39 (4.7)	0.23 (6.3)	0.22 (7.7)
NVLL.035	0.52 (2.8)	0.37 (4.3)	0.21 (5.7)	0.26 (7.0)
NVSL.026	0.53 (2.8)	0.34 (4.3)	0.20 (5.7)	0.23 (7.0)
NVLL.036	0.50 (2.5)	0.35 (3.9)	0.20 (5.2)	0.24 (6.4)
NVLL.046	0.52 (3.2)	0.34 (4.9)	0.26 (6.5)	0.25 (8.0)
NVSL.056	0.55 (2.9)	0.36 (4.4)	0.23 (5.9)	0.20 (7.2)
NVSL.007	0.72 (3.7)	0.43 (5.6)	0.26 (7.5)	0.15 (9.3)
NVLL.017	0.69 (3.5)	0.45 (5.4)	0.29 (7.2)	0.20 (9.0)
NVSL.027	0.72 (3.9)	0.44 (5.8)	0.25 (7.7)	0.15 (9.6)
NVLL.037	0.79 (3.3)	0.55 (5.0)	0.24 (6.7)	0.13 (8.4)
NVSL.047	0.65 (3.6)	0.37 (5.6)	0.21 (7.4)	0.17 (9.2)
NVLL.057	0.69 (4.9)	0.21 (7.8)	0.15 (9.9)	0.06 (11.9)
NVSL.067	0.46 (5.5)	0.19 (8.1)	0.10 (10.6)	0.10 (12.8)
NVLL.077	0.55 (4.5)	0.31 (6.7)	0.17 (8.9)	0.07 (10.9)
NVLL.138	0.47 (3.6)	0.30 (5.7)	0.18 (7.6)	0.15 (9.4)
NVSL.128	0.46 (3.7)	0.31 (5.9)	0.19 (7.8)	0.16 (9.7)
NVSL.098	0.45 (3.6)	0.30 (5.7)	0.20 (7.5)	0.18 (9.4)
NVLL.088	0.48 (3.6)	0.29 (5.7)	0.21 (7.5)	0.18 (9.3)
NVSL.009	0.61 (2.3)	0.35 (3.6)	0.22 (4.8)	0.19 (6.0)
NVLL.019	0.62 (2.3)	0.37 (3.5)	0.23 (4.8)	0.22 (5.9)

Table G3.4

Relative amplitude (for the first four harmonics) and the corresponding frequency for blood pressure pulses analysed in the frequency domain.

File No	Relative amplitude (frequency)			
	5	6	7	8
NVSL.005	0.23 (7.0)	0.15 (8.2)	0.11 (9.4)	0.12 (10.5)
NVLL.025	0.19 (8.5)	0.14 (10.0)	0.11 (11.3)	0.09 (12.7)
NVSL.015	0.14 (9.2)	0.09 (10.6)	0.08 (11.9)	0.07 (13.3)
NVLL.035	0.22 (8.3)	0.14 (9.7)	0.13 (11.0)	0.10 (12.3)
NVSL.026	0.17 (8.3)	0.12 (9.7)	0.11 (10.9)	0.09 (12.3)
NVLL.036	0.22 (7.6)	0.16 (8.9)	0.15 (10.1)	0.13 (11.3)
NVLL.046	0.18 (9.6)	0.14 (11.1)	0.11 (12.7)	0.08 (14.2)
NVSL.056	0.16 (8.6)	0.10 (9.7)	0.08 (11.3)	0.06 (12.6)
NVSL.007	0.11 (11.0)	0.07 (12.7)	0.05 (14.3)	0.06 (15.8)
NVLL.017	0.12 (10.8)	0.05 (12.5)	0.06 (14.1)	0.05 (15.6)
NVSL.027	0.07 (11.4)	0.06 (13.0)	0.06 (14.8)	0.05 (16.3)
NVLL.037	0.08 (13.5)	0.13 (15.1)	0.08 (16.9)	0.06 (22.5)
NVSL.047	0.10 (10.9)	0.09 (12.7)	0.05 (14.5)	0.05 (19.1)
NVLL.057	0.15 (14.1)	0.11 (16.4)	0.09 (18.7)	0.08 (20.9)
NVSL.067	0.10 (15.1)	0.07 (17.5)	0.07 (19.8)	0.07 (22.1)
NVLL.077	0.07 (12.8)	0.07 (14.8)	0.07 (16.8)	0.05 (18.7)
NVLL.138	0.14 (11.2)	0.14 (13.1)	0.15 (14.9)	0.15 (16.9)
NVSL.128	0.15 (11.6)	0.14 (13.5)	0.13 (15.4)	0.12 (17.3)
NVSL.098	0.18 (11.1)	0.16 (13.0)	0.14 (14.8)	0.11 (16.6)
NVLL.088	0.16 (11.1)	0.15 (12.9)	0.11 (14.7)	0.11 (16.4)
NVSL.009	0.13 (7.0)	0.10 (8.1)	0.08 (9.3)	0.07 (10.4)
NVLL.019	0.15 (6.9)	0.10 (8.1)	0.08 (9.2)	0.07 (10.2)

Table G3.5

Relative amplitude (for harmonics 5 to 8) and the corresponding frequency for blood pressure pulses analysed in the frequency domain.

G4 Calculated frequency response parameters for catheter-
manometer systems.

Equations 2.9 and 2.10 were used to calculate the damping factor and resonant frequency respectively. The values ascribed to the parameters are:

$$p = 1.0046 \times 10^{-3} \text{ kg} \cdot \text{m}^{-3} \quad (\text{Greiner labortechnik, 1987})$$

$$E = 0.2 \times 10^9 \text{ Pa} \quad (\text{Goodfellow metals manual, 1987})$$

$$\nu = 0.9 \times 10^{-3} \text{ kg/m} \cdot \text{s} \quad (\text{Bueche, 1979})$$

System ID	Length (mm)	Type	f_p (Hz)	f_d (Hz)	β
A	300	PE	42.08	42.39	0.07
B	300	PE	38.34	38.71	0.08
H	300	PE	43.97	44.30	0.07
I	300	PE	46.64	46.89	0.06
J	300	PE	39.75	40.14	0.08
C	300	T	50.46	50.47	0.01
G	300	T	45.27	45.28	0.01
E*	400	PE	34.63	35.16	0.10
E*	600	PE	20.61	21.79	0.19
E*	900	PE	12.03	14.98	0.36
E*	1000	PE	10.43	14.29	0.42
D	1200	PE	7.58	20.09	0.62
K	1200	PP	14.05	14.26	0.10
L	1200	PP	10.69	11.01	0.14
F	1500	PP	9.01	9.59	0.20

Table G3.6

Calculated frequency responses using the Bruner (1978) model.

Equations B1.24 and B1.25 and the Bessel functions given in table B1.2 were used to determine the characteristic impedance of a pressure tube. The impedance is substituted in equation B1.22 and the resonant frequency and damping factor are calculated.

System ID	Length (mm)	Type	f_p (Hz)	f_d (Hz)	β
A	300	PE	41.28	41.45	0.09
B	300	PE	39.24	39.43	0.10
H	300	PE	42.14	42.24	0.07
I	300	PE	44.33	44.41	0.06
J	300	PE	37.03	37.25	0.11
C	300	T	49.24	49.30	0.05
G	300	T	44.67	44.78	0.07
E*	400	PE	35.21	35.43	0.11
E*	600	PE	21.65	22.07	0.19
E*	900	PE	13.01	13.51	0.26
E*	1000	PE	11.78	12.48	0.31
D	1200	PE	10.21	11.27	0.39
K	1200	PP	13.56	13.76	0.16
L	1200	PP	10.35	10.07	0.15
F	1500	PP	8.75	9.03	0.24

Table G3.7

Calculated frequency responses using the Yeomanson and Evans model.

APPENDIX H

EQUIPMENT SPECIFICATIONS

CONTENTS

H1	Racal store 7DS FM tape recorder	H2
H2	Bio-Tek blood pressure system calibrator frequency response characteristics	H6
H3	Blood pressure amplifier BAP 001	H7
H4	HP Vectra	H8
H5	Microlink	H9

H1 RACAL STORE 7DS FM TAPE RECORDER (RACAL, 1987)

SPECIFICATION

The policy of Racal Recorders Limited is one of continuous development, and consequently the equipment may vary in detail from the description and specification in this publication.

TAPE/HEAD PARAMETERS (Store 4DS)

Tape: Width: 6.25mm ($\frac{1}{4}$ in)
Thickness: 18 to 35 μ m
(.0007 to .0014 in). Triple Play to Long Play.

Spools: Max 210mm ($8\frac{1}{2}$ in) diameter with standard ciné-centre hub. Maximum capacity 1460 m (4800ft) of 18 μ m (Triple Play) tape.

Heads: 4 track in line:
Track width 0.89mm Track pitch 1.78mm Record/Replay distance 50.8mm (2.0 in)
Erase head automatically energised in Forward Record mode only while all four channels are recording. (Optional facility for reverse erase)

Time Base Error (TBE): Peak time displacement between reference track and crystal reference frequency Measured in TAPE mode according to I.R.I.G. 118-73

Tape Speed in/s	TBE μ s zero to peak
60	± 1.5
30	± 1.5
15	± 2
$7\frac{1}{2}$	± 4
$3\frac{3}{4}$	± 8
$1\frac{7}{8}$	± 12
$\frac{1}{2}$	± 20

Interchannel Time Displacement Error (I.T.D.E.): Observed error after record/replay between adjacent tracks. Measured according to I.R.I.G. 118-73

Tape Speed in/s	I.T.D.E. μ s zero to peak
60	± 0.5
30	± 1
15	± 2
$7\frac{1}{2}$	± 4
$3\frac{3}{4}$	± 8
$1\frac{7}{8}$	± 16
$\frac{1}{2}$	± 32

3. TAPE/HEAD PARAMETERS (Store 7DS)

Tape: Width: 12.7mm ($\frac{1}{2}$ in)
Thickness: 26 to 35 μ m or 18 to 26 μ m if alternative tension spring (supplied) is fitted.

Spools: Type: 203mm (8 in) diameter precision metal spools with NAB (or NART8) hubs.

Spool Capacity: 3,600 ft (1100 m) of .0008 in (20 μ m) tape.
2,400 ft (740 m) of .0012 in (30 μ m) tape.
1,800 ft (550 m) of .0015 in (38 μ m) tape.

Heads: Interlaced 3 + 4 record and reproduce head stacks in accordance with I.R.I.G. 106-73. Cue track (for voice) on edge of tape adjacent to track 7. Azimuth ± 1 minute of arc. Gap Scatter - 100 μ in. Inter-stack spacing: 1.5 in ± 0.0005 in.

Time Base Error (TBE): Peak time displacement between reference track and crystal reference frequency. Measured in TAPE mode according to I.R.I.G. 118-73

Tape Speed in/s	TBE (Channel 3) μ s zero to peak
60	± 1.5
30	± 1.5
15	± 2.0
$7\frac{1}{2}$	± 4
$3\frac{3}{4}$	± 8
$1\frac{7}{8}$	± 12
$\frac{1}{2}$	± 20

Interchannel Time Displacement Error (I.T.D.E.) Observed error after record/replay between adjacent tracks on the same head. Measured according to I.R.I.G. 118-73.

Tape Speed	I.T.D.E.
in/s	μ s zero to peak
60	± 0.7
30	± 1.5
15	± 3
$7\frac{1}{2}$	± 6
$3\frac{3}{4}$	± 12
$1\frac{7}{8}$	± 25
$\frac{1}{2}$	± 50

TAPE TRANSPORT

Tape Speeds: 60, 30, 15, $7\frac{1}{2}$, $3\frac{3}{4}$, $1\frac{7}{8}$ and $\frac{1}{2}$ in/s (152.4, 76.2, 38.1, 19.05, 9.52, 4.76, 2.38, cm/s). Electrically selected by front panel rotary switch, or via remote socket.

Tape speed may also be controlled by an external oscillator giving any speed in the range 0.45 in/s to 90 in/s.

Tape Speed Accuracy: $\pm 0.2\%$ (TACH mode).
Flutter: Measured per I.R.I.G. 106-73 (2 sigma) (TACH mode).

Tape Speed in/s	Bandwidth Hz	%Flutter (peak to peak)
60	0.2 to 10,000	0.35
30	0.2 to 5,000	0.35
15	0.2 to 2,500	0.35
$7\frac{1}{2}$	0.2 to 1,250	0.35
$3\frac{3}{4}$	0.2 to 625	0.35
$1\frac{7}{8}$	0.2 to 313	0.45
$\frac{1}{2}$	0.2 to 156	0.55

Tape Position Indicator: 4 digit resettable counter reading in feet to an accuracy of $\pm 2\%$.

Capstan Servo Control: Internal crystal reference 100 kHz at 60 in/s, 50 kHz at 30 in/s and pro rata. Reference Oscillator stability, better than $\pm 50 \times 10^{-6}$ over the operating temperature range.

Servo Control Mode: TAPE or TACH modes selectable by internal switch.

Capstan Servo Performance: Synchronisation of capstan motor to the oscillator maintained to accelerations of 100 rad/s².

Start Time: From Command to meeting flutter specification:-

Speed in/s	Time (seconds)
60	1.5
$\frac{1}{2}$	0.075

Stop Time: 1.5s at 60 in/s

Fast Wind Time: (Store 4DS) Less than 7 minutes for 1,000m (3280 feet) of tape.

Fast Wind Time: (Store 7DS) 4.8 minutes for 700m (2300 feet) of tape.

Tape Movement Controls: Momentary action push buttons for, Stop; Forward; Reverse; Fast Forward; Fast Reverse; Record. (Record electronically interlocked).

5. F.M. SIGNAL ELECTRONICS (Dual Standard). Measurements are taken as laid down in the I.R.I.G. specification 118-73.

(a) Bandwidth and Signal-to-Noise Ratio (Wideband 1).

Tape Speed in/s	Bandwidth* ± 0.5 dB	Signal-to-Noise Ratio dB	
		Store 4DS	Store 7DS
60	DC to 40,000 Hz	48	50
30	DC to 20,000 Hz	48	50
15	DC to 10,000 Hz	48	50
$7\frac{1}{2}$	DC to 5,000 Hz	48	48
$3\frac{3}{4}$	DC to 2,500 Hz	48	48
$1\frac{7}{8}$	DC to 1,250 Hz	46	46
$\frac{1}{2}$	DC to 625 Hz	45	44

* Tchebychef Filter

(b) Bandwidth and Signal-to-Noise Ratio (Intermediate Band).

Tape Speed in/s	Bandwidth * ±0.5 dB	Signal-to-Noise Ratio	
		Store 4DS	Store 7DS
60	DC to 20,000 Hz	48	52
30	DC to 10,000 Hz	48	52
15	DC to 5,000 Hz	48	52
7½	DC to 2,500 Hz	48	50
3¾	DC to 1,250 Hz	48	50
1½	DC to 625 Hz	46	46
¾	DC to 312 Hz	45	45

* Tchebycheff Filter.

(c) Bandwidths for Bessel mode of operation are contained in the following table:-

Tape Speed in/s	Bessel Bandwidths	
	Wideband I +0dB to -3dB	Intermediate Band +0dB to -3dB
60	DC to 32,000 Hz	DC to 16,000 Hz
30	DC to 16,000 Hz	DC to 8,000 Hz
15	DC to 8,000 Hz	DC to 4,000 Hz
7½	DC to 4,000 Hz	DC to 2,000 Hz
3¾	DC to 2,000 Hz	DC to 1,000 Hz
1½	DC to 1,000 Hz	DC to 500 Hz
¾	DC to 500 Hz	DC to 250 Hz

Filter Response: Tchebycheff (Flat response)
Bessel (Linear phase response)

Flutter Compensation: Selected by means of an internal switch; can improve basic signal-to-noise ratio by up to 10 dB at low tape speeds.

Carrier Frequency: Wideband I; 3600 Hz per inch per second of tape speed. Intermediate band; 1800 Hz per inch per second of tape speed.

Carrier Deviation: =40%

System Drift: After 15 minutes setting period, ±0.5% of full scale output in 8 hours with 10°C change in ambient temperature.

Input Sensitivity: A twelve position switch on each Record Board is calibrated in volts peak for full carrier deviation; Range 0.1 volt to 20 volt.

Input Sensitivity: (Contd) Additional positions are:-
OFF record disable.
REF reference frequency.
"- " full negative deviation.
"+ " full positive deviation.

Input Impedance: 100k ohms ±2% in parallel with 50 pF unbalanced.

Input Overload: Input circuits are protected to a maximum continuous input of ±100 volt.

Output: Continuously variable from 0 to 6 volts peak to peak for full deviation.

Output Impedance: Less than 1 ohm.

Output Current: Output short circuit protected. Minimum load impedance 600Ω in parallel with 1000 pF.

Overall System Linearity: ±0.3% deviation from best straight line through zero.

Harmonic Distortion: Less than 1.2% at maximum modulation level.

Intermodulation Distortion: Less than 1%

Variable Offset: Up to ±20 volts referred to input.

Fixed Offset: Switch selectable for recording unipolar signals using full dynamic range.

6. D.R. SIGNAL ELECTRONICS

Frequency Response and Signal/Noise Ratio:

Tape Speed (in/s)	Bandwidth (±3dB)	S.N.R. (dB)
60	300 Hz to 300 kHz	40
30	200 Hz to 150 kHz	40
15	100 Hz to 75 kHz	40
7½	100 Hz to 37.5 kHz	30
3¾	100 Hz to 19 kHz	30
1½	100 Hz to 9.5 kHz	30
¾	100 Hz to 4.75 kHz	20

Input Sensitivity: A twelve position switch on each channel is calibrated in volts peak for normal record level. Range 0.1 to 20V in 8 steps. Additional positions are:-

Input Sensitivity: (Contd). OFF Record Disable
REF Reference Frequency
- Mid-band reference signal *
+ Band-edge reference signal *

* When calibration board is fitted.

Input Impedance: 10k ohms unbalanced shunted by less than 100pF.

Input Overload: Input circuits are protected to a maximum continuous input of $\pm 100V$.

Output: Continuously variable from 0 to $\pm 3V$ for normal record level.

Output Impedance: < 10 ohms.

Output Current: 15mA max. short circuit protected.

Harmonic Distortion: 1% 3rd harmonic at normal record level.

SIGNAL MONITORING

Meter: Simultaneous positive and negative peak indicating meter.

Meter Modes: Peak or D.C. (selected by front panel switch).

Meter Accuracy: $\pm 2\%$

Selector: Front panel slide control selects metered track.

Response: Meter will read the peak amplitude of any pulse greater than $50\mu s$ duration.

VOICE CHANNEL

Microphone/Loudspeaker: Dynamic, hand held, with "press to talk" switch.

Record Level: Determined by A.G.C.

Reproduce Level: Adjustable by front panel control.

Power output: 0.2W maximum

Channel: Interrupts Channel 4 on Store 4DS. Separate channel on Store 7DS.

9. POWER REQUIREMENTS

A.C. 115V $\pm 10\%$ or 230V $\pm 10\%$
48 - 400Hz
80 VA (Store 4DS)
100 VA (Store 7DS)

D.C. 11 - 32V
65W at 24V (Store 4DS)
80W at 24V (Store 7DS)

10. ENVIRONMENT

Operating Temperature: $0^{\circ}C$ to $+50^{\circ}C$

Storage Temperature: $-10^{\circ}C$ to $+70^{\circ}C$

Altitude: 4,500m (15,000 ft)

Humidity: 10-95% relative humidity non-condensing.

Shock: 150m/s² maximum (10ms) non-operating.

11. PHYSICAL

Dimensions (Store 4DS)
Width 483mm (19 in)
Height 140mm (5½ in)
Depth 432mm (17 in)

Dimensions (Store 7DS)
Width 483mm (19 in)
Height 156mm (6¼ in)
Depth 485mm (19½ in)

Weight: 17.5kg (38.5lb) - Store 4DS
22kg (48lb) - Store 7DS (with full reel of tape).

Rack Mounting: May be fitted into standard 19 in racking with removing covers. (See Chapter 2 para 7).

Operational Attitude: Any plane.

H2 BIO-TEK BLOOD PRESSURE SYSTEM CALIBRATOR FREQUENCY RESPONSE
CHARACTERISTICS

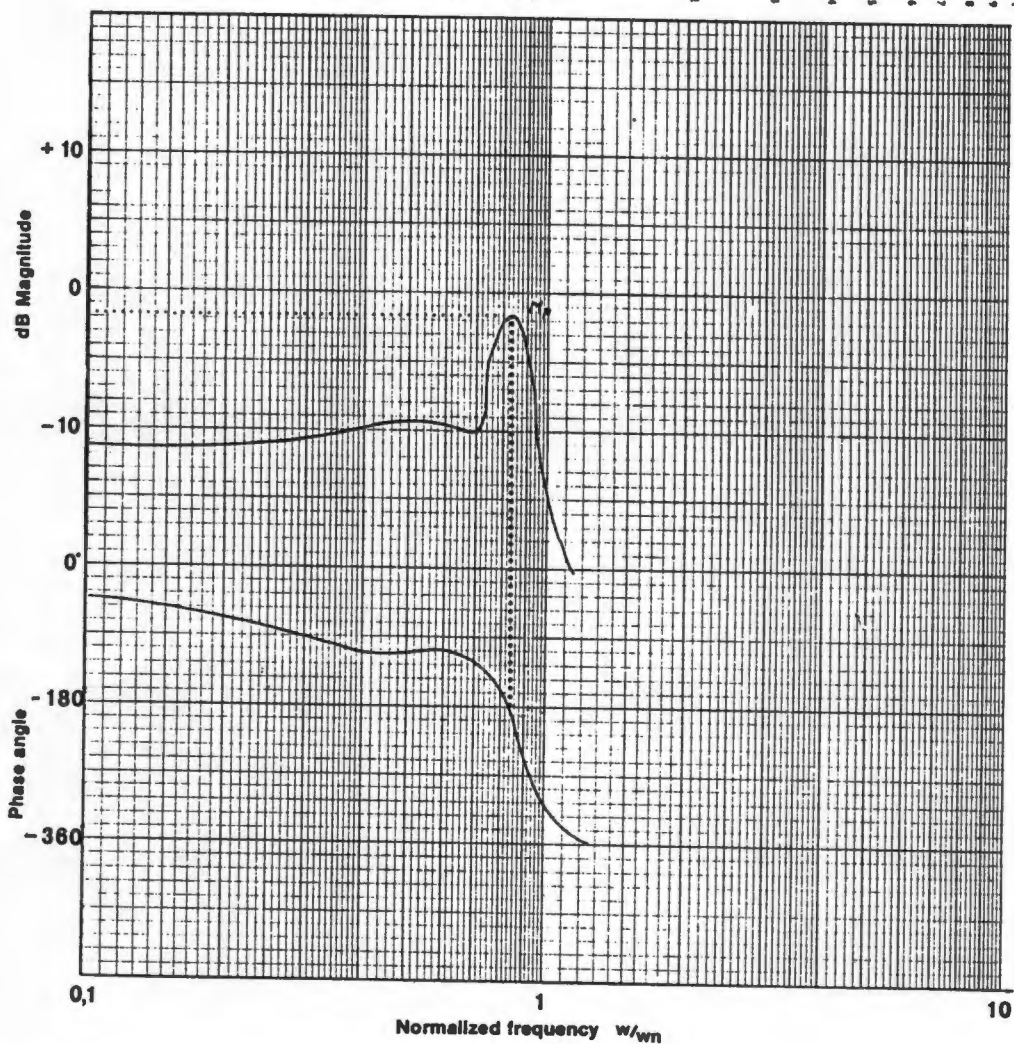


Figure H2.1

Amplitude and phase response of the blood pressure calibrator.

Dimensions:

S&W Standard plug-in module.

Weight:

1 kg (approx. 2 lb 3 oz).

Power Requirements:

Voltage: ± 12 V (± 1 V).

Current: + 250 mA.

- 25 mA.

Input Characteristics:

Mode: differential.

Impedance: 1 M Ω .

Common mode dynamic range: + 4 V.
- 7 V.

Common mode rejection ratio:

≥ 70 dB.

Amplification Characteristics:

Frequency response: 0-200 Hz (- 3 dB).

Gain, range I: X 30-128. Gain, range II: X 128-550.

Noise (BW: 0-200 Hz; input short-circuited): $< 30 \mu\text{V}$ (referred to input).

Zero drift (15-40 $^{\circ}$ C): $< 7 \mu\text{V}/^{\circ}$ C (referred to input).

Semi-automatic zero set deviation (max. gain): $< \pm 8$ mV (referred to output).

Semi-automatic zero set range (max. gain): ± 1 V (referred to output).

Recorder Outputs:

Arterial: X 1.

Venous: X 10.

Mode: single-ended.

Impedance: $< 10 \Omega$.

Max. DC load: 1 k Ω .

Short-circuit protection.

Transducer Excitation:

Voltage: -7.5 V $\pm 5\%$.

Transducer resistance range:

200 Ω -1k Ω . Short-circuit protection.

S&W Patient Safety System:

Leakage current at 50 Hz between chassis and reference electrode
 $\leq 0.07 \mu\text{A}/\text{V}$.

Controls:

Screwdriver-operated calibration.

Pushbutton for automatic zero-setting.

H4 HP VECTRA (Hewlett Packard, 1986)

Chips

HP 45971A 128 KB Memory Expansion

HP 45987A Numeric Coprocessor Chip

Accessory Cards

Video Cards

HP 45984A Multi-Mode Color Adapter Card

Peripheral Cards

HP 24540A Serial/Parallel Interface Card

HP 61062A HP-IB Instrument Interface Card

Memory Cards

HP 45974A 1 MB Memory Expansion Card

Hard Disc Drive Controllers

HP 45816A 20 MB Hard Disc Controller Card

Hard Disc Drives

HP 45816A 20 MB Internal Hard Disc Drive

Flexible Disc Drives

HP 45811A 360 KB Internal Flexible Disc Drive

MICROLINK

HSC

DESCRIPTION

The HSC is a single width module fitting within the Microlink frame, providing facilities for high speed digitisation of analogue signals. To do this it is used in conjunction with an Analogue to Digital converter (A-D) and one or more analogue input modules. These other modules can be used in their normal slow mode even when the HSC is present in the frame. In order to give the HSC control of these modules, it is necessary for the computer to set the HSC enable flag. Having done this, the HSC now controls the rate of sampling of the A-D converter. The module derives this rate from a 1 Mhz crystal clock, by use of 2 programmable dividers. The first divider selects a 'clock unit' of either 1 μ sec, 10 μ sec etc in powers of 10 up to 1 second. The second divider called 'clock number' counts from 1 to 255 of these units. If, for example, the clock unit is selected as 10 msec and the clock number is set to 15, then a sample is taken every 150 msec. Similarly if the clock unit is 100 μ sec and the clock number is set to 39, then a sample is taken every 3,900 μ sec (which is very close to 256 samples/second). In this way times between 1 μ sec and 255 seconds can be set.

The A-D converter is now sampling at a regular programmed rate. In order to deal with several inputs it is necessary to multiplex them (switch in sequence) to the A-D converter. The Microlink achieves this in a very flexible way. The first sample is taken from the leftmost analogue input module (view from the front of the modules). This module then sets a line on the backplane to indicate to the module on its immediate right, that it has been read. This next module now connects itself to the A-D and the second sample is taken from it. It then indicates that it has been read to the module on its right and so on across the frame. Each analogue input module is equipped with 2 programmable flags, Skip and Return. When the Skip flag of a module is set it is omitted from the multiplexing scan. When the Return flag is set, that module becomes the final one in the multiplexing scan. So when a module with its Return flag set has been read, the next module to be read is the leftmost one once again. In order for the multiplexing to work, a Return flag must always be set somewhere in the scan. In the case of modules which have several inputs e.g. ANI6-32, data is sent to them which causes a variable number of inputs to be included in the scan. So if, for example, an ANI6-32 is programmed to include 8 inputs in the multiplex, it will switch the 8 inputs in sequence, at successive sample times, to the A-D before telling the module on its right that it has been read. Having set up the sample rate and the multiplex scan the computer can now read a stream of precisely timed multiplexed data from the A-D converter.

In order to separate the multiplexed channels in the data received by the computer, it is necessary to ensure that the first data received comes from the first channel. The basic way of doing this is to issue a Group Execute Trigger (GET) command. This is a specific IEEE 488 command which causes the HSC to produce a 25 msec long Trigger Out pulse at the front panel BNC socket. For the duration of the pulse the HSC, A-D, and multiplex scan are all reset. Timing, sampling, and multiplexing then restart at the trailing edge of this Trigger pulse, and the first sample from the first channel is taken one sample interval later. The Trigger pulse is made long to ensure that computers can issue their GET command, then proceed to their data entry routines, and then be ready to receive data before the first sample is taken. Sometimes this length is inconvenient, in which case it can be shortened by changing one component on the PCB. In applications where you are measuring the response of a system to a stimulus of some kind, the trailing edge of the Trigger pulse can be used to initiate the stimulus.

Sometimes it is necessary to initiate the data input to the computer from an external event. This is done by connecting a signal marking the event to the Trigger In socket. This input has two modes of operation. In the simplest mode, a rising edge at the Trigger input produces a Service Request (SRQ) signal to the computer which, having set up the HSC and analogue input modules, is monitoring its SRQ input. On receipt of the SRQ, the computer issues the GET command and goes into its data entry routine. This means that sampling actually starts 25 msec after the Trigger In signal. The second mode of operation involves setting up the HSC and analogue inputs and then the computer going straight into its data entry routine. This is made possible by setting the synchroniser flag flip-flop. This, when set, holds the HSC, A-D, and multiplex in the reset condition and holds the Trigger Out signal true. No data can be generated in this condition and so the computer must wait in its data entry routine. A positive edge occurring at the Trigger In resets the synchroniser flip-flop and the first sample occurs exactly one sample time later. This second method is clearly preferable where precise time locking to an incoming trigger signal is required.

As discussed so far all sampling has been on an evenly spaced basis. The effect of this on a multichannel input is to produce a timing skew between channels as shown in Figure 1a. Often this is not a problem and the method does have the virtue of giving the multiplexing elements the maximum time to settle. Figure 1b illustrates the 'burst' mode of sampling. In this mode, at each sample time generated by the HSC, instead of taking a single reading, the Microlink takes one reading from each channel in the analogue input scan. Thus data reaches the computer in regularly spaced bursts. The burst mode is controlled by an 8 position PCB mounted switch. One position switches the mode off whilst the other 7 control the time delay between channels in the burst. This can be set as 16 μ sec, etc in powers of 2 up to 1024 μ sec. The selected setting must be large enough to allow the computer to enter the generated data. Burst mode clearly reduces the time skew between channels and is an approximation to simultaneous sampling across all channels. The ANIDS module, by providing a sample and hold circuit for each channel, allows simultaneous sampling to be truly achieved.

The whole of the above discussion revolves around the HSC producing, at programmable intervals, sample pulses which either cause a single reading or a burst scan. By throwing a PCB mounted switch the external clock input is activated. Now at each positive edge occurring at the clock input, a single sample is taken or a complete burst scan is made. A final facility offered by the HSC involves the SRQ line. This, as described above, is normally controlled by the Trigger In but a PCB mounted switch is fitted which when thrown connects the output of the HSC's programmable sample interval circuits to the SRQ. This produces a regularly spaced series of SRQ pulses which the computer can use for timing purposes.

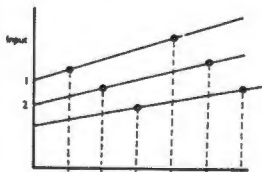


Figure 1a Normal Sampling (Data show samples taken)

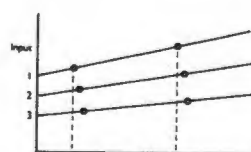


Figure 1b Burst Mode

DESCRIPTION

The ANI is a single width module, fitting within the Microlink mainframe, providing a general purpose single ended voltage input. A block diagram of the module is given below. The functions of the module can be considered in two halves. Firstly to condition the input signal to be suitable for an A-D converter module (A8D, AI2D, INI2D) and secondly, since many analogue input modules can be connected to a single A-D converter, to connect the conditioned signal to the A-D converter only at the appropriate times. Considering first then the analogue section. The input voltage first passes through circuits which protect the module from damage for inputs up to $\pm 50V$. A high input impedance variable gain amplifier then adjusts the signal size to be appropriate for an A-D converter. The gain adjustment is performed by a combination of two front panel controls, a 3 position RANGE switch and a screwdriver operated 20 turn GAIN potentiometer. These together allow the unit to operate with signals anywhere between 10V full scale and 10 mV full scale. The amplified signal then passes through a single pole filter. Normally on leaving the factory this filter is not operational since a capacitor is omitted. This capacitor can be fitted at any time, its value being selected by a simple formula, to limit the frequency response of the module to any desired value. This facility is useful for removing noise from signals or anti-aliasing. Finally the 20 turn OFFSET control is used to offset the signal by a variable amount. This allows the module to cope with all positive, all negative, and bipolar signals. Provision is made on the printed circuit board for the fitting of extra potentiometers which convert the front panel OFFSET and GAIN adjustments to fine trims about ranges defined by the extra potentiometers. This facility is useful when the wide ranging adjustments are not needed but fine trimming is important.

Moving now to the control logic. This has two basic modes of operation; normal and high speed. Normal mode is used where sample rates of a few tens of samples per second or less are required. If higher rates or precise sample timing are required then the high speed mode should be used. This needs the addition of an HSC module. In the normal mode the host computer selects the ANI by means of a secondary address code. This causes the ANI to connect its analogue output to the A-D converter. An A-D conversion is performed and the result passed to the computer as data. A further reading can be taken by a similar procedure or, by substituting a different secondary address, a different analogue input module can be read. When an HSC module is present in the frame, control data sent to it can place the analogue inputs in high speed mode. The sampling rate is now controlled by the HSC with crystal derived accuracy. Also which analogue input module is connected to the A-D converter is now controlled by automatic multiplexing circuitry built into each analogue input. The computer can now obtain from the Microlink a stream of precisely timed multiplexed data and can run at up to its maximum data input rate (typically tens of thousands of bytes per second). The analogue input modules in the Microlink frame are scanned from left to right as viewed from the front of the frame. As with other analogue input modules the ANI is equipped with Skip and Return flags. When set, these cause it to be omitted from the high speed scan or become the final module in a high speed scan respectively. Complete details of the extensive fast sampling facilities provided by the HSC are given in its application note.

PROGRAMMING

When the host computer wishes to communicate with the ANI module, it selects it within the Microlink frame by means of a secondary address code. The code allocated to the ANI is preset by PCB mounted switches. As explained above, receiving its secondary address code causes the ANI to connect its analogue output to the A-D converter, which takes a reading. Also the secondary address can select the ANI to receive its set up data for the Skip and Return flags.

The manual which accompanies each module gives complete details of these transactions with the computer plus example programs for computers supported by BIODATA (see main literature for a list of these). You should state which computer you require programs for when ordering.

APPENDIX I

DATA TABLES

CONTENTS

I1 Data table on polymers

I2

I1 Data tables on polymers (Goodfellow, 1987)

POLYMERS ▶		Poly-styrene	Poly-styrene (Cross-linked)	Poly-tetra-fluoro-ethylene PTFE	PTFE filled with Glass 25% Glass	Polyvinyl-chloride (unplast-icised) uPVC	Polyvinyl-idene-chloride PVDC	Polyvinyl-idene-fluoride PVDF	Silicone Elastomer	
		Property	Units							
Physical	Density	g cm ⁻³	1.05	1.05	2.2	2.2	1.4	1.63	1.76	0.5
	Tensile strength	MPa	30-100	55-70	10-40	7-20	25-70	25-110	25-60	6.5
	Elastic modulus	GPa	2.3-4.1	1.65	0.3-0.8	1.7	2.5-4	0.3-0.55	1-3	-
	Impact strength (IZOD)	J m ⁻¹	19-24	-	160	144	20-1000	16-53	120-320	-
	Hardness (Rockwell)	-	M60-90	110-120	D50-55 (Shore)	D60-70 (Shore)	R106-120	R98-106	R77-83	-
	Abrasion resistance (ASTM D1044)	mg/1000 cycles	-	60-100	-	-	-	-	24	-
	Coefficient of friction	-	-	-	0.05-0.2	0.08-0.10	-	0.24	0.2-0.4	-
	Water absorption	%	<0.4	0.02-0.03	0.01	0.15	0.03-0.4	0.1	0.02-0.06	-
	Flammability	-	Slow burn	Combustible	Non combustible	Non combustible	Self extinguishing	Self extinguishing	Self extinguishing	-
Chemical Resistance	Alcohols		Good	Good	Good	Good	Fair	Good	Good	Fair
	Ketones		Poor	Poor	Good	Good	Poor	Fair	Poor	Fair
	Aromatic hydrocarbons		Poor	Poor	Good	Good	Poor	Fair	Fair	Poor
	Greases and oils		Good-Poor	Fair	Good	Good	Fair	Good	Good	Good
	Acids - concentrated		Good	Fair	Good	Good	Fair	Good	Good	Fair
	Acids - dilute		Good	Good	Good	Good	Good	Good	Good	Good
	Alkalis		Good	Fair	Good	Good	Good	Good	Good	Fair
	Halogens		-	Poor	Good	Good	Fair	Good	Good	Poor
Thermal	Thermal conductivity at 23°C	W m ⁻¹ K ⁻¹	0.04-0.14	0.1	0.25	0.33-0.42	0.12-0.25	0.13	0.1-0.25	-
	Thermal expansivity	×10 ⁻⁶ K ⁻¹	30-210	90	100	75-100	75-100	190	80-140	-
	Lower working temperature	°C	-	-	-260	-	-30	-	-40	-90
	Upper working temperature	°C	95	93	280	260	75	80-100	160-220	-
Electrical	Dielectric constant (at 1 MHz)	-	2.4-3.1	2.5	2.0-2.1	2.2-2.35	2.7-3.1	3-6	8.4	-
	Surface resistivity	Ω	-	10 ¹⁵	10 ¹⁷	10 ¹⁵	-	10 ¹² -10 ¹³	10 ¹³	-
	Volume resistivity	Ω cm	>10 ¹⁶	10 ¹⁶ -10 ¹⁷	10 ¹⁸ -10 ¹⁹	10 ¹⁶	10 ¹⁶	10 ¹² -10 ¹⁶	10 ¹⁴ -	-
Other	Resistance to ultra-violet	-	Fair	Good	Good	Good	Good	Fair	Good	-
	Radiation resistance	-	-	Alpha, Beta, Gamma, X - Good	-	-	-	-	Beta, Gamma, - Good	-

POLYMERS		Poly-ethylene (U.H.M.W.)	Poly-hydroxy-butyrate Biopolymer PHB	Polyimide Kapton®	Poly-methyl-methacrylate Acrylic	Polyoxy-methylene Acetal	Poly-phenylene-oxide Noryl®	Poly-phenylene-sulphide PPS	Poly-propylene	
Property	Units									
Physical	Density	g cm ⁻³	0.94	1.25	1.42	1.2	1.42	1.06	1.66	0.9
	Tensile strength	MPa	20-40	-	70-150	45-85	60-70	62	124-160	25-250
	Elastic modulus	GPa	0.2-1.2	3.5	2-3	2.4-3.3	3.0-3.5	2.5	7-12	1-1.5
	Impact strength (IZOD)	J m ⁻¹	No break	75	80	16-32	64-123	210-370	75-80	21-53
	Hardness (Rockwell)	-	R50-70	-	E52-99	M92-100	M92-94	R120	R123	R80-100
	Abrasion resistance (ASTM D1044)	mg/1000 cycles	-	-	-	-	14-20	20	-	13-16
	Coefficient of friction	-	0.1-0.2	-	0.42	-	0.1-0.3	0.35	-	0.1-0.3
	Water absorption	%	<0.01	-	0.2-2.9	0.3-0.4	0.25-0.4	0.1-0.13	<0.05	<0.05
Flammability	-	Combustible	-	Non combustible	Combustible	Combustible	Self extinguishing	Non combustible	Combustible	
Chemical Resistance	Alcohols		Good	Fair	Good	Fair	Good	Fair	Good	Good
	Ketones		Good	-	Good	Poor	Fair	Fair	Good	Good
	Aromatic hydrocarbons		Poor	-	Good	Poor	Good	Poor	Good	Fair
	Greases and oils		Good	Good	Good	Poor	Good	Fair	Good	Fair
	Acids - concentrated		Fair	-	Good	Fair	Poor	Fair	Fair	Good
	Acids - dilute		Good	Fair	Good	Good	Poor	Good	Good	Good
	Alkalis		Good	Poor	Poor	Good	Fair	Good	Good	Good
	Halogens		Poor	-	-	Poor	Good	Poor	Fair	Poor
Thermal	Thermal conductivity at 23°C	W m ⁻¹ K ⁻¹	0.42-0.51	-	0.1-0.3	0.16-0.25	0.22-0.24	0.2-0.22	0.29-0.45	0.1-0.2
	Thermal expansivity	x10 ⁻⁶ K ⁻¹	130-200	-	30-60	50-90	80-100	50-60	22-35	60-100
	Lower working temperature	°C	-	-	-270	-	-30	-40	-	-10
	Upper working temperature	°C	95	95	250-320	90	80-120	92	195	100-120
Electrical	Dielectric constant (at 1 MHz)	-	2.3	3	3.4	2.1-4.5	3.7	2.6	3.8	2.2-2.6
	Surface resistivity	Ω	10 ¹³	-	-	-	10 ¹⁵	2 x 10 ¹⁶	10 ¹⁶	10 ¹³
	Volume resistivity	Ω cm	10 ¹⁶	10 ¹⁶	10 ¹⁸	10 ¹⁴ -10 ¹⁷	10 ¹⁵	10 ¹⁷	10 ¹⁶	10 ¹⁶ -10 ¹⁸
Other	Resistance to ultra-violet	-	Fair	Fair	Good	Good	Fair	Good	-	Fair
	Radiation resistance	-	-	-	Alpha, Beta, Gamma, X - Good	-	-	-	-	-

POLYMERS		Units	Polyester	Polyester Liquid Crystalline copolymer Vectra®	Polyester/ amide Liquid Crystalline copolymer Vectra®	Polyether- etherketone PEEK	Polyether- sulphone PES	Poly- ethylene (Carbon filled)	Poly- ethylene (High Density)	Poly- ethylene (Low Density)
			Property							
Physical	Density	g cm ⁻³	1.4	1.38	1.37	1.32	1.37	0.96	0.95	0.92
	Tensile strength	MPa	40-200	520-660	600	70-100	70-95	20	15-40	5-25
	Elastic modulus	GPa	2-4	30-45	60	3.7-4	2.4-2.6	-	0.5-1.2	0.1-0.3
	Impact strength (IZOD)	J m ⁻¹	13-35	-	-	85	85	-	20-210	No break
	Hardness (Rockwell)	-	M94-101	-	-	M99	M88	-	D60-73 (Shore)	D41-46 (Shore)
	Abrasion resistance (ASTM D1044)	mg/1000 cycles	-	-	-	-	6	-	-	-
	Coefficient of friction	-	0.2-0.4	-	-	0.18	-	-	0.29	-
	Water absorption	%	<0.8	0.02	0.03	0.1-0.3	0.4-2.0	-	<0.01	<0.015
	Flammability	-	Self extinguishing	Non combustible	Non combustible	-	Self extinguishing	-	-	-
Chemical Resistance	Alcohols		Good	Good	Good	Good	Good	Good	Good	Good
	Ketones		Good	Good	Good	Good	Poor	Fair	Good	Good
	Aromatic hydrocarbons		Fair	Good	Good	Good	Fair	-	Fair-Poor	Poor
	Greases and oils		Good	Good	Good	Good	Good	-	Fair	Poor
	Acids - concentrated		Good	Fair	Fair	Fair	Fair	Fair	Good	Fair
	Acids - dilute		Good	Good	Good	Good	Good	Good	Good	Good
	Alkalis		Poor	Fair	Fair	Good	Good	-	Good	Good
	Halogens		Good	-	-	Good	Good	-	Good	Good
Thermal	Thermal conductivity at 23°C	W m ⁻¹ K ⁻¹	0.15-0.4	-	-	0.25	0.13-0.18	-	0.45-0.52	0.33
	Thermal expansivity	×10 ⁻⁶ K ⁻¹	30-65	-12	-12	60	55	-	100-200	100-200
	Lower working temperature	°C	-40	-	-	-	-110	-	-	-60
	Upper working temperature	°C	130-170	-	-	250	190-200	-	80-120	50-90
Electrical	Dielectric constant (at 1 MHz)	-	3.0	3	-	-	3.5	-	2.3-2.4	2.2-2.35
	Surface resistivity	Ω	10 ¹³	-	-	-	-	10 ² -10 ⁴	-	-
	Volume resistivity	Ω cm	> 10 ¹⁴	10 ¹⁶	-	10 ¹⁵ -10 ¹⁶	10 ¹⁵ -10 ¹⁷	< 10 ⁵	10 ¹⁵ -10 ¹⁸	10 ¹⁵ -10 ¹⁸
Other	Resistance to ultra-violet	-	Good	Good	Good	Fair	Fair	Good	Fair	Fair
	Radiation resistance	-	-	Good	Good	Good	Good	-	-	-